Institut für Erd- und Umweltwissenschaften
Geoökologie

Floods in the Niger River Basin in the face of Global Change – Analysis, Attribution and Projections

Dissertation
zur Erlangung des akademischen Grades
"doctor rerum naturalium"
(Dr. rer. nat.)
in der Wissenschaftsdisziplin "Hydrologie"

kumulativ eingereicht an der
Mathematisch-Naturwissenschaftlichen Fakultät
der Universität Potsdam

von
Valentin Aich

Potsdam, Dezember 2015

Published online at the
Institutional Repository of the University of Potsdam:
URN urn:nbn:de:kobv:517-opus4-91577
http://nbn-resolving.de/urn:nbn:de:kobv:517-opus4-91577

SUMMARY

In the last decade, the number and dimensions of catastrophic flooding events in the Niger River Basin (NRB) have markedly increased. Despite the devastating impact of the floods on the population and the mainly agriculturally based economy of the riverine nations, awareness of the hazards in policy and science is still low. The urgency of this topic and the existing research deficits are the motivation for the present dissertation.

The thesis is an initial detailed assessment of the increasing flood risk in the NRB. The research strategy is based on four questions regarding (1) features of the change in flood risk, (2) reasons for the change in the flood regime, (3) expected changes of the flood regime given climate and land use changes, and (4) recommendations from previous analysis for reducing the flood risk in the NRB.

The question examining the features of change in the flood regime is answered by means of statistical analysis. Trend, correlation, changepoint, and variance analyses show that, in addition to the factors exposure and vulnerability, the hazard itself has also increased significantly in the NRB, in accordance with the decadal climate pattern of West Africa. The northern arid and semi-arid parts of the NRB are those most affected by the changes.

As potential reasons for the increase in flood magnitudes, climate and land use changes are attributed by means of a hypothesis-testing framework. Two different approaches, based on either data analysis or simulation, lead to similar results, showing that the influence of climatic changes is generally larger compared to that of land use changes. Only in the dry areas of the NRB is the influence of land use changes comparable to that of climatic alterations.

Future changes of the flood regime are evaluated using modelling results. First ensembles of statistically and dynamically downscaled climate models based on different emission scenarios are analyzed. The models agree with a distinct increase in temperature. The precipitation signal, however, is not coherent. The climate scenarios are used to drive an eco-hydrological model. The influence of climatic changes on the flood regime is uncertain due to the unclear precipitation signal. Still, in general, higher flood peaks are expected. In a next step, effects of land use changes are integrated into the model. Different scenarios show that regreening might help to reduce flood peaks. In contrast, an expansion of agriculture might enhance the flood peaks in the NRB. Similarly to the analysis of observed changes in the flood regime, the impacts of climate- and land use changes for the future scenarios are also most severe in the dry areas of the NRB.

In order to answer the final research question, the results of the above analysis are integrated into a range of recommendations for science and policy on how to reduce flood risk in the NRB. The main recommendations include a stronger consideration of the enormous natural climate variability in the NRB and a focus on so called “no-regret”

adaptation strategies which account for high uncertainty, as well as a stronger consideration of regional differences. Regarding the prevention and mitigation of catastrophic flooding, the most vulnerable and sensitive areas in the basin, the arid and semi-arid Sahelian and Sudano-Sahelian regions, should be prioritized. Eventually, an active, science-based and science-guided flood policy is recommended. The enormous population growth in the NRB in connection with the expected deterioration of environmental and climatic conditions is likely to enhance the region´s vulnerability to flooding. A smart and sustainable flood policy can help mitigate these negative impacts of flooding on the development of riverine societies in West Africa.

ZUSAMMENFASSUNG

Während des vergangenen Jahrzehnts nahmen die Anzahl und die Ausmaße von katastrophalen Hochwassern im Einzugsgebiet des Nigerflusses (NEZG) deutlich zu. Trotz der verheerenden Auswirkungen der Hochwasserkatastrophen auf die Menschen und die hauptsächlich auf Landwirtschaft basierende Wirtschaft der Anrainerstaaten wird das Thema von Politik und Wissenschaft noch kaum beachtet. Die Relevanz der Thematik und das Forschungsdefizit sind die Motivation für die vorliegende Dissertation.

Sie ist die erste ausführliche Analyse des steigenden Hochwasserrisikos im NEZG. Die Forschungsstrategie leitet sich aus vier Forschungsfragen ab:

(1) Was sind die Merkmale der Veränderungen des Hochwasserrisikos?

(2) Was sind die Ursachen der Veränderungen des Hochwasserregimes?

(3) Welche zukünftigen Entwicklungen des Hochwasserregimes sind auf Grund des Klima- und Landnutzungswandels zu erwarten?

(4) Welche Empfehlungen zur Reduzierung des Hochwasserrisikos im NEZG können aus den vorhergehenden Untersuchungen abgeleitet werden?

Die Frage nach den Merkmalen der Veränderungen im Hochwasserrisiko wurde mithilfe von statistischen Untersuchungen beantwortet. Trend-, Korrelations-, Changepoint- und Varianzanalysen zeigen, dass neben den Risikofaktoren Exponiertheit und Verwundbarkeit auch die Hochwasserstände selbst im NEZG in den letzten Jahrzehnten signifikant und entsprechend der typischen dekadischen Klimamuster Westafrikas angestiegen sind. Die ariden und semi-ariden Teile des NEZG sind dabei am stärksten von den Veränderungen betroffen.

Als potentielle Ursachen des Hochwasseranstiegs werden Klima- und Landnutzungswandel anhand einer Zuschreibungsanalyse untersucht. Zwei verschiedene Ansätze, basierend auf Daten sowie auf Simulationen, führen zu ähnlichen Ergebnissen und zeigen, dass der Einfluss der Klimaveränderungen verglichen mit dem Einfluss von Landnutzungsänderungen im Allgemeinen größer ist. Nur in den trockenen Gebieten des NEZG ist der Einfluss der Landnutzungsänderungen derzeit vergleichbar stark.

Das zukünftige Hochwasserrisiko wird anhand von Modellergebnissen abgeschätzt. Zunächst werden Ensembles statistisch und dynamisch hochaufgelöster Klimamodelle basierend auf verschiedenen Emissionsszenarien untersucht. Die Modelle stimmen in einem deutlichen Temperaturanstieg überein. Das Niederschlagsignal ist jedoch nicht kohärent. Anschließend wird mit den Klimaszenarien ein öko-hydrologisches Modell angetrieben. Der Einfluss des Klimawandels auf das Hochwasserregime ist auf Grund des diffusen Niederschlagssignals unsicher. Tendenziell werden aber höhere Maximalabflüsse erwartet. In einem nächsten Schritt wird der Effekt der Landnutzungsänderung in das Modell einbezogen. Verschiedene Szenarien zeigen, dass Renaturierung hülfe, Hochwasserspitzen zu kappen. Eine Ausweitung der Agrarflächen dagegen würde die

Hochwasser im NEZG weiter verstärken. Wie bei der Analyse der beobachteten Veränderungen sind auch bei den Zukunftsszenarien die Auswirkungen der Klima- bzw. der Landnutzungsänderungen in den trockenen Gebieten am stärksten.

Für die Beantwortung der vierten Forschungsfrage fließen die Ergebnisse der bisherigen Untersuchungen in eine Reihe von Empfehlungen für Wissenschaft und Politik ein. Zentrale Empfehlungen beinhalten eine stärkere Einbeziehung der enorm starken natürlichen Klimavariabilität im NEZG, eine Fokussierung auf sogenannte „no-regret“ Anpassungsstrategien, die der hohen Unsicherheit gerecht werden, sowie eine stärkere Berücksichtigung regionaler Unterschiede. Hinsichtlich Prävention und Minderung der Hochwasser sollte den verwundbarsten und sensibelsten Regionen des Einzugsgebiets, den ariden und semi-ariden Regionen, Priorität eingeräumt werden. Letztendlich wird eine aktive, wissenschaftlich geleitete und begleitete Hochwasserpolitik empfohlen. Die enorme Bevölkerungszunahme im NEZG verbunden mit der zu erwartenden Verschlechterung der Umwelt- und Klimabedingungen wird mit hoher Wahrscheinlichkeit auch die Verwundbarkeit bezüglich Hochwässer weiter ansteigen lassen. Eine vernünftige und nachhaltige Hochwasserpolitik kann helfen, die negativen Folgen auf die Entwicklung der Anrainerstaaten des Nigerflusses abzumindern, und damit beispielsweise dazu beitragen, die Flüchtlingsbewegungen aus Westafrika zu verringern.

ACKNOWLEDGEMENTS

Foremost I would like to thank my supervisors, Dr. habil. Eva Müller and Dr. Fred Hattermann, whose support enabled my work on this dissertation. Dr. Hattermann afforded me a PhD position at the Potsdam Institute of Climate Impact Research (PIK) and, as a supervisor, his door was always open and he provided assistance and encouraging words, regardless of how desperate the problem seemed. Likewise, Dr. Müller was an amazing supervisor in many ways; though she is extremely busy, she always found time to read drafts, comment on manuscripts or help with other challenges. Moreover, her advice and critiques were fundamental for all the research and publications during my PhD. Both of my supervisors gratefully shared their rich knowledge and experience with me and never lost their optimistic view on my research. They supported this PhD way more than is common in the academic world, and their splendid examples will further guide my through my scientific and professional life.

However, I must also note that the original reason for submitting this thesis goes further back to the study at my alma mater, the Julius-Maximilians-Universität Würzburg. I thank Prof. Dr. Roland Baumhauer, Prof. Dr. Heiko Paeth and particularly, Prof. Dr. Barbara Sponholz for not only teaching me the fundamentals of geography but also exemplifying enthusiasm for the subject.

In addition, as this thesis is a cumulative effort, it would not have been possible without the contribution of the coauthors of the included articles, each of whom I thank wholeheartedly. The research of the thesis was also part of the IMPACT2C project, for which I would like to thank all partners, particularly those from the work package on the African case studies for the stimulating atmosphere.

I also owe gratitude to Dr. Stefan Liersch who, especially at the beginning of my PhD, taught me the basics of hydrological modelling as my day-per-day supervisor. He always helped with a smile, no matter how many questions I consulted with him on.

This holds for all my colleagues at PIK, who made my time there so enjoyable and pleasant. I thank Peggy Gräfe for helping me with all administrative issues.

In particular, I want to thank the colleagues of my working group, who are way more than only colleagues. In alphabetic order I thank Dr. Tobias Conradt, Samuel Fournet, Christoph Gornott, Cornelia Hesse, Dr. Shaochun Huang, Dr. Hagen Koch, Anastasia Lobanova, Julia Reinhardt, Maria del Rocio Rivas, Michael Roers, Judith Stagl, Anastassi Stefanova, Julia Tecklenburg, Tobias Vetter, and Michel Wortmann. We had a great time,

and the working atmosphere between Fortran Codes, intriguing discussions and table football was very pleasant and inspiring.

I thank my mother-in-law, Barbara Andre, my colleagues and friends Judith Stagl, Julia Reinhardt and Alec Knuerr, as well as my friend Rosana Aragón Plaza for proofreading this thesis.

My special thanks go to my "Jungs," my friends and former flat mates Andreas Bernhard, Jens Frankenreiter, Philipp Kandal, Julius Kunz, and Heiko Strubel. Our joint familiar everyday life was the perfect contrast to the scientific work and I will certainly never forget our time together in the NB14.

I am indebted to my brothers Gabriel and Romeo Aich, who cared for our parents in difficult times, providing me with valuable time to concentrate on my PhD. This brings me to my parents, Priska and Wolfgang Aich, whom I own my deepest gratitude. They raised me, constantly stimulated my curiosity, and supported me patiently and benevolently throughout the whole of my school and University career. This thesis is dedicated to them.

Finally, I heartily thank my beloved wife Eva Aich for staying by my side through a long-lasting long-distance relationship. She encouraged me in times of doubt and equally shared with me in times of joy. The last of my thanks go to our daughter Antonia Aich, who supported me by waiting for being born until I had finished the draft for my last paper of the PhD.

CONTENTS

Floods in the Niger River Basin 1
SUMMARY iii
ZUSAMMENFASSUNG v
ACKNOWLEDGEMENTS vii
CONTENTS ix
LIST OF TABLES xv
LIST OF FIGURES xvi
LIST OF ABBREVIATIONS xxi
1. INTRODUCTION 1
1.1. Catastrophic flooding in the Niger River Basin 1
1.2. State of research on flooding in the Niger River Basin 2
1.3. Research questions and strategy 3
1.4. The eco-hydrological model SWIM 5
1.5. The Niger River Basin 7
1.5.1. History of the exploration of the Niger River Basin 9
1.5.2. Climate 10
1.5.3. Hydrology 11
1.5.4. Geology, Hydrogeology and Soils 12
1.5.5. Vegetation 12
1.5.6. Agriculture and Socio-economics 14
1.5.7. Flood risk reduction measures 14
1.6. Overview of articles 15
2. TIME SERIES ANALYSIS OF FLOODS ACROSS THE NIGER RIVER BASIN 19
2.1. Introduction 20
2.2. Niger River Basin 21
2.3. Methodology 23
2.3.1. Data 23
2.3.2. Statistics 26
2.4. Results 29

2.4.1. Analysis of long-term dynamics of rainfall and annual flood peaks 29
2.4.2. Analysis of changes in the timing of annual flood peaks 33
2.4.3. Analysis of damage statistics 33
2.5. Discussion 35
2.6. Conclusions 36
Acknowledgements 37
References 37
3. FLOODS IN THE NIGER BASIN – ANALYSIS AND ATTIBUTION 45
3.1. Introduction 46
3.2. Niger basin 47
3.3. Methodology 50
3.3.1. Data 50
3.3.2. Statistics 52
3.4. Results 55
3.4.1. Analysis of damage statistics 55
3.4.2. Analysis of changes in the timing of annual flood peaks 57
3.4.3. Trend analysis of annual flood peaks 58
3.4.4. Attribution of changes in annual flood peaks 59
3.5. Discussion 65
3.5.1. The return to wet conditions and the increasing number of catastrophic floods 65
3.5.2. Attribution of the changes in the flood regime and the "Sahelian paradox" 66
3.6. Conclusions and summary 67
Acknowledgements 68
References 68
4. CLIMATE OR LAND USE? – ATTRIBUTION OF CHANGES IN RIVER FLOODING IN THE SAHEL ZONE 75
4.1. Introduction 76
4.2. Materials and Methods 78
4.2.1. Regional Setting 78
4.2.2. Ecohydrological Model and Model Set-Up 80
4.2.3. Dynamic Land Use Change Module 81
4.2.4. Data 82
4.2.5. Calibration of the Model 86

4.2.6. Sensitivity Analysis of the Effects of LULC on the Hydrological Regime 88
4.2.7. Statistical Methods 89
4.2.8. Hypothesis Testing Framework 90
4.3. Results and Discussion 91
4.3.1. Validation of the Model 91
4.3.2. Attribution of Trends in Annual Maximum Discharges 92
4.3.3. Discussion of the Methodological Framework Employed and Related Uncertainties 96
4.4. Conclusions 98
Acknowledgments 99
References 99
5. MULTI-MODEL CLIMATE IMPACT ASSESSMENT AND INTERCOMPARISON FOR THREE LARGE-SCALE RIVER BASINS ON THREE CONTINENTS 111
5.1. Introduction 112
5.1.1. Hydrology of the basins 112
5.2. Study areas, data and methods 114
5.2.1. Study areas: three river basins 114
5.2.2. Input data and climate scenarios 117
5.2.3. Hydrological models 118
5.2.4. Setup and calibration of three models 119
5.2.5. Method of uncertainty evaluation 122
5.3. Results 124
5.3.1. Calibration and validation of hydrological models 124
5.3.2. Evaluation of climate scenarios 128
5.3.3. Impacts on seasonal dynamics 133
5.3.4. Impacts on trends: magnitude of change and direction 134
5.3.5. Slope of trend 136
5.3.6. Trend significance 137
5.3.7. Evaluation of uncertainty 138
5.4. Summary and discussion 142
5.4.1. Evaluation and validation of models 142
5.4.2. Robust impacts and uncertainty sources 142
5.4.3. Uncertainty related to RCPs 143

5.4.4. Uncertainty related to GCMs 143
5.4.5. Uncertainty related to hydrological models 143
5.4.6. Uncertainties from different sources: what are the ways to reduce them? 144
Acknowledgements 146
References 146
6. COMPARING IMPACTS OF CLIMATE CHANGE ON STREAMFLOW IN FOUR LARGE AFRICAN RIVER BASINS 153
6.1. Introduction 154
6.2. Study sites 155
6.2.1. Hydrology of the basins 155
6.2.2. Human influence on discharge dynamics in the basins 157
6.3. Methodology 159
6.3.1. Model 159
6.3.2. Data 160
6.3.3. Model set-up and calibration 161
6.4. Results 164
6.4.1. Validation of the model 164
6.4.2. Climate trends 165
6.4.3. Climate sensitivity 169
6.4.4. Impact of climate change on discharge and seasonality 171
6.4.5. Changes in extremes 173
6.5. Discussion 175
6.5.1. Differences in climate change sensitivity among the basins 176
6.5.2. Changes of streamflow under climate change 176
6.5.3. Changes in hydrological extremes 177
6.5.4. Sources of uncertainties 179
6.5.5. Implications for adaptation 180
6.6. Summary and conclusions 181
Acknowledgments 182
References 182
7. FLOOD PROJECTIONS FOR THE NIGER RIVER BASIN CONSIDERING FUTURE LAND USE AND CLIMATE CHANGE 193
7.1. Introduction 195

7.2. Materials and Methods 196
7.2.1. Study area 196
7.2.2. Data 198
7.2.3. Ecohydrological Model and Model Set-Up 204
7.2.4. Indicators and statistics 206
7.2.5. Calibration and Validation of the Model 207
7.3. Results 209
7.3.1. Assessment of future climate projections in the Niger Basin 209
7.3.2. Assessment of future land use and land cover changes in the Niger Basin 210
7.3.3. Assessment of future flood projections in the Niger Basin 213
7.4. Discussion 215
7.4.1. Uncertainty 215
7.4.2. Flood trends 217
7.4.3. Managment implications 219
7.5. Conclusions 220
Acknowledgments 220
References 221
8. DISCUSSION AND CONCLUSIONS 229
8.1. Analysis: Characteristics of the changes in flood risk 229
8.2. Attribution: Drivers of the changes in the flood regime 230
8.3. Projections: Expected changes in the flood regime 232
8.4. Recommendations for reducing the flood risk 234
8.5. Overall Conclusions 238
8.6. Outlook 238
9. References 240
10. Appendix 247
10.1. Appendix of Chapter 2 247
10.2. Appendix of Chapter 3 251
10.2.1. Revised version of the data based attribution approach 254
10.3. Appendix of Chapter 4 259
10.4. Appendix of Chapter 5 262
10.5. Appendix of Chapter 6 265

10.6. Appendix of Chapter 7 270

Declaration 275

LIST OF TABLES

Table 1 Correlation of AMAX with heavy precipitation (95th percentile) and annual precipitation.. 34

Table 2 Major reservoirs in the Niger basin. 49

Table 3 Spearman´s correlations of the Atlantic Multidecadal Oscillation with AMAX and precipitation for the regions.. 62

Table 4 Calibrated parameters of the ecohydrological model SWIM 87

Table 5 Calibration and validation results of the eco-hydrological model SWIM in Nash-Sutcliff efficiency (NSE) and percent bias (PBIAS) for three stations. 88

Table 6 Gradient of the trends of AMAX anomalies as estimated with the Theil-Sen approach. 94

Table 7 Characteristics of the three river basins. 115

Table 8 Differences between spatial disaggregation, climate input and representation of main components in the three hydrological models. 121

Table 9 Calibration and validation results with the daily time step.. 124

Table 10 Coefficient of correlation and percent bias for the three runoff quantiles (Q_{90}, Q_{50}, Q_{10}) in the calibration and the validation period 126

Table 11 Basin and river characteristics 158

Table 12 Earth System Models driving the SWIM model 161

Table 13 Characteristics of basin models and validation results 163

Table 14 Summary of modeling results. 177

Table 15: Hydrological parameters for catchments.. 198

Table 16: Overview on the climate models used in the study. 201

Table 17: Calibration and validation results for daily values. 202

Table 18 Reservoirs of the Niger River Basin included in the model. 205

Table S 1 Correlation of AMAX with heavy precipitation (95th percentile) and annual precipitation. 255

Table S 2 Calibration results for additional stations in the Niger basin model. 265

LIST OF FIGURES

Figure 1 Research strategy for assessing catastrophic flooding in the Niger River Basin 4

Figure 2 The Niger River Basin. 7

Figure 3 Regions of the Niger River Basin 8

Figure 4 Annual precipitation and mean annual temperature in the Niger River Basin 11

Figure 5 Vegetation zones of the Niger River Basin. 13

Figure 6 Niger River Basin: Source areas of floods in the Guinean, Sahelian and Benue regions, location and number of catastrophic floods.. 22

Figure 7 Flood risk in the Niger River Basin as result of hazard, exposure, and vulnerability. 23

Figure 8 Hydrograph of the Niamey gauging station with Sahelian flooding and Guinean flooding for the period from 2003 to 2012. 25

Figure 9 AMAX, annual precipitation and heavy precipitation for the three subregions of the Niger River Basin as an anomaly from 1979-2012. 29

Figure 10 Annual maximum discharge (AMAX), precipitation and people affected by floods in the NRB, separated for the three subregions 30

Figure 11 Atlantic Multidecadal Oscillation with LOESS 31

Figure 12 Non-stationary extreme value probability distributions for Kouroussa, Alcongui and Garbe-Kourou. 32

Figure 13 Shift in day of AMAX for the stations influenced by the Inner Niger Delta for the Guinean flood. 33

Figure 14 People affected by catastrophic floods per year in the Niger River Basin from 1980 to 2014 for three different data sources.. 34

Figure 15 Niger basin and source areas of floods in the Guinean, Sahelian, Sudanian and Benue regions. 49

Figure 16 Population density in the Niger basin. 50

Figure 17 People affected by catastrophic floods per year in the Niger basin from 1985 to 2012 for three different data sources.. 55

Figure 18 People affected by floods in the Niger basin, annual maximum discharge (AMAX) and precipitation separated for the four subregions.. 57

Figure 19 Shift in day of AMAX for the Guinean stations upstream of the Inner Niger Delta and for the stations influenced by the Inner Niger Delta. 58

Figure 20 Non-stationary extreme value probability distributions for Kouroussa, Niamey and Malanville. 59

Figure 21 AMAX, annual precipitation, heavy precipitation and runoff coefficient for the four subregions of the Niger basin as an anomaly. 60

Figure 22 Anomaly of Richards-Baker flashiness index and heavy precipitation (95th percentile) for representative gauges in the Guinean (Koulikoro), Sahelian (Niamey), Sudanian (Malanville) and Benue (Lokoja) subregions. 61

Figure 23 Atlantic Multidecadal Oscillation with LOESS curve. 62

Figure 24 Hydrograph of the Niamey gauging station with Sahelian flooding and Guinean flooding.. 63

Figure 25, top: Sahelian AMAX for the Niamey station and annual/ heavy precipitation from WFD and WFDEI for the Sahelian region. 64

Figure 26 Map of the research area in West Africa including land use classes. 79

Figure 27 Land use and land cover changes between 1950 and 2005. 80

Figure 28 Changes in the main land use classes of crop, savannah, and pasture. 80

Figure 29 Comparison of precipitation from interpolated PGFv2 reanalysis data with observations from six weather stations in the research area. 83

Figure 30 Comparison of mean annual temperature of interpolated PGFv2 reanalysis data with observations from six weather stations in the research area. 84

Figure 31 Exemplary process of how the information from the Land Use and Land Cover data of the Land-Use Harmonization project is used.. 86

Figure 32 Comparison of discharges with four different land use coverages for the Sirba and Goroul watersheds. 89

Figure 33 Validation and calibration of the SWIM model for the watersheds of Alcongui, Garbe-Kourou and Niamey.. 92

Figure 34 Anomalies of annual maximum discharges for the gauging stations Alcongui (Goroul River), Garbe-Kourou (Sirba River) and differentiated between the Red and the Guinean Flood for Niamey (Niger River).. 93

Figure 35 Land-use maps of the three basins under study: the Upper Niger, the Rhine and the Upper Yellow 116

Figure 36 Results of calibration and validation of three models in three basins.. 126

Figure 37 Comparison of simulated and observed annual values of Q90, Q50 and Q10 in the calibration and validation periods for three basins: the Upper Niger, Upper Yellow and Rhine. 128

Figure 38 Evaluation of precipitation (P) and temperature (T) simulated by five climate models in three basins.

Figure 39 Comparison of the long-term average seasonal observed discharge in 1961–1990 with discharge driven by five climate models and three hydrological models. 131

Figure 40 Simulated long-term average seasonal dynamics of river discharge in the reference period 1961–1990 and scenario period 2061–2090. 134

Figure 41 Two examples showing annual median flows Q_{50} estimated from simulations. 135

Figure 42 Boxplots for the slopes of the linear trend for the Upper Niger, Upper Yellow and Rhine. 135

Figure 43 Direction of trends in Q_{90}, Q_{50} and Q_{10} for the Upper Niger, Upper Yellow and Rhine. 136

Figure 44 Contribution of different sources of uncertainties to overall uncertainty in the projected slopes of trends for the three runoff quantiles Q_{90}, Q_{50} and Q_{10} for the Upper Niger, Upper Yellow and Rhine. 140

Figure 45 Contribution of different sources of uncertainties to the overall uncertainty in the projected long-term average seasonal dynamics for the Upper Niger, Upper Yellow and Rhine basins for two scenario periods. 141

Figure 46 Map of the four modeled basins: Niger, Upper Blue Nile, Oubangui, Limpopo. 157

Figure 47 Structure of the eco-hydrological model SWIM. 159

Figure 48 Validation of SWIM at the outlets of the four basins.. 165

Figure 49 Mean temperature (left) and precipitation (right) trends over the African continent for 19 CMIP5 models from 2006-2100.. 166

Figure 50 Difference in monthly mean temperature in the far projection period (2070-2099) relative to the base period (1970-1999). 167

Figure 51 Difference in monthly precipitation in the far projection period (2070-2099) relative to the base period (1970-1999).. 169

Figure 52 Climate sensitivity in the four basins. Change in modeled annual discharge per change of precipitation for 2006-2099. 170

Figure 53 Seasonality of monthly discharge for the reference period; second and 172

Figure 54 Change in Q10 (high flows) of five bias corrected model projections. 174

Figure 55 Change in Q90 (low flows) of five bias corrected model projections 175

Figure 56: Overview map with four focus sub-regions and land use and land cover of 2005. 196

Figure 57: Annual precipitation, mean temperature and mean short wave downwelling radiation for the Koulikoro catchment in the Upper Niger Basin.. 199

Figure 58: Calibration and validation results for the stations analyzed in the study. 209

Figure 59: Relative changes of heavy (95th percentile of days >1 mm) and annual mean precipitation for all 18 climate models. 210

Figure 60: Land use and land use and land cover changes for cropland, pasture and urban land. 212

Figure 61: Quantification of changes of % crop and pasture areas of the catchments. 212

Figure 62 Boxplots for relative change (in %) for the 90th percentile of annual discharges 214

Figure 63 Boxplots for relative change (in %) for the 20th-year flood 215

Figure 64 Schematic representation of the causal chain leading to the increase in flood risk in the Niger River Basin 230

Figure S 1 Validation of precipitation reanalysis data.. 248

Figure S 2 Top: Annual/ heavy precipitation from WFD and WFDEI and AMAX for Niamey, and the mean of Alcongui and Garbe-Kourou for the Sahelian region. 249

Figure S 3 Top: AMAX time series with local regression curve 250

Figure S 4 Correlation between AMAX and people affected by floods for the subregions of the Niger basin. 250

Figure S 5 Decadal changes, trends and people affected by floods for all gauging stations affected primarily by the Guinean flood. 251

Figure S 6 Top: Wavelet power spectrum for Guinean, Sahelian, and Sudanian flooding. 252

Figure S 7 Correlation between Atlantic Multidecadal Oscillation and AMAX. 253

Figure S 8 Anomaly of Richards-Baker flashiness index for representative gauges in the Guinean, Sahelian and Benue subregions. 256

Figure S 9 Comparison of precipitation of interpolated PGFv2 reanalysis datawith observations of six weather stations in the research area. 259

Figure S 10 Comparison of mean annual temperature of interpolated WATCH reanalysis data with observations of six weather stations in the research area. 259

Figure S 11 Validation of precipitation reanalysis data. 260

Figure S 12 Comparison of precipitation of interpolated GSWP3 reanalysis data with observations of six weather stations(black) in the research area. 261

Figure S 13 Comparison of mean annual temperature of interpolated GSWP3 reanalysis data (red) with observations of six weather stations (black) in the research area. 261

Figure S 14 Slopes of trends in (a, b) low-flow percentile Q_{90}, (c, d) medium discharge Q_{50} and (e, f) high-flow percentile Q_{10} for the Upper Niger. 262

Figure S 15 Slopes of trends in (a, b) low-flow percentile Q_{90}, (c, d) medium discharge Q_{50} and (e, f) high-flow percentile Q_{10} for the Upper Yellow. 263

Figure S 16 Slopes of trends in (a, b) low-flow percentile Q_{90}, (c, d) medium discharge Q_{50} and (e, f) high-flow percentile Q_{10} for the Rhine. 264

Figure S 17 Mean monthly precipitation of corrected and uncorrected ISI-MIP climate models and 19 other CMIP-5 ESMs for the Niger basin. 266

Figure S 18 Mean monthly precipitation of corrected and uncorrected ISI-MIP climate models and 19 other CMIP-5 ESMs for the Upper Blue Nile basin. 267

Figure S 19 Mean monthly precipitation of corrected and uncorrected ISI-MIP climate models and 19 other CMIP-5 ESMs for the Ubangi basin. 268

Figure S 20 Mean monthly precipitation of corrected and uncorrected ISI-MIP climate models and 19 other CMIP-5 ESMs for the Limpopo basin.. 269

Figure S 21 Annual precipitation, mean temperature and mean short wave downwelling radiation for the Garbe-Kourou. 270

Figure S 22 Similar to Figure S 21 but for the Ibi subcatchment in the Benue Basin. 271

Figure S 23 Similar to Figure S 21 but for the Lower Niger Basin. 272

Figure S 24 Annual flow regimes on monthly basis for different parts using climate models input of the base period compared to reanalysis data which was used for calibration. 273

Figure S 25 Similar to Figure 7, but with outliers.. 274

LIST OF ABBREVIATIONS

Listed are abbreviations that are used in more than one Chapter.

AMAX	Annual maximum discharge
AMO	Atlantic Multidecadal Oscillation
CMIP5	Coupled Model Intercomparison Project Phase 5
CORDEX	Coordinated Regional Downscaling Experiment
ESM	Earth System Model
GCM	Global Circulation Model
GSWP3	Global Soil Wetness Project Phase 3
HDI	Human Development Index
IND	Inner Niger Delta
IPCC	Intergovernmental Panel on Climate Change
ITCZ	Intertropical Convergence Zone
LULC	Land use and land cover
NBA	Niger Basin Authority
NRB	Niger River Basin
NSE	Nash-Sutcliff efficiency
NSGEV	Non-stationary Generalized Extreme Value
PBIAS	Percent bias
PGFv2	Global Meteorological Forcing Dataset for land surface modeling of Princeton University version 2
RCM	Regional Climate Model
RCP	Representative Concentration Pathway
SWIM	Soil and Water Integrated Model
WAM	West African Monsoon
WFD	WATCH Forcing data ERA 40
WFDEI	WATCH Forcing data ERA interim

1. INTRODUCTION

1.1. Catastrophic flooding in the Niger River Basin

Annual floods are characteristic of rivers with a tropical pluvial regime (Pardé, 1963). In riverine societies living alongside this type of river, floods are traditionally perceived as positive and often they even carry religious connotations. This is commonplace for the Nile River in Africa, but it holds, to a smaller extent, also for the Niger River and its tributaries. The monsoon rainfalls and the related river floods are a fundamental part of local livelihoods in the Niger River Basin (NRB), providing freshwater and enabling agriculture, fisheries, transport, livestock and, in an increasingly important manner, also energy production. Occasionally, however, these river floods can turn into catastrophes, drowning people and washing away the homes and belongings of hundreds of thousands of persons living in the NRB. Such flooding has also destroyed world cultural heritage sites in Timbuktu, Mali (UNESCO, 2012).

Catastrophic flooding affects people and their livelihoods not only directly, but also in many indirect ways. Flooding impacts food security by washing away crops, killing livestock and spoiling stocks. In addition, floods contaminate water and deteriorate the hygienic and sanitary conditions of the area affected, causing an increasing risk of malaria, respiratory diseases, diarrhea, and even cholera (Hashizume et al., 2008; Shimi et al., 2013).

These adverse and catastrophic impacts of floods in the NRB have been increasingly observed in the recent decades. Practically every year during the rainy season, new catastrophic floods are reported, some of them of tremendous proportions. For eight of the last 15 years, for example, floods are reported to have affected more than 100,000 people, in 2009 and 2010 over 1 million and in 2012 over 10 million people.

The increasing flood risk can, however, not be simply attributed to an increase of flooding. Flood risk is understood as product of hazard, exposure and vulnerability (1) (IPCC, 2012; Kron, 2005; Merz, 2006)

$$Flood\ risk = Hazard * Exposure * Vulnerability \quad (1)$$

The pronounced vulnerability of developing riverine nations enhances the adverse effects of the hazard, which in turn hinders development. As indicator for exposure, the immense population growth in West Africa is also likely to contribute to the increase of people affected by floods. This context has to be taken into account when regarding the flood risk in the NRB.

The impacts of catastrophic flooding, however, are not limited to the specific regions directly affected. Commonly, extreme events do not lead to large-scale, permanent mass-migration of affected population (L. Perch-Nielsen et al., 2008), but in cases of a spiral of

environmental deteriorations like climatic pressure, land degradation and an increasing frequency of hazards including floods, the likelihood of environmentally-induced migration increases (Black et al., 2011; Renaud et al., 2011; Tschakert et al., 2010). Therefore, floods are also indirectly relevant in a larger-scale context, for example for other African countries or European migration policy.

Despite the awareness of environmental degradation and climatic deterioration as major factors for poverty and calamities in the region, the political and scientific recognition of catastrophic flooding as a relevant threat in the NRB is indeed growing but still remains low. In West Africa, the widespread "desertification narrative in which heavy rainfall events and flooding have no place" (Tschakert et al., 2010) is still dominant. Therefore, this thesis is intended to encourage greater awareness of catastrophic flooding, in addition to its main goal of contributing to the scientific debate on flood risk in the NRB.

1.2. State of research on flooding in the Niger River Basin

The first scientific approach to catastrophic flooding in the NRB was undertaken by Tarhule (2005), who focused on floods in the Sahelian parts of the basin. He referred to the catastrophic flooding as "the other Sahelian hazard", alluding to the fact, that droughts are commonly the primary natural disaster in West Africa. Subsequently, several studies described an increase in flooding over the last decade within the NRB or parts of it (Amogu et al., 2010; Descroix et al., 2012; Jury, 2013; Kundzewicz et al., 2013; Mahe et al., 2013; Oyerinde et al., 2014; Tschakert et al., 2010). A comprehensive overview on the existing literature on NRB flooding is provided in Chapter 2.1. The characteristics of flood risk changes have not yet been analyzed for the NRB.

Some studies point to an increasing vulnerability to flooding in the NRB as way to explain the increasing flood risk (Di Baldassarre et al., 2010; Mertz and Mbow, 2011; Tschakert et al., 2010). They suppose, however, as well, that this increasing vulnerability is most probably only one factor among others, namely increases in flood magnitude and/or frequency. Increased flood magnitudes in the NRB have, however, not been described or analyzed in detail. They have been vaguely associated to a general "return to wet conditions" (Jury, 2013) in West Africa. This increase in flood magnitudes is mostly attributed to two different drivers. On the one hand, human influence through land use and land cover (LULC) changes are related to increases in flood magnitude and/or frequency (Descroix et al., 2012; Mahe et al., 2013; Sighomnou et al., 2013). Sealed soils, crusting and deforestation increase direct runoff due to reduced infiltration, which in turn leads to a higher river runoff, even if the overall amount of water in the system decreases. On the other hand, a general change in the precipitation pattern can be observed during the past few decades (Lebel and Ali, 2009; Paeth et al., 2011a; Panthou et al., 2012, 2014).

Recently, Tarhule et al. (2015) analyzed hydroclimatic variability in the NRB between 1901 and 2006, finding a positive trend in precipitation and streamflow time series after

1969, and thus confirming the wetting trend. Findings of overall increasing precipitation and flood magnitudes, however, do not apply for the entire NRB. One remarkable feature of the positive discharge trends in the arid and semi-arid parts of the NRB is the so-called "Sahel Paradox", described first by Albergel (1987). Paradoxical refers to the fact that discharges are increasing despite decreasing rainfalls. This phenomenon has been attributed to adverse LULC change and crusting of soils, which leads to an increase of surface runoff, even though the climate in the region tends to become drier (Amogu et al., 2010; Descroix et al., 2012). Still, there is no study that systematically attributes the changes in the flood regime, taking into account climate and LULC changes.

With regard to future hydro-meteorological conditions for the NRB, several studies confirmed that temperature projections are robust and coherent, showing show a strong increase above those of average global warming levels. A meridional warming gradient is projected, with temperature increases at the end of the 21st century between approximately 2 °C – 3 °C at the coast in the South and 4 °C – 6 °C in the Sahel region in the North, depending on the emission scenario (Diallo and Sylla, 2012; Gbobaniyi et al., 2013; Sylla et al., 2013). For precipitation, projections are not coherent and model robustness is low. Projections show either increasing or decreasing trends with strong regional heterogeneities (Diallo et al., 2013; Druyan, 2011; Klutse et al., 2015; Nikulin et al., 2012; Paeth et al., 2011b; Vizy et al., 2013). The impact of climate change on vegetation is projected to be severe, and to shift climate zones to more arid conditions, mainly due to the temperature increase (Sylla et al., 2015; Yu et al., 2015).

Hydrological projections for the NRB exist mostly for parts of the basin (Kamga, 2001; Oguntunde and Abiodun, 2013; Okpara et al., 2009; Ruelland et al., 2012) or as part of global studies (Falloon and Betts, 2006; Manabe et al., 2009; Murray et al., 2012; van Vliet et al., 2013). Roudier et al. (2014) recently reviewed the existing literature and found high uncertainty amongst the models, with a tendency to rather increasing streamflow for the NRB. They identified mainly changes in precipitation as the main driver of the changes and, to a lesser extent, also evapotranspiration. However, with regard to flooding, they stated that they "[…] especially underline the lack of information concerning projections of future floods […]."

1.3. Research questions and strategy

A review of the existing literature on flooding in the NRB reveals several research deficits and open questions. Particularly in the face of the rapidly increasing adverse impacts of flooding in the NRB, it seems important to (1) understand the trends in flood risk and the role of the hazard, (2) identify the drivers for the changes in flood magnitudes, (3) project future flood regimes taking into account the drivers found before and (4) eventually identify further research needs and provide adaptation/mitigation options to reduce the flood risk in the NRB.

These gaps in the scientific research on catastrophic flooding in the NRB are the motivation for the present thesis. In order to assess flooding and its context, four explicit research questions (RQ) have been identified:

(1) What are the characteristics of the changes in flood risk?
(2) What are the drivers of the changes in the flood regime?
(3) What changes in the flood regime can be expected in the future, taking into account the identified drivers?
(4) How can the flood risk be reduced?

In order to answer these questions, a systematic research strategy has been developed (Figure 1). In a first step (RQ 1), the role of hazard for flood risk in the context of vulnerability and exposure is analyzed. In addition, changes in the hazard, i.e. the available discharge time series from gauging stations along the Niger River and its tributaries, are analyzed using state-of-the-art statistical methods with a focus on trends, correlations, changepoints, and variance (Chapters 2 and 3).

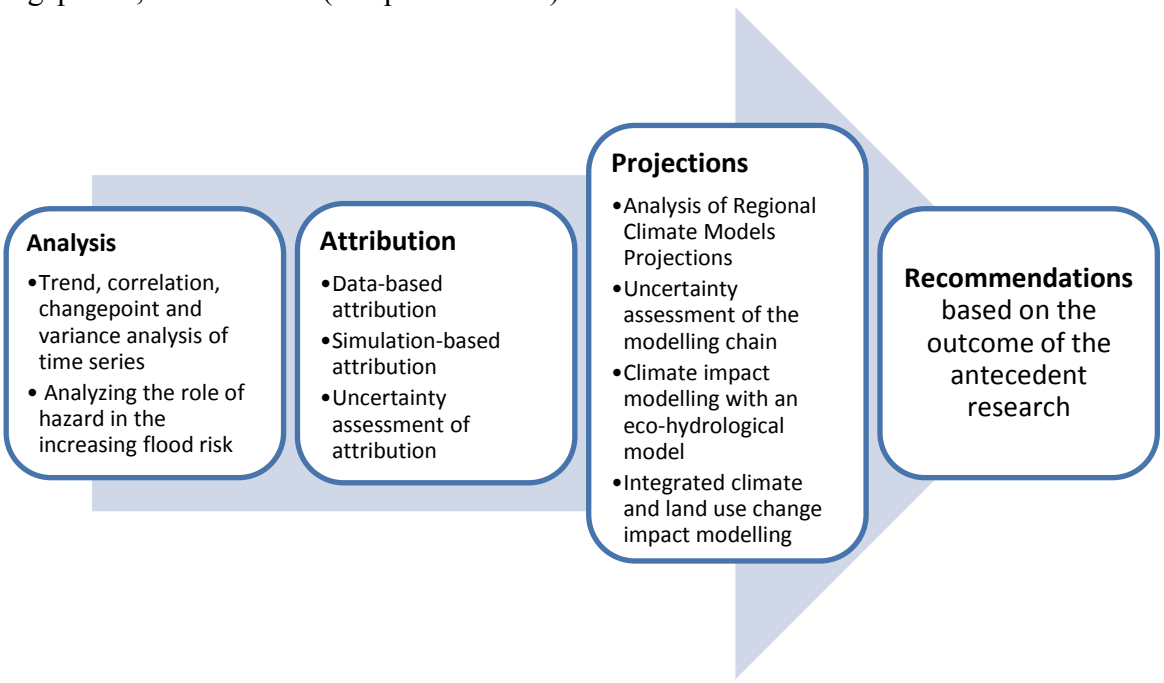

Figure 1 Research strategy for assessing catastrophic flooding in the Niger River Basin on the basis of the identified research questions.

In a second step (RQ 2) the causes for the changes in the flood regime are analyzed. Therefore a strategy proposed by Merz et al. (2012) is applied. It consists of both data-based and simulation-based methods within a hypothesis-testing framework in order to attribute changes in the flood regime to potential drivers. Both methods are applied to

identify the contribution of climate and LULC changes to variations in the flood regime in the NRB; moreover the uncertainty of the attribution is assessed (Chapter 3 and 4).

The third part (RQ 3) focuses on the future flood regime in the NRB. Therefore climate projections of statistically and regionally downscaled climate models are analyzed. Subsequently, impacts of climate change scenarios on the flood regime are projected applying the eco-hydrological Soil and Water Integrated Model (SWIM) in the NRB. The SWIM model has been selected due to the fact that it integrates all relevant eco-hydrological processes and has already been applied successfully in the NRB. In order to evaluate the different sources of uncertainty along the modelling chain, the uncertainty of each research step is assessed individually and eventually a systematic analysis of variance (ANOVA) is applied (Chapter 5). Finally scenarios of future LULC changes and future Climate Change are included in the modelling projections (chapter 6 and 7). LULC changes are, however, not adequately represented in the current version. Therefore, a dynamic LULC module is developed here for the SWIM and, amongst other adaptations, is included in the model code (see model description in Chapter 1.4). The results of the antecedent analyzes are the basis for comprehensive discussion and conclusion in Chapters 8.1 to 8.3.

RQ 4 relates to all references from the aforementioned research and also includes thoughts on a meta-level about the research context of floods in the NRB itself. This and all the individual conclusions for flood assessment are integrated into the recommendations given in Chapter 8.4. Finally, overall conclusions summarize the results (Chapter 8.5), and a short outlook on future assessments of catastrophic flooding in the NRB is provided (Chapter 8.6).

1.4. The eco-hydrological model SWIM

For the simulation-based attribution of the flood risk in the NRB and the climate and LULC change projections on the flood regime, the eco-hydrological model SWIM is applied. SWIM is a process-based and spatially semi-distributed model of intermediate complexity for river basins. It integrates hydrological processes and vegetation growth at the basin scale on a daily time step, integrating hydrological processes, vegetation growth, nutrient cycling, erosion and sediment transport (Figure 47). Hydrological processes are simulated in four main segments: (1) the soil surface, (2) the root zone of the soil, (3) the shallow aquifer, and (4) the deep aquifer. Represented processes include precipitation, surface runoff, evapotranspiration, subsurface runoff, and percolation. At the soil surface, the surface runoff is estimated as a non-linear function of precipitation and a retention coefficient. It depends on soil water content, land use, and soil type. The vegetation component is based on the Environmental Policy Integrated Climate (EPIC) approach (Williams et al., 1983) and includes arable crops and other general vegetation types (e.g. pasture, savannah, evergreen forest). The effects of vegetation on the hydrological

processes include a cover-specific retention coefficient, impacting surface runoff and influencing the amount of transpiration. Transpiration is simulated as a function of the potential evapotranspiration and leaf area index.

The hydrological processes of the shallow aquifer represented in the model are groundwater recharge, capillary rise to the soil profile, lateral flow, and percolation to the deep aquifer. Potential evapotranspiration is calculated using the Turc-Ivanov method (Wendling and Schellin, 1986). Actual evaporation from soil and transpiration by plants are simulated following Ritchie (1972). The model is described in more detail in the respective chapters and a comprehensive description of SWIM has recently been published by Krysanova et al. (2014).

Since the current model version of SWIM does not include all the relevant processes needed for answering the research questions, a LULC module and three other substantial improvements and enhancements have been developed and included, amongst smaller changes and adaptations.

(1) The dynamic land use change module modifies the land classes of SWIM at any frequency or given point in time, while keeping constant the instantaneous balance of water and other modelled fluxes during the change. This means that the number and areas of hydrotopes within a sub-basin can fluctuate: new hydrotopes can appear or existing ones may disappear. The LULC module has been used for the studies presented in Chapters 3 and 7 and is described in detail in the latter. The module is designed for further enhancement as a fully coupled eco-hydrological-LULC model.

(2) The climatological data which drives SWIM often lacks information on short wave downwelling radiation. This holds also for parts of the climate model data used for the NRB. Since this radiation parameter is crucial for calculating evapotranspiration, a method developed by Hargreaves and Samani (1982) has been adopted and implemented in SWIM. When genuine short wave downwelling radiation data is missing, the parameter can be calculated on the basis of information on maximum and minimum daily temperatures as well as on latitude.

(3) SWIM commonly uses the Muskingum method for calculating the routing of the water (McCarthy, 1938). Under certain circumstances, the formula becomes unstable and results in an oscillation of values or negative values. This effect has been corrected in the SWIM code using a solution proposed by Viessman et al. (1989).

(4) The Inner Niger Delta (IND) fundamentally alters the Niger River´s hydrograph by delaying the maximum runoff and smoothing the peak. In order to incorporate this effect into the model, Liersch et al. (2013) developed a process based inundation module which has been used for the study in Chapter 6. Since no detailed results for the IND have been necessary for the other studies, and furthermore considering that the process-based module is computationally relatively time-consuming, a simpler method has been included. It simulates the effect using the inflow-outflow relation, including storage and evapotranspiration over the flooded area as a power law modified from Zwarts (2010).

1.5. The Niger River Basin

"Egerou n-igereou", "river of rivers", is the original Tuareg name of the Niger River (Tarhule, 2006). This designation bears testimony to its importance and significance for the regional societies. The Niger River is the dominant geographic feature in West Africa, spreading over ten countries and an area of approximately 2.15 million km² (Figure 2). The geographic heterogeneity of the land it flows through ranges from arid deserts to moist mountain forests. Its location between the arid Sahara desert and the equator, however, results in the curious fact, that only approximately 59 % (1.27 million km²) of the area is actually contributing to the river´s discharge. Still, the Niger is vital for the agriculture, economy, and cultural identity of the riverine nation's societies. The following chapters provide a short overview of the current knowledge of the physical and human geography of the NRB, in order to illustrate the context, in which catastrophic flooding occurs in the region.

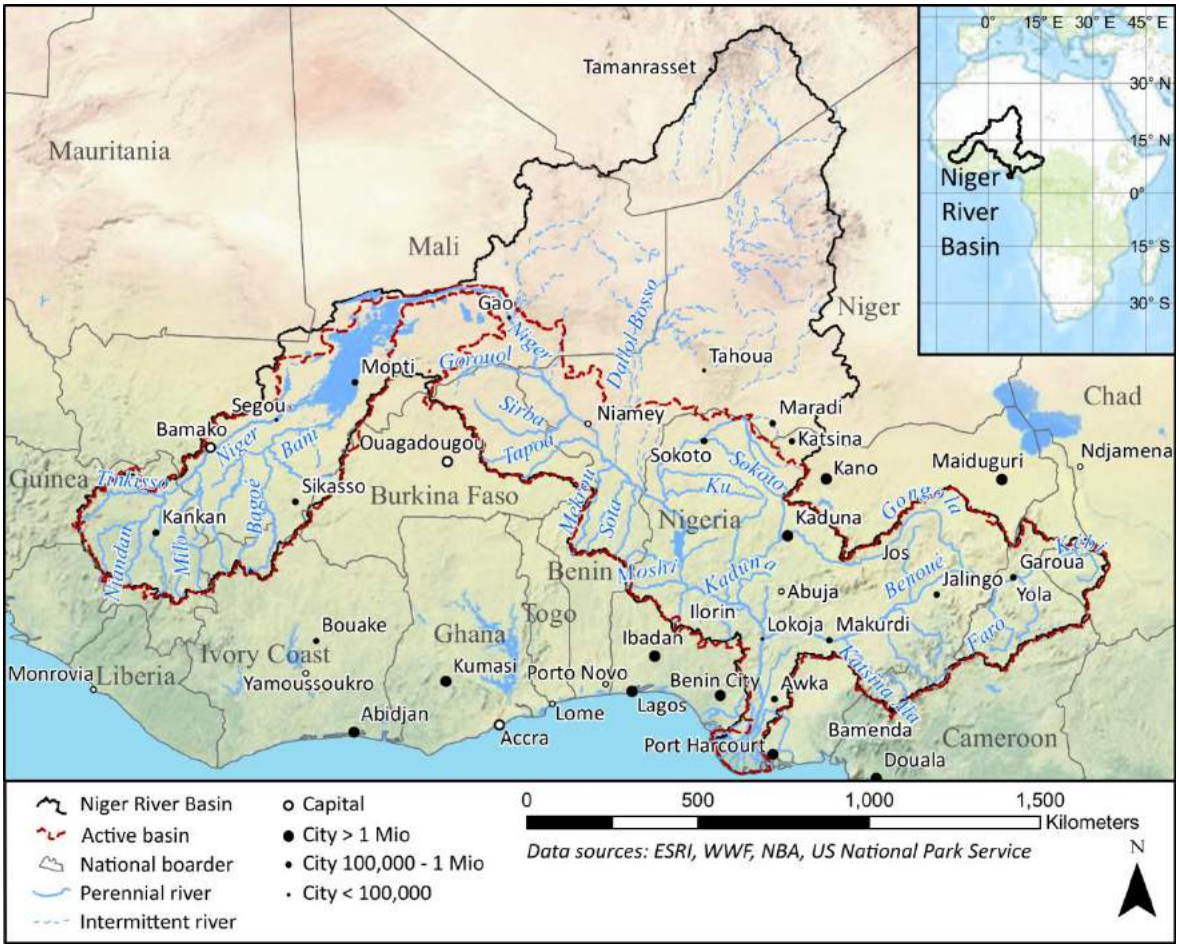

Figure 2 The Niger River Basin.

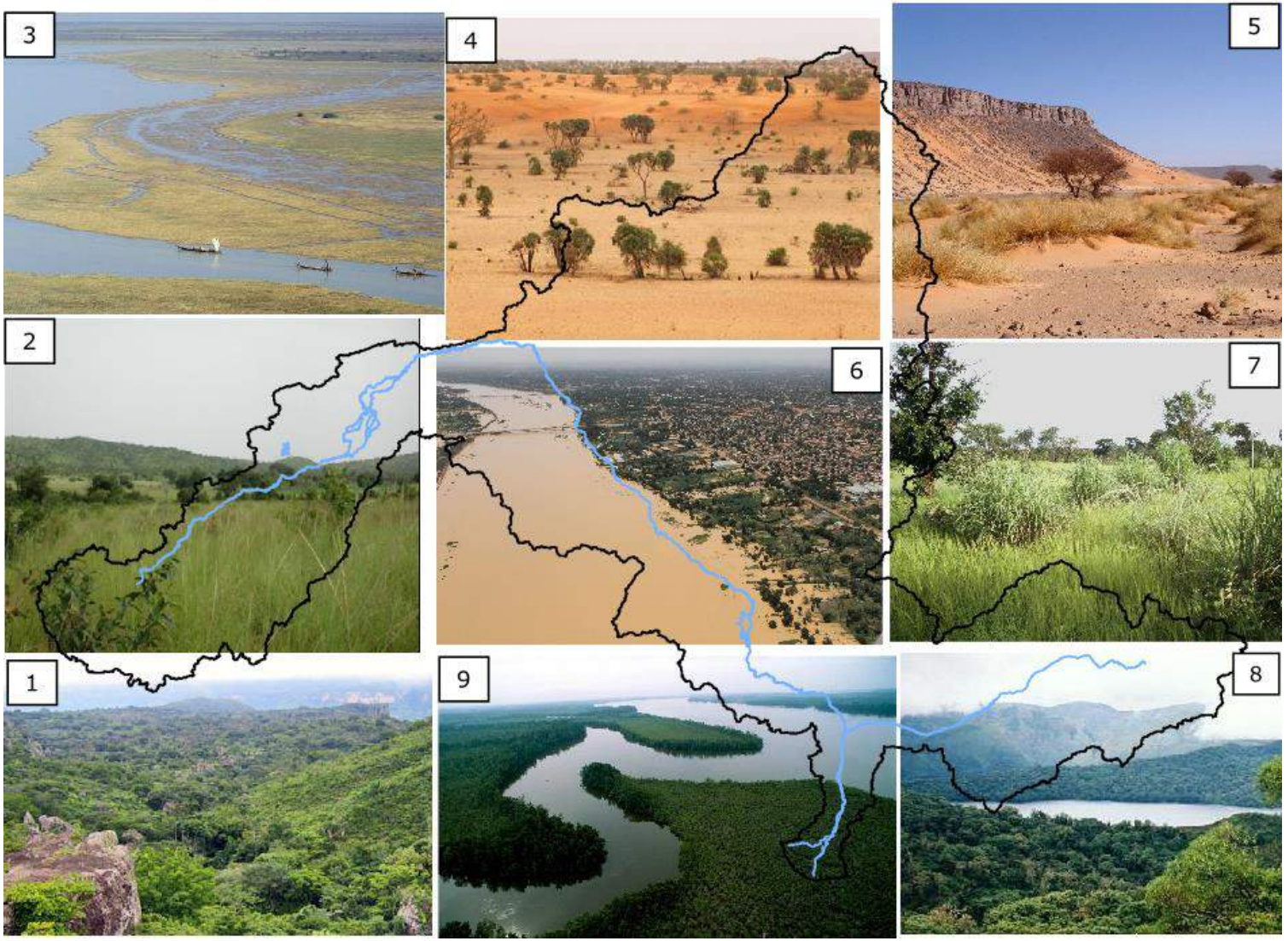

Figure 3 Regions of the Niger River Basin

1. Guinean Highlands *M. Tenidl, eoearth.org*
2. Sudanian Savannah *sudaniansavannas. blogspot.de*
3. Inner Niger Delta *L. Zwartz, wetwin.eu*
4. Acacia Savannah *english.egi.cas.cn*
5. Sahara desert *F. Devouard, wikimedia.org*
6. Flooded Niger River at Niamey *caritas.org*
7. Sudanian Savannah *M. Schmidt, wikimedia.org*
8. Cameroonian highland forest *M. Gawler, eoearth.org*
9. Niger Delta *G. Steinmetz, Science Photo*

1.5.1. History of the exploration of the Niger River Basin

Occidental written records of the Niger River go back to the first historian, Herodotus (484-425 B.C.). He described the geographical features of the Niger in his description of the Phoenicians and Carthaginian exploration voyages, albeit without mentioning the river´s name (Herodotus, Bk IV). The name "Niger" was first mentioned by the Roman writer Vitruvius Pollio around 10 B.C. Since then, many classical authors such as Ptolemy, Sueton, Pliny and Strabo and, later in the Mediaeval period, Leo Africanus and Ibn Battuta mentioned and described the river (Meek, 1960). But, even before the classical period, the NRB was home to human societies. A comprehensive overview on the history of cultures in the basin is given in Collins and Burns (2013). However, there are no local historical traditions derived from the region´s cultural history such as the Nok culture, and only archeological finds remain (Breunig, 2014; Collins and Burns, 2013). Therefore, the above-mentioned European and Arabic sources are the only references available for the classical and mediaeval periods. As of the 11th century, different empires have dominated the basin; during the 16th and 17th centuries trade with European nations along the coast of West Africa started to influence the local cultures (Andersen et al., 2005).

Interestingly, all reports from the first classics until the 19th century regard the Niger as a tributary of the Nile (Meek, 1960). Responsible for the long ignorance of the Niger River´s geography was presumably also its uncommon and curious course, running away from the sea into the Sahara desert at what is known as the Niger bend, where it turns towards the sea again and finally disembogues into the Gulf of Guinea.

The first to finally shed light on the course of the Niger River was Scottish explorer Mungo Park. He published his findings in the famous book "Travels in the Interior of Africa" in 1799 (Park, 1858), which was a bestseller and fueled the era´s enthusiasm for Africa (Lupton, 1979). Despite this great public interest, the support of the British Government and the efforts of countless expeditions (Gramont, 1991), it was not before 1947, that a French expedition succeeded in travelling the entire length of the river from the Guinean Highlands to its Delta (Rouch, 1954).

However, modern scientific exploration of Niger River Basin´s geography started mainly with the colonial interest of European Nations in the 19th century. A comprehensive overview of the Niger River´s history until the colonial times is provided by Gramont (1991). Ever since then, the basin has been the object of scientific explorations and surveys: in particular, continuous river discharge measurements have been performed since the very early 20th century (e.g. the daily discharge time series of Koulikoro, Mali, starts in 1907 and has almost no missing data until today (GRDC, 2013)). Unfortunately, the network of hydro-climatic measurements was not significantly extended, and even decreased in certain regions throughout the 20th and 21st centuries. This phenomenon can be explained, however, by the political and economic conditions prevailing during the post-colonial era. Regular monitoring and data availability are thus very limited, despite

their socio-economic significance. The availability of long-term satellite data and other modern techniques like climatic reanalysis may help to close these gaps. But, research is still limited by a lack of data, as was often experienced during the research for this dissertation.

1.5.2. Climate

The large-scale climate of the NRB is mainly determined by its location within the West African Monsoon (WAM) system, which is described in detail in Janicot et al. (2011). The movement of the Intertropical Convergence Zone (ITCZ), which essentially follows the maximum insolation between the Tropics of Capricorn and Cancer, causes the typical tropical seasonal cycle of dry and rainy seasons. The rise of the South Atlantic high-pressure (also called St. Helena High) in June toward the North and the related northbound movement of the ITCZ are associated with the beginning of the monsoon season in West Africa (Sun et al., 2010). Moist and relatively cool air masses move from the Atlantic Ocean in north-eastern direction towards the Sahara desert. Therefore the WAM is characterized by a distinct spatio-temporal meridional gradient, with precipitation amounts of up to 2000 mm from June until September at the coast and around 50-150 mm in July and August at its northern edges. As the ITCZ wanders back towards the equator, the high-pressure zone stays over the Sahara desert. The northeasterly trade wind, which is underlain by the southwestern monsoon winds during the rainy season, blows at the surface during the dry season from December to May, and is known as “Harmattan”. It blows dry and hot air from the Sahara to the coast, transporting fine dust and sand particles.

Compared to the Asian monsoon, the WAM has a very distinct, high interannual rainfall variability. These large variations are characteristic of West Africa and especially the Sahel region. Illustrative were the famines during the 1970s and 1980s, caused by droughts brought by a WAM that had been extremely week over several years (Janicot et al., 2011).

Due to the meridional gradient of the WAM, three to five different eco-climatic zones are commonly distinguished over West Africa, and the NRB has a share of each (Figure 4). They range from the arid North at the bend of the Niger (Saharan, < 150 mm/a), the semi-arid desert zone (Sahelian, 150-300 mm/a), the semi-arid tropical (Sudano-Sahelian 300 - 750 mm/a), and pure tropical zones (Sudanian/Sudanese 750-1200 mm/a) to the transitional tropical zone (Guinean, > 1200 mm/a). (The classification and names of the climate zones are modified following Andersen et al. (2005) and FAO (2004)). This classification is used throughout the entire dissertation unless noted otherwise. The mean annual temperature is highest in the Sahelian zone of the NRB between 28 °C and 30° C. In the other parts of the basin it ranges from 24° C to 28 °C (Figure 4). Due to the coastal effect, the temperature range has a meridional gradient, extending from an annual average

temperature range between 21 °C and 28 °C at the coast to distinctly larger variations between 12 °C and 29 °C in the North (Andersen et al., 2005).

The effect of global climate change on West Africa is subject to research and scientific debate, and is described comprehensively in Paeth (2005). Particularly the complexity of the WAM and its extremely large natural variability make it difficult to understand and project the characteristics of regional climate change and even the direction of trend signals, for example for precipitation, is highly uncertain (see Chapters 5, 6 and 7).

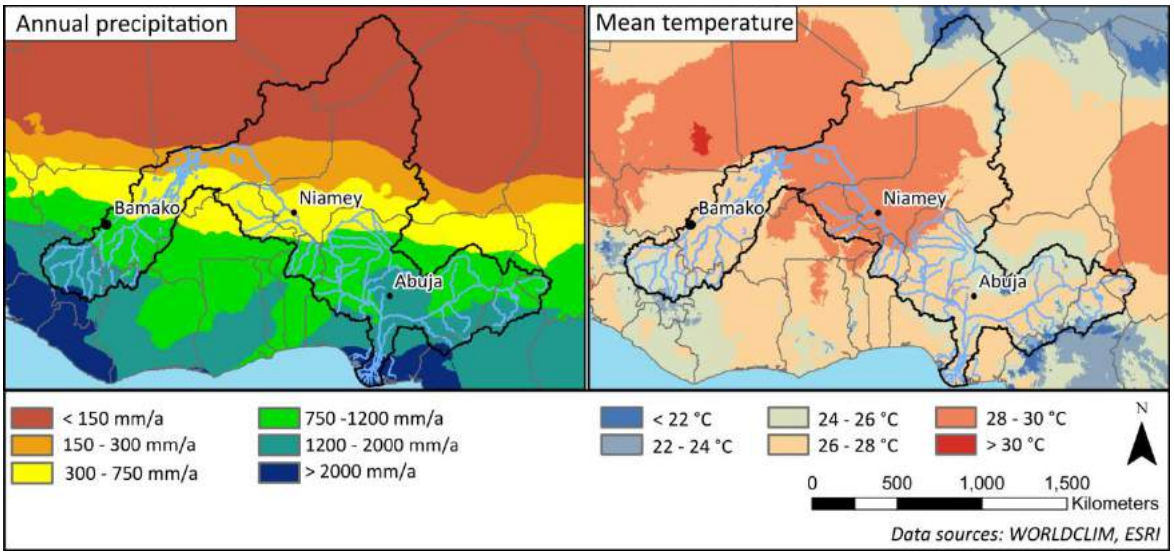

Figure 4 Annual precipitation and mean annual temperature in the Niger River Basin (1950-2000).

1.5.3. Hydrology

The flow regime differs within the active part of the NRB, and six main hydrographic regions are generally distinguished (Andersen et al., 2005; Ogilvie et al., 2010). The Upper Niger Basin is a typical tropical headwater with an extensive network of tributaries. Here, the annual Guinean flood occurs during the rainy season, whose flood peak is still noticeable in the Delta 4200 km downstream. However, in the shallow-sloped floodplains of the IND, the annual flood forms a huge marsh, which can in some years cover a surface of over 80,000 km². The section stretching from the IND to Lokoja (Nigeria) is the Middle Niger, which is again subdivided into left and right banks. The left bank reaches far to the north, and mainly the so-called Wadis, or dry river valleys, contribute episodically to the Niger. The right bank is a low-altitude plateau with periodic tributaries, amongst which the Sirba and Goroul Rivers have been the subject of detailed studies (see Chapter 4).

The Benue River is the major tributary, contributing more than the actual Niger River at the confluence. It originates from the Adamawa Plateau in Cameroon and has a length of 1200 km until Lokoja, where it enters the Niger. From Lokoja to the Delta, the river travels for another 200 km through a plane landscape with few, small tributaries. The Delta itself

covers around 30,000 km² and has over 30 outlets to the Gulf of Guinea. Although all sectors of the Niger seem to be prone to catastrophic flooding, there is a clustering of floods in the drier parts of the river basin (see Chapter 3 and Figure 6).

1.5.4. Geology, Hydrogeology and Soils

The basin is mainly located on the West Africa Craton, one of the five cratons that form the Precambrian basement of Africa (Wright et al., 1985). These mainly crystalline rocks make up the foundation of the basin in all parts that are not overlain with sediment deposits. These rocks are mainly impermeable and have very limited groundwater resources, predominantly in weathered zones (fractured aquifers) (Fontes et al., 1991). Still, there are vast groundwater aquifers in the NRB (intergranular aquifers), mainly in the tertiary, quaternary and recent deposits of the IND, the Lower Niger Basin and parts of the Benue valley (Wright et al., 1985). Withdrawal of groundwater is not systematically reported but is estimated to still be very low despite the high potential of groundwater resources (Jäger and Menge, 2012; World Water Assessment Programme (WWAP), 2009).

Since West Africa was not covered by glaciers during the glacial periods, soils are generally old and deep compared to European soils. Typical, tropical feralitic soils which result from chemical weathering dominate the basin. They usually have a high iron but low silica content and limited fertility. In West Africa, their depth varies commonly from 3 m to 10 m, but can also exceed this depth locally. With regard to hydrological characteristics, feralitic soils feature high porosity and permeability despite their relatively high clay content, due to micro-aggregates and bioturbation (Wiese, 1997). Also, typical of tropical soils are the hardened lateritic layers that result from ferrous oxides and can hinder or impede agriculture. Locally bleached layers of feralitic soils occur where water stands periodically, for example around the IND. In the flood context, LULC-induced changes in the soil are relevant. For example can compression of soils influence the generation of surface-runoff which again alters the flashiness of river regimes.

1.5.5. Vegetation

The Niger River flows through all vegetation zones of West Africa, ranging from arid deserts to evergreen forests (Figure 5) (Hogan, 2013). The strong meridional climatic gradient causes a distinct stratification of ecoregions, running mainly in the east-west direction. The headwaters of the Niger River are located in the Guinean Highlands, where montane forest grows as part of the Guinean forest-savanna mosaic (Figure 3/1). On its way to the IND, the river flows through the West Sudanian savanna composed of long grasses, shrubs, herbs and major trees (Figure 3/2). The IND itself is a major wetland dominated by grasses and aquatic plants (Figure 3/3). The northern part of the basin is dominated by Sahelian acacia savanna which consists mainly of deciduous bushland

(Figure 3/4). After the bend of the Niger on its way to the Delta, the Niger passes again through West Sudanian savanna (Figure 3/7) and Guinean forest-savanna mosaic. The Benue River shares also the savannah types the Niger flows through, with the addition of Cameroonian Highland forests (Figure 3/8) and Northern Congolian forest-savanna mosaic. The Delta of the Niger is subdivided into the upper coastal Delta, which is dominated by swamp forests and the lower coastal Delta with Central African mangroves (Figure 3/9).

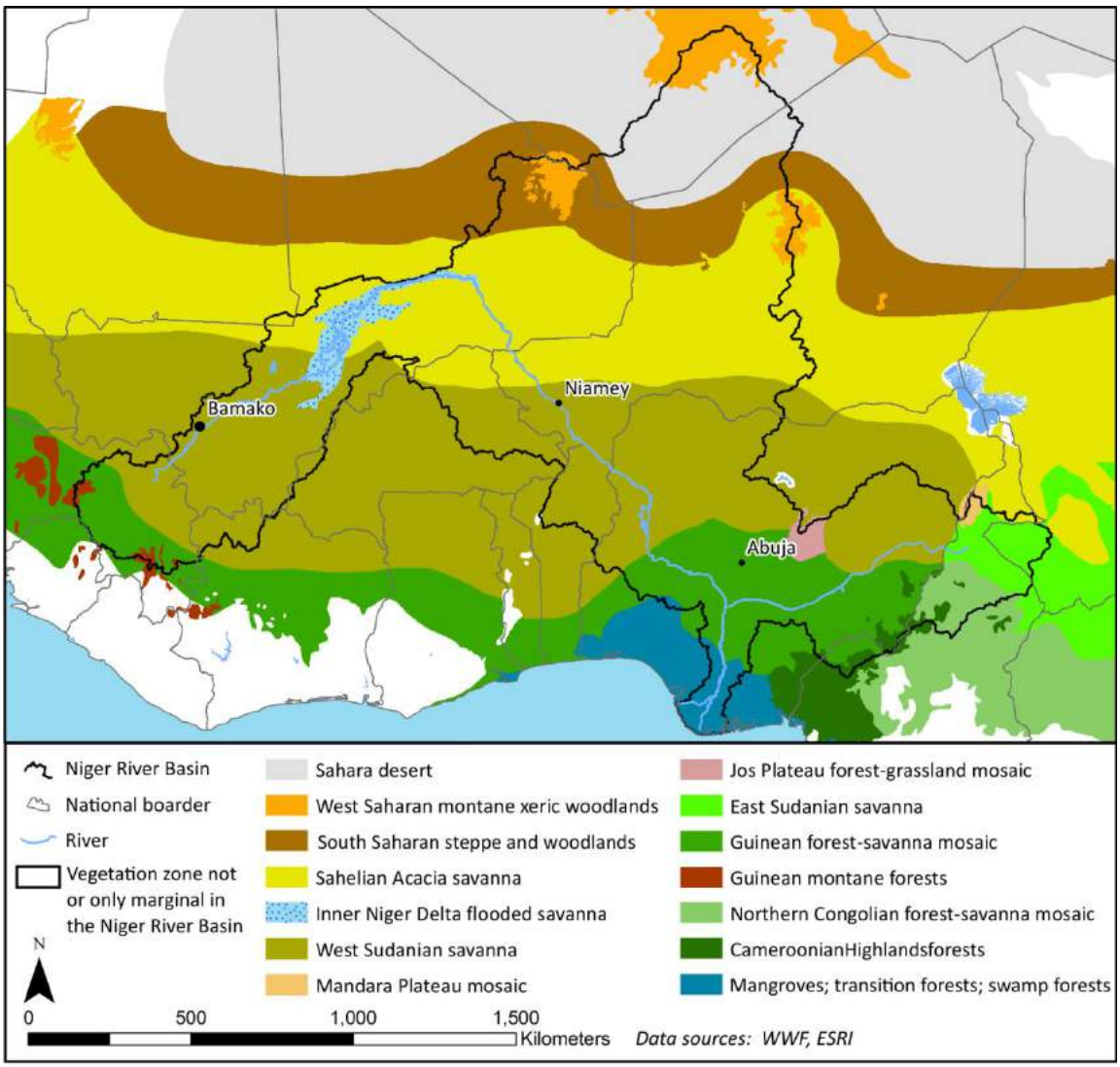

Figure 5 Vegetation zones of the Niger River Basin.

The semi-natural vegetation described here, has, however, been always subject to human intervention. Even though there are strong indications of a regreening of many parts of the Sahel and Sudano-Sahelian ecozones, many other areas are still degraded or undergoing degradation (Kaptué et al., 2015). In addition, the natural climatic variability has always challenged and altered the area´s vegetation and shifted vegetation zones.

Meanwhile, however, human intervention seems to be the most significant driver of vegetational changes which greatly influence discharge and, hence, floods (Chapter 7).

1.5.6. Agriculture and Socio-economics

Livelihoods in the NRB are mostly based on agriculture, usually for subsistence food production and cash sales. The main crops are yams, rice, sorghum, millet, maize and cassava, depending on the respective ecological zone (Ferguson, 1983). However, of the 2.5 million ha of arable land in the NRB, only approximately 20 % is actually exploited. Currently 85 % of the cultivation is rain fed; irrigation is increasing but still poorly developed (Ogilvie et al., 2010).

Similar to agriculture, the large hydropower potential of the NRB remains relatively untapped. Currently, there are five major reservoirs which are used to generate hydropower: Selingué (Mali), Kainji, Jebba, Shiroro (all three in Nigeria) and Lagdo (Cameroon). Additional reservoirs are planned and some are already under construction. The future strategy of the Niger Basin Authority (NBA) includes its member states joint investment in several hydropower plants that will feature 760 GWh installed capacity under the umbrella of the "Cooperation in International Waters in Africa" (CIWA) (Worldbank, 2014).

The Niger River itself has for a long time been the only supraregional way of exchange within the basin, and it is still used today for the transportation of people and goods. Of the approximately 4200 km covered by the river, most parts are navigable, and the stretch between Koulikoro (Mali) until the Delta, even admits larger boats during the rainy season.

1.5.7. Flood risk reduction measures

The high and growing numbers of people affected by floods in the NRB show that there is an existing lack of adaptation to the current flood risk. However, there are different existing measures and initiatives aimed at reducing the flood risk in the basin. The NBA, which was originally founded by the riverine states of the basin in order to jointly manage the water resources, also coordinates flood protection measures (Niger Basin Authority, 1980). The NBA has listed approximately 75 existing reservoirs for the whole basin (Niger Basin Authority and BRL, 2007) that can potentially be used for flood management. However, there are plans to build several new major dams and some are already under construction (Zwarts et al., 2005). Current efforts increasingly include integrated flood management at the local (e.g. Aletan et al., 2012) as well as the international level (e.g. GIZ, 2013).

A Flood Early Warning System for the NRB was agreed upon in 2011 by the Council of Ministers of the NBA and is partly implemented under the name "Forecasting Computer

System – SIP". Although, it seems not to be currently functional, there are initiatives to improve the system (Niger Basin Authority and GIZ, 2015).

The occurrence of more frequent flooding is often associated with decreasing vulnerability. This so-called "adaptation effect" is described by Baldassarre and Viglione (2015) and might in the future also help to reduce flood risk in the NRB, even under increasing flood magnitudes. However, given the large size of the basin and the frequent reports of catastrophic floods, the current initiatives to mitigate hazardous floods and increase resilience, still seem to be insufficient.

1.6. Overview of articles

The present dissertation comprises six different articles in Chapters 2 – 7, which follow the overall structure explained in chapter 1.3. The analyses for RQ 1 resulted in two research papers which form Chapters 2 and 3). The attribution of changes in the flood regime (RQ 2) is divided in a data-based approach which is part of the analysis research paper of chapter 3 and a simulation-based approach published separately and included in chapter 4. The projections for future flood regimes (RQ 3) are analyzed in three research articles. The first study treats the uncertainty of the modelling chain (Chapter 5), the second publication focuses on the impacts of climate change on the basin hydrology (Chapter 6) and the last article covers the impacts of climate and LULC scenarios on the flood regime (Chapter 7). All manuscripts except the one featured in Chapter 5 have been completely drafted by Valentin Aich, including all figures, tables and calculations unless otherwise noted below.

Chapter 2, Page 19:

Title: *Time series analysis of floods across the Niger River Basin*

Authors: Valentin Aich[1], Bakary Kone[2], Fred F. Hattermann[1] and Eva N. Müller

[1] Potsdam Institute for Climate Impact Research (PIK), Potsdam, Germany
[2] Wetlands International, Mali Office, Mopti, Mali
[3] Institute of Earth and Environmental Science, University of Potsdam, Potsdam, Germany

Journal:
Year and status: 2015, under review

Bakary Kone organized and provided discharge data from the NBA for this paper. The general idea and structure were discussed with Dr. Fred F. Hattermann and Dr. habil. Eva N. Müller, who also helped in shaping the text. The paper contains analyses also undertaken in the discussion article in Chapter 3. However, the general structure and all

parts beside the methodology and site description are completely new and independent of the discussion paper.

Chapter 3, Page 45:

Title: *Floods in the Niger Basin – Analysis and Attribution*

Authors: Valentin Aich [1], Bakary Kone [2], Fred F. Hattermann [1] and Eva N. Müller [3]

[1] Potsdam Institute for Climate Impact Research (PIK), Potsdam, Germany
[2] Wetlands International, Mali Office, Mopti, Mali
[3] Institute of Earth and Environmental Science, University of Potsdam, Potsdam, Germany

Journal: Natural Hazards and Earth System Sciences Discussion (Nat. Hazards Earth Syst. Sci. Discuss.)

Year and status: 2014, published as discussion paper

The data for this paper is similar to the previously mentioned, and was similarly provided by Bakary Kone. The general idea and structure were discussed with Dr. Fred F. Hattermann and Dr. habil. Eva N. Müller, who also contributed to shaping the text.

Since the paper has been published as discussion paper the first version has been revised including the recommendations of the discussion. Especially the approach used for the data-based attribution has been improved substantially, since it was the main subject of the discussions. Therefore, the relevant revised version is added in the appendix.

Chapter 4, Page 75:

Title: *Climate or Land Use? – Attribution of Changes in River Flooding in the Sahel Zone*

Authors: Valentin Aich [1], Stefan Liersch [1], Tobias Vetter [1], Jafet C.M. Andersson [2], Eva N. Müller [3] and Fred F. Hattermann [1]

[1] Potsdam Institute for Climate Impact Research (PIK), Potsdam, Germany
[2] Wetlands International, Mali Office, Mopti, Mali
[3] Institute of Earth and Environmental Science, University of Potsdam, Potsdam, Germany

Journal: Water (Water)

Year and status: 2015, published

Observed discharge was provided by Dr. Jafet C. M. Andersson. Dr. habil. Eva N. Müller helped to structure the article and all co-authors contributed to the final version of the manuscript.

Chapter 5, Page 111:

Title: *Multi-model Climate Impact Assessment and Intercomparison for three large-scale River Basins on three Continents*

Authors: Tobias Vetter [1], Shaochun Huang [1],Valentin Aich [1], Tao Yang [2], Xiaoyan Wang [2], Valentina Krysanova [1], and Fred F. Hattermann [1]

[1] Potsdam Institute for Climate Impact Research (PIK), Potsdam, Germany
[2] Hohai University, Nanjing, China

Journal: Earth System Dynamics (Earth Syst. Dynam.)
Year and status: 2015, published

For this paper, Valentin Aich contributed modelling results of the SWIM model for the NRB and helped to shape the text. All analysis, figures and tables as wells the draft were are the work of Tobias Vetter.

Chapter 6, Page 153:

Title: *Comparing Impacts of Climate Change on Streamflow in four large African River Basins*

Authors: Valentin Aich [1], Stefan Liersch [1], Tobias Vetter [1], Shaochun Huang [1,] Julia Tecklenburg [1], Peter Hoffmann [1], Hagen Koch [1], Samuel Fournet [1], Valentina Krysanova [1], Eva N. Müller [1] and Fred F. Hattermann [1]

[1] Potsdam Institute for Climate Impact Research (PIK), Potsdam, Germany
[2] Institute of Earth and Environmental Science, University of Potsdam, Potsdam, Germany

Journal: Hydrology and Earth System Sciences (Hydrol. Earth Syst. Sci.)
Year and status: 2014, published

Tobias Vetter, Julia Tecklenburg and Dr. Shaochun Huang provided modelling results from African catchments, namely the Oubangui, the Upper Blue Nile and the Limpopo Basins, respectivley. Peter Hoffmann contributed one figure (43), showing the mean temperature and precipitation trends for Africa. All co-authors contributed to the final text version of the manuscript.

Chapter 7, Page 193:

Title: *Flood Projections for the Niger River Basin considering future Land Use and Climate Change*

Authors: Valentin Aich [1], Stefan Liersch [1], Tobias Vetter [1], Samuel Fournet [1], Jafet C.M. Andersson [2], Sandro Calmanti [3], Frank H.A. van Weert [4], Fred F. Hattermann [1], Eva N. Müller [5]

[1] Potsdam Institute for Climate Impact Research (PIK), Potsdam, Germany
[2] Swedish Meteorological and Hydrological Institute (SMHI), Norrköping, Sweden
[3] Italian National Agency for New Technologies, Energy and Sustainable Economic Development (ENEA), Roma , Italy
[4] Wetlands International (WI), Wageningen, The Netherlands
[5] Institute of Earth and Environmental Science, University of Potsdam, Potsdam, Germany

Journal: Science of the Total Environment (Sc. Total Environ.)
Year and status: 2015, under review

Dr. habil. Eva N. Müller helped to structure the article and all co-authors contributed to the final version of the manuscript.

2. TIME SERIES ANALYSIS OF FLOODS ACROSS THE NIGER RIVER BASIN

Valentin Aich [1,*], Bakary Kone [2], Fred F. Hattermann [1] and Eva N. Müller [3]

[1] Potsdam Institute for Climate Impact Research (PIK), Potsdam, Germany
[2] Wetlands International, Mali Office, Mopti, Mali
[3] Institute of Earth and Environmental Science, University of Potsdam, Potsdam, Germany

* Corresponding author: Valentin Aich

Journal: Hydrological Sciences Journal (Hydrolog. Sci. J.)
Status: Submitted

Abstract: This study analyses the increasing number of catastrophic floods in the Niger River Basin, focusing on the relation between long term hydro-climatic variability and flood risk over the last 40 to 100 years. Time series for three subregions (Guinean, Sahelian, Benue) show a general consistency between the annual maximum discharge (AMAX) and climatic decadal patterns in West Africa regarding both trends and major changepoints. Variance analysis reveal rather stable AMAX distributions except for the Sahelian region, implying that the changes in flood behavior differ within the basin and affect mostly the dry Sahelian region. The timing of the floods within the year has changed only downstream of the Inner Niger Delta due to retention processes. The results of the hydro-climatic analysis generally correspond to the presented damage statistics on people affected by catastrophic floods. The damage statistics shows positive trends for the entire basin since the beginning in the 1980s, with the most extreme increase in the Middle Niger.

Keywords: Niger River Basin, Floods, Flood risk, Climate Change

2.1. Introduction

In the last two decades, the occurrence of extensive catastrophic flooding has increased drastically in the Niger River Basin (NRB) (Amogu et al., 2010a; Descroix et al., 2012; Mahe et al., 2013; Panthou et al., 2014). Kundzewicz et al. (2013) set the regional flooding, also for Africa, in a global perspective, mentioning that losses have increased greatly globally and regional assessments are needed. However, little research is currently being conducted for the NRB on the factors contributing to flood risk and the associated flood damages. Tarhule (2005) addressed the catastrophic flooding in the Sahel for the first time scientifically, calling the floods "the other Sahelian hazard", alluding to the lesser significance of catastrophic floods in the face of the dominant water scarcity in the region. Since then, several studies have contributed to the discussion from different perspectives studying either climatic or hydrological time series or both.

Paeth et al. (2011) looked at the meteorological patterns that led to the extreme flooding of 2007 and connected it to a La Niña event. Panthou et al. (2014, 2012), Ozer et al. (2009) and Lebel and Ali (2009) detected changes in rainfall patterns in the region. Okpara et al. (2013) analyzed general rainfall discharge patterns, however without considering data after 2002. The studies of Panthou et al. (2014, 2012) analyzed changes in rainfall and heavy rainfall, concluding that there has been a recent increase in heavy precipitation. Jury (2013) analyzed streamflow trends in Africa, including one station in the NRB (Niamey), and found an increase in streamflow that matched their general finding of a "return to wet conditions" in Africa in recent decades. Tarhule et al. (2015) analyzed the hydroclimatic variability between 1901 and 2006 in the NRB, and found a general changepoint in the year 1969, after which both rainfall and streamflow timeseries show a positive trend in the NRB, confirming the wetting trend. Descroix et al. (2012, 2011) examined increasing river discharges in the NRB and came to the conclusion that adverse land-use change and crusting of soils have led to an increase in flooding as the climate in the region tends to become drier. Using modelling approaches, Aich et al., (2015) and Séguis et al. (2004) also found a strong influence of land use change effects on the flood trends in the region. Sighomnou et al. (2013) backs up their findings and attributed the extreme flooding of 2012 to the aforementioned changes in land use and crusting for the region around Niamey. Descroix et al. (2009) and Amogu et al. (2010) also addressed this phenomenon, finding an increasing trend for streamflow of rivers in the Sahelian zone.

Whilst mean discharges have been evaluated extensively, the role of climatic variability for high or extreme flows and the increased flood risk in the NRB has not been systematically addressed yet; neither has the associated impact on people been systematically collected and quantitatively evaluated. This study aims to contribute to this discussion with a comprehensive analysis of the hydroclimatic attributes and trends of catastrophic floodings and the associated impacts on the local population in the NRB. The specific objectives were a) to analyze time series of rainfall and annual maximum

discharge (AMAX) to assess changes and trends over the last 40 to 100 years using changepoint and variance analysis methods, b) to detect changes in the timing of annual flood peaks, and c) to assess and relate damage statistics on the impacts of floods to the results of this flood analysis.

In order to take the regional heterogeneity of the NRB into account, we differentiate between a Guinean, a Sahelian and the Benue subcatchment according to their main source areas and data availability Figure 6. Specific emphasis is put on the Sahelian sub-catchment in the Middle Niger, where two annual flood peaks occur (generally called the Guinean and Sahelian floods). The results are then discussed with a holistic view of the increasing flood risk, taking into account the changes in the hydroclimatic hazards, and vulnerability and exposure.

2.2. Niger River Basin

The NRB covers a total area of approximately 2,156,000 km², of which only approximately 1,270,000 km² contribute to the river discharge (Figure 6) (Ogilvie et al., 2010). The whole basin is spread over the territory of ten countries: Guinea, Côte d´Ivoire, Mali, Burkina Faso, Algeria, Benin, Niger, Chad, Cameroon and Nigeria (Zwarts et al., 2005). It extends over different agro-climatic and hydrographic regions with individual topographic and drainage characteristics. The Niger runoff regime is affected by different types of reoccurring floods, which result from the geographic locations and characteristics of their main source areas. The first one is the Guinean Flood, which originates from the headwaters of the Niger in the low-altitude plateaus known as the Guinean highlands during the rainy season between July and November. From here, the Niger and Bani Rivers flow into the Inner Niger Delta (IND). This vast wetland covers an area of approximately 36.000 km² in central Mali and comprises lakes and floodplains that are regularly flooded with large annual variations. It influences the hydrological regime of the Niger significantly by flattening and slowing down the peak of the annual flood (Liersch et al., 2013; Zwarts, 2010).

Most of the inflow in the middle section of the NRB comes from the plateaus of the right-bank subbasins. The vast subbasins to the left reach up into the central Sahara but only contribute a minor amount of inflow, and local tributaries are endorheic most of the time (Amogu et al., 2010a). The annual peak during the rainy season (July to November) in the mid-section of the Niger downstream of the IND is called the “Red Flood” or “Sahelian Flood”, the latter of which will be used in this study for the second subregion (For the definition of the region please see Descroix et al., 2012). The third flood we focus on here is the flooding of the Benue River, which flows into the Niger at the Nigerian city of Lokoja. Coming from a high-altitude plateau, it is the largest tributary in terms of discharge and surpasses the Niger by about one-third at the confluence near Lokoja. This part of the NRB will henceforth be referred to as “Benue”. Finally, the Niger flows into the

Gulf of Guinea, forming the Niger Delta, a flat region characterized by swamps and lagoons (Andersen et al., 2005a). As no discharge data were available for the region between Yidere Bode and the confluence of the Benue, nor for the part after the confluence, these parts are not included in the analysis.

The population density in the NRB ranges from less than one person per km² in the deserts of the North to over 1,000 in rural areas in Nigeria and Mali (Figure 6) (FAO GEONETWORK, 2015). Of the three regions on which this study focuses, Benue is the most densely populated, with many regions containing over 100 persons per km². Also in the areas along the Niger River, however, many regions in the Upper NRB and the Middle Niger have similar population densities. The population growth rate in the countries of the NRB is extreme, ranging from 2% to 3.5% with the highest increases in the Sahelian countries of Mali and Niger (Central Intelligence Agency, 2013).

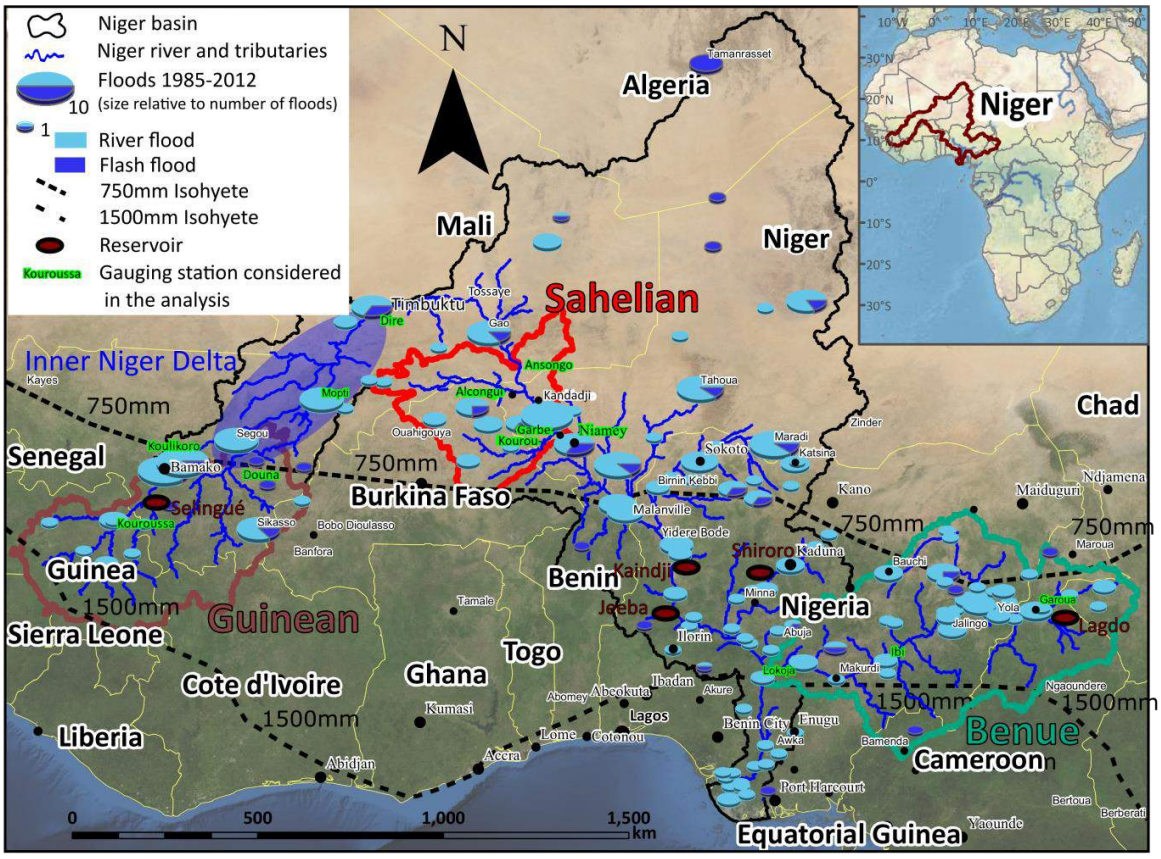

Figure 6 Niger River Basin: Source areas of floods in the Guinean, Sahelian and Benue regions, location and number of catastrophic floods plotted as blue pies, discharge gauging stations used for analysis are marked in green and reservoirs as red ovals.

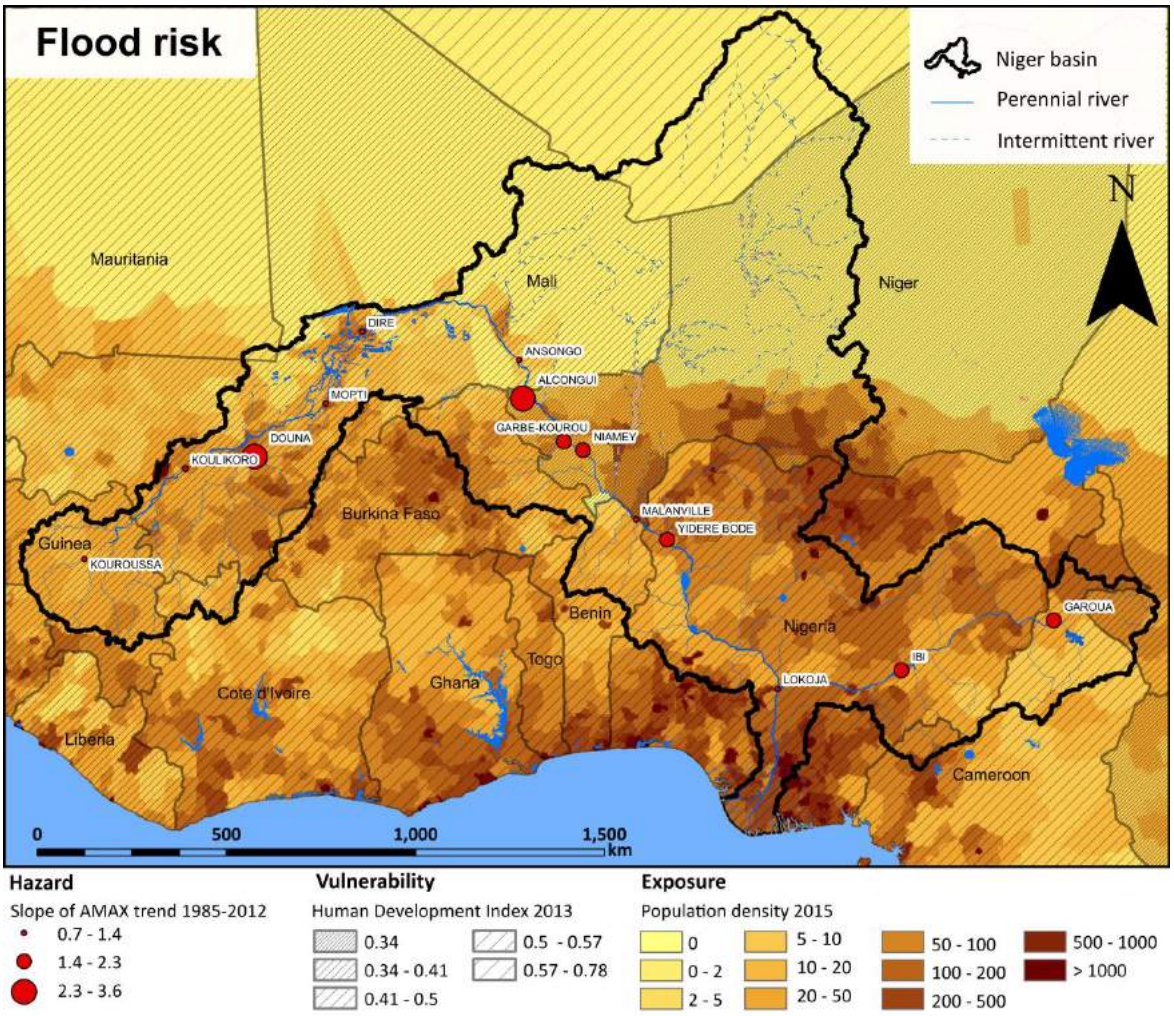

Figure 7 Flood risk in the Niger River Basin as result of hazard (AMAX trend for gauging stations 1985-2012), exposure (population density 2015), and vulnerability Human Development Index 2013).

2.3. Methodology

2.3.1. Data

2.3.1.1. Discharge, precipitation data and Atlantic Multidecadal Oscillation data

Observed river discharge at a daily resolution was provided by the Global Runoff Data Centre (Fekete et al., 1999) and the NRB Authority. In stations where the flood peak originating from the Guinean flood occurred after the 31st of December, the value was attributed to the previous year. The annual maximum discharge (AMAX) value of a certain year was only used if it was the overall change point of the annual hydrograph and if we could reasonably eliminate the possibility that any missing values might have been higher. Missing values were ignored for the analysis. Peaks for the Guinean and Sahelian floods occur at the Ansongo and Niamey stations. The flood originating in the Guinean highlands

experiences its peak before it enters the IND, usually around October. Due to the increasing distance and the buffering/retention effect of the wetlands, the flood peak leaves the IND with a delay of approximately three months. Therefore, it arrives in the middle section of the Niger around January, although rainfall in the Sahelian region falls at the same time as in the Guinean highlands. Thus, here the Guinean and Sahelian regimes generate a flood which can usually be clearly distinguished (an example is shown for the Niger at Niamey in Figure 8). The Sahelian peaks are limited to August through October and do not occur every year. Therefore, the AMAX time series for the Sahelian flood at these gauging stations along the Niger River have gaps for years where a separate peak could not be distinguished. Due to these gaps, the time series cannot be analyzed statistically. Therefore, two gauging stations at Sahelian tributaries to the Niger River, which are not influenced by the Guinean flood and therefore have no gaps, were used for statistical analysis. The Alcongui station at the Gouroul River and the Garbe-Kourou station at the Sirba River (Figure 6) were not available in their entirety from GRDC data, and the missing years have been read-out from hydrographs which are available from the "Nigerhycos" (Niger Basin Authority, 2014).

To analyze precipitation in the regions, we used reanalysis data from the WATCH Forcing data ERA 40 (WFD) (Weedon et al., 2011) for the period from 1960 to 2001 and the WATCH Forcing data ERA interim, which is processed similarly on the ERA 40 reanalysis data set for the period from 1979 to 2012 (WFDEI) (Weedon et al., 2014). The precipitation parameter of both data sets is sampled on a 0.5 ×0.5 grid. For the analysis of the means, only the months during the rainy season (June-November) within the different subregions have been included (Figure 6). For the analysis of heavy precipitation, we derived the 95^{th} percentile of the daily precipitation for each year. Both parameters of the reanalysis time series of WFD and WFDEI were validated with observed rainfall data from stations in all subregions (Bamako in Mali, Gao in Mali, Niamey in Niger, Maradi in Niger, and Garoua in Cameroon, Figure 6). The reanalysis data was interpolated via the Inverse Distance Weighting method to the location of the stations, and it shows good performance with regard to annual and heavy precipitation (Figure S 1, Supplementary material).

The Atlantic Multidecadal Oscillation (AMO) is a mode of variability occurring in the northern Atlantic Ocean and is derived from sea surface temperatures (Dijkstra et al., 2006). It is closely connected to the rainfall in West Africa (Knight et al., 2006; Nicholson et al., 2000). The data on the AMO is provided by the National Oceanic and Atmospheric Administration (NOAA) in an unsmoothed version (Enfield et al., 2001) which is based on the Kaplan Extended Sea Surface Temperature dataset.

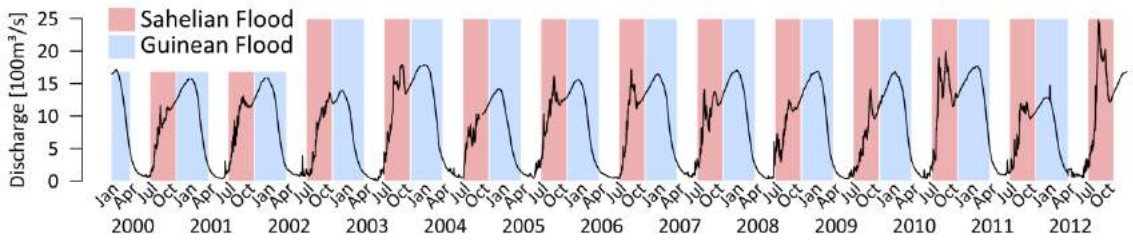

Figure 8 Hydrograph of the Niamey gauging station with Sahelian flooding (red) and Guinean flooding (blue) for the period from 2003 to 2012.

2.3.1.2. Data on people affected by floods

Data on people affected by catastrophic flooding were derived from three different sources: the NatCatService of the Munich Reinsurance Company (MunichRe, 2015), the EM-disaster database of the University of Leuven, Brussels (EM-DAT, 2015) and the Global Active Archive of Large Flood Events of the Darthmouth flood observatory (Brakenridge, 2015). All data are based on media reviews of the respective organization and the collection of data from official sources. The latter archive derives additional information from remote sensing data. Only the period from 1980 to 2012 is considered for the analysis, since only for this period climatic reanalysis are available. All three sources provide additional information on whether the flood was a flash or river flood. The EM-disaster database distinguishes between "general river flood" and "flash flood", the NatCatService and the dataset of the Darthmouth flood observatory between "flood" and "flash flood". None of them are specific about the exact definition of flash flooding. Since the majority of the information is derived from the media, the discrimination between flood types is most probably not homogeneous; however, the rough differentiation is assumed to be correct. The data for West Africa is not systematically and uniformly collected. Some reports are on the village level, others on the regional or even national level. The numbers for the whole NRB or the individual regions have been summed up from the provincial or village level. For the Sahelian zone, most of the data was grouped and could not be distinguished from other regions in the Middle Niger. Therefore, the data also comprises the people affected for the whole Middle Niger until Yideré Bodé (Figure 6). Since most of the reports come from the media, the numbers reported are not verifiable and often differ substantially between sources. Another open question concerns a bias in media coverage, which might have increased during the last decades and could result in an increasing number of flood reports. This issue has been analyzed by Tarhule (2005) for the region around Niamey by comparing flood reports in the media with rainfall data. The conclusion of the study is that the quality of the environmental reporting of the newspapers is reasonable for the Niamey region from 1970 to 2000, allowing some confidence on data consistency over the last decades. Another aspect of the media coverage bias is the better coverage of urban areas compared to rural areas. However, as we do not analyze the spatial distribution of the flooding on the subregional scale, this bias does not affect the analyses

directly. In sum, the datasets of people affected by floods are uncertain and should be interpreted with caution. Still, they are the best available source for damage data on catastrophic floods in West Africa, and even though their absolute numbers might be uncertain, the general trend of the combined three data sets are assumed to be reliable.

Data on population density was derived from the latest estimation of the Food and Agriculture Organization (FAO GEONETWORK, 2015) and data for the Human Development Index on country level as indicator for vulnerability was derived from the latest Human Development Index ranking of the United Nations for 2013 (Malik, 2014).

2.3.2. Statistics

In order to visualize tendencies in the data more clearly, the local regression-fitting technique LOESS was used (Cleveland and Devlin, 1988). It is a nonparametric regression method that combines multiple regression models in a k-nearest-neighbor-based meta-model. When plotted, it generates a smooth curve through a set of data points (LOESS Curve).

For analyzing the relation between time series, Spearman's rank correlation was applied. This is a nonparametric measure of the statistical dependence between two variables and is widely used to assess monotonic relationships.

Monotonic linear trends in the precipitation, discharge and damage data were identified using the Mann-Kendall test (Mann, 1945). This is a robust nonparametric test in which each element is compared with its successors and ranked as larger, equal or smaller. On this basis, it is possible to test the statistical significance of rejecting the null hypothesis (for all tests $\alpha = 0.05$). The linear trend was estimated using the Theil-Sen approach (Sen, 1968; Theil, 1950). Since serial independence is a requirement of the Mann-Kendall test, we checked beforehand for autocorrelations in all precipitation and hydrologic time series using the Durbin-Watson statistic test (Durbin and Watson, 1950, 1951). If an autocorrelation of the first order was found, trend-free pre-whitening was applied according to the method proposed by Yue et al. (2002): First, the trend estimated with the Theil-Sen approach was removed from the time series. Then, the first-order autocorrelation coefficient was calculated and subtracted from the time series. Finally, the trend was added back to the autocorrelation data and the Mann-Kendall test was applied in order to test for its significance.

2.3.2.1. Changepoint identification

Since the West African climate is strongly dominated by a decadal pattern (e.g. Nicholson et al., 2000; Sarr et al., 2013), changepoints are identified in order to see whether the AMAX follows this decadal pattern as well. The resulting changepoints are eventually compared with the periods of Atlantic Multidecadal Oscillation (AMO). For changepoint analysis, the cumulative sums method (CUSUM) given by Page (1954) is a

common approach. Combined with an algorithm to minimize the cost function (1), it is able to detect multiple changepoints (Killick et al., 2012):

$$\sum_{i=1}^{m+1} [C(Y(t_{i-1}+1):t_i)] + \beta f(m) \quad (2)$$

C is the cost function of the time series segment $Y(t_{i-1}+1):t_i$ and $\beta f(m)$ and is the penalty function. The cost function relates to the cost of segmentation. Different algorithms exist to minimize this function, and for this study the Segmented Neighborhood (SN) method of Auger and Lawrence (1989) is appropriate because it is an exact approach and the datasets are relatively small so that the generally high computational cost of this method is acceptable. The cost functions for all possible segments are iteratively calculated. By that means, SN is able to compute the segments; however, it does not provide information about the number of segments which would be identical with the number of observations without restrictions. In order to prevent this overfitting, the penalty function was introduced. In this study, we used Akaike's Information Criterion (AIC) (Akaike, 1974)

$$AIC = 2k - 2\ln(L) \quad (3)$$

where k is the number of parameters in the model and L is the maximized value of the likelihood function.

2.3.2.2. Non-stationary Generalized Extreme value distribution

In order to detect non-linear and non-stationary trends in the AMAX time series, non-stationary Generalized Extreme value models (NSGEV) (Coles et al., 2001) have been used. This method has proven to be an effective tool, not only to detect trends in the flood average, but also in flood variability (e.g. Delgado et al., 2010; Hundecha et al., 2008). The method is described in detail by Delgado et al. (2010) and is based on the generalized extreme value function (GEV), which is cumulatively written as:

$$F(x) = \begin{cases} exp\left[-\left(1-\frac{\xi}{\sigma}(x-\mu)\right)^{\frac{1}{\xi}}\right] \; if \; \xi \neq 0 \\ exp\left[-exp\left(-\frac{x-\mu}{\sigma}\right)\right] \; if \; \xi = 0 \end{cases} \quad (4)$$

with μ as the location parameter, σ as the scale parameter and ξ as the shape parameter. This cumulative distribution is then fitted systematically with different combinations of linear, second- and third-degree time-dependent parameters, but only for the location and scale parameters. These time-dependent parameters were then inserted in a maximum likelihood function.

$$L = \prod_{t=1}^{n} \sigma(t)^{-1} \, exp\left[-\left(1 - \xi\frac{x(t) - \mu(t)}{\sigma(t)}\right)\right] \quad (5)$$

Instead of the different parameters, the linear, second- or third-degree terms were inserted in the likelihood function. In order to identify the parameter setting which best fits with the data, a likelihood deviance statistic was applied. By this means, it could be tested whether the model of higher complexity from stationary to third-degree is an improvement, and whether this improvement is not just obtained by chance but is instead significant. So, each model M_1 was tested against the simpler model M_0. The deviance statistic of the models $M_0 \subset M_1$ is defined as

$$D = 2\{\ell_1(M_1) - \ell_0(M_0)\} \quad (6)$$

where $\ell_1(M_1)$ and $\ell_0(M_0)$ are the maximized log-likelihoods for the models. The distribution D is asymptotic, and its degree of fit can be tested with a Chi-square test (χ_k^2). The degrees of freedom k express the difference in dimensionality between M_0 and M_1. So, larger values of D suggest that model M_1 explains the variation in the data better than M_0 and is therewith accepted as the NSGEV distribution. Since an analysis of the mean for all stations in one subregion might balance out changes in the frequency, the most complete time series for each subregion was selected for the trend detection. For the Guinean region, Kouroussa was selected because the flow is not influenced by the IND. For the Benue region, no time series was long enough for the analysis. In order to avoid the complex distributions of the whole time series that change their directions several times, the analysis was limited to the period after the changepoint around 1970 which was identified by the changepoint analysis in all regions.

2.3.2.3. Wavelet analysis of annual maximum discharge time series

To detect changes in the frequency of AMAX, we applied a wavelet power spectrum (Torrence and Compo, 1998) This can be described as a correlation coefficient between a dataset and a given function. This function slides over the dataset and is scaled to account for different frequencies. In our case, we used the Morlet function, a complex nonorthogonal function which is commonly used for hydrographical time series (e.g. Delgado et al., 2010) The wavelet analysis is a powerful tool used to show changes in the frequency over time, and indicates whether trends exist in the variance of the time series.

2.4. Results

2.4.1. Analysis of long-term dynamics of rainfall and annual flood peaks

2.4.1.1. Analysis of trends of rainfall and annual flood peaks

Figure 9 shows a significant increase of annual precipitation, heavy precipitation and the annual maximum discharge (AMAX) for the time period 1979-2012 averaged over all available stations from the three investigated regions of the NRB (Guinean, Sahelian and Benue).

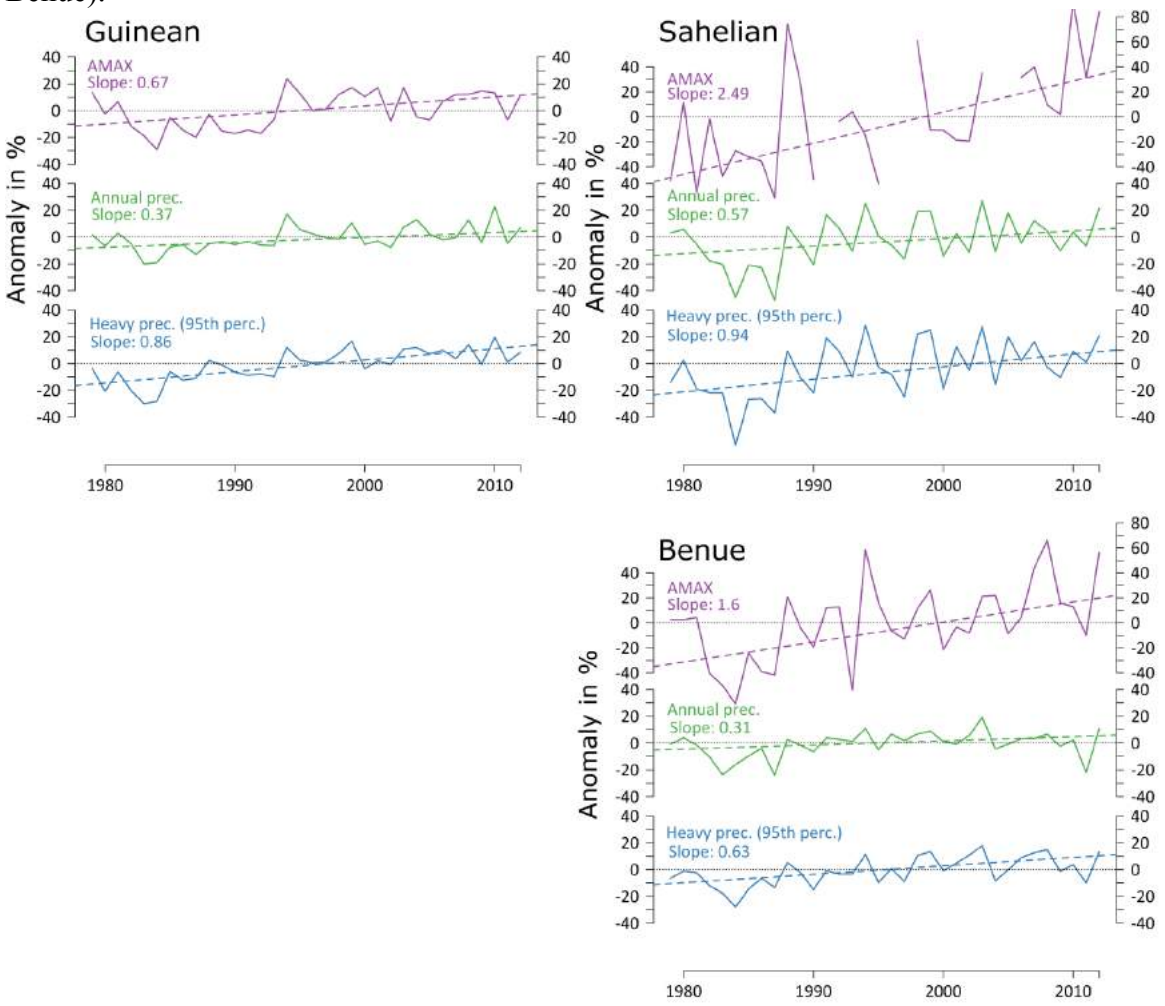

Figure 9 AMAX, annual precipitation and heavy precipitation for the three subregions of the Niger River Basin as an anomaly from 1979-2012. All trends are significant (α=0.05) and the Theil-Sen estimator trend is added as a dashed line and the slope as number.

Considering a longer time period (although with incomplete data records), Figure 10 depicts the rainfall values and AMAX values of all available years and all single investigated stations of the three regions. The precipitation from 1960 to 2001 from the Watch Forcing Data (WFD) and from 1979 to 2012 from the Watch Forcing Data ERA

Interim (WFDEI) show the same pattern in the three regions of the Niger: the mean annual rainfall decreases until the mid-1980s up to -10% and again increases afterwards by around 10%. The anomalies in the Sahelian region are with more than +/- 30% the most distinct ones.

The longest times series of the Guinean region (1907-2012) shows an increase of AMAX from 1910 to the 1950s, a decrease of AMAX until the mid 1980s followed by the increase which was already depicted in Figure 4 for the last 35 years. AMAX of the current period are generally smaller than the AMAX values which were reached in the peak period of the 1950s. The shorter time series from Benue (1970-2012) shows a decrease of AMAX until the mid 1980s, followed by an increase as before. The AMAX time series of the Sahelian region (1950-2012) shows a decrease until the 1970s and a continuous increase since then, which is not in accordance with the rainfall trends ("Sahelian Paradox"). This interesting phenomenon is further analyzed in the supplementary material chapter 10.1 since it shows the differences between the hydro-climatic dynamics of the Guinean and the Sahelian flood. Both the Sahelian and the Benue time series are too short to give information on the larger peak in the 1950s which is visible in the Guinean time series.

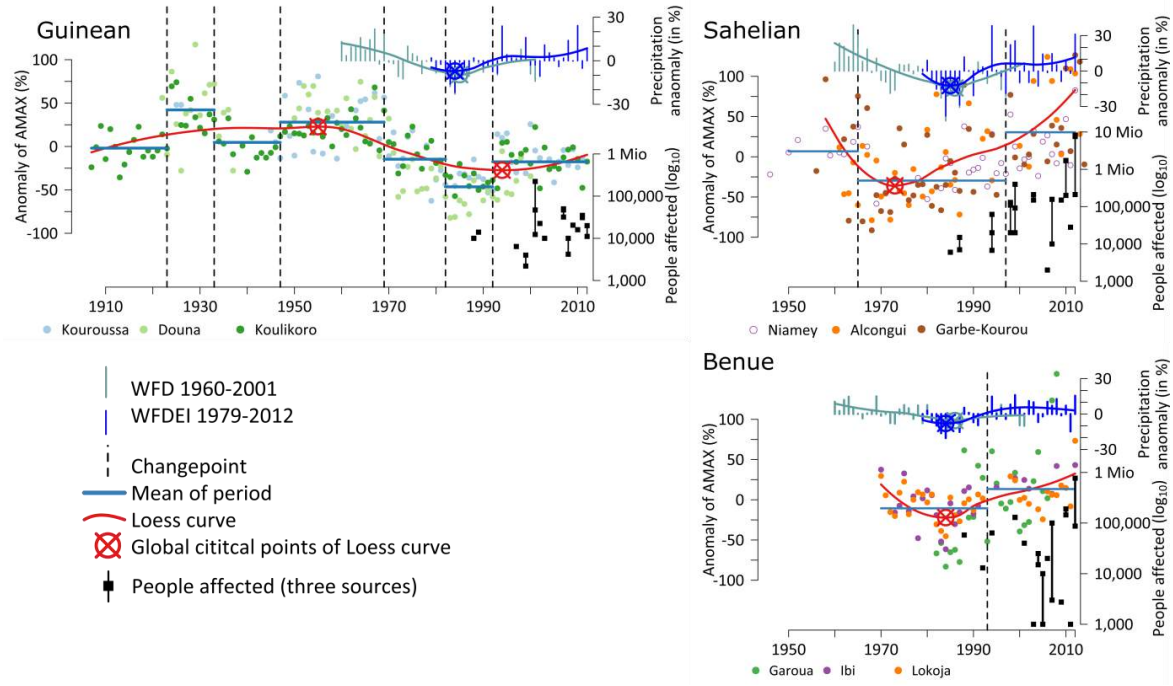

Figure 10 Annual maximum discharge (AMAX), precipitation and people affected by floods in the NRB, separated for the three subregions. Detected changepoints for the mean AMAX in each region are plotted as black dashed lines. Note that for the Sahelian region the numbers of people affected by catastrophic floods are plotted for the whole Middle Niger (see chapter 2.3.1.2). Please also note for the Sahelian region that only stations on the tributaries (Alcongui, Garbe-Korou) have been used for the Loess curve. The station Niamey has gaps where the red flood was covered by the Guinean flood in the hydrograph

2.4.1.2. Analysis of changepoints of annual flood peaks

Changepoint analysis was carried out to assess if these changes of AMAX are predominantly related to decadal pattern of the Atlantic Multidecadal Oscillation (AMO), which is here used as a proxy for longer-term climatic pattern of West Africa (the available rainfall time series were thought to be too short and inconsistent for this analysis). Changepoints of the AMO were detected for mid 1920s, beginning of 1960s and mid 1990s (Figure 6). Corresponding changepoints were detected for the AMAX series of all three regions in the mid 1990s (Figure 5); for the longer time series in Guinean region, a corresponding changepoint was detected for the mid 1920s, only for the Sahelian region was a corresponding changepoint detected for the mid 1960s, whereas the Guinean region showed a changepoint later in that time period at the end of the 1960s (Benue data set was too short to be included). This correspondence shows that for the identified periods of higher and lower AMAX are roughly consistent with the periods of the Atlantic Multidecadal Oscillation (AMO), i.e. the West African decadal pattern. However, the AMAX series in Figure 5 show several changepoints which corresponding ones in the AMO series, which might be either due to limitations of the method (and data availability) or potentially a sign that other factors than rainfall and climatic variability influenced the changes of AMAX, such as for example land-use change.

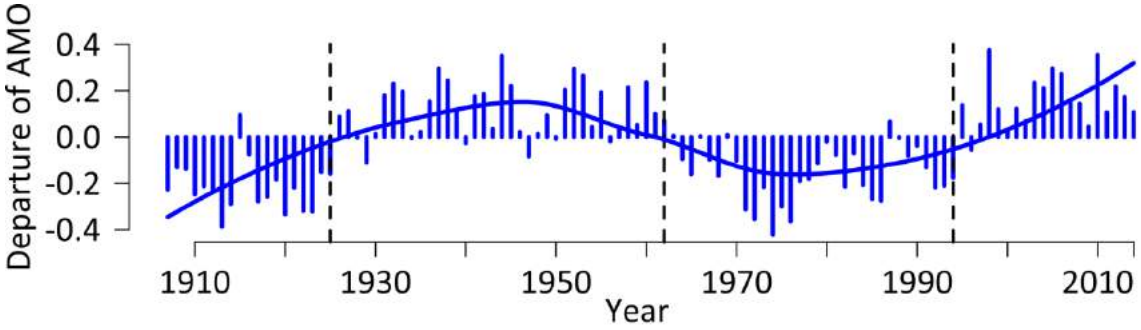

Figure 11 Atlantic Multidecadal Oscillation with LOESS

2.4.1.3. Analysis of changes in the variance of annual flood peaks

In contrast to the trend analysis in Figure 9, the AMAX time series have been analyzed using non-stationary generalized extreme value functions (NSGEV) in Figure 12, in order to see if there are changes in their variability. For the Guinean region, a model with a constant scale parameter but a third-degree location parameter has the highest value in the Chi-square test and is therefore the most suitable for explaining the distribution of probabilities for the AMAX time series. The curve changed from higher (approx. 1200 m^3s^{-1}) discharge in 1969 to lower (approx. 500 m^3s^{-1}) discharges in the 1970s and 1980s, and then half-way back up (approx. 800 m^3s^{-1}) by 2012. This implies that the frequency of the AMAX in the Guinean subregion changed rather linearly.

In contrast, the time series of the Sahelian tributaries Gouroul (Alcongui) and Sirba (Garbe-Kourou) can be explained with the best model fit by exponential location parameters and linear scale parameters. The NSGEV for these time series show not only the same characteristics but also similar probability values, which adds confidence to the result. For both stations, the peak moved from approximately 150 m^3s^{-1} to 300 $m^3s^{-1,}$ with an increasing rate at the end. The distributions of both of the latter stations become flatter over time, which implies a linear increase in variability and an exponential increase trend in flood magnitude.

In order to verify the results of the NSGEV, wavelet power spectra are applied to the same time series (Figure S 3, Supplementary material). For the Guinean time series wavelet, there is no significant change in variance during the last four decades. This supports the finding that no changes in variability occurred in the AMAX of this region, but only linear trends for the flood magnitude. The wavelet analysis for the time series of Garbe-Kourou also confirms the findings of the NSGEV. There is a change in frequency during the 1970s and 1980s and a return to the patterns of the 1950s and 1960s afterwards. This return to wet conditions is reflected in the change in probability of the NSGEV for this station, beginning in 1969 and lasting until 2012. The results show, that only in the dry catchments of the Middle Niger, a significant change of the variability towards more extreme AMAX can be detected. The reason for this inconsistency of more strongly increasing AMAX compared to precipitation is probably due to a stronger effect of land-use change compared to other regions (Aich et al., 2015).

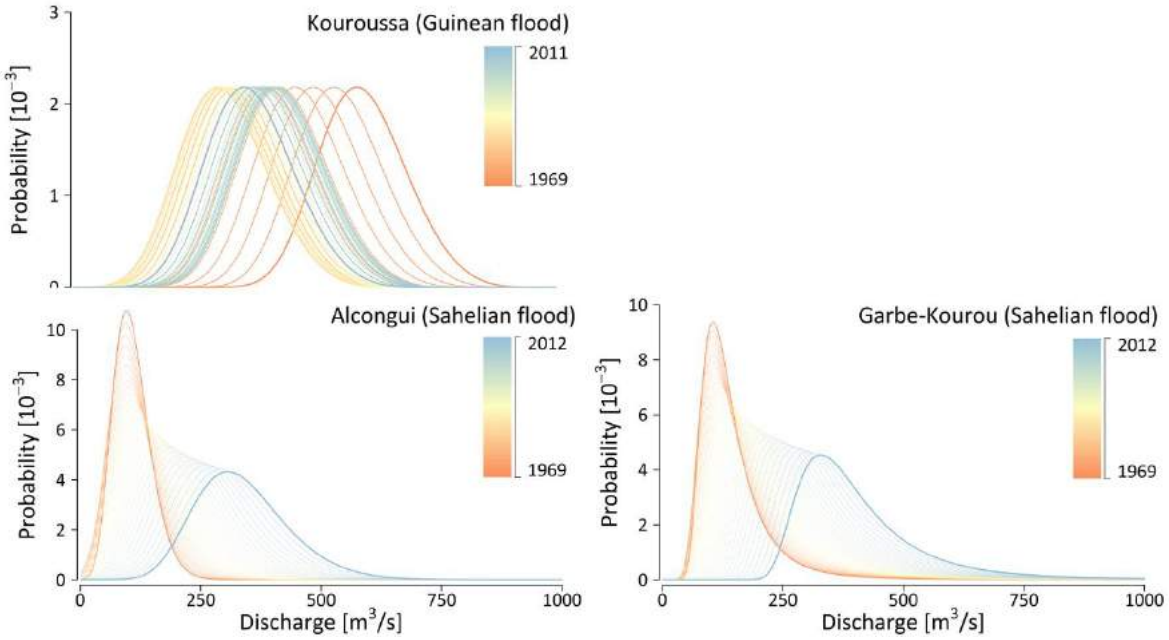

Figure 12 Non-stationary extreme value probability distributions for Kouroussa, Alcongui and Garbe-Kourou.

2.4.2. Analysis of changes in the timing of annual flood peaks

The temporal occurrence of AMAX (day of the year) was analyzed for all regions. No significant trend could be detected except for the stations downstream of the IND Figure 13. Here, AMAX timing of the Guinean flood shifted from February/March in the 1950s and 1960s to December/January in the 1970 to 1980s, and since then occurs again slightly later during January/February (see e.g. for the Malanville station in Figure 13).

This AMAX shift of regions downstream of the IND is attributed not directly to shifts in the rainfall regime, but may be explained by retention processes within the IND: water from the Guinean subregion accumulates in the Delta and only a limited amount can pass through its outlet near Diré at any time. In the time periods of generally lower AMAX (as e.g. during the 1980s to 1990s), the floods reached the downstream stations considerably earlier in the year, whereas higher AMAX values as observed in the 1950s or 2010 resulted in a delay of the AMAX at gauging stations affected by the retention processes of the Inner Niger Delta.

In summary, the timing of AMAX for the period 1910-2012 changes for the stations downstream of the IND where the Guinean flood occurs and depends on the total amount of water stored in the Delta.

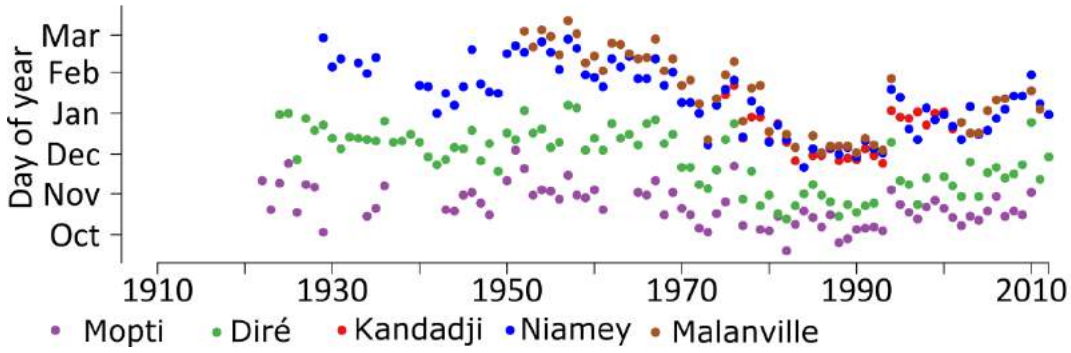

Figure 13 Shift in day of AMAX for the stations influenced by the Inner Niger Delta for the Guinean flood.

2.4.3. Analysis of damage statistics

The locations with the largest number of catastrophic floods between 1980 and 2012 were reported along the main stem of the Niger River, e.g. around the cities of Bamako, Niamey, Maradi and in the upper Benue, while they were less frequent in the Delta. The number of people affected by catastrophic floods in the NRB per year for the period from 1980 to 2014 is displayed in Figure 14 (note the logarithmic scale in the plot). The differences between the numbers for the three employed sources (see 2.3.1.2) is small for most of the years, though for some years at least one source has strong underestimations, e.g. the NatCatService for 1988 or the Darthmouth Flood Observatory data for 2009 and

2011. The increase in frequency of hazardous floods since the new millennium is striking. During the 1980s, around 120,000 people were affected by catastrophic flooding according to the reports, over 500,000 in the 1990s, and well over 10 million from 2000 until 2012.

In Figure 14, the catastrophic floods are spatially plotted and flash floods were separated from areal and river floods, since both have different underlying mechanisms according to the differentiation of the three data sources (as detailed in 2.3.1.2). The majority of the floods are river and areal floods and only a small proportion of the catastrophic floods are flash floods. For the trend and correlation analysis, only the data on people affected by river floods were considered. Figure 6 also shows that floods in the NRB were relatively homogeneously distributed along the river and its main tributaries.

For the individual regions, the number of people affected by catastrophic floods is plotted in Figure 6. Please note that it was not possible to distinguish the numbers of the Sahelian region from the other parts of the Middle Niger in the data sources because information was, in many cases, not clearly localized in the data sources (see chapter 3.1.2). The scale is logarithmic, but a distinct positive trend is nevertheless visible for the Sahelian and Benue regions. It is not visible for the Guinean region, but in all three regions there is a statistically significant linear trend when tested with the Mann-Kendall test. In addition, there is a strong correlation between AMAX and the number of people affected for the Sahelian and Benue regions (Spearman's ρ: 0.67, 0.63) (Figure S 4, Supplementary material). For the Guinean region, the correlation is moderate at ρ = 0.37.

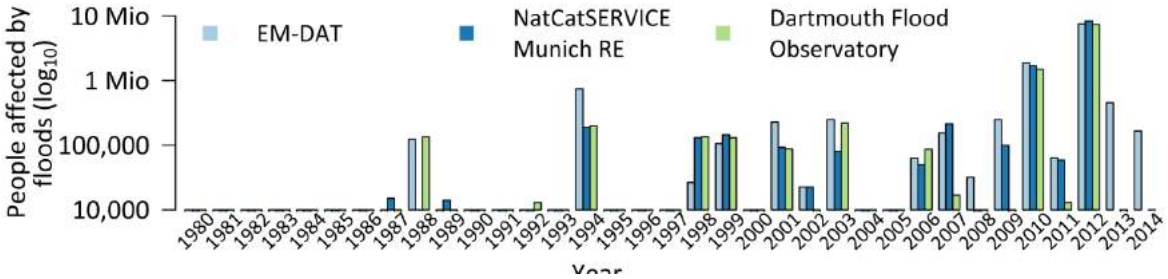

Figure 14 People affected by catastrophic floods per year in the Niger River Basin from 1980 to 2014 for three different data sources. Note that the scale of the y-axis is logarithmic. Please note that for 2013 and 2014 no data from Munich RE was available.

Table 1 Correlation of AMAX with heavy precipitation (95th percentile) and annual precipitation. All correlations are significant (α = 0.05).

	Guinean	Sahelian	Benue
Heavy precipitation	0.72	0.64	0.71
Annual precipitation	0.72	0.6	0.65

2.5. Discussion

The presented results related to research question a) on the long term statistics of rainfall and AMAX dynamics showed that the previously established high variability of rainfall and mean discharge holds also true for large floods, as was shown for the AMAX time series; the results also revealed a remarkably strong regional heterogeneity for the later.

The period from approximately 1970 to approximately 1990 was, in general, exceptionally dry in West Africa. In the Sahelian and Benue regions, the mean rainfall during this period was approximately 35% lower compared to the preceding period. This dry period is followed by a return to wetter conditions in West Africa (e.g. Jury, 2013; Tarhule et al., 2015). During the return to a wet phase, the annual precipitation up to 2012 did not exceed values that have been measured during the 1960s. For the AMAX, these findings are mainly consistent, and the correlation between precipitation and AMAX is strong for all regions (Table 1). The variation of AMAX and the detected changepoints during the analyzed period of up to 100 years follow the decadal climatic pattern in West Africa. However, the magnitude of the trends is only consistent for the Guinean region, where the levels of AMAX do not exceed values from the 1950s and 1960s. For the Benue subregion, there is only one changepoint detectable and therefore the antecedent periods before 1970 cannot be compared.

In the Sahelian region, however, the AMAX levels of recent decades exceed the levels of the 1960s. Particularly remarkable is the increase in frequency and magnitude of Sahelian flooding, which was also found by Descroix et al. (2012). Even during the wet 1960s, the Guinean flood peak was always higher than the Sahelian peak. Starting in 1980, the Sahelian flood was higher than the Guinean in nine of the years. In Niamey, the flood peak of 2012 was the highest peak since the beginning of records in 1929. This particular case of the Sahelian region is also reflected by the probability distribution. While the scale of the distribution stays constant for the Guinean region, it causes a flattening of the curve in the Sahelian region, implying that rare floods with a certain return period at the tail of the curve are more extreme during wet periods. The reason for this inconsistency of more strongly increasing AMAX compared to precipitation is probably due to land-use change and heavy precipitation (Aich et al., 2015).

Research question b) on temporal shifts in the AMAX revealed a shift of the AMAX timing of the Guinean flood downstream of the IND. This shift is not related to the timing of the rainfall regime, but rather to the amount of rainfall and a related retention process in the IND. The IND is responsible for a basin effect, where large Guinean floods occur up to 3 months later than small floods. The trend of the timing of the Guinean flood downstream of the IND reflects therefore the long-term trend of AMAX magnitudes.

The answer on research question c) on the links between the increasing AMAX trends and the impact of catastrophic floods is complex. The consistent trends of Figure 10

suggest a simple relationship between a return to wet conditions and increasing flood risk in the NRB, however this inference would neglect the complexity of catastrophic flood generation. Flood risk is not defined by flood frequency and magnitude alone, but by the product of exposure, vulnerability and hazard (IPCC, 2012; Kim et al., 2006; Kron, 2005; Merz, 2006), and we argue that exposure (population density) and vulnerability has increased significantly since the 1980s.

In West Africa, the population has multiplied by a factor of approximately 2.5 since 1980 (United Nations, Department of Economic and Social Affairs, 2013); the increase in population is matching the trend of people affected by floods for the same period. For all countries in the NRB, the population growth rate is over 2%, and for the Sahelian countries of Mali and Niger even more than 3% (Central Intelligence Agency, 2013). In the Sahelian subbasin, where the strongest trend in catastrophic floods occurs, the population increase is also about one percentage point greater compared to the other subregions; Figure 2 shows the spatial distribution of population density for 2015 (Central Intelligence Agency, 2013).

Regarding the vulnerability, the Human Development Index ranking (HDI) (Malik, 2014) was used in this study as an indicator for the spatial distribution of vulnerability (as depicted in Figure 2), since underdevelopment is closely linked to high vulnerability to disasters such as flooding (e.g. Yamin et al., 2005). Even if the general state of underdevelopment decreased in the countries of the NRB in contrast to their flood statistics, the absolute numbers of HDI still relate to the spatial patterns of catastrophic flood increase. The Republic of Niger, where most of the Middle Niger with its extreme increase in flood risk is located, is the country with the lowest development in the whole region since the HDI started to be recorded in the 1980s.

Figure 7 provides an overview on current flood risk in the NRB, taking into account the three described dimensions of flood risk hazard (changes in AMAX), vulnerability (Human Development Index) and exposure (population density). The figure indicates that the increase in flood risk in the NRB is attributed not only to increases in flood discharge but to a complex overlay of the regionally heterogeneous patterns

2.6. Conclusions

In all regions, the number of people affected by catastrophic floods increased drastically, although this increase can only partly be explained by increasing flood magnitudes and frequencies. Our results denote that the increasing flood risk in the NRB is caused by an increase in all three relevant factors: population, vulnerability and flood attributes such as intensity and frequency. The substantial increase in inhabitants affected by floods in the Middle Niger is the result of the greatest increase in all of these factors in this subregion. Our statistical analysis confirms previous studies regarding a general return to wet conditions since the end of the 1980s and, moreover, detects an increase in annual maximum discharge (AMAX) in the NRB for the same time period. However, the

relationship between the climatic drivers and discharge is complex and varies significantly between the regions of the basin. Several studies have shown that the changes in precipitation patterns in the region are very heterogeneous (e.g. Lebel and Ali, 2009; Panthou et al., 2014). This holds also for the sensitivity of the catchments in terms of changes. The dry Sahelian region is more sensitive to changes compared to the Guinean or Benue regions. The AMAX amplitude for dry (e.g. 1970s-1980s) and wet (e.g.1950s-1960s, 2000s-2012) periods differ substantially between the regions, and the discharge regime of the Sahelian catchment shows the strongest reactions compared to the wetter regions. Only in the dry Sahelian part, the AMAX variability increases significantly during wet periods, and extremer flood magnitudes become more probable. In order to account for dynamics of the entire basin and include climate change induced flood risk, detailed modelling studies on a subregional level are a prerequisite in order to project future flood risks in the NRB and discuss uncertainties (Döll et al., 2014). Such an effort should include land-use change, population density and vulnerability, all of which have been proven to be strong factors for flood risk in the basin.

Other implications can be derived from the decadal AMAX patterns. Since West Africa is currently experiencing a period of relative wetness, the likelihood of high AMAX in the coming years remains high, taking into account the consistent decadal patterns. This implies that short-term responses are needed in order to halt the trend of increasing flood risk, especially in the Middle Niger. A promising way includes the ongoing research activities on short- and medium-term hydrological forecasting systems, which should be connected with a flexible early-warning system. In the longer run, the existing action plan of the NRB Authority should be implemented, which includes, for example, more dams for flood control. These measures on the supranational level need to be accompanied by complementary actions from the national to the household level.

Acknowledgements

We thank the IMPACT2C project for financing this study and the Niger Basin Authority (NBA) for providing data. In addition we thank Munich RE, the Centre for Research on the Epidemiology of Disasters (CRED) of the University of Leuven and the Darthmouth Flood Observatory for sharing their data on people affected by floods.

References

Aich, V., Liersch, S., Vetter, T., Andersson, J., Müller, E. and Hattermann, F.: Climate or Land Use?—Attribution of Changes in River Flooding in the Sahel Zone, Water, 7(6), 2796–2820, doi:10.3390/w7062796, 2015.

Akaike, H.: A new look at the statistical model identification, IEEE Trans. Automat. Contr., 19(6), 716–723, doi:10.1109/TAC.1974.1100705, 1974.

Amogu, O., Descroix, L. and Yéro, K.: Increasing river flows in the Sahel?, Water [online] Available from: http://www.mdpi.com/2073-4441/2/2/170 (Accessed 11 November 2013), 2010.

Andersen, I., Dione, O., Jarosewich-Holder, M. and Olivry, J. C.: Niger River Basin: A Vision for Sustainable Management (Directions in Development), edited by K. G. Golitzen, World Bank Publications, Washington DC. [online] Available from: http://www.amazon.com/Niger-River-Basin-Sustainable-Development/dp/0821362038 (Accessed 11 November 2013), 2005.

Auger, I. and Lawrence, C.: Algorithms for the optimal identification of segment neighborhoods, Bull. Math. Biol., 51(1), 39–54, doi:10.1016/S0092-8240(89)80047-3, 1989.

Brakenridge, G. R.: Global Active Archive of Large Flood Events, [online] Available from: http://floodobservatory.colorado.edu/Archives/index.html., 2015.

Central Intelligence Agency: The World Factbook 2013-14, [online] Available from: https://www.cia.gov/library/publications/the-world-factbook/index.html, 2013.

Cleveland, W. S. and Devlin, S. J.: Locally Weighted Regression: An Approach to Regression Analysis by Local Fitting, J. Am. Stat. Assoc., 83(403), 596–610, doi:10.1080/01621459.1988.10478639, 1988.

Coles, S., Bawa, J., Trenner, L. and Dorazio, P.: An introduction to statistical modeling of extreme values, Springer London, London, UK., 2001.

Delgado, J. M., Apel, H. and Merz, B.: Flood trends and variability in the Mekong river, Hydrol. Earth Syst. Sci., 14(3), 407–418, doi:10.5194/hess-14-407-2010, 2010.

Descroix, L., Mahé, G., Lebel, T., Favreau, G., Galle, S., Gautier, E., Olivry, J.-C., Albergel, J., Amogu, O., Cappelaere, B., Dessouassi, R., Diedhiou, A., Le Breton, E., Mamadou, I. and Sighomnou, D.: Spatio-temporal variability of hydrological regimes around the boundaries between Sahelian and Sudanian areas of West Africa: A synthesis, J. Hydrol., 375(1-2), 90–102, doi:10.1016/j.jhydrol.2008.12.012, 2009.

Descroix, L., Esteves, M., Souley Yéro, K., Rajot, J.-L., Malam Abdou, M., Boubkraoui, S., Lapetite, J. M., Dessay, N., Zin, I., Amogu, O., Bachir, A., Bouzou Moussa, I., Le Breton, E. and Mamadou, I.: Runoff evolution according to land use change in a small Sahelian catchment, Hydrol. Earth Syst. Sci. Discuss., 8(1), 1569–1607, doi:10.5194/hessd-8-1569-2011, 2011.

Descroix, L., Genthon, P., Amogu, O., Rajot, J.-L., Sighomnou, D. and Vauclin, M.: Change in Sahelian Rivers hydrograph: The case of recent red floods of the Niger River in the Niamey region, Glob. Planet. Change, 98-99, 18–30, doi:10.1016/j.gloplacha.2012.07.009, 2012.

Dijkstra, H. A., Raa, L., Schmeits, M. and Gerrits, J.: On the physics of the Atlantic Multidecadal Oscillation, Ocean Dyn., 56(1), 36–50, doi:10.1007/s10236-005-0043-0, 2006.

Döll, P., Jiménez-Cisneros, B., Oki, T., Arnell, N. W., Benito, G., Cogley, J. G., Jiang, T., Kundzewicz, Z. W., Mwakalila, S. and Nishijima, A.: Integrating risks of climate change into water management, Hydrol. Sci. J., 60(1), 4–13, doi:10.1080/02626667.2014.967250, 2014.

Durbin, J. and Watson, G.: Testing for serial correlation in least squares regression. I, Biometrika, 37(3-4), 409–428 [online] Available from: http://www.jstor.org/stable/2332325 (Accessed 10 March 2014), 1950.

Durbin, J. and Watson, G.: Testing for serial correlation in least squares regression. II, Biometrika, 38(1-2), 159–178 [online] Available from: http://www.jstor.org/stable/2332325 (Accessed 10 March 2014), 1951.

EM-DAT: The OFDA/CRED International Disaster Database, Univ. Cathol. Louvain, Brussels, Belgium [online] Available from: www.emdat.be, 2015.

Enfield, D. B., Mestas-Nuñez, A. M. and Trimble, P. J.: The Atlantic Multidecadal Oscillation and its relation to rainfall and river flows in the continental U.S., Geophys. Res. Lett., 28(10), 2077–2080, doi:10.1029/2000GL012745, 2001.

FAO GEONETWORK: Global population density estimates (2015 (FGGD))., Rome, Italy., 2015.

Fekete, B. M., Vorosmarty, C. J. and Grabs, W.: Global, composite runoff fields based on observed river discharge and simulated water balances., Water System Analysis Group, University of New Hampshire, and Global Runoff Data Centre. Koblenz, Germany: Federal Institute of Hydrology (BfG), Koblenz, Germany., 1999.

Hundecha, Y., St-Hilaire, A., Ouarda, T. B. M. J., El Adlouni, S. and Gachon, P.: A Nonstationary Extreme Value Analysis for the Assessment of Changes in Extreme Annual Wind Speed over the Gulf of St. Lawrence, Canada, J. Appl. Meteorol. Climatol., 47(11), 2745–2759, doi:10.1175/2008JAMC1665.1, 2008.

IPCC: Managing the Risks of Extreme Events and Disasters to Advance Climate Change Adaptation. A Special Report of Working Groups I and II of the Intergovernmental Panel on Climate Change, edited by C. B. Field, V. Barros, T. F. Stocker, D. J. D. Qin, Dokken, K. L. Ebi, M. D. Mastrandrea, K. J. Mach, G.-K. Plattner, S. K. Allen, M. Tignor, and P. M. Midgley, Cambridge University Press, Cambridge, UK, and New York, NY, USA., 2012.

Jury, M. R.: A return to wet conditions over Africa: 1995–2010, Theor. Appl. Climatol., 111(3-4), 471–481, doi:10.1007/s00704-012-0677-z, 2013.

Killick, R., Fearnhead, P. and Eckley, I. A.: Optimal Detection of Changepoints With a Linear Computational Cost, J. Am. Stat. Assoc., 107(500), 1590–1598, doi:10.1080/01621459.2012.737745, 2012.

Knight, J. R., Folland, C. K. and Scaife, A. A.: Climate impacts of the Atlantic Multidecadal Oscillation, Geophys. Res. Lett., 33(17), L17706, doi:10.1029/2006GL026242, 2006.

Kron, W.: Flood Risk = Hazard • Values • Vulnerability, Water Int., 30(1), 58–68, doi:10.1080/02508060508691837, 2005.

Kundzewicz, Z. W., Kanae, S., Seneviratne, S. I., Handmer, J., Nicholls, N., Peduzzi, P., Mechler, R., Bouwer, L. M., Arnell, N., Mach, K., Muir-Wood, R., Brakenridge, G. R., Kron, W., Benito, G., Honda, Y., Takahashi, K. and Sherstyukov, B.: Flood risk and climate change: global and regional perspectives, Hydrol. Sci. J., 59(1), 1–28, doi:10.1080/02626667.2013.857411, 2013.

Lebel, T. and Ali, A.: Recent trends in the Central and Western Sahel rainfall regime (1990–2007), J. Hydrol., 375(1-2), 52–64, doi:10.1016/j.jhydrol.2008.11.030, 2009.

Liersch, S., Cools, J., Kone, B., Koch, H., Diallo, M., Reinhardt, J., Fournet, S., Aich, V. and Hattermann, F. F.: Vulnerability of rice production in the Inner Niger Delta to water resources management under climate variability and change, Environ. Sci. Policy, 34, 8–33, doi:10.1016/j.envsci.2012.10.014, 2013.

Mahe, G., Lienou, G., Descroix, L., Bamba, F., Paturel, J. E., Laraque, A., Meddi, M., Habaieb, H., Adeaga, O., Dieulin, C., Chahnez Kotti, F. and Khomsi, K.: The rivers of Africa: witness of climate change and human impact on the environment, Hydrol. Process., 27(15), 2105–2114, doi:10.1002/hyp.9813, 2013.

Malik, K.: Human development report 2014. Sustaining human progress: Reducing vulnerabilities and building resilience, New York United Nations Dev. Program. … [online] Available from: https://scholar.google.de/scholar?q=Human+Development+Report+2014%2C+Sustaining+Human+Progress%3A+Reducing+Vulnerabilities+and+Building+Resilience+&btnG=&hl=de&as_sdt=0%2C5#0 (Accessed 21 August 2015), 2014.

Mann, H. B.: Nonparametric Tests Against Trend, Econometrica, 13(3), 245–259, 1945.

Merz, B.: Hochwasserrisiken: Möglichkeiten und Grenzen der Risikoabschätzung, E. Schweizerbartsche Verlagsbuchhandlung, Stuttgart. [online] Available from: http://www.amazon.de/Hochwasserrisiken-Möglichkeiten-Risikoabschätzung-Bruno-Merz/dp/3510652207 (Accessed 3 June 2014), 2006.

MunichRe: NatCatSERVICE, [online] Available from: http://www.munichre.com/en/reinsurance/business/non-life/georisks/natcatservice/default.aspx, 2015.

Nicholson, S. E., Some, B. and Kone, B.: An Analysis of Recent Rainfall Conditions in West Africa, Including the Rainy Seasons of the 1997 El Niño and the 1998 La Niña Years, J. Clim., 13(14), 2628–2640, doi:10.1175/1520-0442(2000)013<2628:AAORRC>2.0.CO;2, 2000.

Niger Basin Authority, (NBA): Nigerhycos, hydrographs [online] Available from: http://nigerhycos.abn.ne/user-anon/htm/ (Accessed 15 November 2014), 2014.

Ogilvie, A., Mahé, G., Ward, J., Serpantié, G., Lemoalle, J., Morand, P., Barbier, B., Diop, A. T., Caron, A., Namarra, R., Kaczan, D., Lukasiewicz, A., Paturel, J.-E., Liénou, G. and Clanet, J. C.: Water, agriculture and poverty in the Niger River basin, Water Int., 35(5), 594–622 [online] Available from: http://www.tandfonline.com/doi/abs/10.1080/02508060.2010.515545 (Accessed 11 November 2013), 2010.

Okpara, J. N., Tarhule, A. A. and Perumal, M.: Study of Climate Change in Niger River Basin, West Africa: Reality Not a Myth, Clim. Chang. IMPACTS OVER ICE CAP, SEA Lev. RISKS, 1 [online] Available from: http://www.researchgate.net/publication/236020406_Climate_Change__Realities_Impacts_Over_Ice_Cap_Sea_Level_and_Risks/file/9c960515cf2209693a.pdf#page=17, 2013.

Ozer, P., Hountondji, Y. and Manzo, O. L.: Evolution des caractéristiques pluviométriques dans l'est du Niger de 1940 a 2007, Geo-Eco-Trop., 33, 11–30 [online] Available from: http://orbi.ulg.ac.be/handle/2268/78267 (Accessed 6 February 2014), 2009.

Paeth, H., Fink, A. H., Pohle, S., Keis, F., Mächel, H. and Samimi, C.: Meteorological characteristics and potential causes of the 2007 flood in sub-Saharan Africa, Int. J. Climatol., 31(13), 1908–1926, doi:10.1002/joc.2199, 2011.

Page, E.: Continuous inspection schemes, Biometrika, 41(1/2), 100–114 [online] Available from: http://www.jstor.org/stable/2333009 (Accessed 2 March 2014), 1954.

Panthou, G., Vischel, T., Lebel, T., Blanchet, J., Quantin, G. and Ali, A.: Extreme rainfall in West Africa: A regional modeling, Water Resour. Res., 48(8), doi:10.1029/2012WR012052, 2012.

Panthou, G., Vischel, T. and Lebel, T.: Recent trends in the regime of extreme rainfall in the Central Sahel, Int. J. Climatol., doi:10.1002/joc.3984, 2014.

Sarr, M. A., Zoromé, M., Seidou, O., Bryant, C. R. and Gachon, P.: Recent trends in selected extreme precipitation indices in Senegal – A changepoint approach, J. Hydrol., 505, 326–334, doi:10.1016/j.jhydrol.2013.09.032, 2013.

Séguis, L., Cappelaere, B., Milési, G., Peugeot, C., Massuel, S. and Favreau, G.: Simulated impacts of climate change and land-clearing on runoff from a small Sahelian catchment, Hydrol. Process., 18(17), 3401–3413, doi:10.1002/hyp.1503, 2004.

Sen, P.: Estimates of the regression coefficient based on Kendall's tau, J. Am. Stat. Assoc., 63(324), 1379–1389 [online] Available from:

http://amstat.tandfonline.com/doi/abs/10.1080/01621459.1968.10480934 (Accessed 10 March 2014), 1968.

Sighomnou, D., Descroix, L., Genthon, P., Mahé, G., Moussa, I. B., Gautier, E., Mamadou, I., Vandervaere, J.-P., Bachir, T., Coulibaly, B., Rajot, J.-L., Issa, O. M., Abdou, M. M., Dessay, N., Delaitre, E., Maiga, O. F., Diedhiou, A., Panthou, G., Vischel, T., Yacouba, H., Karambiri, H., Paturel, J.-E., Diello, P., Mougin, E., Kergoat, L. and Hiernaux, P.: La crue de 2012 à Niamey: un paroxysme du paradoxe du Sahel?, Sci. Chang. planétaires / Sécheresse, 24(1), 3–13, doi:10.1684/sec.2013.0370, 2013.

Son H. Kim, J. E. J. L. S. J. S. and M. W.: The objECTS Framework for integrated Assessment: Hybrid Modeling of Transportation, Energy J., Hybrid Mod(Special Issue #2), 63–92 [online] Available from: http://ideas.repec.org/a/aen/journl/2006se_jaccard-a04.html (Accessed 25 June 2015), 2006.

Tarhule, A.: Damaging Rainfall and Flooding: The Other Sahel Hazards, Clim. Change, 72, 355–377, doi:10.1007/s10584-005-6792-4, 2005.

Tarhule, A., Zume, J. T., Grijsen, J., Talbi-Jordan, A., Guero, A., Dessouassi, R. Y., Doffou, H., Kone, S., Coulibaly, B. and Harshadeep, N. R.: Exploring temporal hydroclimatic variability in the Niger Basin (1901-2006) using observed and gridded data, Int. J. Climatol., 35(4), 520–539, doi:10.1002/joc.3999, 2015.

Theil, H.: A rank-invariant method of linear and polynomial regression analysis, Ned. Acad. Wetensch. Proc, 53, 386–392 [online] Available from: http://link.springer.com/chapter/10.1007/978-94-011-2546-8_20 (Accessed 10 March 2014), 1950.

Torrence, C. and Compo, G. P.: A Practical Guide to Wavelet Analysis, Bull. Am. Meteorol. Soc., 79(1), 61–78, doi:10.1175/1520-0477(1998)079<0061:APGTWA>2.0.CO;2, 1998.

United Nations, Department of Economic and Social Affairs, P. D.: World Population Prospects: The 2012 Revision, Key Findings and Advance Tables. Working Paper No. ESA/P/WP.227, New York., 2013.

Weedon, G. P., Gomes, S., Viterbo, P., Shuttleworth, W. J., Blyth, E., Österle, H., Adam, J. C., Bellouin, N., Boucher, O. and Best, M.: Creation of the WATCH Forcing Data and Its Use to Assess Global and Regional Reference Crop Evaporation over Land during the Twentieth Century, J. Hydrometeorol., 12(5), 823–848, doi:10.1175/2011JHM1369.1, 2011.

Weedon, G. P., Balsamo, G., Bellouin, N., Gomes, S., Best, M. J. and Viterbo, P.: The WFDEI meteorological forcing data set: WATCH Forcing Data methodology applied to ERA-Interim reanalysis data, Water Resour. Res., n/a–n/a, doi:10.1002/2014WR015638, 2014.

Yamin, F., Rahman, A. and Huq, S.: Vulnerability, adaptation and climate disasters: a conceptual overview, IDS Bull. [online] Available from: https://www.ids.ac.uk/files/dmfile/0Overview.pdf (Accessed 21 August 2015), 2005.

Yue, S., Pilon, P., Phinney, B. and Cavadias, G.: The influence of autocorrelation on the ability to detect trend in hydrological series, Hydrol. Process., 16(9), 1807–1829, doi:10.1002/hyp.1095, 2002.

Zwarts, L.: Will the inner Niger delta shrivel up due to climate change and water use upstream. A & W report 1537, Feanwâlden. [online] Available from: http://www.wetlands.org/Portals/0/publications/Report/Will the Inner Niger Delta shrivel up due to climate change and water use upstream.pdf (Accessed 11 November 2013), 2010.

Zwarts, L., Beukering, P. Van, Kone, B. and Wymenga, E.: The Niger, a Lifeline: Effective Water Management in the Upper Niger Basin, Altenburg & Wymenga Ecologisch Onderzoek BV, Leylstad, Netherlands., 2005.

Nat. Hazards Earth Syst. Sci. Discuss., 2, 5171-5212, 2014
doi:10.5194/nhessd-2-5171-2014

3. FLOODS IN THE NIGER BASIN – ANALYSIS AND ATTIBUTION[1]

Valentin Aich [1,*], Balary Kone [2], Fred F. Hattermann [1] and Eva N. Müller [3]

[1] Potsdam Institute for Climate Impact Research (PIK), Potsdam, Germany
[2] Wetlands International, Mali Office, Mopti, Mali
[3] Institute of Earth and Environmental Science, University of Potsdam, Potsdam, Germany

* Corresponding author: Valentin Aich

Journal: Natural Hazards and Earth System Sciences Discussion (Nat. Hazards Earth Syst. Sci. Discuss.)
Status: Published (discussion paper)

Abstract: This study addresses the increasing flood risk in the Niger basin and assesses the damages that arise from flooding. Statistics from three different sources (EM-DAT, Darthmouth Flood Observatory, NatCat Munich RE) on people affected by floods show positive trends for the entire basin beginning in the 1980s. An assessment of four subregions across the Niger basin indicates even exponential trends for the Sahelian and Sudanian regions. These positive trends for flooding damage match up to a time series of annual maximum discharge (AMAX): the strongest trends in AMAX are detected in the Sahelian and Sudanian regions, where the population is also increasing the fastest and vulnerability generally appears to be very high. The joint effect of these three factors can possibly explain the exponential increase in people affected by floods in these subregions. In a second step, the changes in AMAX are attributed to changes in precipitation and land use via a data-based approach within a hypothesis-testing framework. Analysis of rainfall, heavy precipitation and the runoff coefficient shows a coherent picture of a return to wet conditions in the basin, which we identify as the main driver of the increase in AMAX in the Niger basin. The analysis of flashiness (using the Richards–Baker Index) and the focus on the "Sahel Paradox" of the Sahelian region reveal an additional influence of land-use change, but it seems minor compared to the increase in precipitation.

[1] A revised version of the attribution approach is in the Appendix 10.2.1. This version incooporates the comments and suggestions on the discussion paper but is unpublished.

3.1. Introduction

In the last two decades, the occurrence of extensive flooding has increased drastically in the Niger basin (Amogu et al., 2010a; Descroix et al., 2012; Mahe et al., 2013; Panthou et al., 2014); however, very little research is currently being conducted on both factors contributing to flood risk and the associated flood damages. Tarhule (2005) addressed the flooding in the Sahel for the first time scientifically, calling the floods "the other Sahelian hazard" referring to the lesser significance of floods in the face of the dominant water scarcity in the region. Since then, several studies have contributed to the discussion from different perspectives.

Paeth et al. (2011) looked at the meteorological patterns that lead to the extreme flooding of 2007. Panthou et al. (2014, 2012) and Ozer et al. (2009) detected changes in rainfall patterns in the region and connected them to changes in flood occurrence. Jury (2013) analyzed streamflow trends in Africa, including one station in the Niger basin (Niamey) and found an increase of streamflow that matched their general finding of a "return to wet conditions" in Africa in recent decades. Descroix et al. (2012, 2011) examined increasing river discharges in the Niger basin and came to the conclusion that adverse land-use change and crusting of soils lead to an increase in flooding as the climate in the region tends to become drier. For the Sahelian zone, this effect of increasing discharge despite decreasing rainfall is called the "Sahelian Paradox", first described by Albergel (1987). Sighomnou et al. (2013) attributed the extreme flooding of 2012 to the aforementioned changes in land use and crusting for the region around Niamey. Descroix et al. (2009) and Amogu et al. (2010) also addressed this phenomenon and found an increasing trend for streamflow of rivers in the Sahelian zone and a decreasing trend for rivers in the Sudanian zone. Descroix et al. (2013) summarized the results on the "Sahelian Paradox" and argued for a more regionalized assessment of the floods. Still, the role of climatic variability for the increased flood risk in the Niger basin has not been systematically addressed; neither has the associated damage been quantified.

Flood risk is not defined by flood frequency and magnitude alone, but by the product of value, vulnerability and hazards (Kron, 2005; Merz, 2006). Value in the formula is represented by the population that could be affected by floods in the basin. In West Africa, the population has multiplied ~2.5 times since 1980 (United Nations, Department of Economic and Social Affairs, 2013). For all countries in the Niger basin, the population growth rate is over 2%, and for the Sahelian countries of Mali and Niger, even over 3% (Central Intelligence Agency, 2013). The studies of Di Baldassarre et al. (2010) and Tschakert et al. (2010) provided evidence that the vulnerability of the population with regard to catastrophic floods has increased in the past due to several reasons, e.g. the loss of traditional knowledge about flood adaptation.

This study aims to contribute to the discussion with a comprehensive analysis of flooding and its damages in the Niger basin, thus attempting to disaggregate the total risk

and attribute it to different flood risk components in the Niger basin. In order to take the regional heterogeneity of the Niger basin into account, we differentiate four subcatchments according to their main source areas and data availability (Guinean, Sahelian, Sudanian and Benue, Figure 15).

We first evaluate the three most extensive databases on floods in Africa (NatCat database of Munich Re, Dartmouth Flood Observatory, International disaster database EM-DAT). The numbers of people affected are visualized spatially in order to see how the increase in people affected by floods during the past decades is associated with corresponding annual maximum discharges (AMAX) and rainfall in the subcatchments. In a second step, we focus on the timing of the AMAX and look for temporal shifts. Then, the time series are analyzed with regard to non-stationary trends and decadal patterns. Decadal patterns are correlated to the Atlantic Multidecadal Oscillation (AMO) in order to see whether this mode of variability can indicate flooding in the region.

Based on the systematic trend analysis, we use a data-based approach within a hypothesis-testing framework to attribute the detected trends (Merz et al., 2012). Therefore, rainfall data is analyzed and correlated to AMAX, and the flashiness of the discharge is examined in order to distinguish between the influence of climatic variability and land-use change effects. A focus on the special case of the "Sahelian Paradox" allows a qualitative estimation of the magnitude of influence of land-use change compared to climate change signals. The results are then discussed with a holistic view of the increasing flood risk, taking into account the hazards, vulnerability and population growth.

3.2. Niger basin

The Niger basin covers a total area of approximately 2,156,000 km², of which only ~1,270,000km² contribute to the river discharge (Figure 15) (Ogilvie et al., 2010). The whole basin is spread over the territory of ten countries: Guinea, Côte d´Ivoire, Mali, Burkina Faso, Algeria, Benin, Niger, Chad, Cameroon and Nigeria (Zwarts et al., 2005). It extends over different agro-climatic and hydrographic regions with individual topographic and drainage characteristics. The Niger runoff regime is affected by different types of reoccurring floods, which result from the geographic locations and characteristics of their main source areas. The first one is the Guinean Flood, which originates from the headwaters of the Niger in the low-altitude plateaus called the Guinean highlands during the rainy season between July and November (Figure 25, Descroix et al., 2012). From here, the Niger and Bani Rivers flow into the Inner Niger Delta (IND). This vast inland delta covers an area of ~36.000km² in central Mali and comprises lakes and floodplains that are regularly flooded with large annual variations. It influences the hydrological regime of the Niger significantly by flattening and slowing down the peak of the annual flood (Liersch et al., 2013; Zwarts, 2010).

Most of the inflow in the middle section of the Niger basin comes from the plateaus of the right-bank subbasins. The vast subbasins to the left reach up into the central Sahara but only contribute a minor amount of inflow, and local contributories are endorheic most of the time (Amogu et al., 2010a). The annual peak during the rainy season (July to November) in the mid-section of the Niger downstream of the IND is called the "Red Flood" or "Sahelian Flood", the latter of which will be used in this study for the second subregion (Figure 25, Descroix et al., 2012). The third flood we define in this study is the "Sudanian Flood", which originates from the part of the basin downstream of the Sahelian zone and contributes to the gauge Yidere Bode in Nigeria, also reaching into the Sahelian climate zone. The fourth flood we focus on here is the flood of the Benue River, which flows into the Niger at the Nigerian city of Lokoja. Coming from a high-altitude plateau, it is the largest tributary in terms of discharge and outreaches the Niger by about a third at the confluence near Lokoja. This part of the Niger basin will henceforth be referred to as "Benue" (Figure 15). Finally, the Niger disembogues into the Gulf of Guinea forming the Niger Delta, a flat region characterized by swamps and lagoons (Andersen et al., 2005a). As no discharge data were available for the region between Yidere Bode and the confluence of the Benue, nor for the part after the confluence, these parts are not included in the analysis.

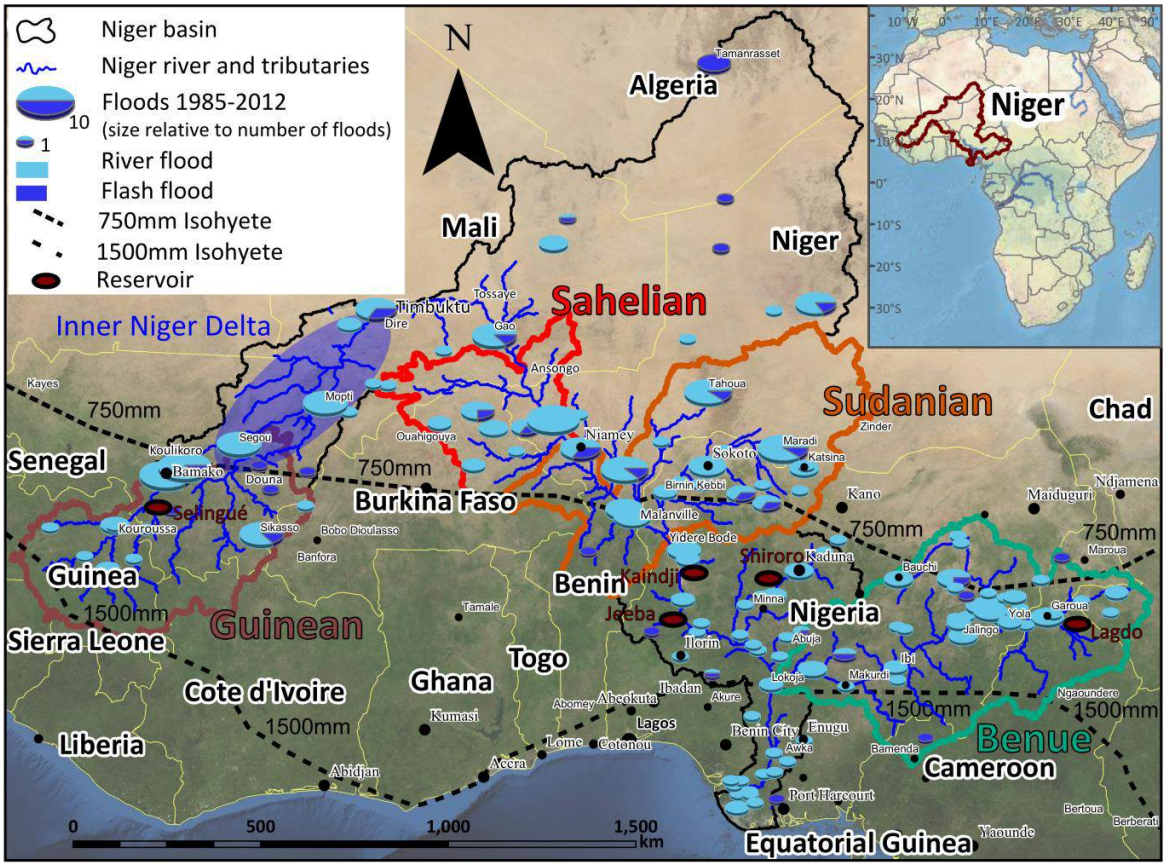

Figure 15 Niger basin and source areas of floods in the Guinean, Sahelian, Sudanian and Benue regions.

There are five major dams in the Niger basin which influence the discharge regime of the Niger and its tributaries (Table 2). In the Action Plan for the Niger Basin of the Niger Basin Authority (NBA), several scenarios with additional major dams are listed, such as Fomi in Guinea and Taoussa in Mali, for example (Niger Basin Authority, 2007). Currently, only the Kandadji dam in the Niger is actually under construction.

Table 2 Major reservoirs in the Niger basin.

Reservoir	Country / River	Completion date	Max. volume [million m³]*
Kainji	Nigeria / Niger River	1968	15000
Selingué	Mali / Sankarani River	1982	2135
Lagdo	Cameroon / Benue River	1982	7800
Jeeba	Nigeria / Niger River	1984	3880
Shiroro	Nigeria / Kaduna River	1990	7000

*including dead storage

The population density in the Niger basin ranges from less than one person per km² in the deserted North to over 1,000 in rural areas in Nigeria and Mali (Figure 16) (Nelson, 2004). Of the four regions on which this study focuses, the Sudanian zone and the Benue are the most densely populated, with many regions containing over 100 persons per km². But also in the riverine areas along the Niger River, many regions in the Upper Niger basin and the middle section have similar population densities. The population growth rate in the countries of the Niger basin is extreme, ranging from 2% to 3.5% with the highest increases in the Sahelian countries of Mali and Niger (Central Intelligence Agency, 2013).

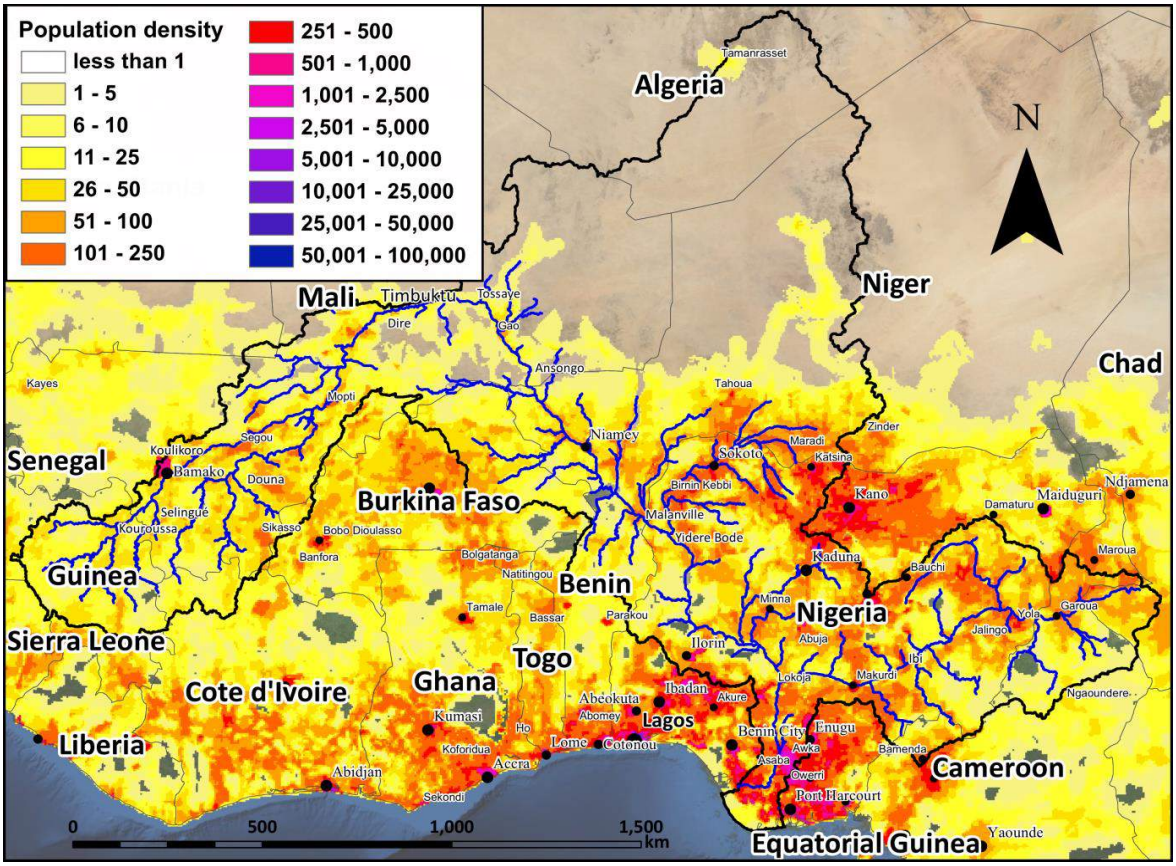

Figure 16 Population density in the Niger basin (data derived from Nelson, 2004)**.**

3.3. Methodology

3.3.1. Data

3.3.1.1. Data on people affected by floods

Data on people affected by catastrophic flooding were derived from three different sources: the NatCatService of the Munich Reinsurance Company (MunichRe, 2015), the EM-disaster data base of the University of Leuven, Brussels (EM-DAT, 2015) and the Global Active Archive of Large Flood Events of the Darthmouth flood observatory

(Brakenridge, 2015). All data are based on media reviews of the respective organization and the collection of data from official sources. The latter archive derives additional information from remote sensing data. Only the period from 1980 to 2012 is considered here, because all datasets provide input for this period. All three sources provide additional information on whether the flood was a flash or river/ areal flood. However, the quality of the data for West Africa is low, as there is no systematic and uniform assessment of floods. Some reports are on the village level, others on the regional or even national level. Therefore, a distinction between people affected in the Sudanian and Sahelian zones was not possible because most reports grouped the number of people affected for both these regions together (Figure 16). Since most of the reports come from the media, the numbers reported are not verifiable and differ often substantially between sources. Still, they are the best available source for damage data on catastrophic floods in West Africa. The data was analyzed equally, and so even if absolute numbers are uncertain, trends in the data are assumed to be reliable.

3.3.1.2. Discharge, precipitation and Atlantic Multidecadal Oscillation data

Observed river discharge at a daily resolution was provided by the Global Runoff Data Centre (Fekete et al., 1999) and the Niger Basin Authority. In stations where the flood peak originating from the Guinean flood occurred after the 31st of December, the value was attributed to the previous year. The annual maximum discharge (AMAX) value of a certain year was only used if it was the global change point of the annual hydrograph and if we could reasonably eliminate the possibility that any missing values might have been higher. At the Ansongo, Niamey and Malanville stations, peaks for the Guinean and the Sahelian/Sudanian floods occur. The Sahelian and Sudanian peaks are limited to August through October and do not occur every year. Therefore, the AMAX time series for the Sahelian and Sudanian floods at these gauging stations have gaps for years where a separate peak could not be distinguished.

To analyze precipitation in the regions, we used reanalysis data from the WATCH Forcing data ERA 40 (WFD) (Weedon et al., 2011) for the period from 1960 until 2001 and the WATCH Forcing data ERA interim, which is processed similarly on the ERA 40 reanalysis data set for the period from 1979 until 2012 (WFDEI) (Dee et al., 2011). The precipitation parameter of both data sets is sampled on a 0.5 ×0.5 grid. For analysis of the means, only the months during the rainy season (June-November) within the different subregions have been included (Figure 15). For the analysis of heavy precipitation, we derived the 95th percentile of the daily precipitation per year. Both parameters of the reanalysis time series of WFD and WFDEI have been validated with observed rainfall data from stations in all subregions (Bamako in Mali, Gao in Mali, Niamey in Niger, Maradi in Niger, Garoua in Cameroon, Figure 15) (Figure S1). The reanalysis data was interpolated

to the location of the stations, and it shows good performance with regard to annual and heavy precipitation.

The Atlantic Multidecadal Oscillation (AMO) is a mode of variability occurring in the northern Atlantic Ocean and is derived from sea surface temperatures (Dijkstra et al., 2006). It is closely connected to the rainfall in West Africa (Knight et al., 2006; Nicholson et al., 2000). The data on the AMO is provided by the National Oceanic and Atmospheric Administration (NOAA) in an unsmoothed version (Enfield et al., 2001) which is based on the Kaplan Extended Sea Surface Temperature dataset.

3.3.2. Statistics

3.3.2.1. Standard statistical methods

For the analysis of several time series, the local regression fitting technique LOESS was used (Cleveland and Devlin, 1988). It is a nonparametric regression method that combines multiple regression models in a k-nearest-neighbor-based meta-model. When plotted, it generates a smooth curve through a set of data points (LOESS Curve).

For correlation analysis, Spearman's rank correlation was applied. It is a nonparametric measure of the statistical dependence between two variables and is widely used to assess monotonic relationships between parameters.

Monotonic linear trends were identified using the Mann-Kendall test (Mann, 1945). This is a robust nonparametric test in which each element is compared with its successors and ranked as larger, equal or smaller. On this basis, it is possible to test the statistical significance of rejecting the null hypothesis (for all tests $\alpha = 0.05$). The linear trend was estimated using the Theil-Sen approach (Sen, 1968; Theil, 1950). Since serial independence is a requirement of the Mann-Kendall test, we checked beforehand for autocorrelations in all precipitation and hydrologic time series using the Durbin-Watson statistic test (Durbin and Watson, 1950, 1951). If an autocorrelation of the first order was found, trend-free pre-whitening was applied according to the method proposed by Yue et al. (2002): First, the trend estimated with the Theil-Sen approach was removed from the time series. Then, the first-order autocorrelation coefficient was calculated and subtracted from the time series. Finally, the trend was added back to the autocorrelation data and the Mann-Kendall test was applied in order to test for its significance.

In order to determine whether there was a trend influencing AMAX in addition to the trend in the rainfall amount, we detrended the AMAX and the precipitation time series for the corresponding rainy season in the region by subtracting the residuals of the linear trend. We then formulated the coefficient between these two time series analogous to the common runoff coefficient between mean discharge and precipitation (Figure 21).

3.3.2.2. Changepoint identification

In order to detect changepoints in the means of datasets, the cumulative sums method (CUSUM) of Page (1954) is a common approach. Combined with an algorithm to minimize the cost function (1) it is able to detect multiple changepoints (Killick et al., 2012):

$$\sum_{i=1}^{m+1} [C(Y(t_{i-1}+1):t_i)] + \beta f(m) \quad (7)$$

C is the cost function of the time series segment $Y(t_{i-1}+1):t_i$ and $\beta f(m)$ is the penalty function. Different algorithms exist to minimize this function, and for this study the Segmented Neighborhood (SN) method of Auger and Lawrence (1989) is appropriate because it is an exact approach and the datasets are relatively small so that the generally high computational cost of this method is acceptable. The cost functions for all possible segments are iteratively calculated. By that means, SN is able to compute the segments; however, it does not provide information about the number of segments which would be identical with the number of observations without restrictions. In order to prevent this overfitting, the penalty function was introduced. In this study, we used Akaike's Information Criterion (AIC) (Akaike, 1974)

$$AIC = 2k - 2\ln(L) \quad (8)$$

where K is the number of parameters in the model and L is the maximized value of the likelihood function.

3.3.2.3. Wavelet analysis of annual maximum discharge time series

For detecting changes in the frequency of AMAX, we applied a wavelet power spectrum (Torrence and Compo, 1998). This can be described as a correlation coefficient between a dataset and a given function. This function slides over the dataset and is scaled to account for different frequencies. In our case we used the Morlet function, a complex nonorthogonal function which is commonly used for hydrographical time series (e.g. Delgado et al., 2010). The wavelet analysis is a powerful tool to show changes in the frequency over time, and indicates whether trends exist in the variance of the time series.

3.3.2.4. Non-stationary Generalized Extreme value distribution

Non-stationary Generalized Extreme value models (NSGEV) (Coles et al., 2001) have been proven to be an effective tool not only to detect trends in the flood average but also of flood variability (e.g. Delgado et al., 2010; Hundecha et al., 2008). The method is

described in detail by Delgado et al. (2010) and is based on the generalized extreme value function (GEV), which is cumulatively written as:

$$F(x) = \begin{cases} exp\left[-\left(1-\frac{\xi}{\sigma}(x-\mu)\right)^{\frac{1}{\xi}}\right] \; if \; \xi \neq 0 \\ exp\left[-exp\left(-\frac{x-\mu}{\sigma}\right)\right] \; if \; \xi = 0 \end{cases} \quad (9)$$

with μ as the location parameter, σ as the scale parameter and ξ as the shape parameter. This cumulative distribution is then fitted systematically with different combinations of linear, second- and third-degree time-dependent parameters, however only for the location and shape parameters. These time-dependent parameters were then inserted in a maximum likelihood function.

$$L = \prod_{t=1}^{n} \sigma(t)^{-1} \, exp\left[-\left(1-\xi\frac{x(t)-\mu(t)}{\sigma(t)}\right)\right] \quad (10)$$

Instead of the different parameters, the linear, second- or third-degree terms were inserted in the likelihood function. In order to identify the parameter setting which fits best to the data, a likelihood deviance statistic was applied. By this means, it could be tested whether the model of higher complexity from stationary to third-degree is an improvement, and whether this improvement is not just obtained by chance but is rather significant. So, each model M_1 was tested against the simpler model M_0. The deviance statistic of the models $M_0 \subset M_1$ is defined as

$$D = 2\{\ell_1(M_1) - \ell_0(M_0)\} \quad (11)$$

where $\ell_1(M_1)$ and $\ell_0(M_0)$ are the maximized log-likelihoods for the models. The distribution D is asymptotic, and its degree of fit can be tested with a Chi-square test (χ_k^2). The degrees of freedom k express the difference in dimensionality between M_0 and M_1. So, larger values of D suggest that model M_1 explains the variation in the data better than M_0 and is therewith accepted as the NSGEV distribution.

3.3.2.5. Richards-Baker flashiness index

Changes in flashiness of the streamflows are quantified using the Richards-Baker Flashiness Index (Baker et al., 2004). This index F_{R-B} is based on the ratio of absolute day-to-day fluctuations in streamflow relative to the total flow in a year:

$$F_{R-B} = \frac{\sum_{i=1}^{n}|q_i - q_{i-1}|}{\sum_{i=1}^{n} q_i} \quad (12)$$

where q is the daily discharge of day i of the year (n=365).

3.4. Results

3.4.1. Analysis of damage statistics

In Figure 17, the number of people affected by catastrophic floods in the Niger basin per year for the period from 1980 to 2012 is displayed (note the algorithmic scale in the plot). The differences between the numbers for the three sources (see chapter 503.3.1.1) is small for most of the years, though for some years at least one source has strong underestimations, e.g. the NatCatService for 1988 or the Darthmouth Flood Observatory data for 2009 and 2011. The increase in flood frequency since the new millennium is striking. During the 1980s, around 120,000 were affected by catastrophic flooding according to the reports, over 500,000 in the 1990s, and well over 10 million from 2000 until 2012. In addition, the increase in people affected appears exponential when taking into account that the scale is logarithmic.

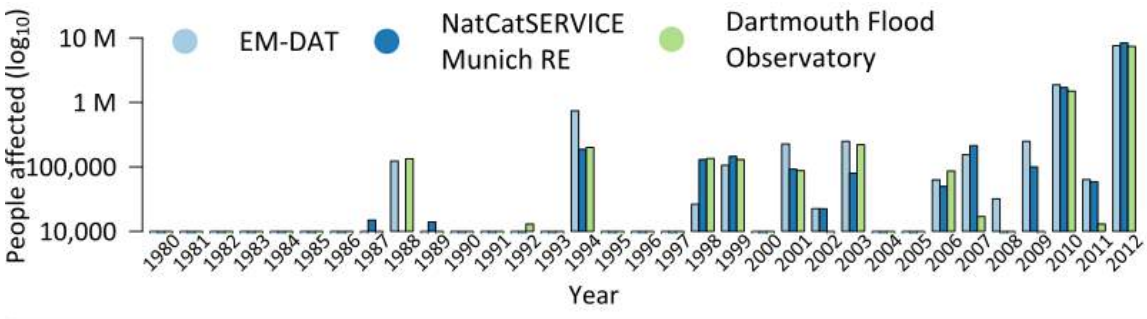

Figure 17 People affected by catastrophic floods per year in the Niger basin from 1985 to 2012 for three different data sources. Note that the scale of the y-axis is logarithmic.

In Figure 15, these floods are spatially plotted and flash floods were separated from areal and river floods, since both have different underlying mechanisms. The majority of the floods are river and areal floods and only a small proportion of the catastrophic floods are flash floods. Figure 15 also shows that floods in the Niger basin are relatively homogeneously distributed along the river and its tributaries, and that clustering is limited. The locations with the largest number of catastrophic floods between 1985 and 2012 have been reported along the main stem of the Niger River, e.g. around the cities of Bamako, Niamey, Maradi and in the upper Benue, while they have been less frequent in the Delta.

In Figure 18, the numbers of people affected by floods are plotted in relation to the anomalies of the annual maximum discharge (AMAX) and the anomalies of the rainfall from reanalysis products (WFD, WFDEI) for each subregion. Changepoints were detected for the mean of the AMAX time series for each subregion. Since the Inner Niger Delta (IND) has a strong influence on the AMAX, stations within the reach of the wetland were excluded in the analysis for the Guinean region and only the stations upstream of the Delta (Kouroussa, Koulikoro and Douna) were considered. The Guinean region includes the

gauges with the longest discharge observations and six changepoints were detected between 1910 and 2012. For the Sahelian and Sudanian regions, data is available starting in the 1950s and for both regions two changepoints were detected. For these three regions, there was a changepoint around 1970 and an additional one around 1990. For the Benue basin, data is only available from 1970 and only one changepoint at the beginning of the 1990s was detected. For the Guinean, Sudanian and Benue sub-basins, the last changepoint was detected in 1992, and for the Sahelian subregion the last changepoint was detected 5 years earlier in 1987. When all stations affected by the Guinean flood, including the IND, were taken into account, the latter two changepoints were not detected. This effect can be explained by retention processes in the wetland that smooth the hydrograph (Figure S2).

The AMAX Loess curves of all regions show a decrease after 1970 that reaches its lowest point in the Guinean region after 1990 and in the other regions around 1980. For the Sahelian, Sudanian and Benue regions, the mean for the last period beginning around 1990 is approximately 25% higher than the mean of the antecedent period beginning around 1970. In the Guinean region, the mean of the last period beginning here around 1970 is around 25% lower than the antecedent period in the 1960s. In the Sahelian and Sudanian regions, this step is around -50%.

The precipitation anomalies from 1960 to 2001 from the Watch Forcing Data (WFD) and from 1979 to 2012 from the Watch Forcing Data ERA Interim (WFDEI) show the same pattern in all regions. The mean decreases until the mid-1980s up to -10% and again increases afterwards by around 10%. The anomalies in the Sahelian region are the most distinct (more than +/- 30%).

The number of people affected per year from 1985 to 2012 (see chapter 3.1.1) are plotted at the bottom of each region. Note that it was not possible to distinguish between the Sudanian and Sahelian regions in the data sources, so the joint numbers are plotted for both of the regions (see chapter 3.1.1). The scale is logarithmic, but a positive trend is nevertheless visible for the Sahelian, Sudanian and Benue regions. It is not visible for the Guinean region, but in all four regions there is a statistically significant linear trend when tested with the Mann-Kendall test. In addition, there is a strong correlation between AMAX and the number of people affected for the Sahelian, Sudanian and Benue regions (Spearman's ρ: 0.67, 0.63, 0.63). For the Guinean region, the correlation is weak at ρ = 0.37.

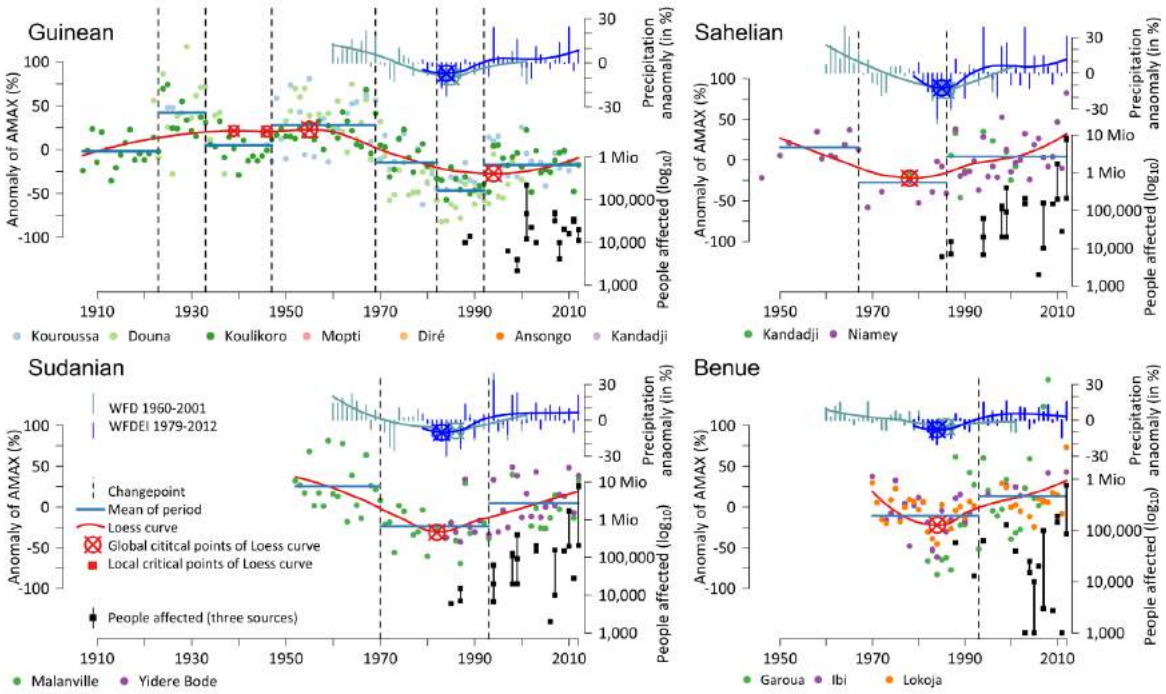

Figure 18 People affected by floods in the Niger basin, annual maximum discharge (AMAX) and precipitation separated for the four subregions. Note that the same numbers of affected people are plotted for the Sudanian and Sahelian regions (see chapter 3.3.1.1). Detected changepoints for the mean AMAX in each region are plotted as black dashed lines.

3.4.2. Analysis of changes in the timing of annual flood peaks

The occurrence of the flood peak as one day of the year was analyzed for all regions. A trend test starting in the year of the last changepoint could not reveal a significant linear trend for any of the time series (Guinean, Sudanian, Benue: 1992, Sahelian: 1987) (for example, see Figure 19, left). This does not hold for the stations influenced by the dynamics of the Inner Niger Delta (IND) (Figure 19, right). For these stations, significant trends exist which reflect the trends of the AMAX time series. This can be explained by the strong correlation between AMAX and the day of the year, caused by the basin effect of the IND. The water from the Guinean subregion accumulates in the IND and only a limited amount can pass through the outlet near Diré. Accordingly, the delay in AMAX at the affected downstream stations is dependent on the total amount of water in the Delta. Due to this correlation, the positive trend in AMAX causes a significant change in the timing of the AMAX of the Guinean Flood in and downstream of the IND.

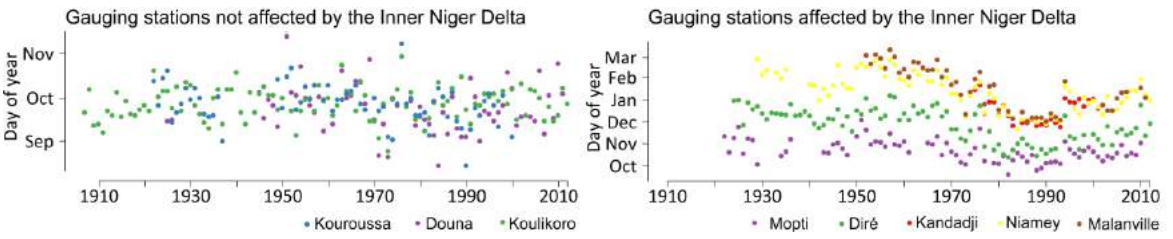

Figure 19 Shift in day of AMAX for the Guinean stations upstream of the Inner Niger Delta (left) and for the stations influenced by the Inner Niger Delta (right).

3.4.3. Trend analysis of annual flood peaks

In Figure 20, the AMAX time series are analyzed using non-stationary generalized extreme value functions (NSGEV). Since an analysis of the mean for all stations in one subregion might balance out changes in the frequency, the most complete time series for each subregion has been selected for the trend detection. For the Guinean region, Kouroussa was selected because the flow is not influenced by the IND. For the Benue region, no time series was long enough for the analysis. In order to avoid the complex distributions of the whole time series that change their directions several times, the analysis was limited to the period after the changepoint around 1970 which was identified by the changepoint analysis in all regions. For the Guinean region, a model with a constant shape parameter but a third-degree location parameter was most suitable for explaining the distribution of probabilities for the AMAX time series. The curve changed from higher discharge (~1200 m^3s^{-1}) in 1969 to lower (~500m^3s^{-1}) discharges in the 1970s and 1980s, and then half-way back up (~800 m^3s^{-1}) by 2012. For the Sahelian and Sudanian time series models, a linear trend in the location parameter and again a constant shape parameter show the best fit. In the Sahelian region, the peak moved from ~750 m^3s^{-1} to 1500 m^3s^{-1} and in the Sudanian region from ~1200 m^3s^{-1} to 1700 m^3s^{-1}. In the Sudanian and Sahelian regions together, the distributions are flatter than in the Guinean region. This means that the frequency of the AMAX in the analyzed subregions do change linearly, meaning that an exemplary increase in the mean annual flood peak of 100 m^3s^{-1} would result in a corresponding increase for the 50- or 500-year return interval of 100 m^3s^{-1}, as well. The analysis suggests that linear models are sufficiently complex to explain the dynamics of AMAX during the period analyzed, from the beginning of the dry conditions around 1970 until 2012. In addition, the linear trends found confirm the positive trends observed in AMAX (chapter 3.4.1) for the Sahelian and Sudanian time series since the 1970s and for the Guinean time series since the 1980s.

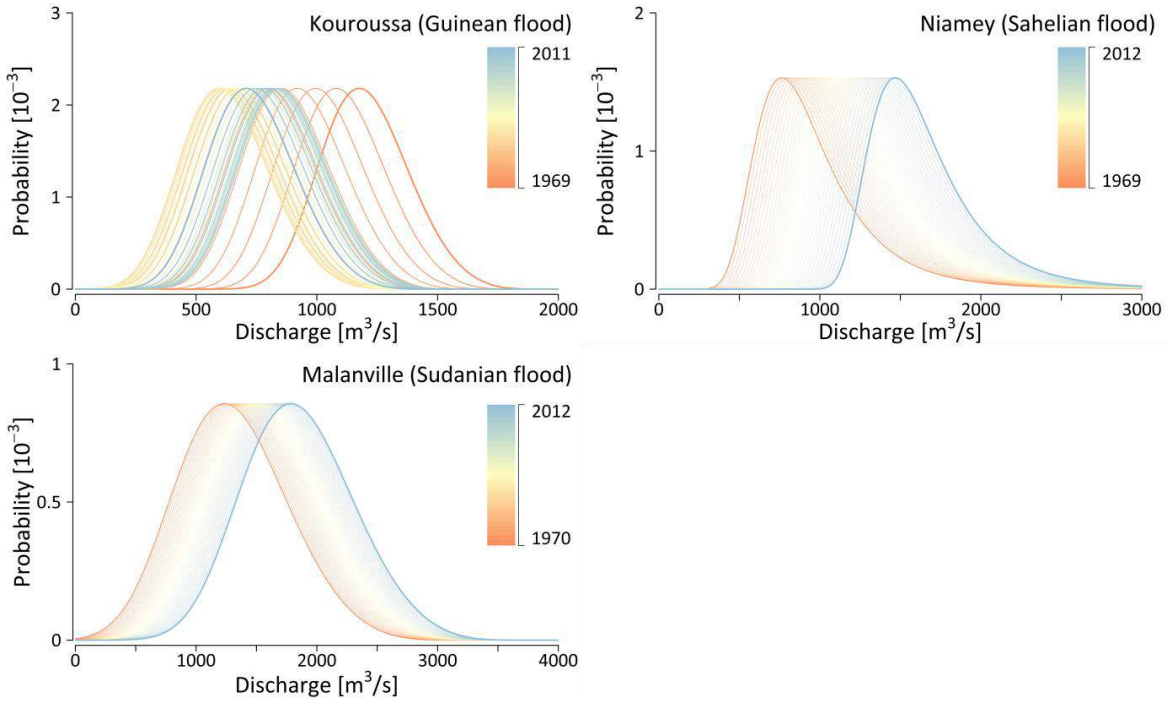

Figure 20 Non-stationary extreme value probability distributions for Kouroussa, Niamey and Malanville.

In order to verify the results of the NSGEV, wavelet power spectra are applied to the same time series (Figure S3) none of the wavelets could a significant change in variance be detected during the last four decades, which supports the finding that no changes in variability occurred in AMAX, but only linear trends for the flood magnitude.

3.4.4. Attribution of changes in annual flood peaks

3.4.4.1. Analysis of precipitation, heavy precipitation, runoff coefficients and flashiness

Figure 21 presents the AMAX, the annual precipitation in the corresponding hydrological year and, as a measurement for heavy precipitation, the 95th percentile of the daily precipitation for the four subregions. Since the NSGEV distribution of the subregions revealed linear models to be best suitable after 1980, we limited the analysis to this time period. In addition, this timespan also corresponds to the period when the data on people affected by floods was available.

We found a significant positive trend for the AMAX, annual precipitation and heavy precipitation in all four regions. The test for autocorrelation was only positive for the AMAX time series of the Guinean region. Here, we then removed the autocorrelation as described in chapter 3.2.1. The strongest trend for AMAX with an increase between 30% and 40% can be found in the Sahelian, Sudanian and Benue regions. In the Guinean region, the trend for AMAX is ~20% until 2012. The annual precipitation during the same period increased ~15% in the Guinean, Sahelian and Sudanian regions, and only ~10% in

the Benue region. The heavy precipitation expressed by the 95th percentile increased proportionally in all regions between 20% and 30%.

The coefficient between the detrended AMAX and the detrended precipitation time series in the corresponding rainy season did not show a significant trend in any of the regions. We also tested trends for the runoff coefficient with the detrended time series of the mean discharge and the rainfall in the rainy season. It showed the same temporal characteristics, and the curve was very similar to the coefficient for AMAX and contained neither trend (not shown).

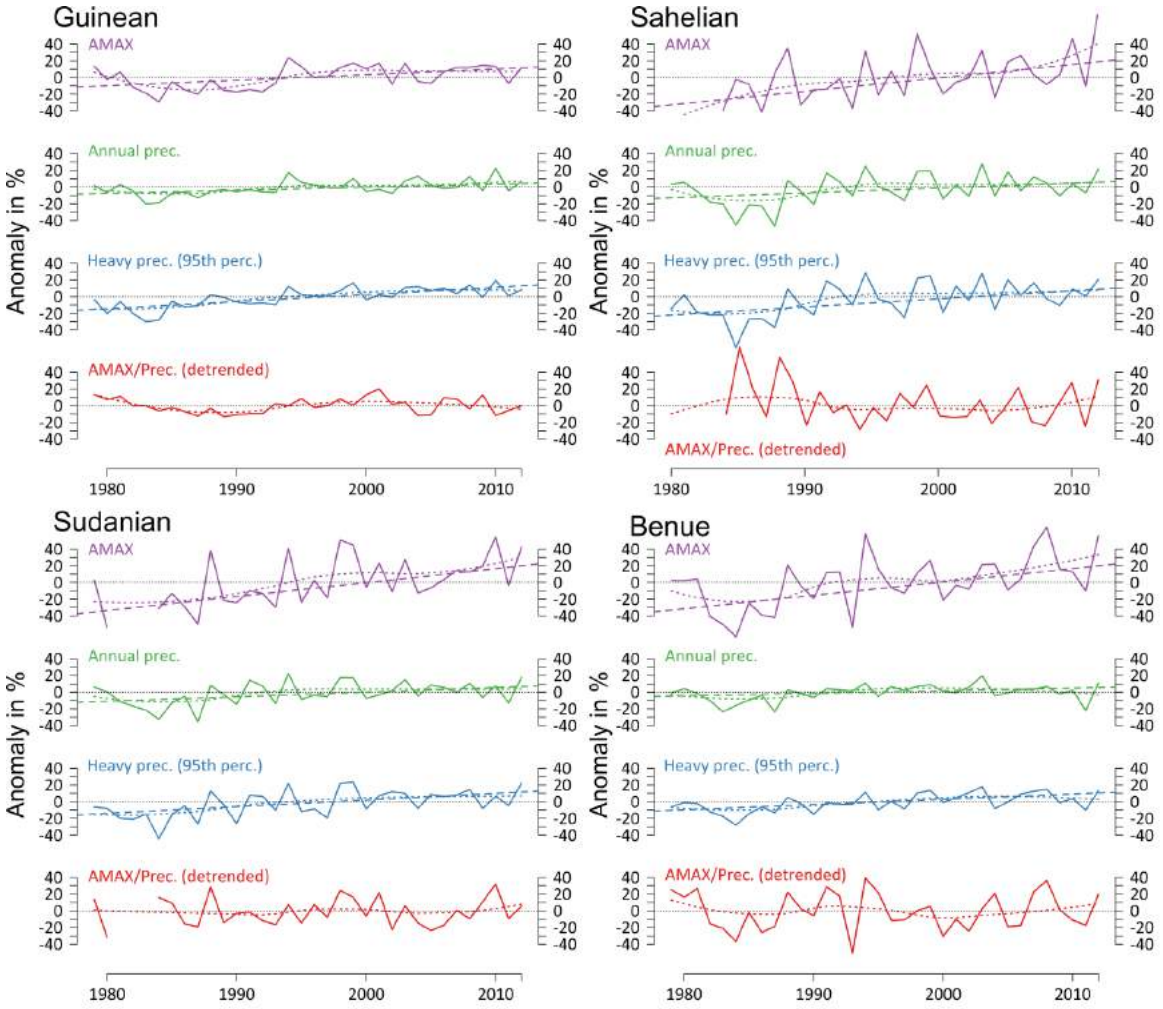

Figure 21 AMAX, annual precipitation, heavy precipitation and runoff coefficient (AMAX/Prec.) for the four subregions of the Niger basin as an anomaly, with Loess curve (dotted line). The Theil-Sen estimator trend is added as a dashed line when the Mann Kendall test was positive (α=0.05).

Figure 22 shows the anomaly of flashiness via the yearly Richards-Baker index for discharge data and heavy precipitation as the 95th percentile for the four subregions. For Koulikoro and Niamey, there are significant positive trends in flashiness since 1960, which increase greater than heavy precipitation. Especially for the Sahelian gauge Niamey, this

increase is extreme, from ~-50% to ~+40%. For Malanville in the Sudanian region, the gaps in the daily data are too large to estimate a trend in the flashiness. Still, the available data also indicates an increase in flashiness. In contrast, the gauge at Lokoja indicates a minor decrease in flashiness after the millennium.

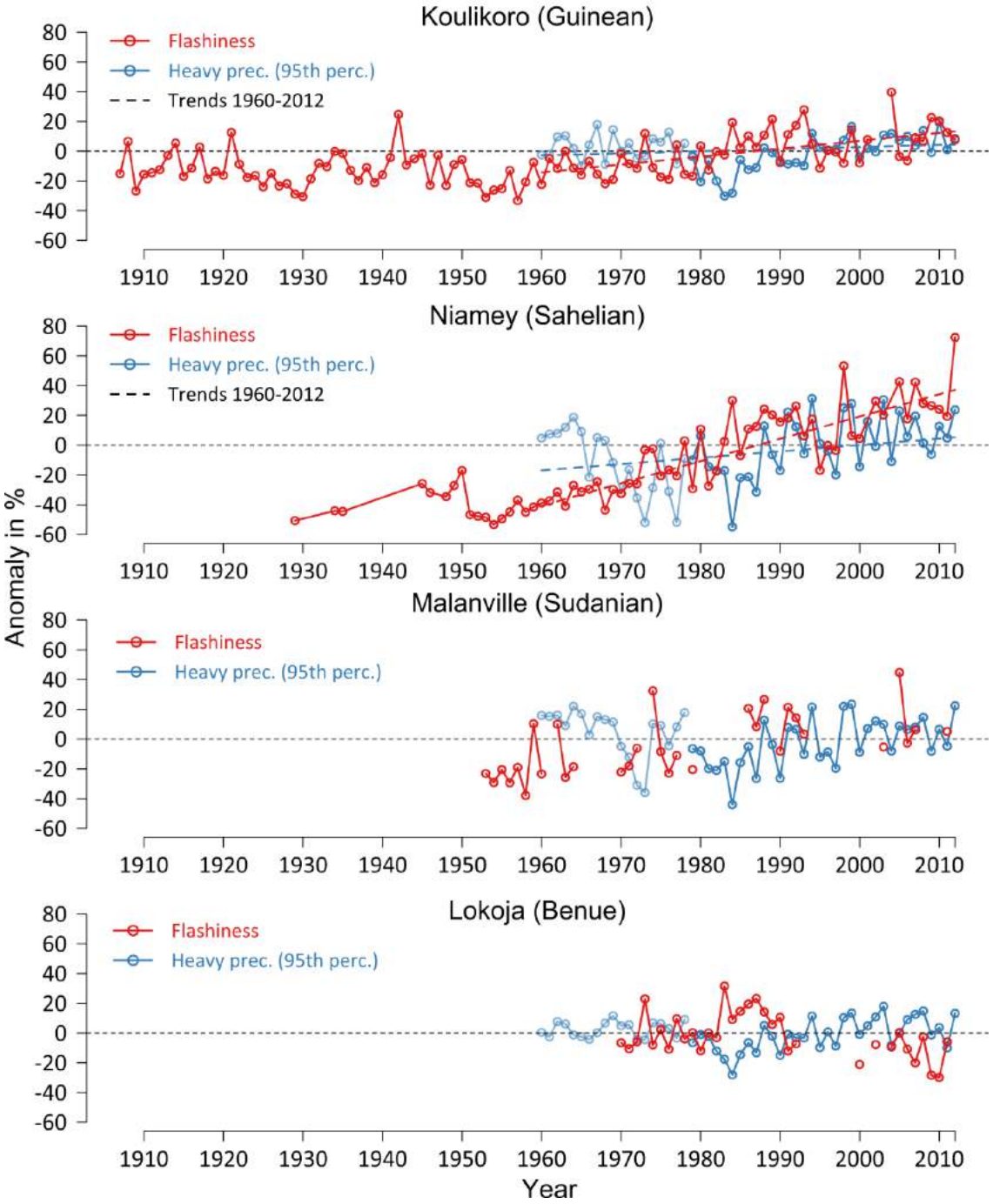

Figure 22 Anomaly of Richards-Baker flashiness index and heavy precipitation (95th percentile) for representative gauges in the Guinean (Koulikoro), Sahelian (Niamey), Sudanian (Malanville) and Benue (Lokoja) subregions. The normalization is based on the years 1960-2012 for which precipitation data is available. The Theil-Sen estimator trend is added as a dashed line for Koulikoro and Niamey. For Malanville and Lokoja, measurements are not sufficient to estimate the trend.

3.4.4.2. Correlations with the Atlantic Multidecadal Oscillation

In order to determine whether the Atlantic Multidecadal Oscillation (AMO) could provide information on flood magnitudes and trends, the similarity of patterns and correlations were evaluated. The changepoints in the AMO were identified for the same period for which discharge data is available (1907-2012) (Figure 23). The three changepoints found for the AMO correspond to points found for the AMAX time series. The point in the beginning of the twenties is reflected in the changepoint in the Guinean AMAX and the changepoint at the beginning of the 1990s in the Benue, Sudanian and Guinean regions upstream of the IND. However, the changepoint detected for the AMO at the beginning of the 1960s is delayed in the AMAX time series of all regions around 1970. The correlation between the AMO and AMAX is moderate for all regions and has a ρ of around 0.5 (Table 3, supplementary material Figure S 7). The correlation of the AMO with the precipitation is also moderate in the respective source regions. In the Guinean region, the value is higher compared to the AMAX, with ρ = 0.54. For the other regions, ρ is slightly smaller (around 0.45, see Table 3).

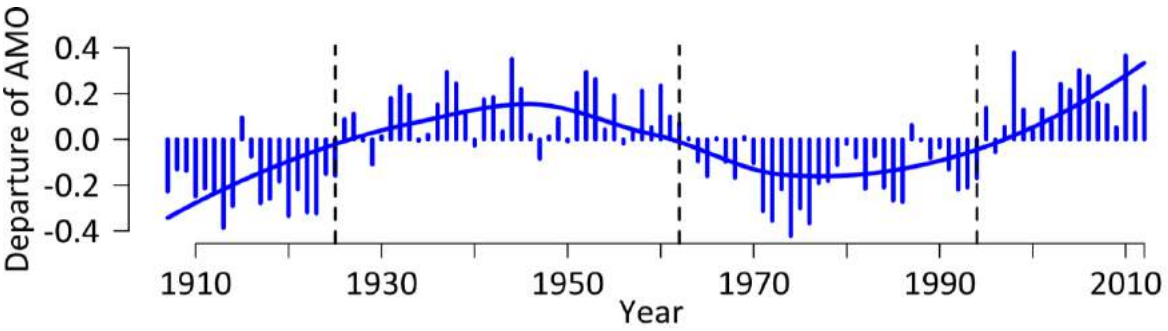

Figure 23 Atlantic Multidecadal Oscillation with LOESS curve as a blue line and detected changepoints as dotted black lines.

Table 3 Spearman´s correlations of the Atlantic Multidecadal Oscillation with AMAX and precipitation for the regions. All correlations are significant.

	Guinean	Sahelian	Sudanian	Benue
Corr (AMAX, AMO)	0.47	0.51	0.55	0.48
Corr (Prec., AMO)	0.54	0.46	0.45	0.45

3.4.5. The "Sahel Paradox"

The flood originating in the Guinean highlands experiences its peak before it enters the IND, usually around October. Due to the increasing distance and the buffering/retention effect of the wetlands, the flood peak leaves the IND with a delay of approximately three months. Therefore, it arrives in the middle section of the Niger around January although

rainfall in the Sahelian region falls at the same time as in the Guinean highlands. Thus, here the Guinean and Sahelian regimes generate a flood which can usually be clearly distinguished (exemplarily shown for the Niger at Niamey in Figure 24). The peak of the Guinean flood is already smoothed due to the large watershed and by the dynamics of the IND, whereas the peak of the local Sahelian flood is more jagged and separated into different peaks for local tributaries (Descroix et al., 2012).

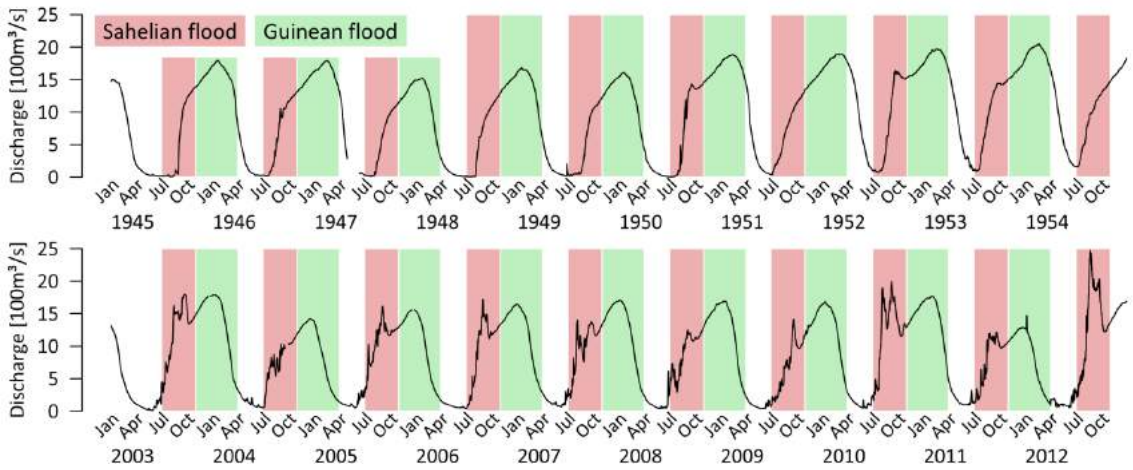

Figure 24 Hydrograph of the Niamey gauging station with Sahelian flooding (red) and Guinean flooding (green) for the period from 1945 to 1954 (dominant feature: single peak) and 2003 to 2012 (dominant feature: multiple peaks).

In Figure 25, the evolution of AMAX for both flood peaks at Niamey is plotted in relation to the annual precipitation in the corresponding source area. For the Sahelian peak, heavy precipitation is also plotted. For the Guinean peak, heavy precipitation is not shown, since the source area in the Guinean highlands is located ~1500km from the gauge in Niamey and these events do not have a noticeable effect here. The systematic detection of the Sahelian peak supports the finding of Descroix et al. (2012) that the AMAX regime in the middle section of the Niger has changed distinctively over the past 30 years. Between 1930 and 1980, a year with a separate peak for the Sahelian flood was rather an exception in Niamey (see also the differences in Figure 24). Since 1983, only one year showed no separate Sahelian peak and since then, the peak was even higher for nine years compared to the Guinean flood (Figure 25, top). This effect is connected to the "Sahelian Paradox", which is illustrated in Figure 25 for the Sahelian peak. The positive trend in AMAX of the Sahelian peak already started in the 1970s. In contrast, the related rainfall data shows a further decrease in annual precipitation until the middle of the 1980s. The data for heavy precipitation in the region shows similar trends and turning points as that for annual precipitation. Therefore, heavy precipitation cannot explain the paradox of increasing discharge despite decreasing rainfall. Since the end of the 1980s, all three trends show the same direction and hence the paradox does not exist anymore, even if the underlying process might still be continuing. For the Guinean peak, this effect is completely absent

and the evolution of the AMAX series corresponds to the annual precipitation. For the time series of the Guinean flood peak, the minimum for AMAX and precipitation are located in the middle of the 1980s, i.e. analogues to the precipitation in the Sahelian region. Hence, the Sahelian and Guinean flood peaks are decoupled even when observed at the same gauging station.

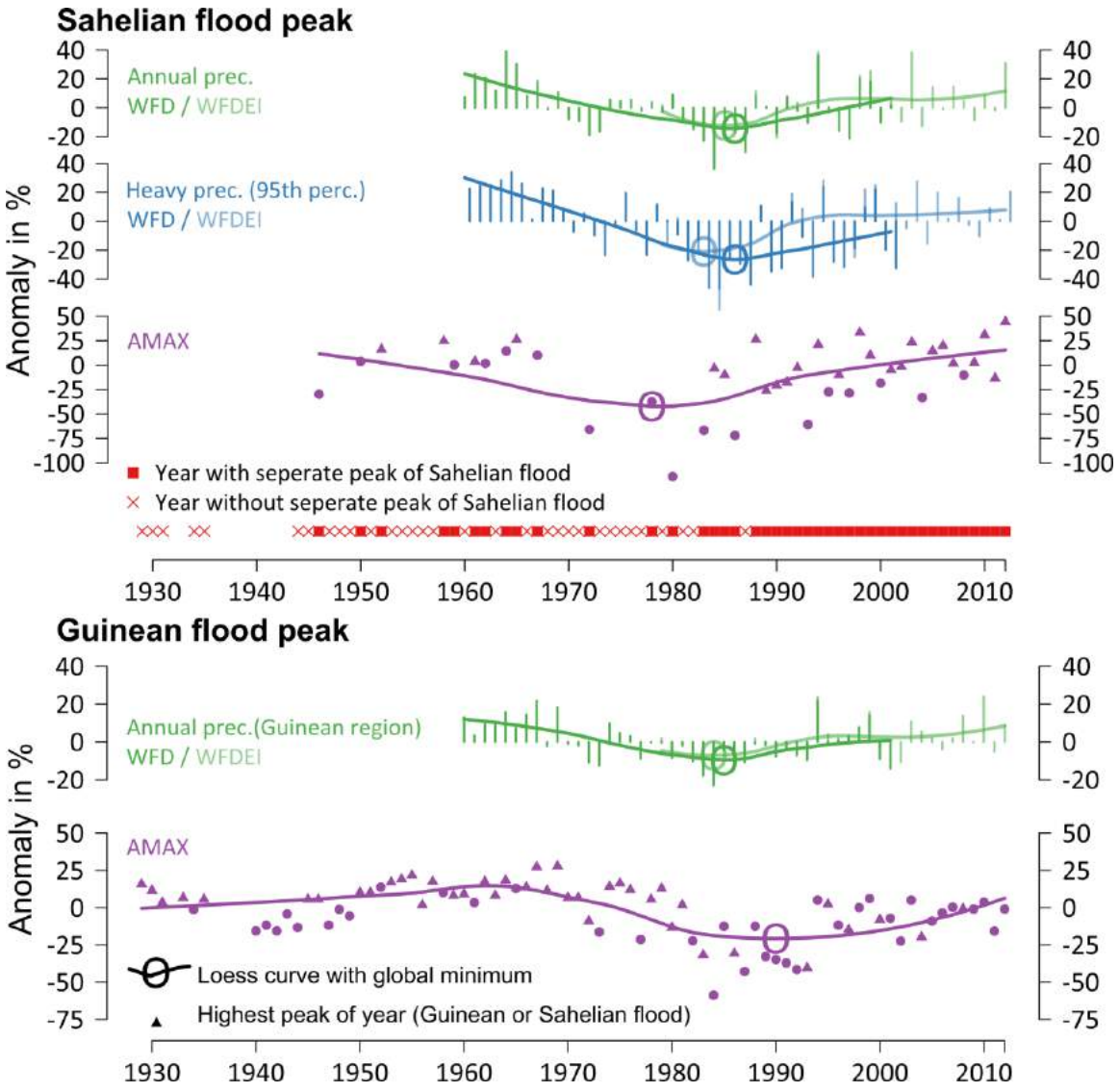

Figure 25, top: Sahelian AMAX for the Niamey station and annual/ heavy precipitation from WFD and WFDEI for the Sahelian region. The red squares and crosses at the bottom of the upper figure mark years with and without separate peaks of Sahelian flooding. Bottom: Guinean AMAX for the Niamey station and annual precipitation from WFD and WFDEI for the Guinean region, all with Loess curves and global minima and as an anomaly in %.

3.5. Discussion

3.5.1. The return to wet conditions and the increasing number of catastrophic floods

The concurrence of changepoints for the annual maximum discharge (AMAX) time series in the regions with a changepoint around 1970 and another around 1990 (Figure 18) supports the findings by previous studies of a decadal climatic pattern in West Africa (e.g. Nicholson et al., 2000; Sarr et al., 2013). The period from ~1970 to ~1990 was in general exceptionally dry in West Africa, and this also holds for the flood peaks. In the Sahelian, Sudanian and Benue regions, the mean during this period was ~35% lower compared to the preceding period. The subsequent return of wetter conditions in West Africa (Jury, 2013) is again reflected in increased flood peaks which almost reach the same level as before the dry period. In the Guinean region, the recovery is less distinct and the flood peaks started to increase again later. In all regions, the positive trend is continuing (Figure 21). Especially in the Sahelian region, the AMAX reached levels in recent years that have not been observed since recording began (Figure 25). Particularly remarkable is the increase in frequency and magnitude of Sahelian flooding, which was also found by Descroix et al. (2012). Even in the wet 1960s, the Guinean flood peak was always higher than the Sahelian peak. This changed during the last three decades, and the trend for the Guinean and Sahelian floods are now decoupled. Since 1980, the Sahelian flood was higher than the Guinean in nine of the years. In Niamey, the flood peak of 2012 was the highest peak since the beginning of records in 1929 (Figure 25, top). Further downstream in the Sudanian region, we see the same decoupled patterns; however, the trend is less distinct and the AMAX does not reach the values of the 1960s (Figure 8, bottom).

The increasing AMAX in all four regions is not connected to a change in the flood regime. The distribution of the extreme stays the same, but on a different level (Figure 20). Especially in the case of the Kouroussa gauge in the Guinean region, we can see that the shape of the distribution moved from the higher level at the beginning of the 1970s to a lower level, and stabilized in the recent past to a level between the two latter stages. This holds also for the Sahelian and Sudanian regions; however, the change in the location parameter is more distinct for the Sahelian station Niamey.

The patterns of increasing AMAX magnitudes are reflected by the number of people affected by floods in all the regions (Figure 17). The trend is significant as well, and strongly correlated to the AMAX in all regions (Figure 18). The most extreme increase, an exponential increase, occurs in the Sahelian and Sudanian regions. In Figure 15, we can see no difference in the number of catastrophic floods reported for the four regions. The marks are distributed along the Niger River and its tributaries without showing a distinct cluster in the Sahelian and Sudanian regions. However, the number of people affected shows distinct differences in the recent past for these two regions when compared to the other parts of the basin. We explain the more extreme increase in people affected by floods

for the Sudanian and Sahelian regions with two main causes. First, the increase in the level of AMAX compared to the preceding periods is more pronounced than in the other regions (see chapter 3.5.2). In the Guinean and Benue regions, flood plains such as the IND or the Benue wetlands (Uluocha and Okeke, 2004) are inundated in case of a flood event and thereby reduce high flood peaks, while in the drier regions these retention areas are missing, leading to higher flood peaks and subsequently more "catastrophic" events in these areas. Second, the population increase in these subregions is about 1% greater compared to the more southern subregions (Central Intelligence Agency, 2013). In addition, in these regions the traditional knowledge of strategies for handling flood magnitudes might be less widespread than in wetter subregions (Tschakert et al., 2010). In the Guinean and Benue regions some of the traditional knowledge might still exist, since in these regions the current flood levels are still lower than those experienced during the 1960s.

3.5.2. Attribution of the changes in the flood regime and the "Sahelian paradox"

The evolution of AMAX in the Niger basin is closely related to the evolution of the Atlantic Multidecadal Oscillation (AMO) (Figure 23). The correlations between the AMO and the AMAX, as well as for the precipitation, are high for all subregions. The dry periods around the 1970s and 1980s (Figure 18) reflect the negative values of the AMO, and the recovery occurring since the 1990s can be also explained by its changes. The extremely high AMO values in the years 1998 and 2012 resulted in major flooding events in the same years in the Niger basin, with exceptional high AMAX values (Figure 18).

The question of whether climatic variabilities or land-use changes are the dominant drivers of the increasing AMAX is complex. The focus on the "Sahelian Paradox" reveals most clearly the influence of both drivers. The extreme increase in flashiness for Niamey after 1960 supports the influence of land-use change (Figure 22). Sealed soils, crusting and deforestation lead to more direct runoff due to less infiltration, as proposed by Descroix et al. (2012). Figure 25 illustrates the fact that the increase in heavy precipitation started later than the increase in AMAX. Therefore, heavy precipitation can be excluded as the cause of the "Sahelian Paradox"; instead, land-use change is the most plausible explanation.

Descroix et al. (2012) concluded that, based on their findings of decreasing rainfall, the recent increase in flooding in the Sahelian region and especially in the region around Niamey are not related to a climatic changes but only to land cover changes due to more intensive agricultural use. However, our findings contradict this conclusion for the Sahelian region and the other subregions. The trend prevailing since the 1990s in rainfall as well as in extreme events is significant and can at least partly explain the increase in AMAX. In addition, the absence of a trend in the detrended runoff coefficient time series indicates that land-use change at least plays no dominant role in the increase in AMAX (Figure 21). The increase in precipitation as the driver for the increased flooding in the

Sahelian region is a fact also supported by Aich et al. (2014). The study shows that for four basins in Africa an increase in precipitation in drier regions with a rather low runoff coefficient leads to proportionally higher increases in discharge compared to regions with a wetter climate, where an increase in precipitation has less influence. Hence, wet years in the dry Sahelian and, less distinctly, in the Sudanian region, lead to proportionally higher discharges than in the Guinean or Benue regions of the Niger basin.

Also, the non-linear trend in heavy precipitation (Figure 21) supports the view that climatic variability is the main driver of the change. The study by Panthou et al. (2014) comes to the same results by analyzing a multitude of rainfall stations in the Sahel region with up-to-date statistical methods. They were also able to detect a significant trend of extreme events increasing. These results contradict the findings of Descroix et al. (2012) for the Sahelian region, who detected trends neither for total precipitation nor for heavy precipitation. In their study, they analyzed station data from one weather station at Niamey collectively for 5 decades from 1960 to 2010. However, there is a significant trend in the observed data for Niamey for the period 1980-2013 in the annual precipitation and an even stronger trend in the heavy precipitation (Figure S 1, Niamey), both of which correspond to the trends detected in the reanalysis data.

3.6. Conclusions and summary

The increasing flood risk in the Niger basin is caused by an increase in all three relevant factors: population, vulnerability and hazards. The substantial increase in inhabitants affected by floods in the Sahelian and Sudanian subregions is the result of the greatest increase in all of these factors in these subregions. With regard to the hazards, we find evidence for a general return to wet conditions since the end of the 1980s in time series of annual maximum discharge (AMAX) and precipitation in the Niger basin. The Non-stationary Generalized Extreme value (NSGEV) and wavelet analysis show linear trends in AMAX. No change in the variance and form of distribution occurred in the last three decades. The Atlantic Multidecadal Oscillation is strongly correlated to the AMAX, and might be worth considering for use as an indicator of flood risk, e.g. for dam management.

With regard to the causes of the increased flood hazards and the AMAX, we identified the variability and trends in precipitation in the Niger basin as the main causes. The changes in flashiness prove the influence of land-use change on the hydrograph; however, the analysis of changes in the runoff coefficient reveals that this effect does not determine the magnitude of AMAX. In the special case of the “Sahel Paradox”, the effect of land-use change on the magnitude of AMAX becomes visible, but also here precipitation seems to play the major role in the increase. In order to quantify the share of annual precipitation, land-use change, and the non-linear increase in heavy precipitation, a detailed modelling study could bring more clarity and provide conclusive evidence. In addition, the role of groundwater in the region is very complex (Leduc et al., 2001; Mahé, 2009) and should be

addressed systematically. Detailed modelling studies on a subregional level are also necessary to project future flood risks in the Niger basin. Such an effort should include land-use change and population vulnerability. In order to halt the trend of increasing flood risk, especially in the Sahelian and Sudanian subregions, the action plan of the NBA should be implemented, which includes more dams. In addition, more adapted settlement and housing policies are required and early warning systems based on forecasting and hydrological modelling should be implemented in the Niger basin.

Acknowledgements

We thank the IMPACT2C project for financing this study and the Niger Basin Authority (NBA) for providing data.

References

Aich, V., Liersch, S., Vetter, T., Huang, S., Tecklenburg, J., Hoffmann, P., Koch, H., Fournet, S., Krysanova, V., Müller, E. N. and Hattermann, F. F.: Comparing impacts of climate change on streamflow in four large African river basins, Hydrol. Earth Syst. Sci., 18(4), 1305–1321, doi:10.5194/hess-18-1305-2014, 2014.

Akaike, H.: A new look at the statistical model identification, IEEE Trans. Automat. Contr., 19(6), 716–723, doi:10.1109/TAC.1974.1100705, 1974.

Albergel, J.: Sécheresse, désertification et ressources en eau de surface. Application aux petits bassins du Burkina Faso, Influ. Clim. Chang. Clim. Var. Hydrol. Regime Water Resour. (Proceedings Vancouver Symp. August 1987)., 168 [online] Available from: http://itia.ntua.gr/hsj/redbooks/168/hysj_168_01_0355.pdf (Accessed 6 February 2014), 1987.

Amogu, O., Descroix, L. and Yéro, K.: Increasing river flows in the Sahel?, Water [online] Available from: http://www.mdpi.com/2073-4441/2/2/170 (Accessed 11 November 2013), 2010.

Andersen, I., Dione, O., Jarosewich-Holder, M. and Olivry, J. C.: Niger River Basin: A Vision for Sustainable Management (Directions in Development), edited by K. G. Golitzen, World Bank Publications, Washington DC. [online] Available from: http://www.amazon.com/Niger-River-Basin-Sustainable-Development/dp/0821362038 (Accessed 11 November 2013), 2005.

Auger, I. and Lawrence, C.: Algorithms for the optimal identification of segment neighborhoods, Bull. Math. Biol., 51(1), 39–54, doi:10.1016/S0092-8240(89)80047-3, 1989.

Baker, D. B., Richards, R. P., Loftus, T. T. and Kramer, J. W.: A new Flashiness Index: Characteristics and Applications to Midwestern Rivers and Streams, J. Am. Water Resour. Assoc., 40(2), 503–522, doi:10.1111/j.1752-1688.2004.tb01046.x, 2004.

Di Baldassarre, G., Montanari, A., Lins, H., Koutsoyiannis, D., Brandimarte, L. and Blöschl, G.: Flood fatalities in Africa: From diagnosis to mitigation, Geophys. Res. Lett., 37(22), doi:10.1029/2010GL045467, 2010.

Brakenridge, G. R.: Global Active Archive of Large Flood Events, [online] Available from: http://floodobservatory.colorado.edu/Archives/index.html., 2013.

Central Intelligence Agency: The World Factbook 2013-14, [online] Available from: https://www.cia.gov/library/publications/the-world-factbook/index.html, 2013.

Cleveland, W. S. and Devlin, S. J.: Locally Weighted Regression: An Approach to Regression Analysis by Local Fitting, J. Am. Stat. Assoc., 83(403), 596–610, doi:10.1080/01621459.1988.10478639, 1988.

Coles, S., Bawa, J., Trenner, L. and Dorazio, P.: An introduction to statistical modeling of extreme values, Springer London, London, UK., 2001.

Dee, D. P., Uppala, S. M., Simmons, A. J., Berrisford, P., Poli, P., Kobayashi, S., Andrae, U., Balmaseda, M. A., Balsamo, G., Bauer, P., Bechtold, P., Beljaars, A. C. M., van de Berg, L., Bidlot, J., Bormann, N., Delsol, C., Dragani, R., Fuentes, M., Geer, A. J., Haimberger, L., Healy, S. B., Hersbach, H., Hólm, E. V., Isaksen, L., Kållberg, P., Köhler, M., Matricardi, M., McNally, A. P., Monge-Sanz, B. M., Morcrette, J.-J., Park, B.-K., Peubey, C., de Rosnay, P., Tavolato, C., Thépaut, J.-N. and Vitart, F.: The ERA-Interim reanalysis: configuration and performance of the data assimilation system, Q. J. R. Meteorol. Soc., 137(656), 553–597, doi:10.1002/qj.828, 2011.

Delgado, J. M., Apel, H. and Merz, B.: Flood trends and variability in the Mekong river, Hydrol. Earth Syst. Sci., 14(3), 407–418, doi:10.5194/hess-14-407-2010, 2010.

Descroix, L., Bouzou, I., Genthon, P., Sighomnou, D., Mahe, G., Mamadou, I., Vandervaere, J.-P., Gautier, E., Faran, O., Rajot, J.-L., Malam, M., Dessay, N., Ingatan, A., Noma, I., Souley, K., Karambiri, H., Fensholt, R., Albergel, J. and Olivry, J.-C.: Impact of Drought and Land – Use Changes on Surface – Water Quality and Quantity: The Sahelian Paradox, in Current Perspectives in Contaminant Hydrology and Water Resources Sustainability, edited by P. Bradley, InTech., 2013.

Descroix, L., Esteves, M., Souley Yéro, K., Rajot, J.-L., Malam Abdou, M., Boubkraoui, S., Lapetite, J. M., Dessay, N., Zin, I., Amogu, O., Bachir, A., Bouzou Moussa, I., Le Breton, E. and Mamadou, I.: Runoff evolution according to land use change in a small Sahelian catchment, Hydrol. Earth Syst. Sci. Discuss., 8(1), 1569–1607, doi:10.5194/hessd-8-1569-2011, 2011.

Descroix, L., Genthon, P., Amogu, O., Rajot, J.-L., Sighomnou, D. and Vauclin, M.: Change in Sahelian Rivers hydrograph: The case of recent red floods of the Niger River in

the Niamey region, Glob. Planet. Change, 98-99, 18–30, doi:10.1016/j.gloplacha.2012.07.009, 2012.

Descroix, L., Mahé, G., Lebel, T., Favreau, G., Galle, S., Gautier, E., Olivry, J.-C., Albergel, J., Amogu, O., Cappelaere, B., Dessouassi, R., Diedhiou, A., Le Breton, E., Mamadou, I. and Sighomnou, D.: Spatio-temporal variability of hydrological regimes around the boundaries between Sahelian and Sudanian areas of West Africa: A synthesis, J. Hydrol., 375(1-2), 90–102, doi:10.1016/j.jhydrol.2008.12.012, 2009.

Dijkstra, H. A., Raa, L., Schmeits, M. and Gerrits, J.: On the physics of the Atlantic Multidecadal Oscillation, Ocean Dyn., 56(1), 36–50, doi:10.1007/s10236-005-0043-0, 2006.

Durbin, J. and Watson, G.: Testing for serial correlation in least squares regression. I, Biometrika, 37(3-4), 409–428 [online] Available from: http://biomet.oxfordjournals.org/content/37/3-4/409.short (Accessed 10 March 2014), 1950.

Durbin, J. and Watson, G.: Testing for serial correlation in least squares regression. II, Biometrika, 38(1-2), 159–178 [online] Available from: http://www.jstor.org/stable/2332325 (Accessed 10 March 2014), 1951.

EM-DAT: The OFDA/CRED International Disaster Database, Univ. Cathol. Louvain, Brussels, Belgium [online] Available from: www.emdat.be, 2013.

Enfield, D. B., Mestas-Nuñez, A. M. and Trimble, P. J.: The Atlantic Multidecadal Oscillation and its relation to rainfall and river flows in the continental U.S., Geophys. Res. Lett., 28(10), 2077–2080, doi:10.1029/2000GL012745, 2001.

Fekete, B. M., Vorosmarty, C. J. and Grabs, W.: Global, composite runoff fields based on observed river discharge and simulated water balances, Koblenz, Germany., 1999.

Hundecha, Y., St-Hilaire, A., Ouarda, T. B. M. J., El Adlouni, S. and Gachon, P.: A Nonstationary Extreme Value Analysis for the Assessment of Changes in Extreme Annual Wind Speed over the Gulf of St. Lawrence, Canada, J. Appl. Meteorol. Climatol., 47(11), 2745–2759, doi:10.1175/2008JAMC1665.1, 2008.

Jury, M. R.: A return to wet conditions over Africa: 1995–2010, Theor. Appl. Climatol., 111(3-4), 471–481, doi:10.1007/s00704-012-0677-z, 2013.

Killick, R., Fearnhead, P. and Eckley, I. A.: Optimal Detection of Changepoints With a Linear Computational Cost, J. Am. Stat. Assoc., 107(500), 1590–1598, doi:10.1080/01621459.2012.737745, 2012.

Knight, J. R., Folland, C. K. and Scaife, A. A.: Climate impacts of the Atlantic Multidecadal Oscillation, Geophys. Res. Lett., 33(17), L17706, doi:10.1029/2006GL026242, 2006.

Kron, W.: Flood Risk = Hazard • Values • Vulnerability, Water Int., 30(1), 58–68, doi:10.1080/02508060508691837, 2005.

Leduc, C., Favreau, G. and Schroeter, P.: Long-term rise in a Sahelian water-table: the Continental Terminal in South-West Niger, J. Hydrol., 243(1-2), 43–54, doi:10.1016/S0022-1694(00)00403-0, 2001.

Liersch, S., Cools, J., Kone, B., Koch, H., Diallo, M., Reinhardt, J., Fournet, S., Aich, V. and Hattermann, F. F.: Vulnerability of rice production in the Inner Niger Delta to water resources management under climate variability and change, Environ. Sci. Policy, 1–16, doi:10.1016/j.envsci.2012.10.014, 2012.

Mahé, G.: Surface/groundwater interactions in the Bani and Nakambe rivers, tributaries of the Niger and Volta basins, West Africa, Hydrol. Sci. J., 54(4), 704–712, doi:10.1623/hysj.54.4.704, 2009.

Mahe, G., Lienou, G., Descroix, L., Bamba, F., Paturel, J. E., Laraque, A., Meddi, M., Habaieb, H., Adeaga, O., Dieulin, C., Chahnez Kotti, F. and Khomsi, K.: The rivers of Africa: witness of climate change and human impact on the environment, Hydrol. Process., 27(15), 2105–2114, doi:10.1002/hyp.9813, 2013.

Mann, H. B.: Nonparametric Tests Against Trend, Econometrica, 13(3), 245–259, 1945.

Merz, B.: Hochwasserrisiken: Möglichkeiten und Grenzen der Risikoabschätzung, E. Schweizerbartsche Verlagsbuchhandlung, Stuttgart., 2006.

Merz, B., Vorogushyn, S., Uhlemann, S., Delgado, J. and Hundecha, Y.: More efforts and scientific rigour are needed to attribute trends in flood time series, Hydrol. Earth Syst. Sci. Discuss., 9(1), 1345–1365, doi:10.5194/hessd-9-1345-2012, 2012.

MunichRe: NatCatSERVICE, [online] Available from: http://www.munichre.com/en/reinsurance/business/non-life/georisks/natcatservice/default.aspx, 2013.

Nelson, A.: African Population Database, Sioux Falls., 2004.

Nicholson, S. E., Some, B. and Kone, B.: An Analysis of Recent Rainfall Conditions in West Africa, Including the Rainy Seasons of the 1997 El Niño and the 1998 La Niña Years, J. Clim., 13(14), 2628–2640, doi:10.1175/1520-0442(2000)013<2628:AAORRC>2.0.CO;2, 2000.

Niger Basin Authority, (NBA): Elaboration of an Action Plan for the Sustainalble Development of the Niger Basin. Phase 2: Master Plan for the Development and Managment, Niamey, Niger., 2007.

Ogilvie, A., Mahé, G., Ward, J., Serpantié, G., Lemoalle, J., Morand, P., Barbier, B., Diop, A. T., Caron, A., Namarra, R., Kaczan, D., Lukasiewicz, A., Paturel, J.-E., Liénou, G. and Clanet, J. C.: Water, agriculture and poverty in the Niger River basin, Water Int., 35(5), 594–622 [online] Available from:

http://www.tandfonline.com/doi/abs/10.1080/02508060.2010.515545 (Accessed 11 November 2013), 2010.

Ozer, P., Hountondji, Y. and Manzo, O. L.: Evolution des caractéristiques pluviométriques dans l'est du Niger de 1940 a 2007, Geo-Eco-Trop., 33, 11–30 [online] Available from: http://orbi.ulg.ac.be/handle/2268/78267 (Accessed 6 February 2014), 2009.

Paeth, H., Fink, A. H., Pohle, S., Keis, F., Mächel, H. and Samimi, C.: Meteorological characteristics and potential causes of the 2007 flood in sub-Saharan Africa, Int. J. Climatol., 31(13), 1908–1926, doi:10.1002/joc.2199, 2011.

Page, E.: Continuous inspection schemes, Biometrika, 41(1/2), 100–114 [online] Available from: http://www.jstor.org/stable/2333009 (Accessed 2 March 2014), 1954.

Panthou, G., Vischel, T. and Lebel, T.: Recent trends in the regime of extreme rainfall in the Central Sahel, Int. J. Climatol., doi:10.1002/joc.3984, 2014.

Panthou, G., Vischel, T., Lebel, T., Blanchet, J., Quantin, G. and Ali, A.: Extreme rainfall in West Africa: A regional modeling, Water Resour. Res., 48(8), doi:10.1029/2012WR012052, 2012.

Sarr, M. A., Zoromé, M., Seidou, O., Bryant, C. R. and Gachon, P.: Recent trends in selected extreme precipitation indices in Senegal – A changepoint approach, J. Hydrol., 505, 326–334, doi:10.1016/j.jhydrol.2013.09.032, 2013.

Sen, P.: Estimates of the regression coefficient based on Kendall's tau, J. Am. Stat. Assoc., 63(324), 1379–1389 [online] Available from: http://amstat.tandfonline.com/doi/abs/10.1080/01621459.1968.10480934 (Accessed 10 March 2014), 1968.

Sighomnou, D., Descroix, L., Genthon, P., Mahé, G., Moussa, I. B., Gautier, E., Mamadou, I., Vandervaere, J.-P., Bachir, T., Coulibaly, B., Rajot, J.-L., Issa, O. M., Abdou, M. M., Dessay, N., Delaitre, E., Maiga, O. F., Diedhiou, A., Panthou, G., Vischel, T., Yacouba, H., Karambiri, H., Paturel, J.-E., Diello, P., Mougin, E., Kergoat, L. and Hiernaux, P.: La crue de 2012 à Niamey : un paroxysme du paradoxe du Sahel ?, Sci. Chang. planétaires / Sécheresse, 24(1), 3–13, doi:10.1684/sec.2013.0370, 2013.

Tarhule, A.: Damaging Rainfall and Flooding: The Other Sahel Hazards, Clim. Change, 72, 355–377, doi:10.1007/s10584-005-6792-4, 2005.

Theil, H.: A rank-invariant method of linear and polynomial regression analysis, Ned. Acad. Wetensch. Proc, 53, 386–392 [online] Available from: http://link.springer.com/chapter/10.1007/978-94-011-2546-8_20 (Accessed 10 March 2014), 1950.

Torrence, C. and Compo, G. P.: A Practical Guide to Wavelet Analysis, Bull. Am. Meteorol. Soc., 79(1), 61–78, doi:10.1175/1520-0477(1998)079<0061:APGTWA>2.0.CO;2, 1998.

Tschakert, P., Sagoe, R., Ofori-Darko, G. and Codjoe, S. N.: Floods in the Sahel: an analysis of anomalies, memory, and anticipatory learning, Clim. Change, 103(3-4), 471–502, doi:10.1007/s10584-009-9776-y, 2010.

Uluocha, N. O. and Okeke, I. C.: Implications of wetlands degradation for water resources management: Lessons from Nigeria, GeoJournal, 61(2), 151–154, doi:10.1007/s10708-004-2868-3, 2004.

United Nations, Department of Economic and Social Affairs, P. D.: World Population Prospects: The 2012 Revision, Key Findings and Advance Tables. Working Paper No. ESA/P/WP.227., 2013.

Weedon, G. P., Gomes, S., Viterbo, P., Shuttleworth, W. J., Blyth, E., Österle, H., Adam, J. C., Bellouin, N., Boucher, O. and Best, M.: Creation of the WATCH Forcing Data and Its Use to Assess Global and Regional Reference Crop Evaporation over Land during the Twentieth Century, J. Hydrometeorol., 12(5), 823–848, doi:10.1175/2011JHM1369.1, 2011.

Yue, S., Pilon, P., Phinney, B. and Cavadias, G.: The influence of autocorrelation on the ability to detect trend in hydrological series, Hydrol. Process., 16(9), 1807–1829, doi:10.1002/hyp.1095, 2002.

Zwarts, L.: Will the inner Niger delta shrivel up due to climate change and water use upstream. [online] Available from: http://scholar.google.de/scholar?hl=de&q=Will+the+Inner+Niger+Delta+shrivel+up+due+to++climate+change+and+water+use+upstream?&btnG=&lr=#0 (Accessed 11 November 2013), 2010.

Zwarts, L., Beukering, P. Van, Kone, B. and Wymenga, E.: The Niger, a Lifeline: Effective Water Management in the Upper Niger Basin, Altenburg & Wymenga Ecologisch Onderzoek BV., 2005.

Water 2015, 7(6), 2796-2820
doi:10.3390/w7062796

4. CLIMATE OR LAND USE? – ATTRIBUTION OF CHANGES IN RIVER FLOODING IN THE SAHEL ZONE

Valentin Aich [1,*], Stefan Liersch [1], Tobias Vetter [1], Jafet C.M. Andersson [2], Eva N. Müller [3] and Fred F. Hattermann [1]

[1] Potsdam Institute for Climate Impact Research (PIK), Potsdam, Germany
[2] Swedish Meteorological and Hydrological Institute (SMHI), Norrköping, Sweden
[3] Institute of Earth and Environmental Science, University of Potsdam, Potsdam, Germany

* Corresponding author: Valentin Aich

Journal: Water (Water)
Status: Published

Abstract: This study intends to contribute to the ongoing discussion on whether land use and land cover changes (LULC) or climate trends have the major influence on the observed increase of flood magnitudes in the Sahel. A simulation-based approach is used for attributing the observed trends to the postulated drivers. For this purpose, the ecohydrological model SWIM (Soil and Water Integrated Model) with a new, dynamic LULC module was set up for the Sahelian part of the Niger River until Niamey, including the main tributaries Sirba and Goroul. The model was driven with observed, reanalyzed climate and LULC data for the years 1950–2009. In order to quantify the shares of influence, one simulation was carried out with constant land cover as of 1950, and one including LULC. As quantitative measure, the gradients of the simulated trends were compared to the observed trend. The modeling studies showed that for the Sirba River only the simulation which included LULC was able to reproduce the observed trend. The simulation without LULC showed a positive trend for flood magnitudes, but underestimated the trend significantly.
For the Goroul River and the local flood of the Niger River at Niamey, the simulations were only partly able to reproduce the observed trend. In conclusion, the new LULC module enabled some first quantitative insights into the relative influence of LULC and climatic changes. For the Sirba catchment, the results imply that LULC and climatic changes contribute in roughly equal shares to the observed increase in flooding. For the other parts of the subcatchment, the results are less clear but show, that climatic changes and LULC are drivers for the flood increase; however their shares cannot be quantified. Based on these modeling results, we argue for a two-pillar adaptation strategy to reduce current and future flood risk: Flood mitigation for reducing LULC-induced flood increase, and flood adaptation for a general reduction of flood vulnerability.

Keywords: simulation-based attribution; Sahel; Niger River; climate variability; hydrological modeling; flood mitigation; flood adaptation

4.1. Introduction

Catastrophic flooding in the Sahelian part of the Niger basin has become an increasing threat during the last decades, leading to more than ten million people affected since the year 2000 (Aich et al., 2014b). Tarhule (2005) were some of the first to bring the topic into academic research, referring to it as the "other Sahelian hazard". Aich et al. (2014b) recently published a comprehensive overview of flooding characteristics within the entire Niger basin, including a review of existing literature and damage statistics from different sources. They found that the Sahelian part of the Niger basin was particularly affected by catastrophic floods, with an almost exponential increase in people affected over the last decades. They also showed that the increasing flood risk was related to the extreme population growth, the increasing vulnerability of the population, and an increase in flood magnitude.

However, the reason for the increase in flood magnitude in the Sahel is still not fully understood. Descroix et al. (2012) stated that climate is not the cause of the phenomenon, since the increasing discharges are accompanied by decreasing rainfall rates. This inconsistency is called "the Sahel Paradox" (SP) and is described in detail in Descroix et al. (2013). Based on their statistical analysis and field observations on infiltration, they argued that the effect of land use and land cover change (LULC), from the local to the meso-scale, caused the increased discharge in the region. The main processes were land clearing and the transformation of savannah into pasture, agricultural land or degraded savannah. This led to soil crusting and a decrease in infiltrability, which subsequently led to an increase in flood magnitude during the heavy rains of the Sahelian rainy season.

In contrast to their study, Aich et al. (2014b) identified climatic changes and a return to wet conditions as the major driver of increasing flood magnitudes in the Niger basin, including the Sahelian region. Aich et al. (2014b) used a data-based attribution approach and compared time series of maximum annual discharge (AMAX) with precipitation time series, as well as time series of flashiness of discharge, as a proxy for LULC. They showed that even though the LULC caused an increase in flashiness since at least the 1960s, the AMAX decreased until the 1980s and they concluded that LULC could not be the major driver of the increased flood regime in the Sahel. In addition, they demonstrated that the SP only existed during the 1970s and 1980s, after which the trends of precipitation and discharge again correlated.

This study intends to contribute to the discussion on the reasons for the increasing flood risk in the Sahelian part of the Niger basin. The specific research question is, to which share LULC and/or climatic changes cause the increase of river flooding in the area. To this end, a simulation-based attribution approach proposed by Merz et al. (2012) is used. Merz et al. (2012) introduced a hypothesis testing framework for attributing changes of flood regime, which is based on testing the consistency or inconsistency of plausible

drivers with the observed flood trend and providing a confidence level for the attribution. They distinguished between a data-based and a simulation-based attribution approach.

The data-based attribution compares flood time series or their statistics with those of the assumed driver, for example, by evaluating the correlation between the time series of the potential cause and effect variables. It is common and widely used in the literature (e.g. Aich et al., 2014b; Giuntoli et al., 2013; Mediero et al., 2014; Murphy et al., 2013; Prosdocimi et al., 2014; Villarini and Strong, 2014; Vorogushyn and Merz, 2012). The simulation-based approach has been used in several studies with conceptual rainfall-runoff models (Andréassian et al., 2003; Gebrehiwot et al., 2013; Harrigan et al., 2013; Schreider et al., 2002; Seibert and McDonnell, 2010). Process-based hydrological models have not been widely used for attribution approaches. There are studies, which distinguish climate change and LULC impacts on historical trends in flood magnitude, but not systematically and within one modeling approach (e.g. Hattermann et al., 2012)). To the best of our knowledge, the only study published which follows the protocol of Merz et al. (2012) is that by Hundecha and Merz (2012). Hundecha and Merz (2012) drove a hydrological model with a large number of stationary and non-stationary climate time series in order to study whether the observed flood trend was climate driven.

In this study, we analyze the effects of LULC on the flood trend using the process-based based ecohydrological model SWIM (Soil and Water Integrated Model) with integrated dynamic land use change. The ecohydrological model is applied to simulate flood discharges for the time period 1950–2009 with two different settings. The discharge is simulated with static land cover as of 1950 in order to show how the discharge would have developed over the last 60 years if there had not been any LULC.

The second/control run implicitly includes past LULC. We hypothesize that the comparison of the modelled discharge of these two scenarios will give some initial quantitative insights into the relative share of LULC and climatic changes on changes in the Sahel flood regimes. There is an ongoing debate over whether the observed “return to wet conditions” in West Africa itself can be attributed to global climate change or is still within the boundaries of natural climatic variability (Jury, 2013; Kandji et al., 2006; Mahe et al., 2013); without taking sides, we refer to the recent changes of the precipitation patterns as “climatic” changes.

Since this study is the first to attribute LULC to flood trends via a process-based hydrological model following the proposed protocol of Merz et al. (2012), it might additionally shed first light on the requirements of data quality/availability and the efficiency of the hydrological model in order to achieve robust attribution statements.

4.2. Materials and Methods

4.2.1. Regional Setting

The Sahelian part of the Niger River is located downstream of Diré in Mali and extends to around Niamey in the state of Niger (Figure 26). This part of the Niger basin until Niamey covers around 297,400 km^2. Its landscape is characterized by plateaus and smooth valleys with long slopes. The climate is semi-arid, with annual precipitation ranging from 267 mm in Ansongo to 540 mm in Niamey. The potential evapotranspiration in the area is 3500 mm per year (Descroix et al., 2012). The typically convective rainfalls occur within the rainy season between June and October. The vegetation in the region and its changes since the 1950s are described in detail in Descroix et al. (2012). The original bushy and woody savannah types have been replaced almost completely by crop fields, pasture and a patchwork of woody savannah vegetation called Tiger Bush. The northern part, in which the Sirba catchment is located, is too dry for effective rain fed agriculture and was therefore turned mainly into extensively or intensively used pastoral land (Figure 27 and Figure 28). In contrast, the southern part in which the Sirba catchment is located has mainly been converted into cropland.

Most of the discharge in the Sahelian part of the Niger originates in its upstream regions within the Guinean highlands. The Inner Niger Delta, a large wetland, limits the Upper Niger basin. The wetland smooths the river flow and protracts the peak. The outlet of the delta is close to Diré, and the flood, generated in the Guinean highlands, occurs between November and January. This flood, referred to as the "Guinean Flood", passes through Niamey between December and the beginning of March (Aich et al., 2014b). Transmission losses are high between Diré and Niamey, resulting in higher annual discharge at Diré compared to Niamey. Little additional runoff is generated locally in the Sahelian part (Amogu et al., 2010a). This locally generated discharge comes mainly from the plateaus of the right-bank subbasins and results in another flood peak in the Sahelian Niger, previous to the Guinean Flood. This first peak occurs during the rainy season (July–November) and is called the "Red Flood" due to the red color of the sedimentary load of the local iron oxide rich soils. The two main tributaries are the Goroul (44,900 km^2) and Sirba Rivers (38,750 km^2), which are analyzed in this study (gauging stations Alcongui and Garbe-Kourou). Both are intermittent rivers, and the annual peaks vary substantially, with values between 35 and 300 m^3/s for Alcongui and 20 and 460 m^3/s for Garbe-Kourou (1950–2009). The vast subbasins to the East reach up into the central Sahara and contribute only a minor amount of inflow, and local tributaries are endorheic most of the year. The Guinean and Red Floods can usually be clearly distinguished. The peak of the Guinean Flood is already smoothed due to the large watershed and the dynamics of the Inner Niger Delta, whereas the peak of the Red Flood is more jagged and flashy. However, in years where the Red Flood is very low, a separate peak cannot be distinguished. This happened regularly

during the 1950s and 1970s but has occurred significantly less often since the 1980s (Aich et al., 2014b).

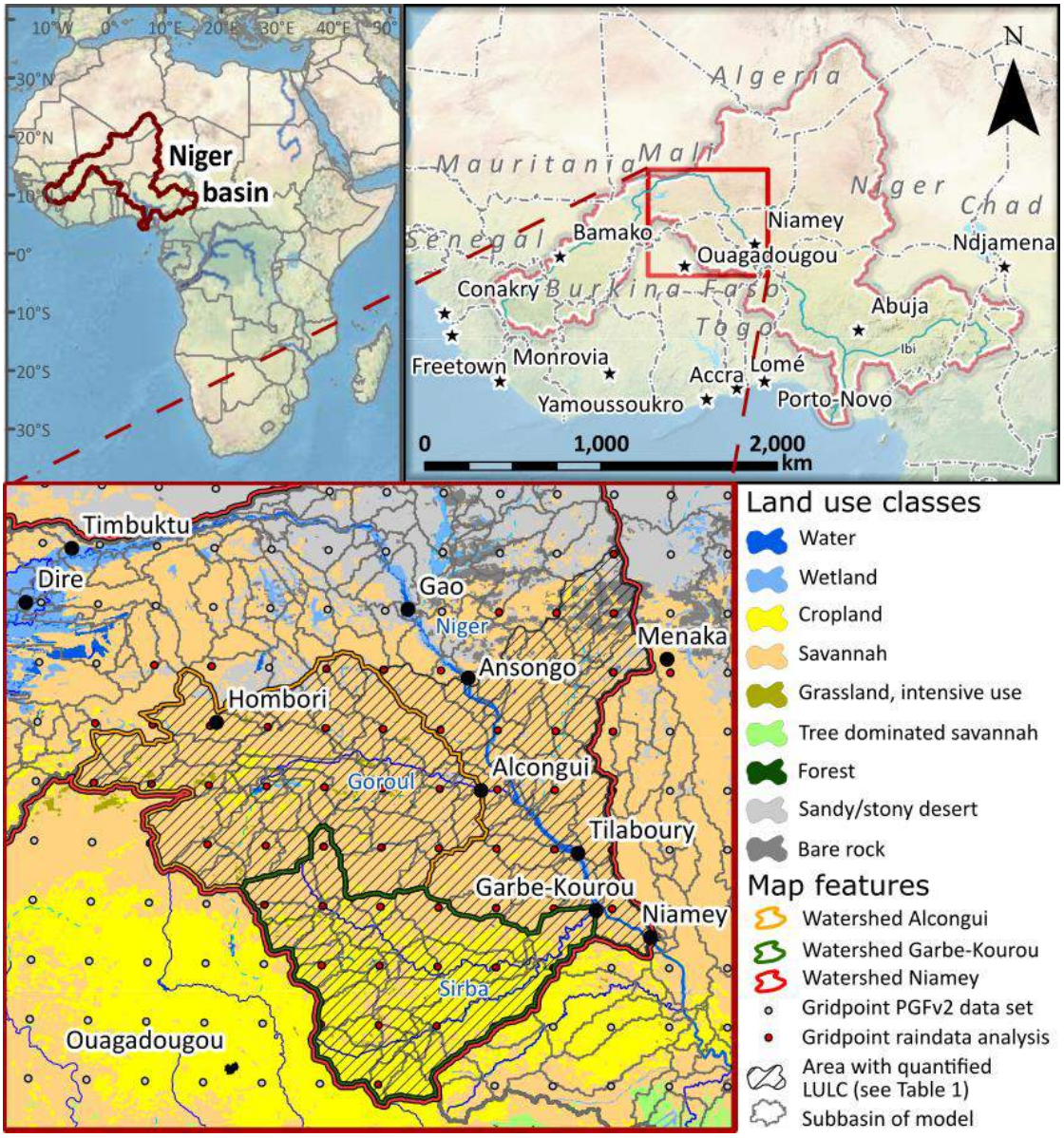

Figure 26 Map of the research area in West Africa including land use classes used in the model as base map in the year 2000. The orange, green, and red outlines mark the watershed of the gauging stations Alcongui (Goroul River), Garbe-Kourou (Sirba River) and the watershed of Niamey (Niger River). The grey dots show the grid of the PGFv2 climate reanalysis data set. The red dots show the grid of the climate data used for the analysis. The hatched area marks the region which is used for the quantification of land use and land cover changes

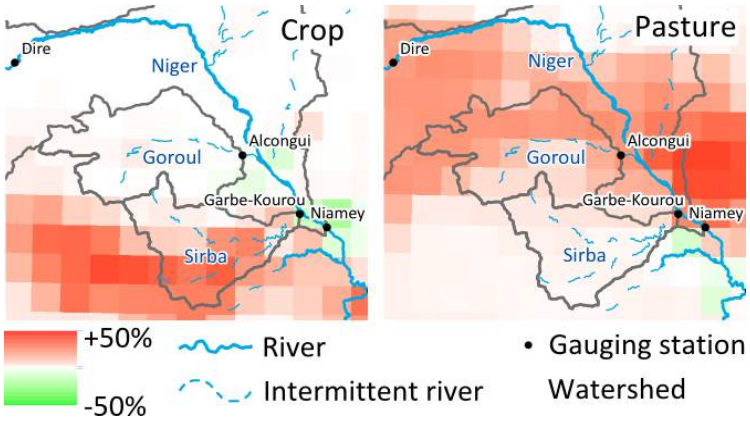

Figure 27 Land use and land cover changes between 1950 and 2005 for crop and pasture after Hurtt et al. (2011).

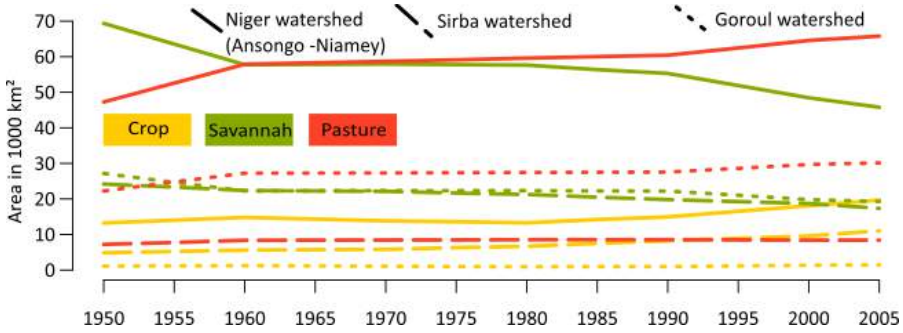

Figure 28 Changes in the main land use classes of crop, savannah, and pasture from 1950 until 2005 for the watershed of the Niger River between Ansongo and Niamey, and the catchments of the Sirba and Goroul Rivers (see area in Figure 26).

4.2.2. Ecohydrological Model and Model Set-Up

The ecohydrological model SWIM (Soil and Water Integrated Model) is a continuous-time (daily) and spatially semi-distributed model of intermediate complexity for river basins (Krysanova et al., 1998). SWIM was developed based on two models: Soil and Water Assessment Tool (SWAT) (Arnold et al., 1993) and MATSALU (Krysanova et al., 1989), with the aim to provide a tool for climate and LULC impact assessment in meso-scale and large river basins. It integrates hydrological processes, vegetation growth, nutrient cycling, erosion and sediment transport at the river basin scale (Huang et al., 2013). The hydrological system of the model comprises four main segments: The soil surface, the root zone of the soil, the shallow aquifer, and the deep aquifer. On the soil surface, the surface runoff is estimated as a non-linear function of precipitation and a retention coefficient. It depends on soil water content, land use, and soil type (modified after the Soil Conservation Service curve number approach (Arnold et al., 1990)). The soil column is subdivided into several layers. In these layers, the water balance is calculated, including precipitation, surface runoff, evapotranspiration, subsurface runoff, and percolation. Hydrological processes

represented in the shallow aquifer are groundwater recharge, capillary rise to the soil profile, lateral flow, and percolation to the deep aquifer. Potential evapotranspiration is calculated using the method of Turc-Ivanov (Wendling and Schellin, 1986). Actual evaporation from soil and transpiration by plants are simulated following the Ritchie concept (Ritchie, 1972).

A simplified Environmental Policy Integrated Climate (EPIC) approach (Williams et al., 1983) is integrated in the model for the simulation of arable crops and other general vegetation types (e.g., pasture, savannah, evergreen forest), using specific parameter values for each crop/vegetation type. The parameter settings of the newest version of the SWAT model are used for the aggregated vegetation types of the SWIM model (Arnold et al., 2013). These parameter settings have been widely used in the African context for LULC studies (e.g., Awotwi et al., 2014; Baker and Miller, 2013; Liersch et al., 2013; Nyeko et al., 2013). The effects of the vegetation on the hydrological processes include the cover-specific retention coefficient, impacting surface runoff and influencing the amount of transpiration. Transpiration is simulated as a function of potential evapotranspiration and leaf area index. A more detailed description of the representation of hydrological processes within SWIM is given in Huang et al. (2013).

SWIM disaggregates a river basin into subbasins and hydrotopes. The subbasins are delineated on the basis of flow accumulation in a Digital Elevation Model. The hydrotopes are created by overlaying the subbasin map with maps of land use and soil. They represent the spatial units used to simulate all water flows and nutrient cycling in soil as well as vegetation growth based on the principle of similarity (*i.e.*, assuming that units within one subbasin that have the same land use and soil types behave similarly). The model was applied for impact studies in several basins in Africa and showed good efficiency for the whole Niger, the Blue Nile, the Limpopo and the Congo (Aich et al., 2014a; Liersch et al., 2013). In addition, a multi-model intercomparison of hydrological models of Vetter et al. (2015) has shown that SWIM is quite capable of simulating flow in the Niger basin.

For this study, the model has been set up for the Sahelian part of the Niger River, from Diré in Mali to Niamey in the state of Niger. Since the model is only used for modeling river flows in the past, monitored discharges are routed into the model at the Diré gauge. The model includes 255 subbasins for the 297,000 km^2 area of the watershed. These subbasins are integrated to form three subcatchments which are the catchments Goroul (station Alcongui), Sirba (station Garbe-Kourou), and Niger (between the stations Diré and Niamey) (Figure 26). These subcatchments were calibrated individually in order to fit the model as closely as possible to the regional conditions (see Chapter 4.2.1).

4.2.3. Dynamic Land Use Change Module

The newly developed land use change module (LUCM) for the SWIM model is used for the first time in this study. It changes the land classes at any frequency or given point in

time, while keeping the instantaneous balance of water and other modelled fluxes constant during the change, for example soil water content (SWC). This means that the number and the areas of hydrotopes within a subbasin can change and new hydrotopes can appear or others disappear.

The land-use status at given points in time (see Chapter 4.2.4.3) are read in by the LUCM (in this study every five years; Shorter frequencies up to a daily change are possible). The LUCM transforms the land classes and rearranges the hydrotopes on the basis of so-called stable units (SU). SU are areas within a subbasin and do not change their extent, like areas with uniform soil, for example. For these SU, fluxes like SWC remain constant during the change, even if the land class changes. Thereby, all given information on LULC on the subbasin level is used, and the transformation of the hydrotopes does not alter the balances of water or other relevant fluxes.

The following two examples shall illustrate the main processes when hydrotopes increase or decrease within a SU. If the shares of crop and pasture increase and the savannah deceases, the SWC of the old hydrotopes have to be newly distributed. The SWC of the savannah is reduced according to its areal share. The residual SWC is then added proportionally to crop and pasture, depending on their areal increase.

In another case, an existing SU consists of cropland and savannah. In the new land use, there is also pasture on the SU. Meanwhile, crop and savannah shrink. In this case, the SWC of crop and savannah is reduced proportionally and the residual SWC is completely added to the new pasture.

These examples show that the balance of the SWC remains constant during the change on the SU. This holds also for all other simulated fluxes. Only parameters connected to vegetation, such as biomass, for example, restart at zero for the additional area or are reduced relative to the areal changes.

4.2.4. Data

4.2.4.1. Climate Data

Climate data are used to drive the simulations and to analyze the total annual precipitation. For the modeling runs, a relatively dense spatial coverage of climate input is needed, since the climate forcing is interpolated for each subbasin (see Chapter 4.2.2). In the data-sparse research area, this can only be provided by reanalysis data sets. For this study, three different data sets have been analyzed and compared to data from six weather stations in the region, in order to check their performance in the face of the requirements for an attribution study with regard to accuracy. The WATCH Forcing Data 20th Century (WATCH) (1950–2001) (Weedon et al., 2011), data from the Global Soil Wetness Project Phase 3 (GSWP3) (Kim, 2014) and the second version of the Global Meteorological

Forcing Dataset for land surface modeling of Princeton University (PGFv2) (Sheffield et al., 2006) (Figure 29 and Figure 30) have been selected as potential model input.

The visual comparison of temperature and precipitation shows that all of the data sets generally have good correspondence with the measured data, yet also all of them have some deficits (PGFv2: Figure 29 and Figure 30, WATCH: Supplementary Material Figure S 9 and Figure S 10, GSWP3: Figure S 12 and Figure S 13). Regarding precipitation, distinct deviations of single years or short periods do occur, as for example in all three data sets for the station Timbuktu during the early 1990s. However, the general trends in precipitation are represented in all three reanalysis products. Annual mean temperatures only rarely deviate more than 1 °C from the observed station data and reproduce the general trends also efficiently. Additional uncertainty derives from the limited evaluation. The comparison only takes six stations into account for the whole region. These points cannot represent the whole area. These uncertainties deriving from the climate data have to be taken into account when discussing the modeling results. The comparison implies that single years should not be compared between the modeling results and observations of discharge. However, since the major trends of the climate data are represented in the analysis, the climate data can be used for reproducing general trends with the model when results are carefully interpreted.

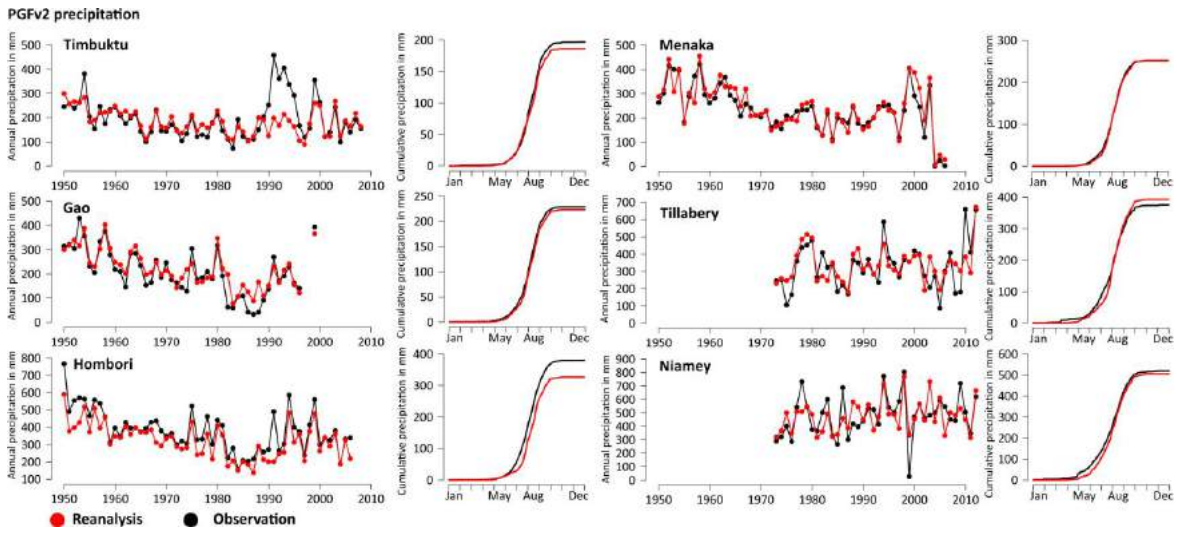

Figure 29 Comparison of precipitation from interpolated PGFv2 reanalysis data (red) with observations from six weather stations (black) in the research area. For each station, the annual precipitation (left) and the cumulative sum of the precipitation of the whole period (right) is depicted.

Since no systematic differences could be detected with regard to data quality, the PGFv2 data set was finally selected since it is the newest of the three data sets. It is a combination of a suite of global observation-based data sets with the National Centers for Environmental Prediction—National Center for Atmospheric Research reanalysis. The

spatial resolution is at 0.5° × 0.5° and for the modeling the 3-hourly data has been aggregated to daily data.

For the precipitation analysis, annual rainfall data is aggregated for each subcatchment (Niger, Sirba, Goroul) by building the mean over all data points in the subcatchment region (Figure 26). Since the Guinean Flood is completely generated in the Upper Niger basin, the related rainfall data was aggregated for this region outside the research area.

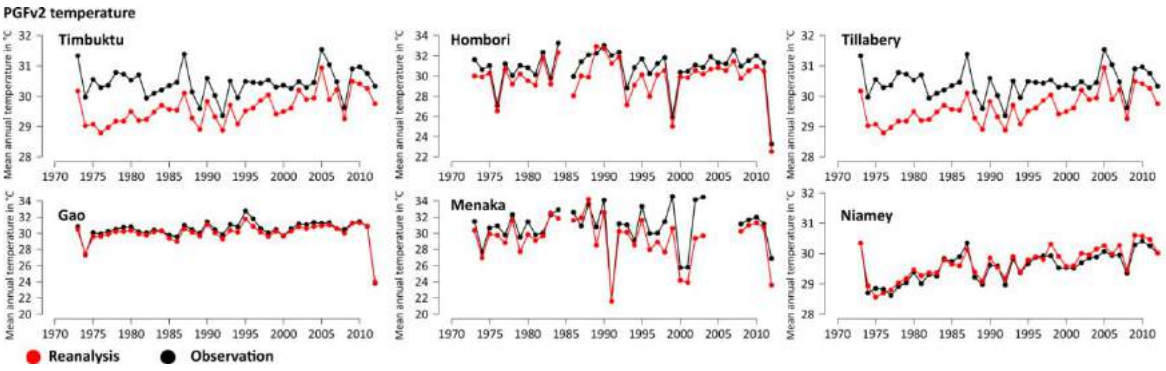

Figure 30 Comparison of mean annual temperature of interpolated PGFv2 reanalysis data (red) with observations from six weather stations (black) in the research area.

4.2.4.2. Discharge Data

Observed discharges from three monitoring stations (Figure 26) were used to calibrate and validate the model and for the analysis of the AMAX. The observed discharge at the Diré station was used as input for the model (see Chapter 4.2.2). The observations are part of the Niger-HYCOS monitoring network, managed by the Niger Basin Authority, which consists of daily water-level readings at more than 100 locations across the basin, as well as accompanying rating curves to compute discharge at these locations (Niger Basin Authority, 2008).

The AMAX for the time series of Alcongui on the Goroul River and Garbe-Kourou on the Sirba River are created by selecting the highest daily discharge per year, with gaps for years where the peak cannot be identified due to missing values. The time series for Niamey has two peaks per year (see Chapter 4.2.1). The second, the Guinean peak, occurs in most of the years after the 31st of December but is still assigned to the rainy season of the previous year. For the Red Flood, the procedure is not straightforward since the peak cannot be distinguished in dry years hidden from the Guinean Flood and thus it cannot be quantified for all years (see Chapter 4.2.1). For the simulation, this problem was solved by simulating the discharge without the inflow of Diré, leading to a clear AMAX value of the Red Flood, generated in the Sahelian part of the Niger basin after Diré. For the observation, it is not possible to filter only the discharge which is generated in the basin downstream of Diré. Therefore, identification of the AMAX depends on a clearly distinguishable first peak of the hydrograph between July and October. For years when the

flood peak cannot be detected since it is too low and hidden under the Guinean flood peak, the AMAX time series contains gaps, which affects the statistical analysis (see Chapter 4.2.7).

4.2.4.3. Land Cover and Land Use Change Data

For the representation of the LULC in the model, maps of the land cover for different periods are needed. For this study, land use maps have been generated in five year steps from 1950 until 2005.

There is no data available which provides this information to the degree of detail necessary for ecohydrological modeling at the meso-scale with regard to land classes. Therefore, the land cover maps have been derived using the information from two different data sets. In the first step, a base map was derived which has the necessary details concerning land cover at a fine spatial resolution. For the base map, land class information was derived from the GLC2000 data set (Bartholomé and Belward, 2005). It differentiates between 27 land classes and has a spatial resolution of $\frac{1}{112}$, which corresponds to 1 km at the equator. It is based on remote sensing data and includes a detailed legend. The GLC2000 classes occurring in the research area have been transformed to the classes of the ecohydrological model (Figure 26, see Chapter 4.2.2).

However, this map only represents the one point in time at which the data was collected (year 2000). Therefore, an additional data set was used which gives information about the change in land cover with regard to crop, pasture, and urban land but for different times in history. The information on areal changes in crop and pasture was obtained from the Land-Use Harmonization project (Hurtt et al., 2011). The harmonized land use scenarios connect historical reconstructions with future scenarios and have been used as a basis for the Earth System Models of the fifth Assessment Report of the Intergovernmental Panel on Climate Change (IPCC). The historical data for the period 1500–2005 are based on the model HYDE (Klein Goldewijk et al., 2010, 2011), and contain information on changes to cropland, pasture and urban land at a 0.5° × 0.5° resolution on an annual basis. The reconstruction of the data set is based on satellite maps for the years they were available and for the more distant past by combining information on population density, soil suitability, distance to rivers or lakes, slopes, and specific biomes. Each grid point of the LULC data contained the percentage of crop, pasture and urban land (Figure 27).

With this information on changes, the base map was altered for each of the 5-year time steps in order to have land use maps which represent the LULC, as shown simplified in Figure 31. The LULC information was added to the base map on the subbasin level of the model, and existing land classes changed accordingly. The land classes of water, wetlands, sandy/stony desert and bare rock have been kept constant in the year 2000. When pasture, crop and/or urban land increase in a subbasin, other natural vegetation land classes like

savannah or forest are proportionally reduced in the same subbasin. If crop, pasture and/or urban land decrease, the land classes of the natural vegetation increase proportionally.

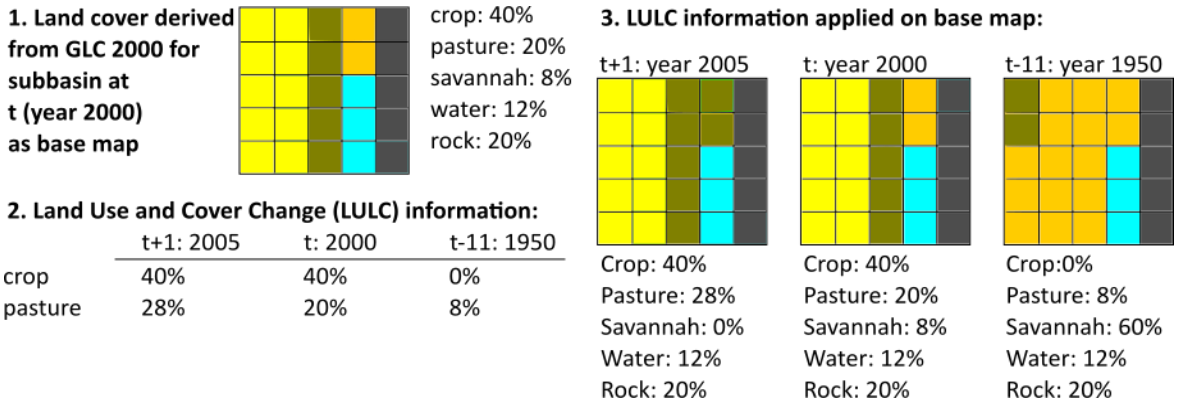

Figure 31 Exemplary process of how the information from the Land Use and Land Cover data of the Land-Use Harmonization project is used on the subbasin level to produce land cover maps for the different years which are then used by the land use change module. The whole square represents one exemplary subbasin, with small squares representing individual stable units (SU).

The emerging land class maps from 1950 until 2005 are used in the model as explained in Chapter 4.2.3. In Figure 28 the changes are quantified for the watershed of Niamey until Ansongo, corresponding to the area marked by climate grid points in Figure 26. The related spatial distribution is shown in Figure 27.

Crop types were derived from a data set for West African crops (Ramankutty, 2004). The four main types in the region are millet, sorghum, cowpea and rice. For every subbasin, the same crop type has been used for the whole period, according to the dominant crop in the data.

4.2.4.4. Soil and Topographic Data

Information on the soils in the research area for the modeling was derived from the Digital Soil Map of the World (FAO et al., 2012). Relevant parameters for the model include depth, clay, silt and sand content, bulk density, porosity, available water capacity, field capacity, and saturated conductivity for each of the soil layers. For the delineation of the subbasins and necessary topographic information, a Digital Elevation Model derived from the Shuttle Radar Topography Missions at a 90 m resolution (Jarvis et al., 2008) was used.

4.2.5. Calibration of the Model

An accurate representation of the main hydrological processes and characteristics of the research is a crucial precondition for a robust modeling attribution. Therefore, the model was calibrated with a standard procedure for SWIM and SWAT (Arnold et al., 2012) via

an automatic calibration using the PEST software package (Doherty, 2005). This is commonly applied, as for example done in the studies of Vetter et al. (2015) on the rivers Rhine (Europe), Upper Niger (Africa), and Upper Yellow (Asia). The calibration was done individually for the Sirba (station Garbe-Kourou), the Goroul (station Alcongui) and the rest of the subcatchment between Diré and Niamey (station Niamey) to take into account the distinctly different geographic attributes. During the calibration, the LUCM was used in order to calibrate/validate the model with correct land use for the respective period and region. The calibrated parameters/factors are static and do not change within a subcatchment and over time. The focus of the calibration and model set-up for all subbasins was to achieve adequate efficiency for streamflow simulations on daily time steps, especially for high flows. Therefore, the main parameters/factors for the calibration were related to groundwater, river routing, saturated conductivity and potential evapotranspiration (Table 4). For the Sirba and Goroul catchments, the parameters related to groundwater and the factors for potential evapotranspiration and saturated conductivity showed the highest sensitivity. Routing parameters were somewhat less sensitive. For the Niger basin between Diré and Niamey without the subcatchments of Goroul and Sirba, the sensitivity for the routing and the potential evapotranspiration was higher and the sensitivity of other parameters lower. This is likely due to the fact that the model is fed monitored data from the Diré gauging station (see Chapter 4.2.2).

Table 4 Calibrated parameters of the ecohydrological model SWIM (Soil and Water Integrated Model) with a short description.

Calibrated Parameter/Factors		Short Description
Groundwater related parameters	Groundwater recession	Rate at which groundwater flow is returned to the stream.
	Groundwater delay	The time it takes for water to leave the bottom of the root zone until it reaches the shallow aquifer where it can become groundwater flow (in days).
	Baseflow factor	The baseflow factor is used to calculate the return flow travel time. The return flow travel time is then used to calculate percolation in the soil from layer to layer.
Correction factor for saturated conductivity		The factor is applied for all soils
Correction factor for potential evapotranspiration		The factor is applied for all subbasins in the respective subbasin.
Routing coefficient		Routing coefficient to calculate the storage time constant of the flow from the initial estimation which is based on channel length and celerity.

Prior to the calibration, the available observed discharge data was checked visually and calibration periods were selected where distinct high and distinct low annual peaks are represented in order to cover a broad range of rainfall-runoff conditions. The period was finally selected when a period of eight years with a low amount of missing data was available (Goroul (Alcongui): 1963–1970, Sirba (Garbe-Kourou): 1986–1994, Niger

(Niamey): 1988–1995). The validation periods are before or after the calibration period, depending on the availability of observations (Goroul (Alcongui): 1971–1978, Sirba (Garbe-Kourou): 1978–1985, Niger (Niamey): 1996–2003). Since there are not enough climatic observations available, reanalysis data is used to drive the model, also during the calibration. The results of the calibration are shown in Table 5.

Table 5 Calibration and validation results of the eco-hydrological model SWIM in Nash-Sutcliff efficiency (NSE) and percent bias (PBIAS) for three stations.

Gauging Stations	Calibration		Validation	
	NSE	PBIAS	NSE	PBIAS
Alcongui (Goroul)	0.58	−0.4	0.55	−16.9
Garbe-Kourou (Sirba)	0.66	22.1	0.49	34.5
Niamey (Niger)	0.86	12.2	0.87	6.9

4.2.6. Sensitivity Analysis of the Effects of LULC on the Hydrological Regime

The representation of the LULC and their effect on the hydrological processes are important for an understanding of the discharge changes. In Figure 32, the effects of different land cover on the modelled hydrological regime are shown for the Sirba and Goroul watersheds. The watersheds have been modelled with three set-ups, with either crop, pasture or savannah vegetation covering the entire subcatchments. The model is run for a period of 10 years (1985–1995). Regarding precipitation, the 10-year period was selected with a rather dry beginning and above-average wet conditions at the end in order to allow for different rainfall-runoff conditions.

The subcatchments covered solely with crops show a strong increase in peak discharges. In the wetter Goroul catchment, this holds true even for the dry years at the beginning of the 10-year period. The results for crop cover correspond to the changes as described in detail in Amogu *et al.* (2010) (Amogu et al., 2010a), Descroix *et al.* 2012 (Descroix et al., 2012) and Descroix *et al.* 2013 (Descroix et al., 2013) for the research area. The LULC processes lead to a decrease in infiltrability and more direct runoff and regeneration of groundwater. They attribute the regeneration of the groundwater to the fast infiltration in the rivers, which carry more water due to the increase in runoff. This effects lead to a higher frequency of flow changes and flashiness. For pasture, this process seems to be much weaker in the modeling results.

These results reflect the sensitivity analysis of different studies of LULC in Africa, using the same land class parameters of the SWAT model. Awotowi *et al.* (2014) (Awotwi et al., 2014) show for West Africa that land use classes of SWAT are generally suitable for West African conditions. They found similar effects of LULC on the hydrology for the Volta basin, where cropland replaced savannah and grassland. Other studies undertaken with SWAT in East Africa studying the effects of LULC focus more on the transformation of forest to cropland (Baker and Miller, 2013; Nobert and Jeremiah, 2012; Nyeko et al.,

2013). Concerning the effect of the transformation from savannah into pasture as taken place mainly in the Goroul catchment, it was not possible to test whether the parameterization of the model reflects the hydrological processes. There is no quantitative data or literature available to the authors which could be used to verify the modelled effects. The potential misparametrization of pasture is discussed in more detail in Chapters 4.3.2 4.3.3.

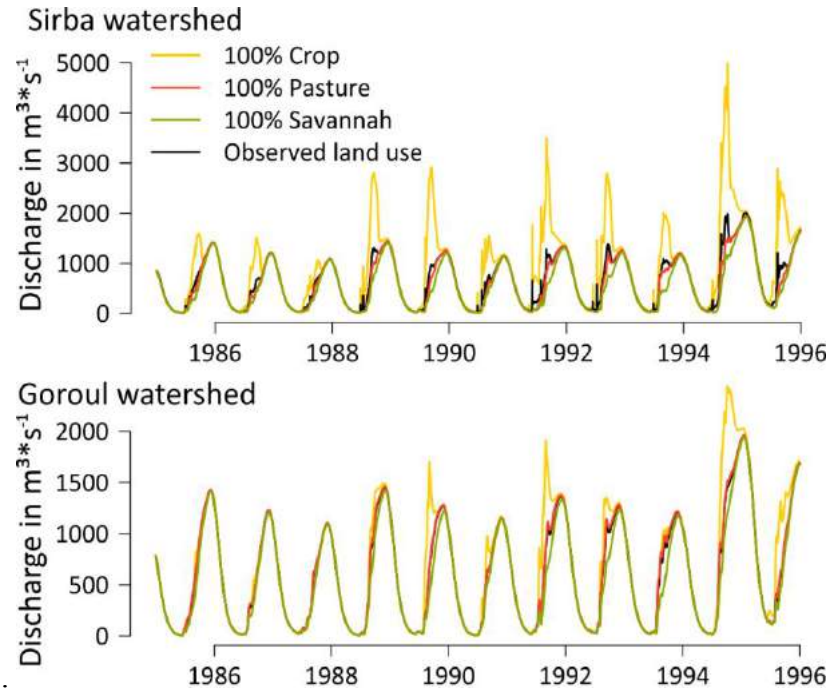

Figure 32 Comparison of discharges with four different land use coverages (100% crop, 100% pasture, 100% Savanna and land use as observed) for the Sirba and Goroul watersheds.

4.2.7. Statistical Methods

In order to make general trends of the time series more clearly visible, the local regression fitting technique LOESS was used (Cleveland and Devlin, 1988). This is a nonparametric regression method that combines multiple regression models in a k-nearest-neighbor-based meta-model (Altman, 2012). When plotted, it generates a smooth curve through a set of data points. It is used to depict nonlinear trends in time series.

Since the absolute values of discharge differ distinctively between the different parts of the catchment, AMAX anomalies are used in order to make the results more easily comparable. The time series of AMAX anomalies is given by the time series of AMAX of the individual years divided by the mean AMAX of the entire AMAX time series of 1950–2009, given as a percentage. The annual rainfall time series are transformed to anomalies accordingly.

Linear trends in the observed and simulated AMAX time series are estimated using the Theil-Sen estimator (Sen, 1968; Theil, 1950). It estimates the slope of a trend and is widely used, since it is insensitive to outliers. Since serial independence is a requirement of the test, the data was checked for autocorrelations using the Durbin-Watson statistic test (Durbin and Watson, 1950, 1951). It tests the null hypothesis that the residuals from an ordinary least-squares regression are not autocorrelated against the alternative that the residuals are autocorrelated. If an autocorrelation of the first order was found, trend-free pre-whitening was applied according to the method proposed by Yue *et al.* (2002) (Yue et al., 2002). It is a procedure to remove serial correlation from time series, and hence to eliminate the effect of serial correlation on the Theil-Sen estimator.

As a result of the gaps in the time series for the Red Flood (see Chapter 4.2.4.2), it is not possible to generate a local regression curve and to identify the minimum of the AMAX time series. The linear trends are therefore only calculated from 1984 to 2009 with five missing years (1986, 1987, 1993, 1995, 1996). This means that the AMAX trends are calculated consistently for the simulations even with these gaps and can therefore be included in the interpretation.

For the calibration and validation, the methods of Nash and Sutcliff (1970) (NSE) (Nash and Sutcliffe, 1970), and percent bias (PBIAS) have been used. The NSE is calculated using the formula.

$$NSE = 1 \frac{\sum_{i=1}^{n}(Q_{obs} - Q_{sim})^2}{\sum_{i=1}^{n}(Q_{obs} - \overline{Q_{obs}})^2} \quad (13)$$

Values for the NSE range from 1 to negative ∞ values. An NSE of 0 means that the model is no better than using average annual discharge as a predictor. If $NSE = 1$, it means that the model is perfectly aligned with the observations. The PBIAS indicates the over- or underestimation of discharge during the calibration or validation period as a percentage. For the evaluation of the NSE and PBIAS the terminology of Moriasi *et al.* (Moriasi and Arnold, 2007) is used (for NSE: very good: $0.75-1.0$, good: $0.65-0.75$, satisfactory: $0.5-0.65$, unsatisfactory: < 0.5; for PBIAS: very good: $< |10|$, good: $|10|-|15|$, satisfactory: $|15|-|25|$, unsatisfactory: $\geq |25|$).

4.2.8. Hypothesis Testing Framework

In order to attribute the increase of discharge observed in the research area to LULC and/or climatic changes, a simulation-based approach within a hypothesis testing framework as proposed by Merz *et al.* (Merz et al., 2012) is applied. The framework consists of the evidence of consistency, the evidence of inconsistency, and the provision of confidence level. In order to show the consistency or inconsistency, the observed trend is compared to the change simulated by the hydrological model, either with or without considering the potential driver LULC. The model which includes all postulated drivers, as

in our case both changes in LULC and climatic regime, should be able to reproduce the observed trends and are therefore control runs. The simulations without one of the postulated drivers, might result in no trends or differing trends. This difference can then be used for the quantification of the influence. In other words, if the model is capable of simulating the observed trend without LULC, it would mean that LULC has no or little influence on the discharge trend and vice versa (within the uncertainty limits of model runs).

In this study, the observed trend is an increase of flood peak magnitude since the 1970s/1980s. Therefore, the AMAX is derived from the observed and simulated daily time series of discharge. The AMAX time series have been transformed from absolute values to anomalies (see Chapter4.2.7) in order to be able to compare the gradients amongst the subcatchments. The gradients of the trends are used as measure for the comparison. Ideally, the second/control run including LULC shows a similar gradient like the observed trend. The difference between the gradients of the run without LULC and the observed then consequently indicates the share of the climatic variability.

Annual rainfall is used as general indicator of the wetness trend in the respective watershed. The rainfall trend mainly helps to illustrate the SP (see Chapter 4.2.1), and whether the simulations are able to reproduce the phenomenon when including LULC.

4.3. Results and Discussion

4.3.1. Validation of the Model

To quantify the efficiency of the model, the NSE and PBIAS were used (see Chapter 4.2.7). The model showed very high efficiency at the gauging station Niamey for the validation period (NSE: 0.87/PBIAS: 6.9) (Figure 33). For the Goroul basin, the results are satisfactory for the NSE (0.55) and slightly unsatisfactory for the Sirba basin (0.49). For the PBIAS, only the validation of the station Alcongui shows satisfactory efficiency (−16.9). At the station Garbe-Kourou, the PBIAS is over 25 and therefore unsatisfactory. The very good performance of the model for the station Niger can be explained by the fact that monitored data was fed into the model at the station Diré, while the reason for the weaker performance of the model in the watersheds of the Goroul and Sirba Rivers after the intensive calibration efforts is unclear. We assume that the climatic reanalysis data for these subcatchments are at above-average deficiency and/or that the land use data for these regions are not accurate. In fact, some years with similar observed hydrographs, like 1974 and 1975 at the Goroul river, for example, are simulated once very accurately and yet in the other year are deficient. An additional reason for the difficulties could be that the discharge of rivers in dry environments is generally more sensitive to climate input due to the low runoff-coefficients (Aich et al., 2014a), which is especially the case for the intermittent rivers Goroul and Sirba. Inaccurate climate forcing is therefore more likely to affect the model performance in drier regions. The reasons, therefore, are the proportionally higher losses in

smaller streams through evapotranspiration, transmission losses, *etc.* compared to large rivers. A certain decrease in rainfall thus leads to a proportionally larger decrease in discharge in dry areas compared to wetter areas (Aich et al., 2014a). Other explanations for the lower performance might be data quality of the streamflow, the parametrization of the land use or other deficits in the model structure, e.g., for the representation of the groundwater. These input data related problems are taken into account in the discussion (see Chapters 4.3.2 and4.3.3).

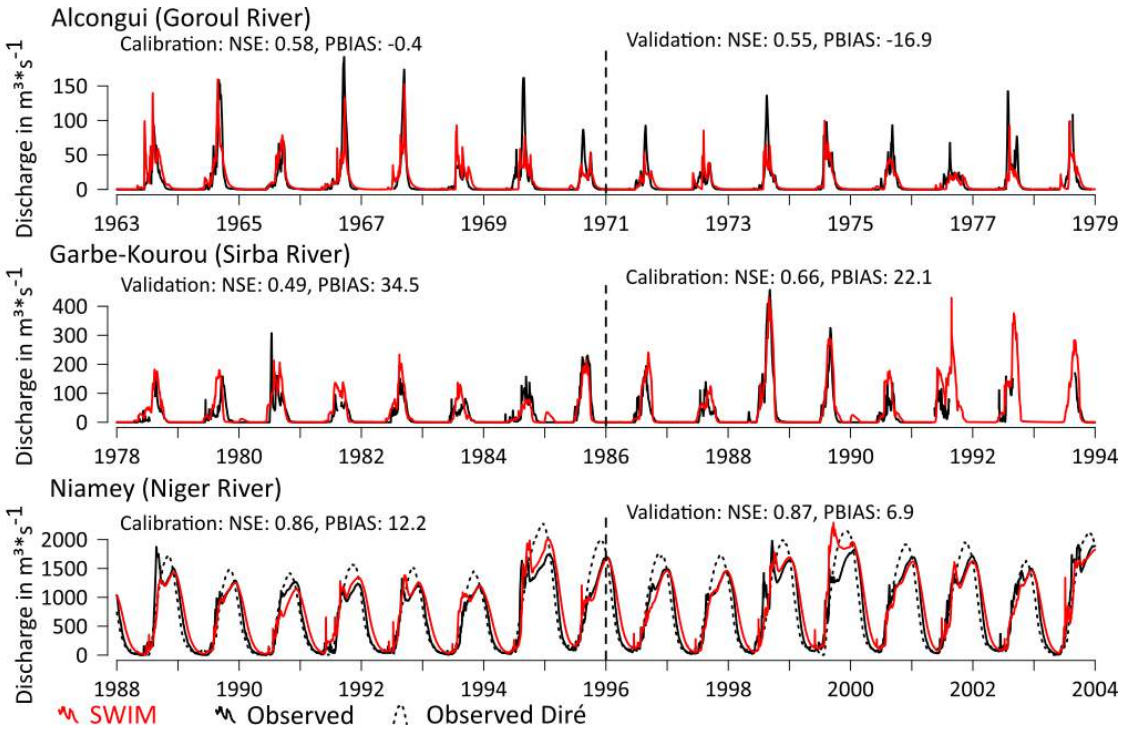

Figure 33 Validation and calibration of the SWIM model for the watersheds of Alcongui, Garbe-Kourou and Niamey for eight-year periods using PGFv2 reanalysis climate forcing. For Niamey, the measured discharge at the Diré gauge is additionally plotted, which is fed into the model.

4.3.2. Attribution of Trends in Annual Maximum Discharges

4.3.2.1. Simulation Results

The gradients of the trend lines for all AMAX anomaly time series are used as a quantitative attribution measure as specified in Chapter4.2.8. (see trend lines in the lower part of Figure 35 and gradients in Table 6) All estimated observed and simulated trends are positive and statistically significant ($\alpha = 0.05$).

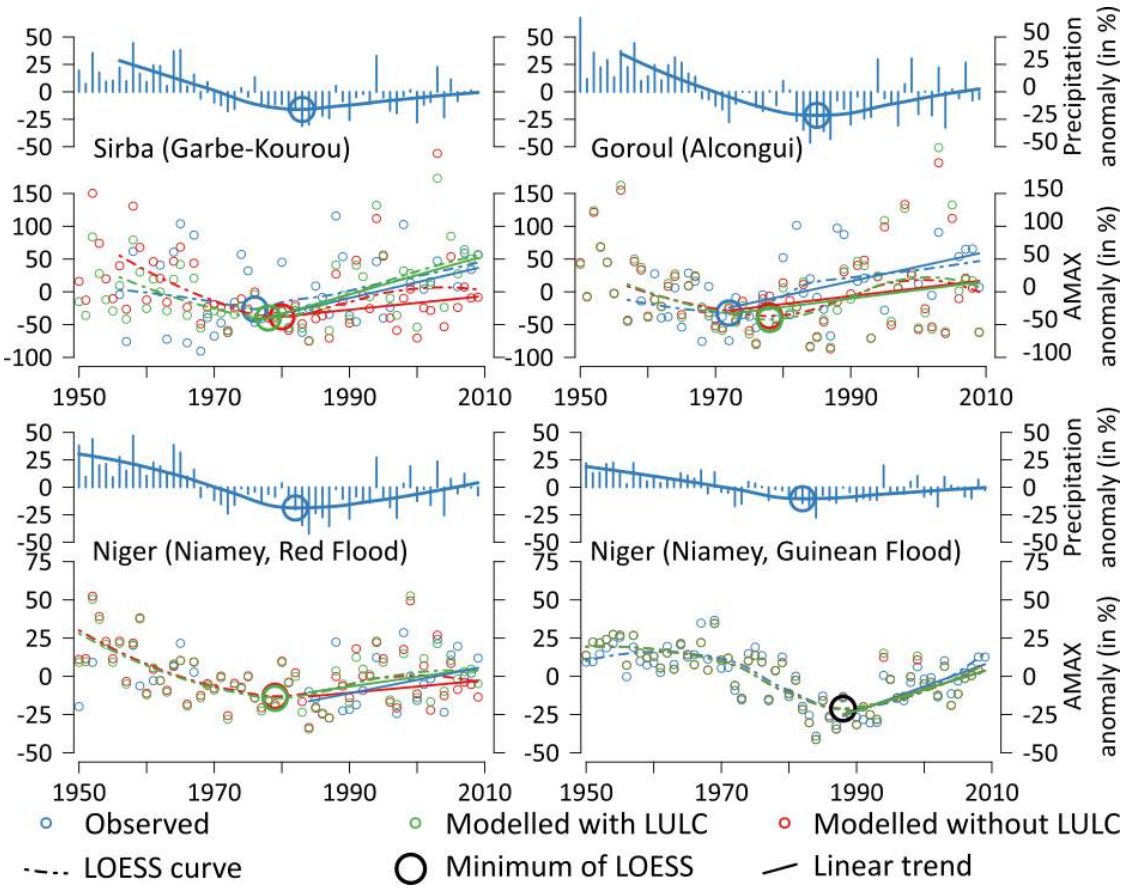

Figure 34 Anomalies of annual maximum discharges for the gauging stations Alcongui (Goroul River), Garbe-Kourou (Sirba River) and differentiated between the Red and the Guinean Flood for Niamey (Niger River). On the top of each region, rainfall anomalies over the respective catchment are plotted. A LOESS curve with a minimum point is added as a dashed line and the Theil-Sen estimators for the discharge trends are plotted as bold lines, beginning at the minimum of the observed discharge points. Please note that, for the observed values of the Red Flood at Niamey, the time series is incomplete (see Chapter 4.2.4.2). Therefore, the LOESS curve is not plotted and the trends start at 1984 (see Chapters 4.2.64.2.7). For the Guinean Flood at Niamey, all minima are on the same point and the circle is plotted in black.

In the Sirba catchment, the simulation run including LULC reproduces the trend of AMAX anomaly adequately (sim_{with} LULC: 2.94, obs.: 2.42, Table 3), whereas the simulation run that assumed no LULC since 1950s does not reproduce the observed trend of AMAX anomaly adequately ($sim_{without}$ LULC: 1.05).In contrast, for the Guinean flood of the Niger River at Niamey, the AMAX anomaly gradients of both simulations are similar to the observed trends of the AMAX anomaly (sim_{with} LULC: 1.37, $sim_{without}$ LULC: 1.36, obs: 1.61). For the so-called Red Flood of the Niger River at Niamey, the simulation with LULC is closer to the observed AMAX trend than the run without considering LULC (sim_{with} LULC: 0.63, $sim_{without}$ LULC: 0.56, obs.: 0.87), but both are not able to reproduce the trend adequately. In the Goroul catchment, the gradients of both simulation runs (sim_{with} LULC: 1.38, $sim_{without}$ LULC: 1.29, obs.: 2.37) significantly underestimate the observed gradient of AMAX anomalies.

The Sahel Paradox (SP) of the Sirba catchment is distinct with an offset between the minima of AMAX and annual rainfall of approximately 10 years. Both simulations show this effect while the SP of the control run is more distinct, with an AMAX minimum close to the observed AMAX minimum.

In the Goroul catchment the SP is very pronounced, too, with an offset of approximately 14 years. Both simulations show the effect while they underestimate the offset by approximately seven years. For the Red Flood at Niamey, it is not possible to detect the magnitude of the SP shift of the observed AMAX due to the missing LOESS curve and minimum (see Chapter 4.2.7). However, both simulations show an offset of around five years, which is in accordance with the findings from the Sirba River.

For the Guinean Flood the effect of the SP does not occur and rainfall and AMAX minima do not show the paradoxical offset.

Table 6 Gradient of the trends of AMAX anomalies as estimated with the Theil-Sen approach.

Gauging Stations	Observed	Simulation w. LULC		Simulation w/o LULC	
		Gradient	% of Observed Gradient	Gradient	% of Observed Gradient
Sirba River (Garbe-Kourou)	2.42	2.94	121%	1.05	43%
Goroul River (Alcongui)	2.37	1.38	58%	1.29	54%
Niger River (Niamey, Red Flood)	0.87	0.63	72%	0.56	64%
Niger River (Niamey, Guinean Flood)	1.61	1.37	85%	1.36	84%

4.3.2.2. Discussion of Simulation Results

The effects of LULC are most pronounced in the model runs for the Sirba subcatchment.

The main LULC in this watershed is a distinct increase in cropland and a reduction of natural savannah (Figure 28). This leads to an increase of surface flow and less evapotranspiration, both represented in the model parametrization. Because the run without LULC generates a trend gradient of 43% of the gradient of the observed trend, this share can be attributed to the climatic changes and, consequently, the other half to the LULC.

The Guinean Flood is almost exclusively controlled by the hydrological setting upstream of the Sahelian Niger. Since this study only simulates the basin downstream of Diré, the LULC effects upstream are not simulated. If there were effects, they are inherent in the observed discharge which was fed into the model at Diré. Still, the absence of any LULC effect when flowing through the Sahelian part, as well as the correlation between the rainfall and the AMAX trends, supports the finding of Aich et al. (2014b). They identified the climate as the main driver of the Guinean Flood. The differences between the trend magnitudes of rain and AMAX can be explained by the sensitivity of the Niger

basin, which causes a higher increase in discharge compared to the magnitude of rainfall (Aich et al., 2014a).

For the Red Flood of the Niger River at Niamey, there is almost no difference in the gradients of the simulations with and without LULC. The runs without LULC and hence with only the climatic forcing causing the trend can explain 64% of the observed AMAX anomaly trend. The modelled effect of LULC is small and reproduces 72% of the observed trend. These results of the Red Flood correspond to the results of the Goroul catchment, which is the beside the Sirba catchment the second major tributary catchment generating the Red Flood (see Chapter 4.2.1). Therefore they are discussed together.

In the Goroul catchment, the poor performance of the model runs with and without LULC only allows a partial quantification of the relative effect of the drivers. Following the simulation results without LULC, the climatic part of the simulations explains 54% of the observed trend gradient. The cause for the remaining 46% is unclear, since the runs with LULC do not reproduce the trend significantly better. Therefore, it is not possible to give robust statements for the Goroul catchment and for the Red Flood as to the influence of the assumed drivers and quantification is a fortiori uncertain. The results might even indicate that there is an additional driver forcing the AMAX trends besides climatic changes and LULC, which is not represented in the model and has not been postulated. Another general point is the quality of the observed discharge data and the reanalyzed climate data. Especially in the Goroul catchment, the validation shows that some peaks are missed completely by the model (e.g., Alcongui 1977), or that peaks which are modelled do not occur at all in the discharge data (e.g., Alcongui 1963). This indicates the general deficit of the employed observed reanalyzed data and needs to be taken into account for the interpretation as well. However, a more probable explanation is the combination of inadequate information on LULC and/or a deficient representation of LULC in the model. The dominant change in the reanalysis data set of LULC in the watershed is a transformation of savannah to pasture (Figure 27). These two land cover types do not differ substantially in their modelled effects on the hydrological regime (see Chapter 4.2.6, Figure 32). Therefore, the similar and poor results for the runs with and without the LUCM are a logical consequence. The parameters for pasture of the SWAT land class parameters are most likely optimized for pastures in the temperate zone. The hydrological effects of pasture in the Sahel differ probably from these temperate pastures. However, since no other data was available to the authors in order to check or even change the effects and the related parameters of pasture in the Sahel, this deficit could neither be verified nor corrected. We assume that especially the infiltration capacities of Sahelian pastures are lower than of pastures in the temperate zones, e.g., due to soil-crusting effects and less dense vegetation. An additional source of uncertainty is the undifferentiated information on LULC with regard to savannah. Descroix et al. (2012) describe the LULC of this region with a change from the original bushy and woody savannah to a degraded savannah (Tiger

Bush, see Chapter 4.2.1) and sandy slopes due to land clearing. These changes are not represented in the LULC data (see Chapter 4.2.4.3).

The SP is a special aspect of the increase of flood magnitudes. Following our results, the same statements and explanations, which can explain the increase in flood magnitude, hold also for the SP. For all time series (except the ones from the Guinean Flood of the Niger River at Niamey, where the SP did not occur), the SP phenomenon could be reproduced without LULC, but to a lower degree than when accounting for LULC. We assume that this effect is based on changes in the frequency of precipitation in the climatic forcing. The findings of Panthou et al. (2012) and Panthou et al. (2014) of increasing convective precipitation supports this theory that heavy precipitation leads to an increase of the run-off coefficient, and finally to an increase in discharge. This effect is also shown by means of measurements in Amogu et al. (2010). Eventually, the combined actions of LULC and changes in precipitation patterns seem responsible for the observed SP in the 1970s/1980s.

Another finding is the non-stationary influence of climate. The model runs without LULC, and hence with only climate as the driver show upward trends in AMAX for both tributaries and the Red Flood of the Niger River at Niamey. These increases are, however, stronger than the respective annual rainfall anomalies would suggest. Therefore, we assume that changes in the rainfall patterns, most likely an increase in the frequency of heavy precipitation, contribute to the trend. This is supported by state-of-the-art analysis of climatic changes in the Sahel, for example by Panthou et al. (2012) and Panthou et al. (2014).

4.3.3. Discussion of the Methodological Framework Employed and Related Uncertainties

We acknowledge that simulation runs and the calibration procedure are affected by a wide range of uncertainties regarding the processes in the model, their parametrization and the driver data.

Relevant processes like evapotranspiration and surface runoff are not entirely physically based in the model but simplified and calibrated with a factor or empirical (e.g., the factor for potential evapotranspiration and the curve number approach). Therefore, the effects of LULC on these processes could be represented inadequately. However, the SWIM model showed in this study, like SWAT model in other LULC studies in the region (Awotwi et al., 2014), that the process-based models are generally able to reproduce the effects of LULC.

The data on LULC as the key driver of the attribution study cannot be easily improved regarding temporal and spatial resolution since no other data products or observation on LULC are available for the region. There is only a qualitative confirmation of the used LULC data by studies which are based on observations (Amogu et al., 2010a; Descroix et

al., 2012). The global LULC data set seemed therefore partly reliable, but, for example degradation of savannah (Tiger Bush, see Chapter 4.2.1), as reported in the studies are not represented in such a detail. We therefore recommended for similar studies the use of regional and more detailed data sets, if available.

Regarding the uncertainty coming from the parametrization, especially the representation of land cover types in the model has to be adequately included in terms of their hydrological attributes.

The robustness of a simulation-based attribution study is therefore not only dependent on the general validation results of the model, but rather on the ability of the model to reflect well-known changes of the postulated driver(s) adequately. Especially the parametrization of pasture in the model is questionable, but could, due to the lack of related field data, not be improved. A way to avoid this uncertainty might be the calibration of each of the main changing land cover types separately by looking at small catchments which are dominated by one of these land uses (Strömqvist et al., 2012). In doing so, the sensitivity of the model against the impact of each change can be verified and tested whether the representation is adequate or not. Unfortunately, discharge data for the validation of the model performance on such homogeneous areas were not available for the research area of this study.

Additional uncertainty is related to the general methodological framework. A modeling attribution study only can provide robust results, if all potential drivers of the observed change were adequately represented in the model. Two drivers, LULC and climatic changes, which are mentioned by qualitative studies as potential sources for the increasing flood trend (Amogu et al., 2010a; Descroix et al., 2012) are tested in this study. However, we cannot exclude the influence of a third or more drivers for the observed changes. For example the effects of the extreme population growth in the region, might influence the hydrological regime, possibly via sealing of soils near settlements. Still, the two considered drivers LULC and climate are the only potential drivers in the current literature of the Niger, which makes the assumption more reliable.

Also the assumption of linear trends in the AMAX anomaly time series and accordingly in the LULC and climatic changes is probably not realistic. However, comparing non-linear trends would request an even higher level of data quality/density, which is not available in the research area.

Another critical issue is model performance with respect to other important state variables of the model like groundwater flows and evapotranspiration. In this study, the performance of the model was only tested with regard to discharge, since no quantitative data was available on groundwater dynamics. However, in the Sahelian part of the Niger, groundwater is known to play a crucial role (Mahé, 2009) and it cannot be excluded that the model underestimates the effects of a potential relevant process related to LULC.

However, keeping model uncertainty in mind, even under conditions of comparatively poor data quality and availability, the simulation-based approach using a process-based

based model, shed new light on attribution of increasing floods in the Sahelian part of the Niger by developing some first quantitative measure of comparing the linear trend estimates of AMAX anomalies. In addition, even without adequately representing the LULC in the Goroul catchment and for the Red Flood at the station Niamey, the method could show that at least climatic changes contribute substantially to the flood increase in the region.

4.4. Conclusions

The research question, to which share LULC and/or climatic changes cause the increase of flooding in the Sahelian part of the Niger basin, can only be answered partly by this study. The most reliable conclusions can be drawn from the results of the Sirba catchment, since the simulation including LULC is able to reproduce the observed trend adequately. The influences of both drivers on the observed trend of AMAX seem to be roughly equal with a share of 43% which can be—within the known limitations—attributed to the climatic changes.

For the Goroul subcatchment and the Red Flood of the Niger River, the results are in the same order of magnitude with shares of the climatic forcing of 54% (Goroul) and 64% (Niamey Red Flood). Since the model was not able to reproduce the influence of LULC adequately, the results for these two stations are uncertain and only partly reliable. For Goroul and the Red Flood, we conclude that climatic changes have a major influence on the observed trend of AMAX and LULC also contributes, but to an unknown amount.

Using a process-based eco-hydrological model seems to be a valid method for attributing an increase of flooding. Even though main processes related to LULC, like e.g., evapotranspiration, are simplified and calibrated in the model or empirical like the curve number approach for surface runoff, the effects of LULC on the hydrology are assumed to be generally well represented since the modelled effects reflect observed effects and other studies could show a general suitability of process-based models for LULC studies. Still we see a general need for hydrological science to overcome the calibration of land use sensitive parameters in favor of more physically-based models, especially for LULC studies.

These efforts are, however, still limited by data availability, computing power and partly also detailed process understanding.

In regard of the specific methodology applied in this study, the gradient proved to be an uncomplicated and intuitive measure for comparing simulated and observed trends and estimating the influence of different drivers. However, the demands for a robust attribution on the model and data quality/density are high. Testing the method in a data-richer environment, where especially more information on LULC are available, would help to get a better understanding of its robustness and reliability.

Regarding flood mitigation and adaptation strategies, the modeling framework could be employed to assess different land management options. If the flood risk is to a significant extent due to LULC (rather than due to a climatic change), it means that it can also be counteracted. State-of-the-art options implemented locally can reduce surface runoff, for example, by reforestation, smart planting techniques which also reduce erosion, shifting cultivation etc., such as those published in the World Overview of Conservation Approaches and Technologies (WOCAT, 2015) or weADAPT (weADAPT, 2015). However, in the face of the existing flood risk in the region and the return to wet conditions, mitigation is not enough.

There is a strong need for immediate adaptation measures and we argue for early-warning systems, investments in flood protection infrastructure and flood-smart settlement policies in the riverine nations. To ensure cost-efficient implementation, a simulation-based approach can be further used to assess the relative merits of both mitigation and adaptation measures (Andersson et al., 2013).

Acknowledgments

We thank the IMPACT2C project for financing this study and the Niger Basin Authority (NBA) for providing data.

References

Aich, V., Liersch, S., Vetter, T., Huang, S., Tecklenburg, J., Hoffmann, P., Koch, H., Fournet, S., Krysanova, V., Müller, E. N. and Hattermann, F. F.: Comparing impacts of climate change on streamflow in four large African river basins, Hydrol. Earth Syst. Sci., 18(4), 1305–1321, doi:10.5194/hess-18-1305-2014, 2014a.

Aich, V., Koné, B., Hattermann, F. F. and Müller, E. N.: Floods in the Niger basin – analysis and attribution, Nat. Hazards Earth Syst. Sci. Discuss., 2(8), 5171–5212, doi:10.5194/nhessd-2-5171-2014, 2014b.

Altman, N. S.: An Introduction to Kernel and Nearest-Neighbor Nonparametric Regression, , 46(3), 175–185 [online] Available from: http://www.tandfonline.com/doi/abs/10.1080/00031305.1992.10475879# (Accessed 23 April 2015), 2012.

Amogu, O., Descroix, L. and Yéro, K.: Increasing river flows in the Sahel?, Water [online] Available from: http://www.mdpi.com/2073-4441/2/2/170 (Accessed 11 November 2013), 2010.

Andersen, I., Dione, O., Jarosewich-Holder, M. and Olivry, J.-C.: The Niger River Baisn: A Vision for Sustainable Management, edited by K. G. Golitzen, Dir. Dev., 144 [online] Available from: http://books.google.com/books?hl=de&lr=&id=DQj7Zpv-IwkC&pgis=1 (Accessed 11 November 2013), 2005.

Andersson, J. C. M., Zehnder, A. J. B., Wehrli, B., Jewitt, G. P. W., Abbaspour, K. C. and Yang, H.: Improving crop yield and water productivity by ecological sanitation and water harvesting in South Africa., Environ. Sci. Technol., 47(9), 4341–8, doi:10.1021/es304585p, 2013.

Andréassian, V., Parent, E. and Michel, C.: A distribution-free test to detect gradual changes in watershed behavior, Water Resour. Res., 39(9), doi:10.1029/2003WR002081, 2003.

Arnold, J., Williams, J., Nicks, A. and Sammons, N.: SWRRB; a basin scale simulation model for soil and water resources management. [online] Available from: http://www.cabdirect.org/abstracts/19911960464.html (Accessed 26 April 2015), 1990.

Arnold, J. G., Allen, P. M. and Bernhardt, G.: A comprehensive surface-groundwater flow model, J. Hydrol., 142(1), 47–69 [online] Available from: http://www.sciencedirect.com/science/article/pii/002216949390004S, 1993.

Arnold, J. G., Moriasi, D. N., Gassman, P. W., Abbaspour, K. C., White, M. J., Srinivasan, R., Santhi, C., Harmel, R. D., Griensven, A. van, Liew, M. W. Van and N. Kannan, M. K. J.: SWAT: Model use, calibration, and validation, Trans. Am. Soc. Agric. Biol. Eng., 55(4), 1491–1508 [online] Available from: http://swat.tamu.edu/media/70993/azdez.asp.pdf (Accessed 26 April 2015), 2012.

Arnold, J. G., Kiniry, J. R., Srinivasan, R., Williams, J. R., Haney, E. B. and Neitsch, S. L.: SWAT 2012 Input/Output Documentation., 2013.

Ashton, P., Love, D., Mahachi, H. and Dirks, P.: An Overview of the Impact of Mining and Mineral Processing Operations on Water Resources and Water Quality in the Zambezi, Limpopo and Olifants Catchments in Southern Africa. Contract Report to the Mining, Minerals and Sustainable Development (SOUTHERN AF., 2001.

Ashton, P., Love, D., Mahachi, H. and Dirks, P.: Impacts of Mining and Mineral Processing on Water Resources in the Zambezi, Limpopo, and Olifants Catchment, World Bank Publications., 2005.

Awotwi, A., Yeboah, F. and Kumi, M.: Assessing the impact of land cover changes on water balance components of White Volta Basin in West Africa, Water Environ. J., n/a–n/a, doi:10.1111/wej.12100, 2014.

Awulachew, S. B., Loulseged, A. D., Loiskandl, M., Ayana, W. and M Alamirew, T.: Water resources and irrigation development in Ethiopia, International Water Management Institute, Colombo, Sri Lanka., 2007.

Baker, T. J. and Miller, S. N.: Using the Soil and Water Assessment Tool (SWAT) to assess land use impact on water resources in an East African watershed, J. Hydrol., 486, 100–111, doi:10.1016/j.jhydrol.2013.01.041, 2013.

Di Baldassarre, G. and Uhlenbrook, S.: Is the current flood of data enough? A treatise on research needs for the improvement of flood modelling, Hydrol. Process., 26(1), 153–158, doi:10.1002/hyp.8226, 2012.

Di Baldassarre, G., Montanari, A., Lins, H., Koutsoyiannis, D., Brandimarte, L. and Blschl, G.: Flood fatalities in Africa: From diagnosis to mitigation, Geophys. Res. Lett., 37(22), L22402, doi:10.1029/2010GL045467, 2010.

Bartholomé, E. and Belward, a. S.: GLC2000: a new approach to global land cover mapping from Earth observation data, Int. J. Remote Sens., 26(9), 1959–1977, doi:10.1080/01431160412331291297, 2005.

Block, P. J., Strzepek, K. and Rajagopalan, B.: Integrated Management of the Blue Nile Basin in Ethiopia, Washington D.C. [online] Available from: http://water.columbia.edu/files/2011/11/Block2007Integrated(1).pdf, 2007.

Boko, M., Niang, I., Nyong, A., Vogel, C., Githeko, A., Medany, M., Osman-Elasha, B., Tabo, R. and Yanda, P.: Africa. Climate Change 2007: Impacts, Adaptation and Vulnerability. Contribution ofWorking Group II to the Fourth Assessment Report of the Intergovernmental Panel on Climate Change, edited by M. L. Parry, O. F. Canziani, J. P. Palutikof, P. J. van der Linden, and C. E. Hanson, pp. 433–467., Cambridge University Press, Cambridge UK. [online] Available from: http://results.waterandfood.org/handle/10568/17019 (Accessed 2 December 2013), 2007.

Vanden Bossche, J.-P. J. P. and Bernacsek, G. M. M.: Source book for the inland fishery resources of Africa Vol. 2, Rome., FAO. [online] Available from: http://www.fao.org/docrep/005/t0360e/T0360E00.htm#TOC, 1990.

Cleveland, W. S. and Devlin, S. J.: Locally Weighted Regression: An Approach to Regression Analysis by Local Fitting, J. Am. Stat. Assoc., 83(403), 596–610, doi:10.1080/01621459.1988.10478639, 1988.

Commission Internationale du Bassin Congo-Oubangui-Sangha: Plan d'Action Stratégique, [online] Available from: http://www.cicos.info/siteweb/uploads/media/1.1._Amelioration_du_Plan_d_Action_Strategique__PAS_.pdf, 2007.

Descroix, L., Genthon, P., Amogu, O., Rajot, J.-L., Sighomnou, D. and Vauclin, M.: Change in Sahelian Rivers hydrograph: The case of recent red floods of the Niger River in the Niamey region, Glob. Planet. Change, 98-99, 18–30, doi:10.1016/j.gloplacha.2012.07.009, 2012.

Descroix, L., Bouzou, I., Genthon, P., Sighomnou, D., Mahe, G., Mamadou, I., Vandervaere, J.-P., Gautier, E., Faran, O., Rajot, J.-L., Malam, M., Dessay, N., Ingatan, A., Noma, I., Souley, K., Karambiri, H., Fensholt, R., Albergel, J. and Olivry, J.-C.: Impact of Drought and Land – Use Changes on Surface – Water Quality and Quantity: The Sahelian Paradox, in Current Perspectives in Contaminant Hydrology and Water Resources Sustainability, edited by P. Bradley, pp. 243–271, InTech, Rijeka, Croatia., 2013.

Doherty, J.: PEST—Model-independent parameter estimation, User Manual, 5th ed., edited by W. N. Computing, Watermark Numerical Computing. [online] Available from: http://www.pesthomepage.org/files/pestman.pdf, 2005.

Durbin, J. and Watson, G.: Testing for serial correlation in least squares regression. I, Biometrika, 37(3-4), 409–428 [online] Available from: http://www.jstor.org/stable/2332325 (Accessed 10 March 2014), 1950.

Durbin, J. and Watson, G.: Testing for serial correlation in least squares regression. II, Biometrika, 38(1-2), 159–178 [online] Available from: http://www.jstor.org/stable/2332325 (Accessed 10 March 2014), 1951.

FAO: Drought Impact Mitigation and Prevention in the Limpopo River Basin: A Situation Analysis, FAO Sub-Regional Office for Southern and East Africa Harare., 2004.

FAO, IIASA, ISRIC, ISSC and JRC: Harmonized World Soil Database v 1.2, [online] Available from: http://webarchive.iiasa.ac.at/Research/LUC/External-World-soil-database/HTML/, 2012.

Faramarzi, M., Abbaspour, K. C., Ashraf Vaghefi, S., Farzaneh, M. R., Zehnder, A. J. B., Srinivasan, R. and Yang, H.: Modeling impacts of climate change on freshwater availability in Africa, J. Hydrol., 480, 85–101, doi:10.1016/j.jhydrol.2012.12.016, 2013.

Fekete, B. M., Vorosmarty, C. J. and Grabs, W.: Global, composite runoff fields based on observed river discharge and simulated water balances., Water System Analysis Group, University of New Hampshire, and Global Runoff Data Centre. Koblenz, Germany: Federal Institute of Hydrology (BfG), Koblenz, Germany., 1999.

Few, R., Brown, K. and Tompkins, E. L.: Public participation and climate change adaptation: avoiding the illusion of inclusion, Clim. Policy, 7(1), 46–59, doi:10.1080/14693062.2007.9685637, 2007.

Frenken, K. and Faurès, J. M.: Irrigation Potential in Africa: A Basin Approach, FAO, Rome. [online] Available from: https://books.google.de/books?id=VzqBfdeSjgQC&printsec, 1997.

Gebrehiwot, S. G., Seibert, J., Gärdenäs, A. I., Mellander, P.-E. and Bishop, K.: Hydrological change detection using modeling: Half a century of runoff from four rivers in the Blue Nile Basin, Water Resour. Res., 49(6), 3842–3851, doi:10.1002/wrcr.20319, 2013.

Giuntoli, I., Renard, B., Vidal, J.-P. and Bard, A.: Low flows in France and their relationship to large-scale climate indices, J. Hydrol., 482, 105–118, doi:10.1016/j.jhydrol.2012.12.038, 2013.

Hargreaves, G. H. and Samani, Z. A.: Estimating Potential Evapotranspiration, J. Irrig. Drain. Div., 108(3), 225–230 [online] Available from: http://cedb.asce.org/cgi/WWWdisplay.cgi?35047, 1982.

Harrigan, S., Murphy, C., Hall, J., Wilby, R. L. and Sweeney, J.: Attribution of detected changes in streamflow using multiple working hypotheses, Hydrol. Earth Syst. Sci. [online] Available from: http://eprints.maynoothuniversity.ie/4947/1/CM_Attribution.pdf (Accessed 20 January 2015), 2013.

Hastenrath, S., Polzin, D. and Mutai, C.: Diagnosing the Droughts and Floods in Equatorial East Africa during Boreal Autumn 2005–08, J. Clim., 23(3), 813–817, doi:10.1175/2009JCLI3094.1, 2010.

Hattermann, F., Kundzewicz, Z. W., Huang, S., Vetter, T., Kron, W., Burghoff, O., Merz, B., Bronstert, A., Krysanova, V., Gerstengarbe, F.-W., Werner, P. C. and Ylva, H.: Flood risk from a holistic perspective–observed changes in Germany, in Changes of flood risk in Europe, edited by Z. W. Kundzewicz, pp. 212–237, IAHS Press, Wallingford. [online] Available from: https://scholar.google.de/scholar?hl=en&as_sdt=0,5&q=flood+risk+holistic+hattermann#0 (Accessed 7 May 2015), 2012.

Hempel, S., Frieler, K., Warszawski, L., Schewe, J. and Piontek, F.: A trend-preserving bias correction – the ISI-MIP approach, Earth Syst. Dyn. Discuss., 4(1), 49–92, doi:10.5194/esdd-4-49-2013, 2013.

Huang, S., Krysanova, V. and Hattermann, F.: Projection of low flow conditions in Germany under climate change by combining three RCMs and a regional hydrological model, Acta Geophys., 61(1), 151–193 [online] Available from: http://link.springer.com/article/10.2478/s11600-012-0065-1 (Accessed 26 April 2015), 2013.

Hundecha, Y. and Merz, B.: Exploring the relationship between changes in climate and floods using a model-based analysis, Water Resour. Res., 48(4), n/a–n/a, doi:10.1029/2011WR010527, 2012.

Hurtt, G. C., Chini, L. P., Frolking, S., Betts, R. a., Feddema, J., Fischer, G., Fisk, J. P., Hibbard, K., Houghton, R. a., Janetos, a., Jones, C. D., Kindermann, G., Kinoshita, T., Klein Goldewijk, K., Riahi, K., Shevliakova, E., Smith, S., Stehfest, E., Thomson, a., Thornton, P., van Vuuren, D. P. and Wang, Y. P.: Harmonization of land-use scenarios for the period 1500-2100: 600 years of global gridded annual land-use transitions, wood harvest, and resulting secondary lands, Clim. Change, 109(1-2), 117–161, doi:10.1007/s10584-011-0153-2, 2011.

IPCC-TGICA: General Guidelines on the Use of Scenario Data for Climate Impact and Adaptation Assessment. Version 2., 2007.

Jarvis, a, Reuter, H. I., Nelson, a and Guevara, E.: Hole-filled seamless SRTM data V4, Int. Cent. Trop. Agric., available from http://srtm.csi.cgiar.org [online] Available from: http://srtm.csi.cgiar.org/ (Accessed 13 January 2015), 2008.

Jury, M. R.: A return to wet conditions over Africa: 1995–2010, Theor. Appl. Climatol., 111(3-4), 471–481, doi:10.1007/s00704-012-0677-z, 2013.

Kandji, S. T., Verchot, L. and Mackensen, J.: Climate change and variability in the Sahel region: Impacts and adaptation strategies in the agricultural sector, Nairobi, Kenya. [online] Available from: http://www.unep.org/Themes/Freshwater/Documents/pdf/ClimateChangeSahelCombine.pdf (Accessed 23 January 2015), 2006.

Kim, H.: GSWP3, Glob. Soil Wetness Proj. Phase 3, Surf. Meteorol., 1 [online] Available from: http://hydro.iis.u-tokyo.ac.jp/GSWP3/exp1.html (Accessed 24 April 2015), 2014.

Klein Goldewijk, K., Beusen, A. and Janssen, P.: Long-term dynamic modeling of global population and built-up area in a spatially explicit way: HYDE 3.1, The Holocene, 20(4), 565–573, doi:10.1177/0959683609356587, 2010.

Klein Goldewijk, K., Beusen, A., Van Drecht, G. and De Vos, M.: The HYDE 3.1 spatially explicit database of human-induced global land-use change over the past 12,000 years, Glob. Ecol. Biogeogr., 20(1), 73–86, doi:10.1111/j.1466-8238.2010.00587.x, 2011.

Koch, H., Liersch, S. and Hattermann, F. F.: Integrating water resources management in eco-hydrological modelling, Water Sci. Technol., 67(7), 1525, doi:10.2166/wst.2013.022, 2013.

Köppen, W.: Das geographische System der Klimate, in Handbuch der Klimatologie., edited by W. Köppen and R. Geiger, p. 44, Gebrüder Borntraeger, Berlin., 1936.

Krysanova, V., Meiner, A., Roosaare, J. and Vasilyev, A.: Simulation modelling of the coastal waters pollution from agricultural watershed, Ecol. Modell., 49(1), 7–29 [online] Available from: http://www.sciencedirect.com/science/article/pii/0304380089900410, 1989.

Krysanova, V., Müller-Wohlfeil, D.-I. and Becker, A.: Development and test of a spatially distributed hydrological/water quality model for mesoscale watersheds, Ecol. Modell., 106(2–3), 261–289, doi:10.1016/S0304-3800(97)00204-4, 1998.

Krysanova, V., Arnold, J. G., Wechsung, F., Srinivasan, R. and Williams, J.: SWIM (Soil and Water Integrated Model) Users Manual, Potsdam Institute for Climate Impact Research, Potsdam, Germany., 2000.

Krysanova, V., Hattermann, F. and Wechsung, F.: Development of the ecohydrological model SWIM for regional impact studies and vulnerability assessment, Hydrol. Process., 19(3), 763–783 [online] Available from: http://onlinelibrary.wiley.com/doi/10.1002/hyp.5619/abstract, 2005.

LBPTC, L. B. P. T. C.: Joint Limpopo River Basin Study Scoping Phase. Final Report, 2010.

Liersch, S., Cools, J., Kone, B., Koch, H., Diallo, M., Reinhardt, J., Fournet, S., Aich, V. and Hattermann, F. F.: Vulnerability of rice production in the Inner Niger Delta to water resources management under climate variability and change, Environ. Sci. Policy, 34, 8–33, doi:10.1016/j.envsci.2012.10.014, 2013.

Mahe, G., Lienou, G., Descroix, L., Bamba, F., Paturel, J. E., Laraque, A., Meddi, M., Habaieb, H., Adeaga, O., Dieulin, C., Chahnez Kotti, F. and Khomsi, K.: The rivers of Africa: witness of climate change and human impact on the environment, Hydrol. Process., 27(15), 2105–2114, doi:10.1002/hyp.9813, 2013.

Mahé, G.: Surface/groundwater interactions in the Bani and Nakambe rivers, tributaries of the Niger and Volta basins, West Africa, Hydrol. Sci. J., 54(4), 704–712, doi:10.1623/hysj.54.4.704, 2009.

Mediero, L., Santillán, D., Garrote, L. and Granados, A.: Detection and attribution of trends in magnitude, frequency and timing of floods in Spain, J. Hydrol., 517, 1072–1088, doi:10.1016/j.jhydrol.2014.06.040, 2014.

Merz, B., Vorogushyn, S., Uhlemann, S., Delgado, J. and Hundecha, Y.: HESS Opinions "More efforts and scientific rigour are needed to attribute trends in flood time series," Hydrol. Earth Syst. Sci. Discuss., 16, 1379–1387, doi:10.5194/hessd-16-1379-2012, 2012.

Mngutyo, A.: An Investigation of the Influence of the Flooded Household Environments on Maternal Health of Flood Plain Dwellers in Makurdi, OIDA Int. J. Sustain. Dev., 4(8), 29–38 [online] Available from: http://papers.ssrn.com/sol3/papers.cfm?abstract_id=2131849, 2012.

Moriasi, D. and Arnold, J.: Model evaluation guidelines for systematic quantification of accuracy in watershed simulations, Trans. …, 50(3), 885–900, doi:10.13031/2013.23153, 2007.

Murphy, C., Harrigan, S., Hall, J. and Wilby, R. L.: Climate-driven trends in mean and high flows from a network of reference stations in Ireland, Hydrol. Sci. J., 58(4), 755–772, doi:10.1080/02626667.2013.782407, 2013.

Murwira, A. and Yachan, A.: Limpopo Basin Strategic Plan for Reducing Vulnerability to Floods and Droughts. Draft for Discussion with Riparian Governments. UN-HABITAT/UNEP, Manager, (July), 25 [online] Available from: http://scholar.google.de/, 2007.

Nash, J. E. and Sutcliffe, J. V.: River flow forecasting through conceptual models part I — A discussion of principles, J. Hydrol., 10(3), 282–290, doi:10.1016/0022-1694(70)90255-6, 1970.

Niger Basin Authority: NIGER-HYCOS, [online] Available from: http://nigerhycos.abn.ne/ (Accessed 1 March 2012), 2008.

Niger Basin Authority, (NBA): Elaboration of an Action Plan for the Sustainalble Development of the Niger Basin. Phase 2: Master Plan for the Development and Managment, Niamey, Niger., 2007.

Nobert, J. and Jeremiah, J.: Hydrological Response of Watershed Systems to Land Use/Cover Change. A Case of Wami River Basin, Open Hydrol. J., 6(1) [online] Available

from: http://benthamopen.com/ABSTRACT/TOHYDJ-6-78 (Accessed 24 April 2015), 2012.

NWP: Summary note of the Nairobi work programme on impacts, vulnerability and adaptation to climate change, UNFCC, Durban, South Africa. [online] Available from: http://unfccc.int/adaptation/workstreams/nairobi_work_programme/items/3633.php, 2011.

Nyeko, M., D'Urso, G. and Immerzeel, W. W.: Adaptive simulation of the impact of changes in land use on water resources in the lower Aswa basin, J. Agric. Eng., 43(4), 24, doi:10.4081/jae.2012.e24, 2013.

Ogilvie, A., Mahé, G., Ward, J., Serpantié, G., Lemoalle, J., Morand, P., Barbier, B., Diop, A. T., Caron, A., Namarra, R., Kaczan, D., Lukasiewicz, A., Paturel, J.-E., Liénou, G. and Clanet, J. C.: Water, agriculture and poverty in the Niger River basin, Water Int., 35(5), 594–622 [online] Available from: http://www.tandfonline.com/doi/abs/10.1080/02508060.2010.515545 (Accessed 11 November 2013), 2010.

Oguntunde, P. G. and Abiodun, B. J.: The impact of climate change on the Niger River Basin hydroclimatology, West Africa, Clim. Dyn., 40(1-2), 81–94, doi:10.1007/s00382-012-1498-6, 2013.

Panthou, G., Vischel, T., Lebel, T., Blanchet, J., Quantin, G. and Ali, A.: Extreme rainfall in West Africa: A regional modeling, Water Resour. Res., 48(8), doi:10.1029/2012WR012052, 2012.

Panthou, G., Vischel, T. and Lebel, T.: Recent trends in the regime of extreme rainfall in the Central Sahel, Int. J. Climatol., doi:10.1002/joc.3984, 2014.

Prosdocimi, I., Kjeldsen, T. R. and Svensson, C.: Non-stationarity in annual and seasonal series of peak flow and precipitation in the UK, Nat. Hazards Earth Syst. Sci., 14(5), 1125–1144, doi:10.5194/nhess-14-1125-2014, 2014.

Ramankutty, N.: Croplands in West Africa: A Geographically Explicit Dataset for Use in Models, Earth Interact., 8(23), 1–22, doi:10.1175/1087-3562(2004)8<1:CIWAAG>2.0.CO;2, 2004.

Richardson, K., Steffen, W. and Liverman, D.: Climate change: Global risks, challenges and decisions, Cambridge University Press. [online] Available from: Richardson, K., Steffen, W. and Liverman, D.: Climate change: Global risks, challenges and decisions, Cambridge University Pres, 2011.

Ritchie, J.: Model for predicting evaporation from a row crop with incomplete cover, Water Resour. Res., 8(5), 1204–1213 [online] Available from: http://onlinelibrary.wiley.com/doi/10.1029/WR008i005p01204/full (Accessed 26 April 2015), 1972.

Rogelj, J., Meinshausen, M. and Knutti, R.: Global warming under old and new scenarios using IPCC climate sensitivity range estimates, Nat. Clim. Chang., 2(4), 248–253, doi:10.1038/nclimate1385, 2012.

Salman, S. M. A.: The Nile Basin Cooperative Framework Agreement: a peacefully unfolding African spring?, Water Int., 38(1), 17–29, doi:10.1080/02508060.2013.744273, 2013.

Schreider, S. Y., Jakeman, A. J., Letcher, R. A., Nathan, R. J., Neal, B. P. and Beavis, S. G.: Detecting changes in streamflow response to changes in non-climatic catchment conditions: farm dam development in the Murray–Darling basin, Australia, J. Hydrol., 262(1-4), 84–98, doi:10.1016/S0022-1694(02)00023-9, 2002.

Seibert, J. and McDonnell, J. J.: Land-cover impacts on streamflow: a change-detection modelling approach that incorporates parameter uncertainty, Hydrol. Sci. J., 55(3), 316–332, doi:10.1080/02626661003683264, 2010.

Sen, P.: Estimates of the regression coefficient based on Kendall's tau, J. Am. Stat. Assoc., 63(324), 1379–1389 [online] Available from: http://amstat.tandfonline.com/doi/abs/10.1080/01621459.1968.10480934 (Accessed 10 March 2014), 1968.

Shahin, M.: Hydrology and Water Resources of Africa, Springer Science & Business Media. [online] Available from: https://books.google.com/books?id=MmjjBwAAQBAJ&pgis=1 (Accessed 26 August 2015), 2006.

Sheffield, J., Goteti, G. and Wood, E. F.: Development of a 50-year high-resolution global dataset of meteorological forcings for land surface modeling, J. Clim., 19(13), 3088–3111, doi:10.1175/JCLI3790.1, 2006.

Solomon, S., Qin, D., Manning, M., Alley, R. B., Berntsen, T., Bindoff, N. L., Chen, Z., Chidthaisong, A., Gregory, J. M. and Hegerl, G. C.: Climate change 2007: The physical science basis, contribution of working group 1 to the fourth assessment report of the Intergovernmental Panel on Climate Change, [online] Available from: http://www.esrl.noaa.gov/search/publications/3792/, 2007.

Strahler, A. H.: Introducing Physical Geography, Wiley. [online] Available from: https://books.google.de/books?vid=ISBN9781118396209&redir_esc=y (Accessed 26 August 2015), 2013.

Strömqvist, J., Arheimer, B., Dahné, J., Donnelly, C. and Lindström, G.: Water and nutrient predictions in ungauged basins: set-up and evaluation of a model at the national scale, Hydrol. Sci. J., 57, 229–247, doi:10.1080/02626667.2011.637497, 2012.

Strzepek, K. and McCluskey, A.: The impacts of climate change on regional water resources and agriculture in Africa, World Bank Policy Res. Work. Pap., (4290) [online] Available from: http://papers.ssrn.com/sol3/papers.cfm?abstract_id=1004404, 2007.

Tarhule, A.: Damaging Rainfall and Flooding: The Other Sahel Hazards, Clim. Change, 72, 355–377, doi:10.1007/s10584-005-6792-4, 2005.

Theil, H.: A rank-invariant method of linear and polynomial regression analysis, Ned. Acad. Wetensch. Proc, 53, 386–392 [online] Available from: http://link.springer.com/chapter/10.1007/978-94-011-2546-8_20 (Accessed 10 March 2014), 1950.

Tschakert, P., Sagoe, R., Ofori-Darko, G. and Codjoe, S. N.: Floods in the Sahel: an analysis of anomalies, memory, and anticipatory learning, Clim. Change, 103(3-4), 471–502, doi:10.1007/s10584-009-9776-y, 2010.

Tshimanga, R. M.: Hydrological uncertainty analysis and scenario-based streamflow modelling for the Congo River Basin, Rhodes University, South Africa. [online] Available from: http://agris.fao.org/agris-search/search.do?recordID=AV2012089066 (Accessed 26 August 2015), 2012.

Tshimanga, R. M. and Hughes, D. A.: Climate change and impacts on the hydrology of the Congo Basin: The case of the northern sub-basins of the Oubangui and Sangha Rivers, Phys. Chem. Earth, Parts A/B/C, 50–52, 72–83, doi:10.1016/j.pce.2012.08.002, 2012.

UN: Water in a changing world, The United Nations World Water Development Report 3, World Water Assess. Program. [online] Available from: http://webworld.unesco.org/water/wwap/wwdr/wwdr3/tableofcontents.shtml, 2009.

Vetter, T., Huang, S., Aich, V., Yang, T., Wang, X., Krysanova, V. and Hattermann, F.: Multi-model climate impact assessment and intercomparison for three large-scale river basins on three continents, Earth Syst. Dyn., 6(1), 17–43, doi:10.5194/esd-6-17-2015, 2015.

Villarini, G. and Strong, A.: Roles of climate and agricultural practices in discharge changes in an agricultural watershed in Iowa, Agric. Ecosyst. Environ., 188, 204–211, doi:10.1016/j.agee.2014.02.036, 2014.

Vorogushyn, S. and Merz, B.: What drives flood trends along the Rhine River: climate or river training?, Hydrol. Earth Syst. Sci. Discuss., 9(12), 13537–13567, doi:10.5194/hessd-9-13537-2012, 2012.

Van Vuuren, D. P., Stehfest, E., Elzen, M. G. J., Kram, T., Vliet, J., Deetman, S., Isaac, M., Klein Goldewijk, K., Hof, A., Mendoza Beltran, A., Oostenrijk, R. and Ruijven, B.: RCP2.6: exploring the possibility to keep global mean temperature increase below 2°C, Clim. Change, 109(1-2), 95–116, doi:10.1007/s10584-011-0152-3, 2011a.

Van Vuuren, D. P., Edmonds, J., Kainuma, M., Riahi, K., Thomson, A., Hibbard, K., Hurtt, G. C., Kram, T., Krey, V. and Lamarque, J.-F.: The representative concentration pathways: an overview, Clim. Change, 109(1-2), 5–31 [online] Available from: http://link.springer.com/article/10.1007/s10584-011-0148-z, 2011b.

weADAPT: weADAPT 4.0, Climate adaptation planning, research and practice, [online] Available from: https://weadapt.org/ (Accessed 21 January 2015), 2015.

Weedon, G. P., Gomes, S., Viterbo, P., Shuttleworth, W. J., Blyth, E., Österle, H., Adam, J. C., Bellouin, N., Boucher, O. and Best, M.: Creation of the WATCH Forcing Data and Its Use to Assess Global and Regional Reference Crop Evaporation over Land during the Twentieth Century, J. Hydrometeorol., 12(5), 823–848, doi:10.1175/2011JHM1369.1, 2011.

Wendling, U. and Schellin, H.: Neue Ergebnisse zur Berechnung der potentiellen Evapotranspiration, Zeitschrift für Meteorol., 36(3), 214–217 [online] Available from: http://cat.inist.fr/?aModele=afficheN&cpsidt=8792552 (Accessed 26 April 2015), 1986.

Wesselink, A. J., Orange, D. and Feizouré, C. T.: Les régimes hydroclimatiques et hydrologiques d'un bassin versant de type tropical humide: l'Oubangui (République Centrafricaine), vol. 238, edited by P. Chevallier and B. Pouyaud, pp. 179–194, IAHS Publication, Wallingford, UK. [online] Available from: http://books.google.de/books?hl=de&lr=&id=azUCAebIN-YC&oi=fnd&pg=PA179&dq=les+regimes+hydroclimatique+et+hydrologique+d'un+bassin+versant+de+type+tropicale+humide:+l´oubangi+&ots=MURoAug2Cy&sig=Fsaqb9mAXNcOg1MXYCWgooWWVUE#v=onepage&q=les regimes hydroclimatique et hydrologique d'un bassin versant de type tropicale humide: l´oubangi&f=false, 1996.

WFD: EU WATCH - Home, [online] Available from: http://eu-watch.org/templates/dispatcher.asp?page_id=25222705, 2011.

Williams, J. R., Renard, K. G. and Dyke, P. T.: EPIC: A new method for assessing erosion's effect on soil productivity, J. Soil Water Conserv., 38(5), 381–383 [online] Available from: http://www.jswconline.org/content/38/5/381.short (Accessed 26 April 2015), 1983.

De Wit, M. and Stankiewicz, J.: Changes in surface water supply across Africa with predicted climate change, Science (80-.)., 311(5769), 1917–1921 [online] Available from: http://www.sciencemag.org/content/311/5769/1917.short, 2006.

WOCAT: World Overview of Conservation Approaches and Technologies, [online] Available from: https://www.wocat.net/ (Accessed 21 January 2015), 2015.

WRDC: World Radiation Data Centre, [online] Available from: http://wrdc-mgo.nrel.gov/, 2000.

Yue, S., Pilon, P., Phinney, B. and Cavadias, G.: The influence of autocorrelation on the ability to detect trend in hydrological series, Hydrol. Process., 16(9), 1807–1829, doi:10.1002/hyp.1095, 2002.

Zhu, T. and Ringler, C.: Climate Change Impacts on Water Availability and Use in the Limpopo River Basin, Water, 4(4), 63–84, doi:10.3390/w4010063, 2012.

Earth Syst. Dynam., 6, 17–43, 2015
doi:10.5194/esd-6-17-2015

5. MULTI-MODEL CLIMATE IMPACT ASSESSMENT AND INTERCOMPARISON FOR THREE LARGE-SCALE RIVER BASINS ON THREE CONTINENTS

Tobias Vetter [1,*], Shaochun Huang [1], Valentin Aich [1], Tao Yang [2], Xiaoyan Wang [2], Valentina Krysanova[1], and Fred F. Hattermann [1]

[1] Potsdam Institute for Climate Impact Research (PIK), Potsdam, Germany
[2] Hohai University, Nanjing, China

* Corresponding author: Tobias Vetter (vetter@pik-potsdam.de)

Journal: Earth System Dynamics (Earth Syst. Dynam.)
Status: Published

Abstract: Climate change impacts on hydrological processes should be simulated for river basins using validated models and multiple climate scenarios in order to provide reliable results for stakeholders. In the last 10-15 years, climate impact assessment has been performed for many river basins worldwide using different climate scenarios and models. However, their results are hardly comparable, and do not allow one to create a full picture of impacts and uncertainties. Therefore, a systematic intercomparison of impacts is suggested, which should be done for representative regions using state-of-the-art models. Only a few such studies have been available until now with the global-scale hydrological models, and our study is intended as a step in this direction by applying the regional-scale models. The impact assessment presented here was performed for three river basins on three continents: the Rhine in Europe, the Upper Niger in Africa and the Upper Yellow in Asia. For that, climate scenarios from five general circulation models (GCMs) and three hydrological models, HBV, SWIM and VIC, were used. Four representative concentration pathways (RCPs) covering a range of emissions and land-use change projections were included. The objectives were to analyze and compare climate impacts on future river discharge and to evaluate uncertainties from different sources. The results allow one to draw some robust conclusions, but uncertainties are large and shared differently between sources in the studied basins. Robust results in terms of trend direction and slope and changes in seasonal dynamics could be found for the Rhine basin regardless of which hydrological model or forcing GCM is used. For the Niger River, scenarios from climate models are the largest uncertainty source, providing large discrepancies in precipitation, and therefore clear projections are difficult to do. For the Upper Yellow basin, both the hydrological models and climate models contribute to uncertainty in the impacts, though an increase in high flows in the future is a robust outcome ensured by all three hydrological models. Introduction Climate change impacts are commonly assessed on two different scales: the global or continental scale allows for a general view of the larger context and patterns, whereas regional studies focus on details, for example flood or drought hazards. By comparing climate change impacts between different regions,

advantages of both approaches can be combined. This way of bridging these two scales is likely to give new insights into the characteristics of climate change in the actual regions, but also beyond.

5.1. Introduction

5.1.1. Hydrology of the basins

The Setting adequate climate stabilization goals and designing appropriate adaptation policies should rely on a sound quantitative understanding of the expected impacts of climate change under different emission scenarios and different levels of global warming. In particular, a comprehensive assessment of climate impacts is urgently needed within the Intergovernmental Panel on Climate Change (IPCC) process. However, the scientific knowledge about the impacts of climate change still remains fragmentary. Very many studies have been undertaken to investigate climate impacts for a number of sectors, globally and on the regional scale, applying different models and emission scenarios, and there are only a few model intercomparison studies using a consistent setup and global-scale models.

Global assessment of climate change impacts is important for informing the global policy makers, especially regarding mitigation efforts. However, climate impacts occur and adaptation policies are implemented on the regional scale, the projections from global impact models may not be precise enough. To make sure that climate impact research meets the demand of stakeholders for reliable information on the regional level, projections of climate impacts should be provided on the regional or river basin scale using validated hydrological models and up-to-date scenarios.

Of course, numerous studies on climate change impacts are of value in their own right by providing useful knowledge. However, a quantitative synthesis of climate impacts for different regions, including consistent estimation of uncertainties from different sources, is still missing. In order to achieve it, a systematic intercomparison of impacts simulated by several state-of-the-art models performed for a set of representative regions on all continents using an ensemble of climate scenarios is needed. It is now planned in the Inter-Sectoral Impact Model Intercomparison Project (ISI-MIP), and the first results of the fast-track modeling using global-scale models are already available (Warszawski et al., 2014).

While comparison of climate model outputs has a long tradition and is well established on the global and continental scales (IPCC, 2000, 2007; Déqué et al., 2007; Jacob et al., 2013), fewer studies can be found that intercompare hydrological models and study propagation of uncertainty along the entire model chain of general circulation model (GCM) – regional climate model (RCM) – impact models. The ones that can be found use a variety of methods and techniques to assess the contribution of different sources of uncertainty to the total uncertainty.

A comprehensive intercomparison of hydrological models has been done, e.g., in the Distributed Model Intercomparison Project (Reed et al., 2004; Smith et al., 2004) comparing the performance of 12 hydrological models in three North American river basins. A hierarchical validation testing scheme for model application to runoff predictions in gauged and ungauged basins has been proposed by Refsgaard and Knudsen (1996) using three types of hydrological models (lumped, physically based, semi-distributed) for a catchment in Zimbabwe. An uncertainty intercomparison of different hydrological models in simulating extreme flows for the Upper Yellow River has been published by Chen et al. (2013) comparing the performance of three different hydrological models under current climate conditions. These studies solely investigate the model performance and related uncertainty of hydrological models without looking at simulation of climate change impacts and the related uncertainty propagation (see also Velázquez et al., 2013).

A set of 10 lumped, semi-distributed and fully distributed hydrological models has been applied in the LUCHEM project aiming at investigating the envelope of predictions of changes in hydrological fluxes due to land-use change, also considering land-use change scenarios (Breuer et al., 2009).

A comprehensive comparison of uncertainty sources for climate change impacts on flood frequency in England has been published by Kay et al. (2009). Six different sources of uncertainty are discussed for two example catchments (future greenhouse gas emissions, GCM structure, downscaling from GCMs, hydrological model structure, hydrological model parameters and the internal variability of the climate system, sampled by applying different GCM initial conditions). The results suggest that uncertainty from GCM structure is by far the largest source of uncertainty. A probabilistic framework for assessing uncertainties in climate change impacts on low-flow scenarios for the River Thames considering a similar set of uncertainty sources is suggested by Wilby and Harris (2006).

All these studies compare results for the regional scale, while Schewe et al. (2014) performed a multi-model assessment of water scarcity under climate change by comparing results of twelve global hydrological models driven by five GCM projections. The study highlights the large uncertainties associated with both, climate models and hydrological models. The uncertainty introduced by the hydrological models is particularly dominant in many regions affected by water resource scarcity, suggesting a high potential for improved water resource projections through further improvement of hydrological models. Another global-scale model intercomparison study was done by Haddeland et al. (2011). They compared simulated runoff and evapotranspiration from six land surface models and five global hydrological models for eight large river basins. Their simulations with uncalibrated models (with one exception) showed high spreads in simulated seasonal and annual river runoff and only little agreement with observed runoff. Doing impact assessment with eight of those eleven models and three GCMs, Hagemann et al. (2013) found that, in some regions, uncertainties caused by the impact models are higher than those caused by the climate models.

Recently, a number of studies were published suggesting the use of the analysis of variance (ANOVA) approach for uncertainty assessment in hydrology and climatology. For example, Yip et al. (2011) use ANOVA to quantify the contribution of different uncertainty sources in climate models, distinguishing between model uncertainty, scenario uncertainty and internal variation. Finger et al. (2012) used ANOVA to estimate impacts of climate model uncertainty on water resource projections and hydro-power production in a glaciated catchment in Switzerland during the 21st century. Ott et al. (2013) applied ANOVA and a nonparametric test to address uncertainty sources in an assessment of high-resolution climate change impacts on medium-sized river catchments in Germany, applying an ensemble of RCM climate forcing data to three hydrological models. Using the ANOVA approach, Bosshard et al. (2013) assessed uncertainties induced by climate models, two different bias correction methods and hydrological models using the output of eight RCMs that are fed into two hydrological models of the Upper Rhine. The results indicate that none of the investigated uncertainty sources is negligible, and some of the uncertainties are not attributable to individual modeling chain components, but rather depend upon their interactions, while in total, climate model uncertainty has the largest contribution to the entire uncertainty. Our study is intended as a contribution to the intercomparison of climate change impacts for the water sector on the regional scale. It was done for three large-scale river basins on three continents, the Rhine in Europe, the Upper Niger in Africa and the Upper Yellow River in Asia, by applying three hydrological models, SWIM (Krysanova et al., 1998), HBV (Bergström and Singh, 1995) and VIC (Liang et al., 1994), after their calibration and validation. The bias-corrected climate scenarios from five GCMs (HadGEM2-ES,IPSL-CM5ALR, MIROCESM- CHEM, GFDL-ESM2M, NorESM1-M) driven by four representative concentration pathways (RCPs) were provided by the ISI-MIP project (Hempel et al., 2013) and used as input for impact assessment. The four RCPs cover a range of emissions and land-use change projections. The objectives were (a) to compare climate impacts on seasonal water discharge, (b) to compare future trends considering three runoff quantiles, Q_{90}, Q_{50} and Q_{10}, in terms of trend direction and slope, and (c) to evaluate uncertainties from different sources, namely related to climate models (CMs) providing scenarios, hydrological models (HMs) and RCPs.

5.2. Study areas, data and methods

5.2.1. Study areas: three river basins

From the general set of possible basins, we selected three basins on three continents, which belong to different climatic zones. Besides, the three chosen basins belong to the ISIMIP Phase 2 (Warszawski et al., 2014) river basins chosen for intercomparison of climate change impacts on water using regional- and global-scale models.

5.2.1.1. The Upper Niger

The Niger River basin is the largest basin of western Africa. Its source is located in the Guinean highlands, from which the river flows in the northeasterly direction through the dry Sahelian zone, and then enters the wetter tropical region north of the Gulf of Guinea. In our study, only the Upper Niger catchment until the Koulikoro gauge station (Figure 35) covering an area of about 122 000 km2 was taken for impact assessment. The complete Niger River basin could not be properly modeled with HBV and VIC, since there is no inundation module included in those models, and the flow of the Niger is very much altered by the existence of the inner Niger Delta and related inundation processes. In another study (Aich et al., 2014), the whole Niger basin was modeled with SWIM, with several intermediate gauges. The same model setup for the Niger as in Aich et al. (2014) was taken in the present study for SWIM simulations.

The studied upper part of the Niger basin spreads over the countries of Guinea and Mali, and includes a small part of the Ivory Coast. The topography of the catchment is quite heterogeneous, with several steep-sloped tributaries in Upper Guinea that flow into the flat plane of the Niger River. The dominant land cover in the Upper Niger catchment is forest (34 %) followed by savannah (30 %). The climate in the Upper Niger basin is characterized by a dry season (November– May) and a rainy season from June to September (see Table 7). The rainfall that feeds the river comes mainly from the Guinean Highlands during the rainy season. The average annual precipitation of 1495mm in the Upper Niger is the highest among the three basins in the study.

The catchment area until Koulikoro is not much influenced by human management. There is only one dam, the Selingue (brought into service in 1982), influencing the discharge downstream until Koulikoro. There are no major irrigation schemes in this part of the catchment.

Table 7 Characteristics of the three river basins.

	Rhine (Rees) Upper Yellow	**Upper Yellow (Tanghaihai)**	**Upper Niger (Koulikoro)**
Area (km2)	160 000	110 000	122 000
Altitude range (min/mean/max) (m)	10/495/4275	2673/4256/6248	289/463/1407
Average temperature (1971–2000) (°C)	8.6	−2.0	26.5
Temp. of coldest/warmest month (°C)	0.3/17.4	−14.2/8.23	23.8/28.6
Annual precipitation (1971–2000) (mm)	987	520	1495
Prec. of driest/wettest month (mm)	69/97	0/113	3/323
Dominant land cover .%/	Cropland 38 Forest 25 Grassland 9	Grassland 90 Bare soil 4 Heather 3	Forest 34 Savanna 30 Cropland 24

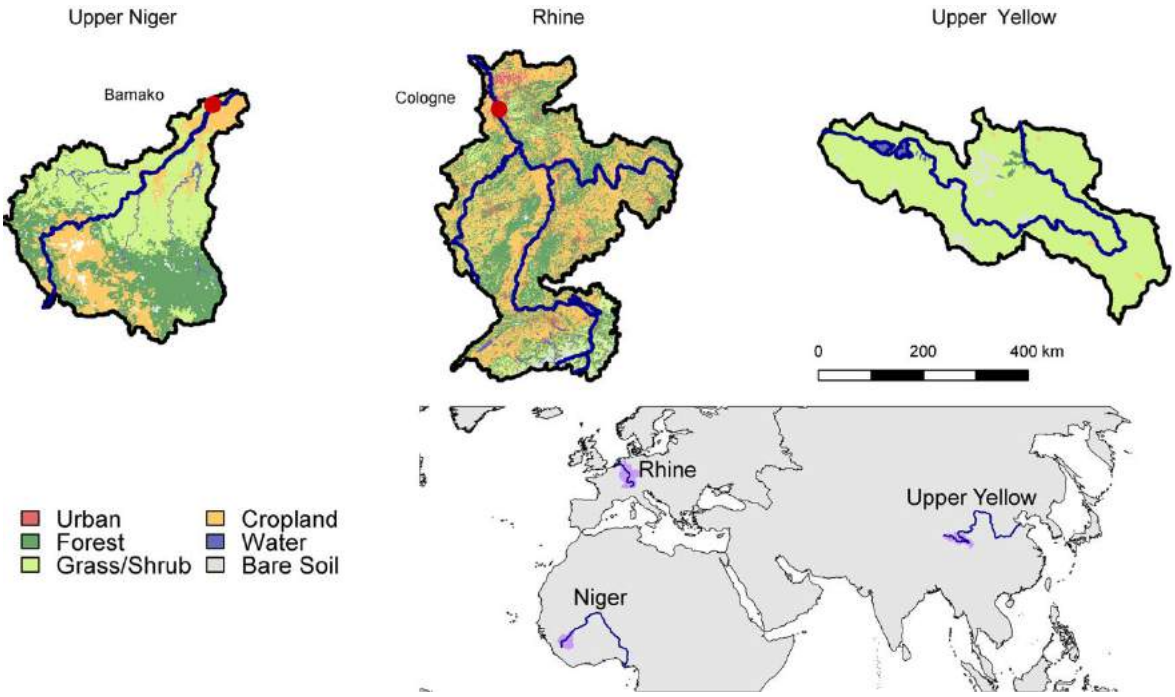

Figure 35 Land-use maps of the three basins under study: the Upper Niger, the Rhine and the Upper Yellow

5.2.1.2. The Upper Yellow

The Yellow River (hereafter called Yellow) in its lower reaches is heavily influenced by human water use like irrigation, and abstraction for industry and municipal purposes. Hydrological modeling of the total river basin requires a lot of water management information, which is not easily available. Therefore, the headwater part, which is crucial for water supply to the whole river basin, was chosen in our case. The Yellow River source region above the Tangnaihai gauging station belongs to the Qing–Tibetan Plateau of China. This Upper Yellow basin with the drainage area of about 122 000 km2 covering approximately 15% of the entire Yellow River's drainage basin, while supplying 38% of the river's total runoff (Chen et al., 2013), was chosen for our study. This area has been designated as a part of the "Three Rivers' Sources" National Nature Reserve, which was created to protect the source region of the Yellow River, the Yangtze and the Mekong (also called China's water tower supplying water to the whole country). The Upper Yellow flows mainly through pastures, swamps, and knolls between mountains, and crystal clear lakes are characteristic of this area. The two major lakes along this part are Lake Zhaling and Lake Eling, with capacities of 4.7 and 10.8 billionm2, respectively. The mean altitude of the drainage area is about 4000 m.

The Yellow River source region belongs to the cold and dry climate zone, with the annual average temperature about −4 C and average annual precipitation lower than 500mm (see Table 7), with 70% of precipitation falling from July to October. The

headwaters of the Yellow River basin are not much influenced by human activities, besides some overgrazing and wild herb digging.

5.2.1.3. The Rhine

The Rhine River basin covers a drainage area of about 185 000 km2 and spreads over nine European countries. The Rhine River starts from the confluence of two small rivers originating in Switzerland, then forms the Swiss–German and French–German borders before flowing through Germany. In its lower part, it enters the Netherlands, where it forms an extensive delta and finally releases into the North Sea. Its main tributaries are the Main, the Neckar and the Moselle. Approximately two thirds of the Rhine drainage basin is located in Germany. The altitude in the drainage area ranges from 4275ma.s.l. in the Swiss Alps to 0ma.s.l. at Rotterdam. Regarding its hydrological characteristics, the basin can be subdivided into three major sub-areas: the Alpine area, the German middle mountain area and the lowland area. Two major land cover types in the drainage basin are arable land (38 %) and forest (25 %).

The average annual precipitation of 987mm in the Rhine is lower than in the Upper Niger but higher than in the Upper Yellow (Table 7), and seasonality is not very distinct. In the Alpine region, the maximum discharge of the Rhine is observed during summer due to snowmelt. Downstream of Basel (close to the Swiss–French–German border crossing), a pluvio-nival hydrological regime of the Rhine gradually becomes dominant. The rainfall-dominated tributaries (Moselle and Neckar) contribute to the second maximum discharge of the Rhine in winter in this part. In the middle and lower Rhine, the winter peak is higher than the summer one, changing the runoff regime into the pluvial type. Compared to the other two rivers in our study, the Rhine is more influenced by human water management. In this study, the Rhine basin was modeled until the Rees gauge (160 000 km2).

5.2.2. Input data and climate scenarios

The digital elevation model (DEM) constructed from the Shuttle Radar Topography Missions with 90m resolution was used for altitude information (Jarvis et al., 2008). Soil parameters (soil depth, texture, bulk density) were derived from the Digital Soil Map of the World (FAO et al., 2009), and other parameters needed by models (field capacity – by HBV – porosity, field capacity, available water capacity and saturated conductivity – by SWIM and VIC) were derived using pedotransfer functions and tables (hoc AGBoden, 2006). Land use was parameterized using the Global Land Cover data (GLCF) (Bartholomé and Belward, 2005). Observed river discharge data from the Global Runoff Data Centre were used to calibrate and validate the hydrological models (GRDC, 1998). As climate input for model calibration, the WATCH reanalysis data were applied with a grid resolution of 0.5° (Weedon et al., 2011).

For the climate impact assessment, the hydrological models were driven with outputs of five bias-corrected earth system models of the Coupled Model Intercomparison Project Phase 5 (CMIP5): HadGEM2-ES, IPSL-5 CM5ALR, MIROC-ESM-CHEM, GFDL-ESM2M, and NorESM1- M. Later, the following abbreviations are used for scenarios produced by these models: Had, IPSL, MIROC, GFDL and Nor. Climate scenarios were downscaled to a grid resolution of 0.5° and bias corrected by the ISI-MIP project using a trend-preserving bias-correction method with the WATCH reanalysis data (Hempel et al., 2013). Four RCPs covering a range of emissions and land-use change projections, from RCP2.6 to RCP8.5, were included in the study.

5.2.3. Hydrological models

Two hydrological models, HBV and VIC, and the SWIM ecohydrological model were used in the study.

5.2.3.1. HBV

The HBV model (Bergström and Forsman, 1973; Bergström and Singh, 1995) is a conceptual rainfall–runoff model. The model was developed for runoff simulation and hydrological forecasting. The advantage of HBV is that it covers the most important runoff generating processes by quite simple and robust structures where topographic and climate parameters serve as driving forces. Besides, HBV does not require extensive data sets.

In our study a modified semi-distributed version of the HBV model (HBV-D, Krysanova et al., 1999), with a finer spatial disaggregation into subbasins and 10 elevation zones and up to 15 land cover types, was applied. The modification was based on the Nordic HBV version (Saelthun, 1996).

HBV has been applied for modeling hydrological processes in countries with different climatic conditions, as, for example, Sweden, China (Zhang and Lindström, 1996), Zimbabwe (Lidén et al., 2001), and Mozambique (Andersson et al., 2011) and the scales ranging from small catchments to the entire Baltic Sea drainage basin (Graham, 1999). The model is also used worldwide in climate impact assessment studies (Menzel et al., 2006; Yu and Wang, 2009).

5.2.3.2. SWIM

The SWIM (Soil and Water Integrated Model, Krysanova et al., 1998) ecohydrological model is a continuous-time spatially semi-distributed model of intermediate complexity for river basins. It integrates hydrological processes, vegetation growth, nutrient cycling, erosion and sediment transport on the river basin scale. SWIM was developed based on two models, SWAT (Arnold et al., 1993) and MATSALU (Krysanova et al., 1989), with the aim of providing a tool for climate and land-use change impact assessment in

mesoscale and large river basins. The spatial disaggregation scheme in SWIM includes subbasins and hydrotopes. The hydrotopes are created by overlaying three maps: subbasins, land use and soil. At the hydrotope level, all soil water flows, nutrient cycling in soil and vegetation growth are simulated, based on the principle of similarity, i.e., assuming that units within one subbasin that have the same land use and soil types behave similarly. The model was validated and applied for impact assessment in many medium and large river basins in Europe, Africa and Asia (Hattermann et al., 2011; Huang et al., 2013; Liersch et al., 2013). An overview of SWIM application for impact studies is given in Krysanova et al. (2015).

5.2.3.3. VIC

The Variable Infiltration Capacity (VIC) model (Liang et al., 1994, 1996) is a semi-distributed hydrological model for large-scale applications. The land surface processes in VIC are modeled as a grid of large (usually >1 km), flat, uniform cells, and the sub-grid heterogeneity (e.g., in elevation, or land cover) is handled using statistical distribution functions. The water and energy balances at the land surface can be simulated at a daily or sub-daily time step. The runoff processes are represented through the variable infiltration curve, parameterization of the effects of sub-grid variability in soil moisture holding capacity and a representation of the non-linear baseflow. The modeler can subdivide each grid cell into an arbitrary number of tiles, each corresponding to the fraction of the cell covered by a particular land cover (i.e., grassland, coniferous forest, etc.). VIC takes into account snow in several forms: ground snow pack, snow in the vegetation canopy, and snow on top of lake ice. The processes in grid cells are simulated independently, and the routing of water flow is performed separately from the land surface simulation. VIC has been applied extensively in climate impact studies for a number of large river basins over the continental US and the globe (Hamlet and Lettenmaier, 1999; Su and Xie, 2003; Christensen and Lettenmaier, 2007).

5.2.4. Setup and calibration of three models

The three models differ in their levels of complexity, mathematical process formulation and spatial resolution. For example, vegetation growth is simulated only in SWIM, whereas HBV and VIC use fixed monthly plant characteristics. Spatial resolution of SWIM and HBV is finer than that in VIC, though statistical distribution functions allow one to account for vegetation and soil processes in VIC as well. On the other hand, VIC describes land–atmosphere processes with more detail than the other two models. Table 8 describes some major differences between the three models. Among them, the differences in soil and vegetation representation are important.

In this study, SWIM and HBV were set up with different spatial representations compared to VIC. For the VIC raster based model, a grid resolution of 0.125° was used for

all basins. For example, for the Rhine basin, 1433 grid cells were simulated by VIC. For the SWIM and HBV applications, the basins were subdivided into subbasins with an average area of 100–200 km2 using the SRTM digital elevation model; so, for the Rhine, 1668 subbasins were created. All the subbasins and grid cells were further disaggregated considering land use and elevation zones. In addition, SWIM used soil information along with land use for disaggregation of subbasins into hydrotopes.

In total, for the Rhine basin, 26,961 units were simulated by VIC, 41,976 hydrotopes were modeled by SWIM, and 69,589 units were simulated by HBV, with average areas of 5.9, 3.8, and 2.3 km^2, respectively.

All hydrological models were calibrated using the observed discharge at the basin outlet. For SWIM and VIC, automatic calibration was performed with the PEST software package (Doherty, 2005) using the mean square error (MSE) between the observed and simulated discharges as an objective function. A multi-objective calibration was applied for all basins modeled with HBV using the NSGA II algorithm (Deb et al., 2002). As an objective function, the Nash and Sutcliffe efficiency (Nash and Sutcliffe, 1970) of untransformed (NSE) and log-transformed (logNSE) observed and simulated discharges was taken. After optimization, the one simulation from the Pareto front was selected, which was closest to the points NSE=1 and logNSE=1, reflecting the theoretically best possible value for NSE and logNSE.

The number of parameters used for calibration differ between the models and the three basins. For VIC, only five parameters were used to calibrate the model, eight for SWIM and 19 for HBV. For the Upper Niger basin, a reduced number of calibration parameters was used, as all snow-related parameters were excluded.

Table 8 Differences between spatial disaggregation, climate input and representation of main components in the three hydrological models used in the study.

Features	HBV	SWIM	VIC
Spatial disaggregation	Subbasins, 10 elevation zones and land-use classes within them	Subbasins and hydrotopes (based on land use and soil types within subbasins)	Grid cells, sub-grid heterogeneity (elevation, land cover) is handled via statistical distributions
Climate data input	Two parameters: T b mean, precipitation	Six parameters: T_{min}, T_{mean}, T_{max}, precipitation, air humidity, radiation	Five parameters: T_{min}, $T_{max,}$ precipitation, air humidity, wind speed
Representation of soils	One soil layer, two soil parameters	Up to 10 soil layers, 11 soil parameters	Typically 3 soil layers, 19 parameters
Representation of vegetation	Fixed monthly plant characteristics	Simulation of plant growth using the EPIC approach	Fixed monthly plant characteristics
Calculation of potential evapotranspiration	Blaney–Criddle	Priestley–Taylor	Penman–Monteith
Method to calculate snowmelt	Degree-day	Extended degree-day method	Two-layer energy balance model at the snow surface
Runoff routing method	Simple time lag method	Muskingum method	Linearized St. Venant equations

5.2.4.1. Methods of trend analysis

Trends in projected runoff were calculated for three runoff quantiles, which reflect the annual high-flow conditions (Q_{10}), the annual low-flow conditions (Q_{90}) and the medium-flow conditions (Q_{50}). To avoid the same event being separated between two adjacent years, the hydrological years have been taken instead of the calendar years for calculation of annual Q_{50} and Q_{10}. As Q_{90} may occur at the end or at the beginning of a new hydrological year, we used a different approach for this quantile. To calculate Q_{90}, a year starts from a month when, on average, the high flow is reached (different months in our three basins). The quantiles were calculated for the scenario period 2010–2099, and then analyzed for trends.

The trends in the projected runoff quantiles were calculated using the robust linear MM estimator (Yohai, 1987; Koller and Stahel, 2011). The MM estimates are calculated by a three-step procedure: (1) a regression estimate with a high breakdown point, (2) an M estimate of the error scale using residuals from step 1, and (3) an M estimate of the regression parameters based on a proper re-descending psi function. The M estimates with a monotone psi function were introduced by Huber (1973). The convergent iterative numerical algorithm for the MM estimates was provided by Yohai (1987), and is included in the R statistical software. For the trend analysis in our study, the "lmrob" function from the "robust" package in R was used.

Compared to the ordinary least squares prediction (OLS), the robust trend estimator is less sensitive to outliers or extreme values and to deviations from the Gaussian

distribution. For example, one extremely wet year at the end of the considered time period would have a significant influence on the predicted trend when using the OLS method (bad leverage point), but it would not influence much the trend prediction using the MM estimator. On the other hand, the MM estimator is usually less efficient (i.e., provides the higher p values) compared to the OLS prediction. In the present study, the standard setup of "lmrob" with an asymptotic relative efficiency of 95% was applied. The statistically significant trends correspond to the p values lower than 0.05.

5.2.5. Method of uncertainty evaluation

For evaluation of different sources of uncertainty, an analysis of variance (ANOVA) is performed. ANOVA is a tool for partitioning observed variances into different sources of contributing variation. In the present study, three factors are used for variance decomposition (three-way ANOVA). The total sum of squares (SST) is defined as

$$SST = \sum_{i=1}^{N_{Hyd}} \sum_{j=1}^{N_{GCM}} \sum_{k=1}^{N_{RCP}} \left(Y_{ijk} - \bar{Y}_{ooo}\right)^2 \tag{14}$$

where Y_{ijk} is the particular value corresponding to hydrological model i, climate model j and RCP k, respectively, and $\bar{Y}_{000}$ is the overall mean. According to to ANOVA theory, SST can be split into seven fractions:

$$SST = \underbrace{SS_{Hyd} + SS_{GCM} + SS_{RCP}}_{main\ effects} + \underbrace{SS_{Hyd*GCM} + SS_{Hyd*RCP} + SS_{GCM*RCP} + SS_{Hyd*GCM*RCP}}_{interaction\ terms} \tag{15}$$

The total sum of squares is partitioned into three main effects SS_{Hyd}, SS_{GCM}, and SS_{RCP}, corresponding to three hydrological models, five GCMs and four RCPs, respectively. In addition, there are four interaction terms $SS_{Hyd*GCM}$, $SS_{Hyd*RCP}$, $SS_{GCM*RCP}$, and $SS_{Hyd*GCM*RCP}$, describing the situation where effects are non-additive or nonlinear. For example, the precipitation trends in the Upper Niger (Figure 36) show noticeable interaction effects. There are strong dependencies of precipitation on the RCPs for each single GCM but, in three cases, GCMs show negative trends and, in two cases, GCMs show positive trends. In the case of no interactions, all the lines would run in parallel. Exemplarily, the calculations of one main effect, one first order interaction term and the second-order interactions are given below:

$$SS_{Hyd} = N_{GCM}N_{RCP}\sum_{i=1}^{N_{Hyd}}(\bar{Y}_{ioo} - \bar{Y}_{ooo})^2 \quad (16)$$

$$SS_{Hyd*GCM} = N_{RCP}\sum_{i=1}^{NHyd}\sum_{j=1}^{N_{GCM}}\left(\bar{Y}_{ij0} - \bar{Y}_{ioo} - \bar{Y}_{ojo} + \bar{Y}_{ooo}\right)^2 \quad (17)$$

$$SST_{Hyd*GCM*RCP} = SST - SS_{Hyd} - SS_{GCM} - SS_{RCP} - SS_{Hyd*RCP} - SS_{Hyd*GCM} - SS_{GCM*RCP} \quad (18)$$

where N_{Hyd}, N_{GCM}, and N_{RCP} describe the number of hydrological models, the number of GCMs and the number of RCPs, respectively. The token ° indicates averaging over a particular index.

Bosshard et al. (2013) showed that different sample sizes of the uncertainty sources result in a biased variance estimation. To avoid such a bias, Bosshard et al. (2013) complemented the ANOVA with a subsampling scheme. Following the general approach from Bosshard et al. (2013), in the present study, the five GCMs, four RCPs and three hydrological models are subsampled in a way that all possible combinations of three hydrological models, three GCMs and three RCPs are fulfilled; so, for the four RCPs, we have four combinations ($c_1 - c_4$) for selecting a subsample with $N_{RCP} = 3$, namely $c_1 = 2.6, 4.5$, an6.5d, $c_2 = 2.6, 4.5$, and 8.5, $c_3 = 2.6, 4.5$and 8.5, and $c_4 = 2.6, 4.5$, and 8.5. For the five GCMs, there are 10 possible combinations. These four possible RCP combinations and 10 possible GCM combinations are finally combined into a total number of 40 subsamples. Each of the 40 subsamples contains 27 simulations (using 3 GCMs, 3 hydrological models and 3 RCPs). For each of these 40 subsamples, the ANOVA calculation using the formulas above is fulfilled After calculation of all the partial sums of squares for all 40 subsamples, the unbiased variance fractions η 2 related to different components can be calculated. For example, the partial variance related to hydrological models can be calculated as

$$\eta^2_{Hyd} = \frac{1}{40}\sum_{m=1}^{40}\frac{SS_{Hyd}(m)}{SST(m)} \quad (19)$$

.

The calculation of the contributing variance fraction for all the other six components is analogous to Eq. (**19**).

5.3. Results

5.3.1. Calibration and validation of hydrological models

The results of calibration and validation in terms of fit NSE and percent bias (PBIAS) are presented in Table 9 and Figure 36 for three models and three basins. In general, the validation results are good, with NSE ranging from 0.81 to 0.93 for the daily time step. The lowest NSE is 0.81 for the VIC application in the Rhine basin. The percent bias values are between −3.6 and +3.8 % for the simulations in the validation period. Figure 36 shows a comparison of a 30 day moving average of daily river discharge, simulated by three hydrological models and observed for 5 years in both the calibration and validation periods, and a comparison of the long-term average seasonal discharges in the calibration and validation periods. As is evident, dynamics are simulated adequately by all three models in the three basins. The river discharges simulated by HBV and SWIM are very similar, and the VIC outputs show some moderate differences in the Upper Yellow, with an underestimation of discharge in the first part of the year and an overestimation of discharge in September and October.

Table 9 Calibration and validation results with the daily time step. NSE = Nash and Sutcliffe efficiency; pbias = percent bias.

	Calibration			Validation		
Rhine	**HBV**	**VIC**	**SWIM**	**HBV**	**VIC**	**SWIM**
Period	19811990	19811990	19811990	1991 2000	19912000	19912000
NSE	0.75	0.81	0.87	0.83	0.81	0.9
Pbias (%)	0.0	−3.6	0.6	3.8	−9.3	−3.6
Upper Yellow	**HBV**	**VIC**	**SWIM**	**HBV**	**VIC**	**SWIM**
Period	19611970	19611970	19611970	19711980	19711980	19711980
NSE	0.89	0.79	0.82	0.88	0.75	0.75
Pbias (%)	1.5	−6.9	−0.1	2.6	0.4	4.6
Upper Niger	**HBV**	**VIC**	**SWIM**	**HBV**	**VIC**	**SWIM**
Period	19611970	19611970	19611970	19711980	19711980	19711980
NSE	0.91	0.88	0.92	0.93	0.87	0.91
Pbias (%)	6.8	3.3	2.8	3.4	−5.7	2.0

In addition, the annual simulated values of Q_{90}, Q_{50} and Q_{10} in the calibration and validation periods were compared to those estimated from the observed time series, and results are presented in Figure 37 and Table 10. All hydrological models show a good performance for high-flow conditions (Q_{10}) in all three basins. The coefficient of correlation ranges from 0.78 to 0.97 for the validation period, and the bias is between −13.6 and +14.6 %, and in seven cases of nine it is between −7 and +8.4 %, for the same period.

In the Rhine basin there is also a good agreement between the observed and simulated Q_{50} and Q_{90} values. The lowest coefficient of correlation for the two quantiles is 0.88 for Q_{90} simulated by VIC. The highest bias for Q_{90} in the validation period is −17.2 % (VIC). For Q_{50} the highest bias is +6.3 % for the simulation run with HBV.

The simulation results for Q_{90} and Q_{50} in the Upper Yellow and the Upper Niger are not as good as for the Rhine basin. For Q_{50} in the Upper Niger, the coefficient of correlation ranges from 0.78 to 0.92 in the validation period, but a large bias of +40.5 % was found for SWIM. In the Upper Yellow, the maximum bias is lower (−20.1 % for VIC), but here the correlation between the observations and simulations is lower (ranges from 0.33 to 0.7). For the low-flow simulations (Q_{90}), the biases in the validation period are even higher than for Q_{50}. The maximum bias of +108.4 % was found for the HBV simulations in the Upper Niger. In the Upper Yellow, VIC showed a maximum bias of −49.5 %. The coefficient of correlation ranges from 0.18 to 0.91 in the Upper Yellow and from 0.52 to 0.72 in the Upper Yellow.

Summarizing the hydrological model validation, we can conclude that, in general, the results are good in terms of NSE and PBIAS for river discharge, in terms of correlation and PBIAS for high flows Q_{10} in all three basins, and for Q_{50} and Q_{90} in the Rhine. However, the results for Q_{50} and Q_{90} in the Upper Yellow and the Upper Niger are weaker. In our view, this could be due to high seasonality in runoff in these basins. For example, in the Niger, the average Q_{10} is nearly 100 times higher than Q_{90}. Therefore, low flow gets small weights in the calibration process, leading to bias in simulations.

In total, there is no hydrological model that outperforms the others.

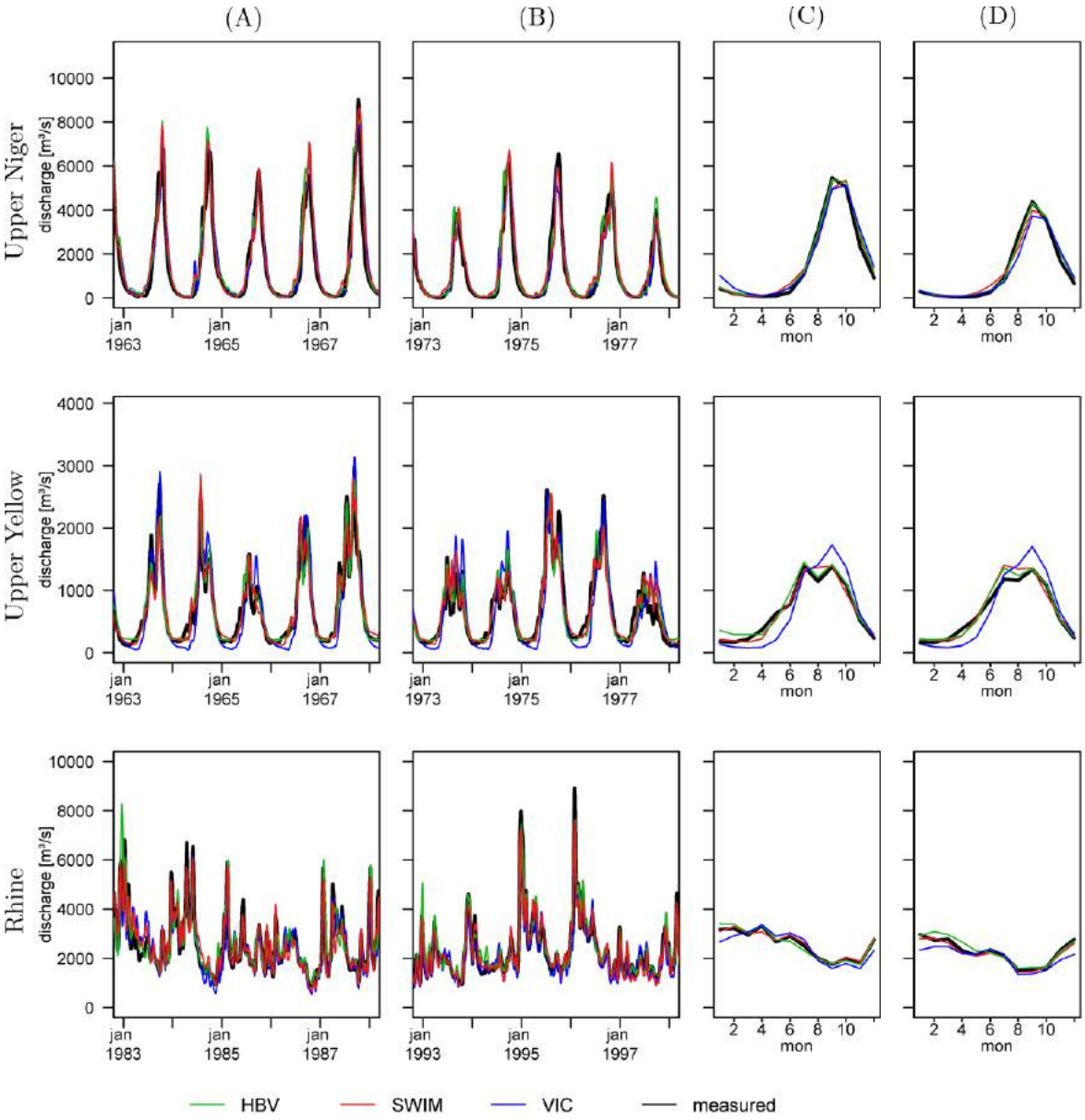

Figure 36 Results of calibration and validation of three models in three basins: comparison of the simulated and observed 30 day moving average discharges for 5 years in the calibration (a) and validation (b) periods, and comparison of the long-term average seasonal discharges in the calibration (c) and validation (d) periods.

Table 10 Coefficient of correlation (cor) and percent bias (pbias) for the three runoff quantiles (Q_{90}, Q_{50}, Q_{10}) in the calibration and the validation period

	Calibration			Validation		
Rhine	**HBV**	**VIC**	**SWIM**	**HBV**	**VIC**	**SWIM**
Period	19811990	19811990	19811990	1991 2000	19912000	19912000
Q_{90} cor	0.96	0.94	0.9	0.93	0.93	0.88
Q_{90} pbias	4.4	0.0	−13.0	5.8	−0.8	−17.2
Q_{50} cor	0.93	0.94	0.94	0.95	0.98	0.98
Q_{50} pbias	3.8	8.0	3.6	6.3	1.1	−4.7
Q_{10} cor	0.95	0.94	0.93	0.96	0.96	0.95

Q_{10} pbias	-3.9	-3.4	-5.8	0.4	-1.9	-7.5
Upper Yellow	**HBV**	**VIC**	**SWIM**	**HBV**	**VIC**	**SWIM**
Period	19611970	19611970	19611970	19711980	19711980	19711980
Q_{90} cor	−0.16	0.66	0.02	0.18	0.91	0.25
Q_{90} pbias	39.6	1.9	−56.2	25.4	14.4	−49.5
Q_{50} cor	0.72	0.82	0.87	0.33	0.70	0.57
Q_{50} pbias	4.2	−3.4	−35.0	−3.5	5.7	−20.1
Q_{10} cor	0.84	0.93	0.88	0.97	0.89	0.79
Q_{10} pbias						
Upper Niger	**HBV**	**VIC**	**SWIM**	**HBV**	**VIC**	**SWIM**
Period	19611970	19611970	19611970	19711980	19711980	19711980
Q_{90} cor	0.74	0.79	0.26	0.52	0.34	0.72
Q_{90} pbias	61.6	4.2	37.6	108.4	27.0	63.2
Q_{50} cor	0.69	0.4	0.08	0.92	0.83	0.78
Q_{50} pbias	30.1	38.1	41.1	9.6	40.5	−4.0
Q_{10} cor	0.71	0.84	0.71	0.78	0.81	0.79
Q_{10} pbias	2.1	−1.7	−2.7	−3.8	−10.9	13.6

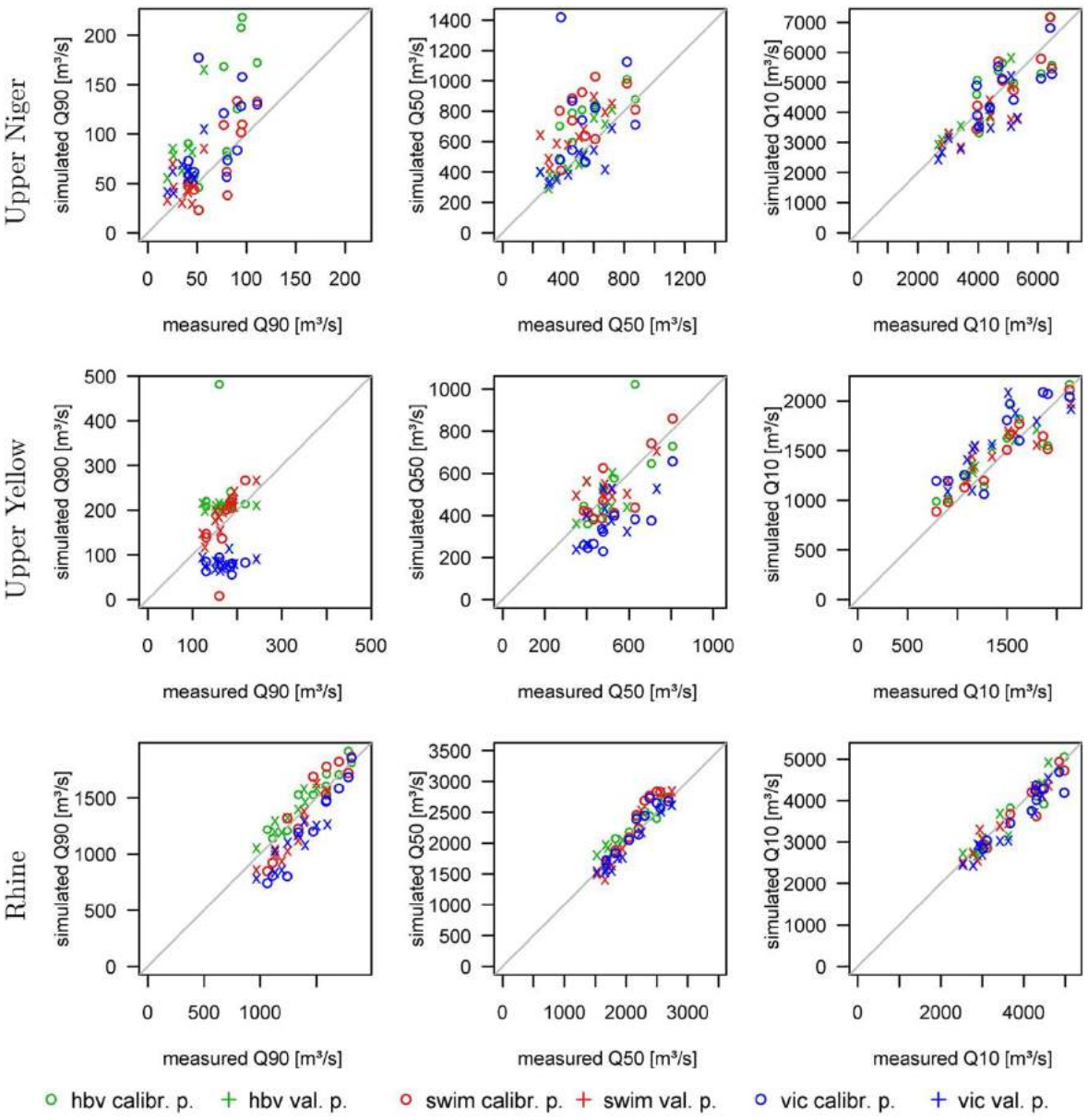

Figure 37 Comparison of simulated and observed annual values of Q90, Q50 and Q10 in the calibration and validation periods for three basins: the Upper Niger, Upper Yellow and Rhine.

5.3.2. Evaluation of climate scenarios

For the assessment, the time period 1961–1990 was chosen as the reference period, and two periods 2021–2050 and 2061–2090 were considered as two scenario periods SP1 and SP2, respectively. The simulated precipitation (P) and temperature (T) were evaluated and compared between the reference and scenario periods for the three basins.

Figure 38 shows the long-term average monthly simulated P by five GCMs in the reference period 1961–1990 in comparison with the observed P. As one can see, the simulated P in the reference period is very close to the observed one. Obviously, this is mainly due to the applied bias correction. The differences between the long-term average

simulated P in two scenario periods 2021–2050 and 2061–2090 and that in the reference period for four RCPs are also shown in Figure 38. Additionally, the long-term average annual changes in P related to the long-term average annual changes in T are given in Figure 38 for the second scenario period.

For the Upper Niger, changes in P vary between climate models, especially in months 4–7: two or three climate scenarios show a decrease in P, and the other three or two an increase. The MIROC scenarios show mostly an increase, which is mostly higher than that simulated by other models, reaching 90–140 mm month−1 in some months of the second scenario period. Panel b shows for the Upper Niger a decrease in P with increasing T projected by two models (IPSL, Nor), and an opposite trend projected by MIROC and GFDL, with the highest increase in P simulated by MIROC. The projected Had P shows the largest differences for RCP2.6 and the smallest differences for RCP8.5, in contrast to the four other GCMs.

Projections for the Upper Yellow show mostly a small or moderate increase in months 5–9, which is mostly below 20 mm month−1 . Only in the second period do MIROC and IPSL project higher increases in some months. According to panel b, the increase in T is accompanied by an increase in P in almost all cases.

The projected changes in monthly P for the Rhine are also moderate, mostly within ±20 mm month−1; only the Had scenarios show a stronger decrease in some months, and MIROC a higher increase in summer months, contradicting other models. For the Rhine, all GCMs project an increase in precipitation for RCP2.6. Except for Nor, all the other GCMs show a smaller increase in P for all the higher level RCPs.

After the model calibration and validation, the simulated long-term average discharge driven by the bias-corrected climate model outputs in the period 1961–1990 was compared with the observed one. As is evident from Figure 39, the simulated and observed discharges agree well for all basins and driving climate models. This is mainly due to the bias correction of climate model outputs. The agreement between 15 simulations for the reference period is very good for the Upper Niger, good for the Rhine, but weaker for the Upper Yellow.

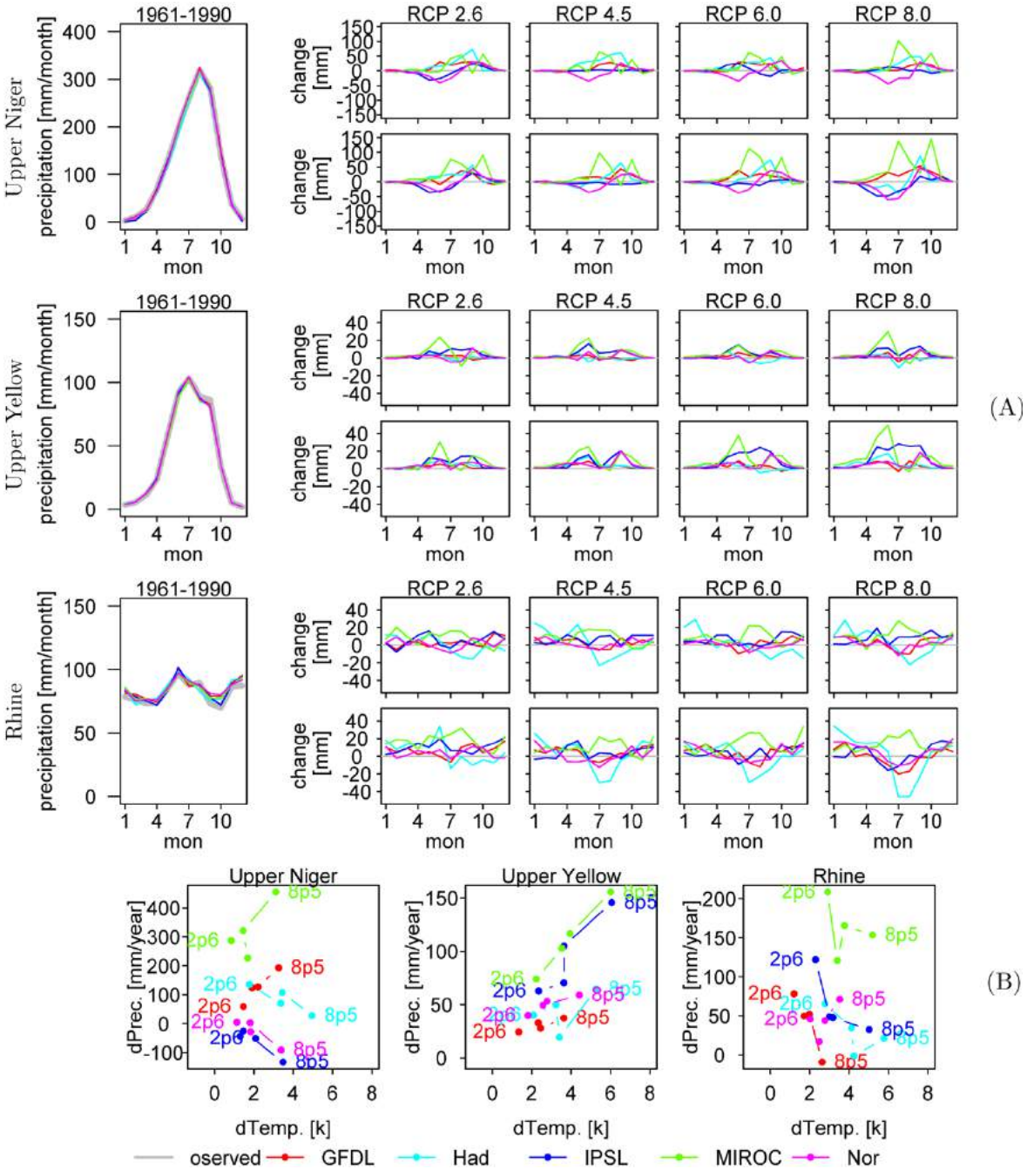

Figure 38 Evaluation of precipitation (P) and temperature (T) simulated by five climate models in three basins. (a) Left: comparison of the observed and simulated long-term average monthly P in the reference period 1961–1990; right: differences between simulated P in two scenario periods 2021–2050 and 2061–2090 and that in the reference period for four RCPs: 2.6, 4.5, 6.0, and 8.5. (b) The long-term average annual changes in P (dPrec) in relation to the long-term average annual changes in T (dTemp) in the second scenario period related to those in the reference period for four RCPs.

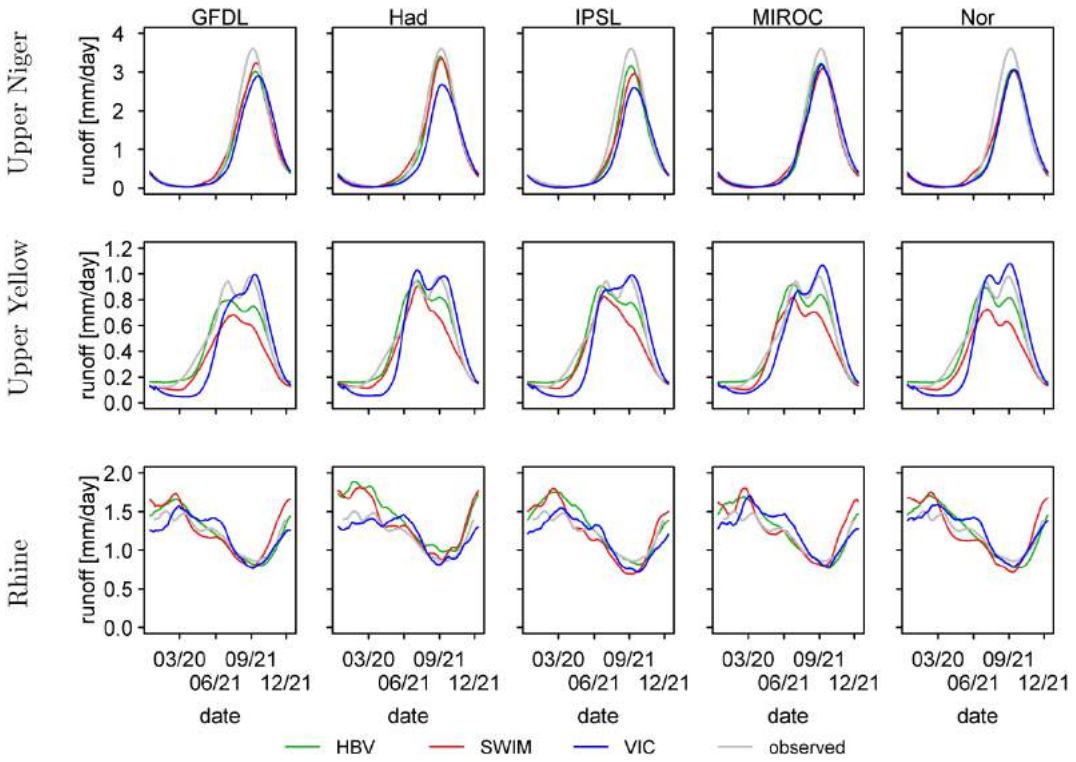

Figure 39 Comparison of the long-term average seasonal observed discharge in 1961–1990 with discharge driven by five climate models and three hydrological models for the same period.

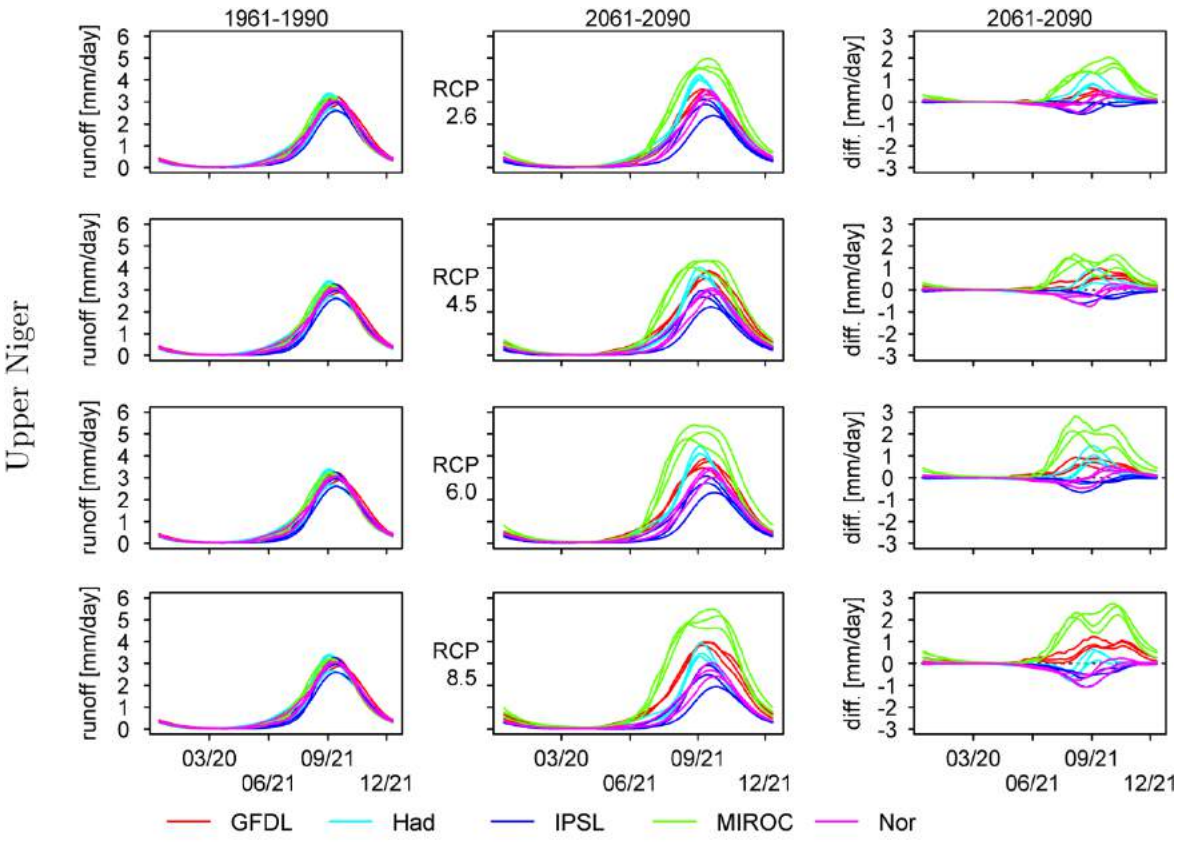
Upper Niger
1961-1990
2061-2090
2061-2090
RCP 2.6
RCP 4.5
RCP 6.0
RCP 8.5
runoff [mm/day]
diff. [mm/day]
03/20
06/21
09/21
12/21
GFDL
Had
IPSL
MIROC
Nor

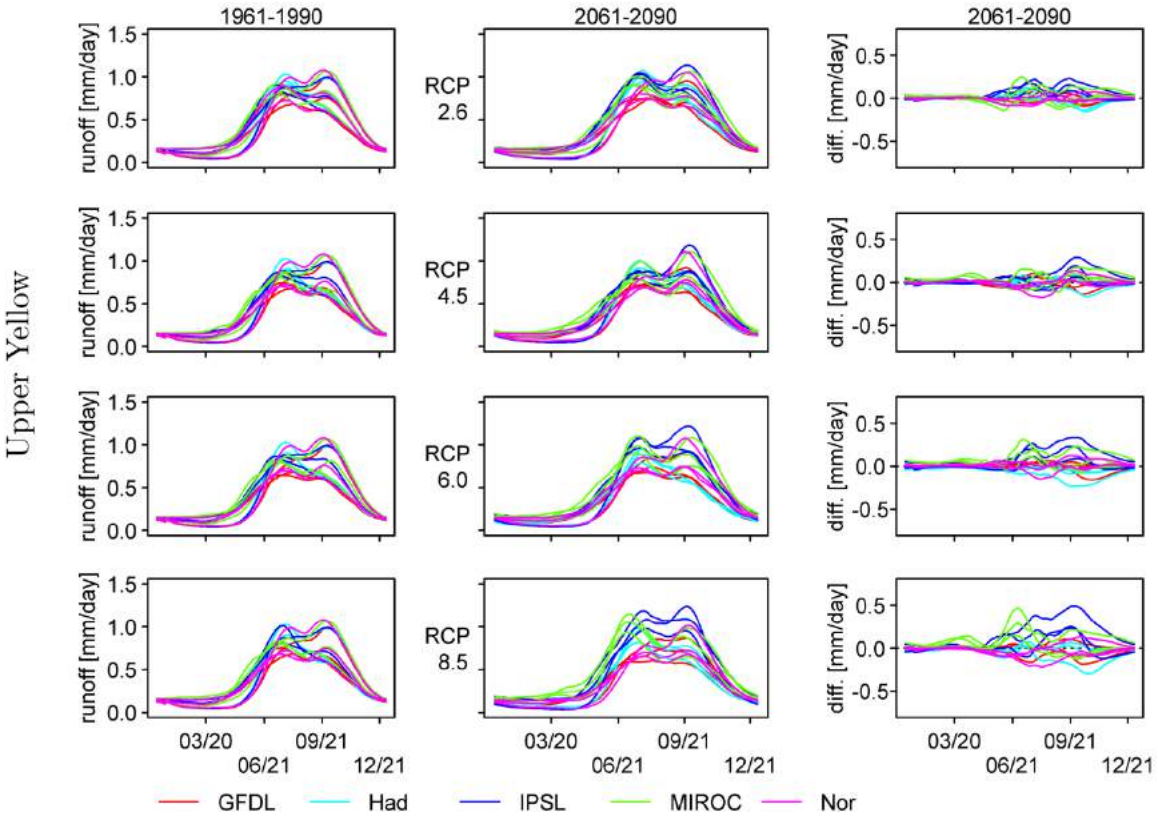
Upper Yellow
1961-1990
2061-2090
2061-2090
RCP 2.6
RCP 4.5
RCP 6.0
RCP 8.5
runoff [mm/day]
diff. [mm/day]
03/20
06/21
09/21
12/21
GFDL
Had
IPSL
MIROC
Nor

5.3.3. Impacts on seasonal dynamics

After the calibration and validation of the three hydrological models, they were run for the period 1971–2099 using five GCM scenarios for four RCPs providing 60 time series, which were analyzed for long-term average seasonal dynamics and trends.

Figure 40 presents the long-term average seasonal discharge for the reference period 1961–1990, for the second scenario period 2061–2090 and the difference between the second scenario and the reference periods.

For the Upper Niger, a high discrepancy between simulations driven by different CMs is visible, and agreement between HMs is higher: three curves of the same color are close to one another. The increase in discharge projected by simulations driven by MIROC is highest in the rainy season from July to December (and increases from RPC2.6 to RCP8.5), followed by those driven by GFDL, which also show an increase. On the opposite end, the IPSl- and Nor-driven projections show a decrease in discharge in this season, and the simulations using Had scenarios are in between.

For the Upper Yellow River, changes in average daily discharge are smaller compared to the Upper Niger. The simulations driven by two CMs, IPSL and MIROC, project an increase in the second half of the year (months 7–11), whereas the results driven by three other CMs show rather moderate changes. The magnitude of the changes clearly and steadily increases from RCP2.6 to RCP8.5.

For the Rhine, a decrease in the summer period (results driven by four CMs of five) and a moderate increase in winter time are projected, which corresponds well to the previous impact assessments for this basin (see, e.g., Huang et al., 2010). The MIROC-driven outputs show mostly an increase for all months and RCPs. Uncertainty related to CM is visually higher compared to that related to HM (clustering of curves with the same color). The projections by SWIM and VIC agree very well (though are not shown in Figure 40).

The results driven by the MIROC climate model for all three basins show the highest discharge in the scenario period compared to the outputs driven by four other CMs in almost all cases. This correlates well with the higher precipitation projected by MIROC for the studied basins. In general, notably lower uncertainty related to HMs compared to CMs is visible in most cases, especially for the Upper Niger and Rhine.

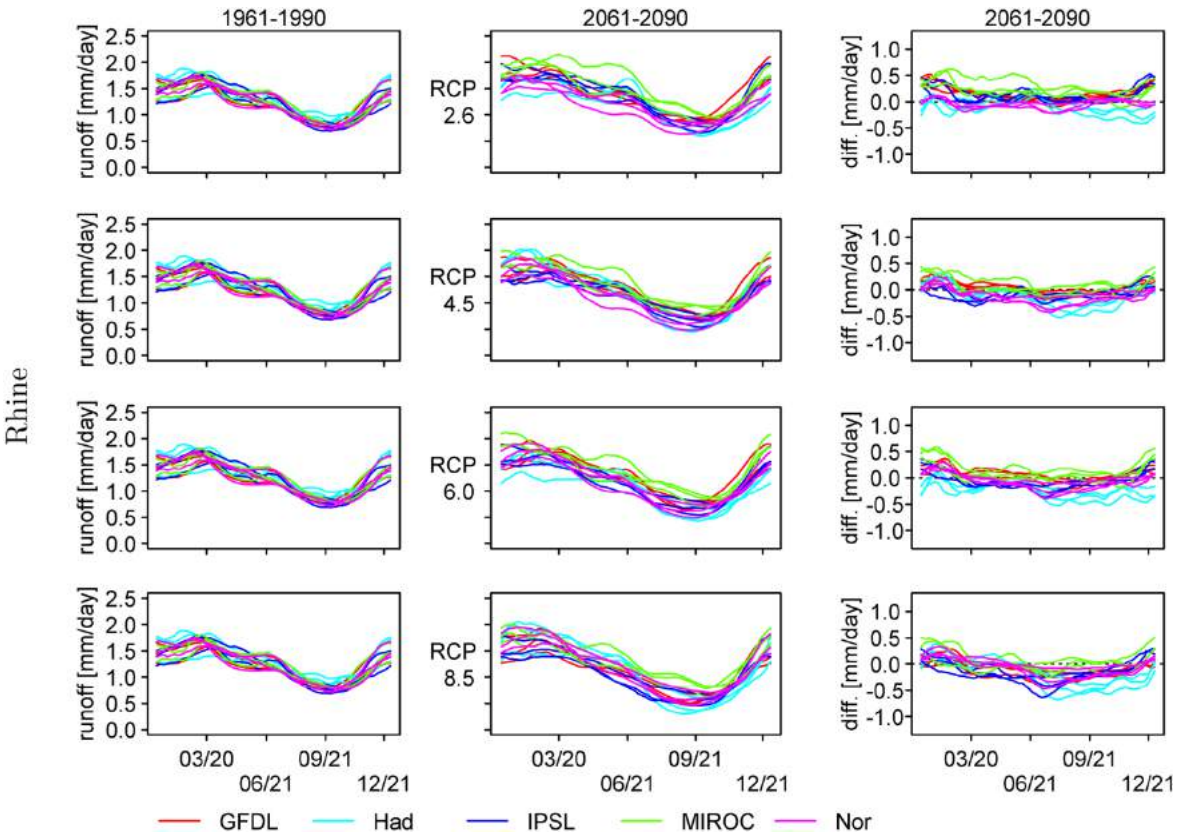

Figure 40 Simulated long-term average seasonal dynamics of river discharge in the reference period 1961–1990 and scenario period 2061–2090 for four RCPs, and the differences in discharge between these two periods; simulations are differentiated by colors corresponding to climate models, whereby three simulations produced by three hydrological models have the same color.

5.3.4. Impacts on trends: magnitude of change and direction

After that, linear trends were calculated using a robust statistical method for three variables: annual median runoff Q_{50}, and low and high annual percentiles Q_{90} and Q_{10} representing the low- and high-flow conditions, respectively. The trends were calculated for the period 2010–2099, and the significance of the trends was evaluated at the 5 % level. The results of trend analysis for the three basins in terms of the slopes of trend and trend direction (and significance) are presented in Figure 41, Figure 42, Figure 43 and Figure S 14, Figure S 15Figure S 16.

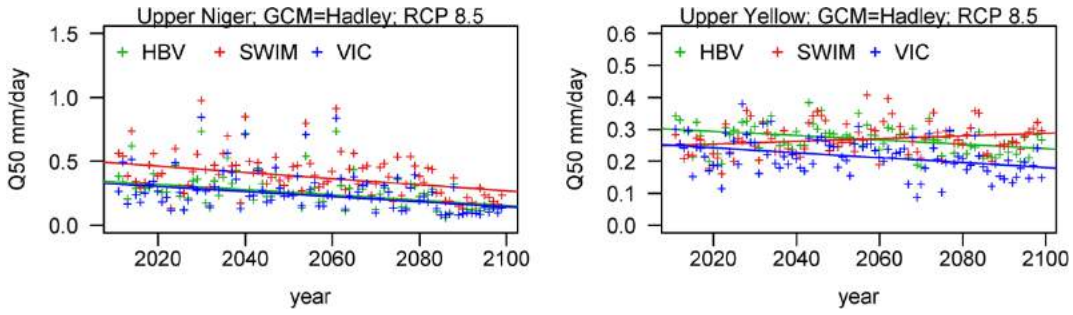

Figure 41 Two examples showing annual median flows Q_{50} estimated from simulations by three models driven by the Had climate scenario data corresponding to RCP8.5 and the corresponding trend lines (all presented trends are significant) for the Upper Niger (left panel) and Upper Yellow (right panel) in the period 2010–2099.

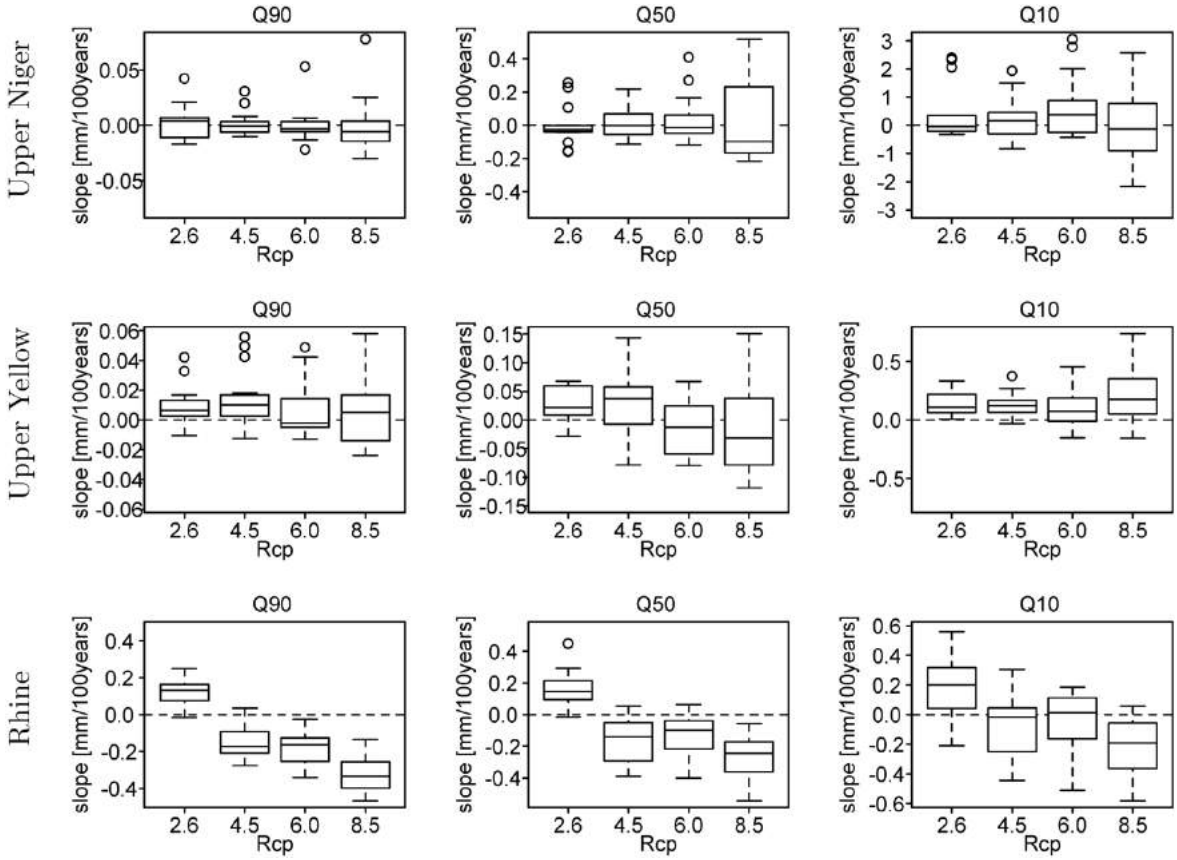

Figure 42 Boxplots for the slopes of the linear trend for the Upper Niger, Upper Yellow and Rhine in three runoff quantiles grouped by RCPs. Outliers as circles. Outlier = distance to median (center line of box) exceeding 2.5 times the interquartile range (length of the box).

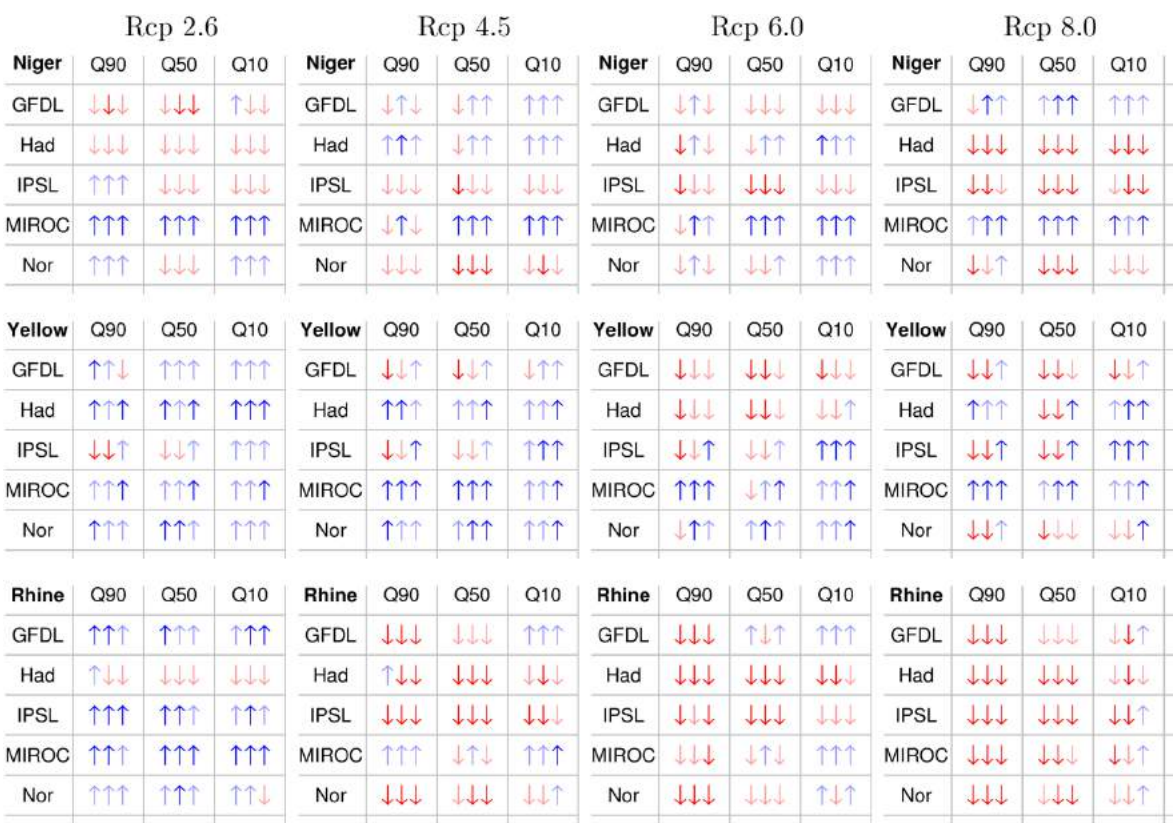

Figure 43 Direction of trends in Q_{90}, Q_{50} and Q_{10} for the Upper Niger, Upper Yellow and Rhine grouped by basins (three horizontal bands), four RCPs (four vertical bands), driving climate models (horizontal lines), and three hydrological models. The first arrow in the small boxes corresponds to HBV, the second one to SWIM, and the third one to VIC. The arrows with statistically significant trends are thicker, and their direction up or down shows an increase or decrease, respectively.

5.3.5. Slope of trend

Two examples of trends for the median flow Q_{50} simulated by the three hydrological models driven by the Had climate scenario and RCP8.5 are presented in Figure 41 for the Upper Niger and Upper Yellow. As is evident, in the first case, all three models agree on a downward trend (all statistically significant). For the Upper Yellow, the models disagree: SWIM shows an increasing trend, and VIC and HBV a decreasing one.

Figure S 14, Figure S 15 and Figure S 16 show the slopes of trends in Q_{90}, Q_{50} and Q_{10}. The results are grouped by climate models and by hydrological models. In addition, Figure 42 shows aggregated results for the slopes of trends as boxplots for four RCPs.

For the Rhine, slopes of the trends in the two variables Q_{90} and Q_{50} are mainly positive under RCP2.6. The trends are negative under three other RCPs, almost steadily decreasing from RCP2.6 to RCP8.5. The slopes of Q_{10} are positive under RCP2.6, negative under RCP8.5, and uncertain under RCP4.5 and RCP6.0.

The results in terms of slopes of the trend for the Upper Niger are highly uncertain for all variables and RCPs. There is no case where at least 75 % of the model runs show the

same trend direction. Only for RCP2.6 and Q50 do more than 75 % of the model runs agree on declining trends.

For the Upper Yellow, all three variables, Q_{90}, Q_{50}, and Q_{10}, show an increase under RCP2.6 and RCP4.5, and the slopes of the trend in Q_{10} representing high flows are positive for all four RCPs.

The Figure S 14Figure S 15Figure S 16 allow one to compare visually uncertainties related to CMs and HMs and to conclude that the agreement between HMs is higher than that between CMs, especially for the Upper Niger and Rhine. The outputs driven by MIROC show the highest slopes for the Upper Niger and Upper Yellow.

5.3.6. Trend significance

Figure 43 summarizes the results of the evaluation of the direction of trends for all 180 time series. The direction of trends in Q_{90}, Q_{50} and Q_{10} are grouped by basins, four RCPs, driving climate models, and three hydrological models. Only statistically significant trends are analyzed below.

For the Niger, much more significant trends were found for RCP8.5 than for the other three. In this case, all simulations (except one) driven by Had and IPSL show a significant downward trend, and almost all simulations driven by MIROC show a significant upward trend. For Q_{50}, the Nor-driven projections corresponding to RCP8.5 agree with those of Had and IPSL, and two of three GFDL projections agree with those of MIROC. The direction of trends in Q_{50} for three other RCPs is positive in all simulations driven by MIROC, and in each of these three cases there is a simulation driven by one of the other CMs that shows a downward trend simulated by all three HMs: GFDL for RCP2.6, Nor for RCP4.5, and IPSL for RCP6.0. The results driven by MIROC show the upward trends in Q_{50} and Q_{10} for all RCPs. In total, a high discrepancy between climate models is obvious for this basin.

For the Upper Yellow, a downward trend in Q_{90} and Q50 simulated by HBV and SWIM driven by three to four climate models was found for RCP8.5, whereas the VIC results either do not show a significant trend, or even disagree and show an upward trend (in three cases). The results for Q_{10} show a moderate agreement in increasing trends, with a growing level of significance from RCP2.6 to RCP8.5. Only for the Yellow could several cases be found, where hydrological models disagree and show significant opposite trends.

Evaluating results for the Rhine, we can conclude with a moderate certainty that all three runoff quantiles show positive trends for RCP2.6. The direction of change is different for three other RCPs. A significant downward trend in Q_{50} and Q_{90} was found in simulations driven by three to four climate models for RCP4.5 and RCP6.0. Q_{90} and Q_{50} show a stronger downward trend in nearly all simulations for RCP8.5. Regarding Q_{10}, there is only a small number of significant trends, and the trend direction changes from a positive trend in the RCP2.6 scenario to a negative one in the RCP8.5 scenario. In general,

a good agreement between CM-driven simulations and HM outputs can be stated for the Rhine.

5.3.7. Evaluation of uncertainty

The sources of uncertainties were analyzed using the ANOVA method described in Sect. 2.5 for the slopes of the linear trend and changes in long-term average seasonal dynamics (Figure 44 and Figure 45). The variance decomposition of the projected slopes for three runoff quantiles is presented in Figure 44.

For the projected high-flow trends (Q_{10}) in the Upper Niger, mainly CMs are important uncertainty contributors, followed by the GCM–RCP interactions and followed by the main effects of RCPs. Together, they contribute about 95 % to the total uncertainty. For Q_{50}, a similar pattern can be observed. For trends in low flow in the Upper Niger, the hydrological models become more important contributors to uncertainty. Their contribution to the overall uncertainty is about as big as the contribution of CMs and the GCM–RCP interactions.

In the Upper Yellow, the contribution of the hydrological models to the overall uncertainty in projected trends is more pronounced than in the Upper Niger. For Q_{90} and Q_{50}, their effect is comparable to the effect of the CMs. Together, they explain 58 % of the variance for Q_{10} and 49 % of the total variance for Q_{10}, respectively. For the high flows, the CMs are the dominant contributors, followed by the hydrological models and the GCM–RCP interaction term.

A different pattern can be seen for the Rhine. Here, the RCPs have the highest influence on the projected trends for all three runoff quantiles. For the trends in low flows, the RCPs contribute 70 % to the overall uncertainty. For Q_{50} and Q_{10}, the CMs become more important contributors of uncertainty, but are still lower than RCPs. For Q_{90}, CMs and RCPs together explain about 70 % and, for Q_{50}, 85 % of the overall uncertainly. In the Rhine basin, there is not much contribution of the hydrological models in the uncertainty of the projected trends.

The sources of uncertainty related to the changes in the long-term average seasonal dynamics of runoff are shown in Figure 45a–c. Figure 45a shows the unscaled results for three basins in two selected scenario periods. To highlight the periods of the year where the changes among the different runoff projections are large (high uncertainty), the graphs presented in Figure 45a were scaled further. The scaling was performed in accordance with the variability in absolute changes (Figure 45b), and also in accordance with the variability in relative changes (Figure 45c). As variance estimators, the interquartile range of absolute changes (Figure 45b) and the interquartile range of relative changes (Figure 45c) were taken for the scaling. When the differences between low-flow and high-flow river runoff are very large, as is the case in the Upper Niger as well as in the Upper Yellow, the scaling of the variance contributions in absolute terms only would lead to an under-representation

of uncertainties with small absolute but high relative changes. This is the reason for using two scaling approaches.

As is evident from Figure 45a–c, in the Upper Niger, the CMs are the main source of uncertainty, especially in the high-flow period. In the first 4 to 5 months of the year, hydrological models have a higher contribution, but the overall uncertainty is low in this period (see Figure 45b). The low-flow periods become more pronounced when looking at the relative scaling (Figure 45c). During these periods, the importance of hydrological models increases. In general, the differences in the variance decomposition between the two selected scenario periods are relatively small.

In the Upper Yellow, the hydrological models are about as important as the climate models. The contribution of hydrological models to the overall uncertainty is highest during the second runoff peak in autumn. In this period, the uncertainty related to hydrological models is higher than that related to climate models. This pattern is present in both scenario periods. The overall uncertainty in projected seasonal changes is highest during the rainy season, when looking at scaling with absolute differences (Figure 45b). Looking at relative scaling (Figure 45c), there is a notable peak at beginning of the year caused by hydrological models. The reason for this peak is not yet clear. The same as in the Upper Niger, the differences between the two scenario periods are small, but the influence of hydrological models becomes higher in the second scenario period.

In contrast to these two basins, for the Rhine, the RCPs also become more important contributors of uncertainty, but only for the second scenario period (2061–2090), and mainly in summer and autumn. As in the other two basins, looking at the whole year, the variance contribution of CMs is highest, followed by that of hydrological models. For the Rhine, a clear difference between the first and second scenario periods regarding sources of uncertainty is visible. In the first scenario period, the highest variability in projected absolute changes is in the late autumn and early winter. For 2061– 2090, the period of high variability is expanded to the late summer period.

Comparing Figure 44Figure 45, we can conclude that the fractions of uncertainties for the slopes of trends and the long-term average seasonal dynamics are mostly consistent. Only for the Rhine basin do the main sources of uncertainties differ; that is, whereas for changes in seasonal dynamics, the uncertainty related to GCMs is the highest, the RCPs are the main contributors to overall uncertainty for the projected trends in runoff quantiles.

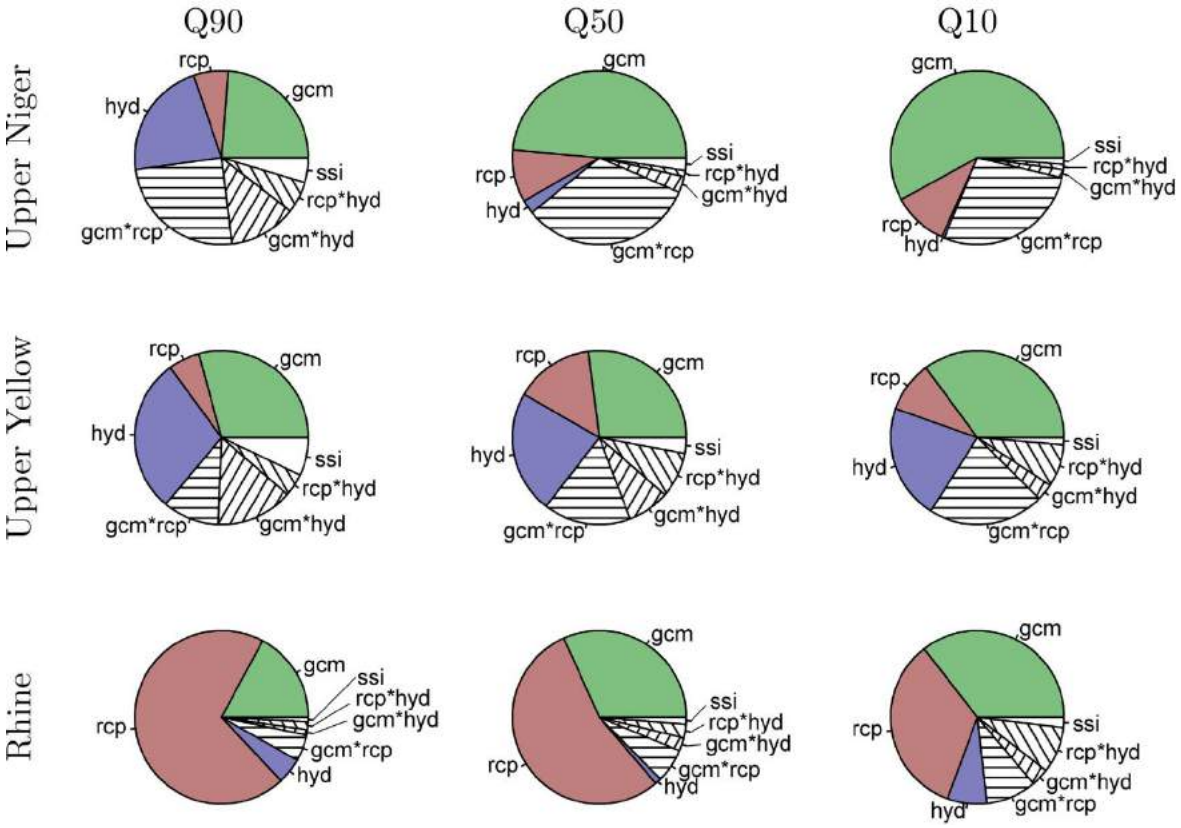

Figure 44 Contribution of different sources of uncertainties to overall uncertainty in the projected slopes of trends for the three runoff quantiles Q_{90}, Q_{50} and Q_{10} for the Upper Niger, Upper Yellow and Rhine.

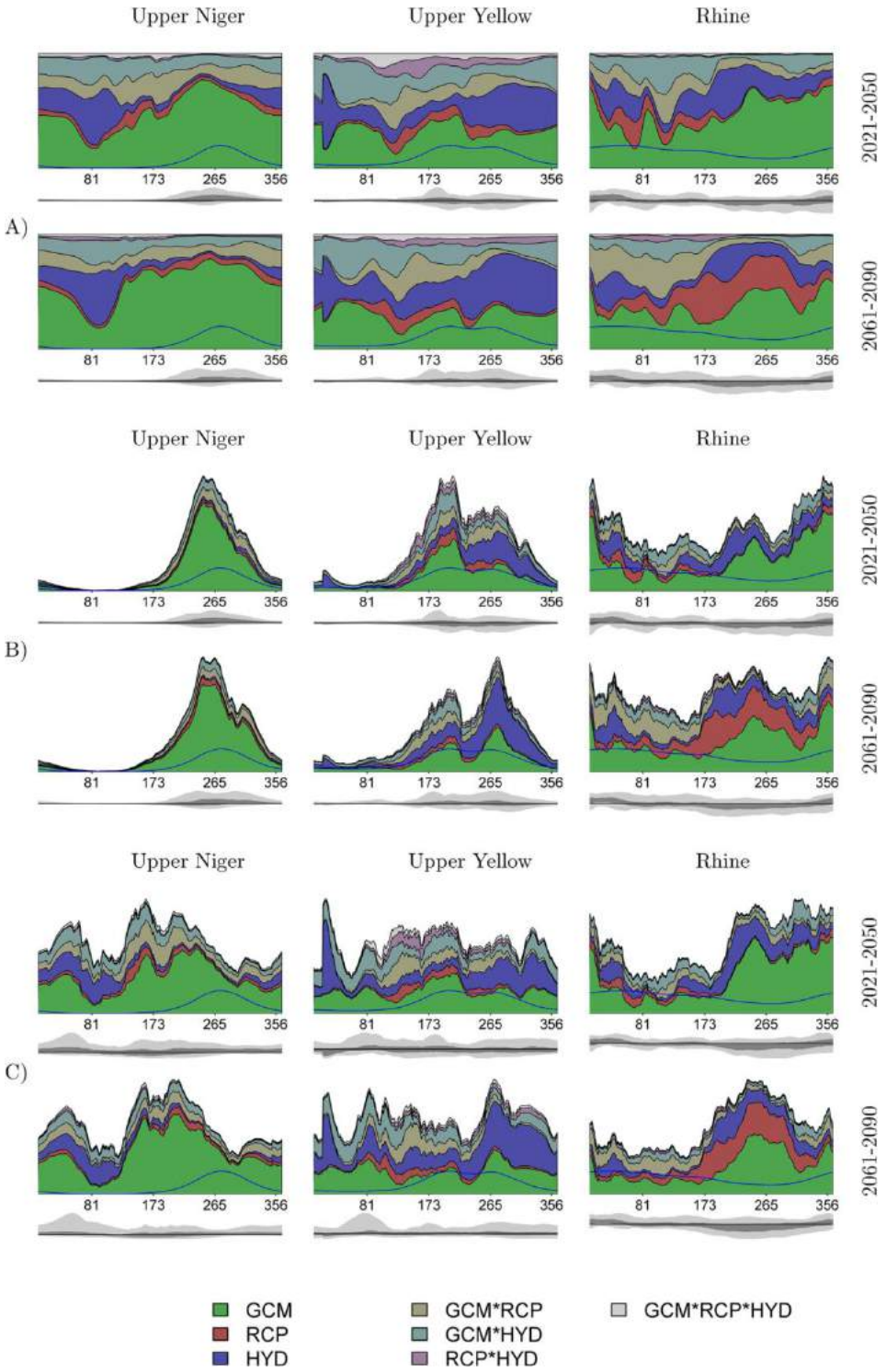

Figure 45 Contribution of different sources of uncertainties to the overall uncertainty in the projected long-term average seasonal dynamics for the Upper Niger, Upper Yellow and Rhine basins for two scenario periods. The blue line denotes the long-term average runoff in the reference period. (a) Unscaled results; (b) results scaled by variability (interquartile range) of absolute changes in river discharge; (c) results scaled by variability (interquartile range) of relative changes in river discharge. Ranges (light gray) and interquartile ranges (dark gray) of projected absolute changes (a, b) and projected relative changes (c) are given below each colored graph.

5.4. Summary and discussion

The study intercompared the climate impacts on runoff generation and river discharge across three river basins on three continents using three hydrological models driven by climate scenarios from five bias-corrected global climate models for four RCPs.

5.4.1. Evaluation and validation of models

The validation of the hydrological models provided good results for river discharge and high flows (Q_{10}) in all three basins, and for the median flow (Q_{50}) and low flow (Q_{90}) in the Rhine. However, the validation results for Q_{50} and Q_{90} in the Upper Yellow and the Upper Niger were weaker, probably due to high seasonality of runoff in these basins. No one of the three hydrological models outperformed the other two. The evaluation of climate model outputs in the historical period by comparing simulations driven by climate models with the observed discharge has shown good agreement.

5.4.2. Robust impacts and uncertainty sources

Regarding the sources of uncertainty in the overall results, we found that the GCM structure is in most cases the largest source of uncertainty for simulated river flows under climate change conditions. The projected impacts show best agreement in the Rhine basin, despite given differences in precipitation projections. Therefore, the robust results in terms of trend direction and slope and changes in seasonal dynamics could be found for the Rhine River basin, regardless of which hydrological model or forcing GCM is used.

For the Upper Niger in Africa, having a monsoonal type of climate, scenarios from climate models are the largest uncertainty source, and therefore clear conclusions on the projections for the future are difficult to draw. It is evident that, during the rainy season, with high and intensive precipitation, the driving GCM simulations dominate river runoff and contribute most to the total uncertainty. However, during the dry season, when evapotranspiration dominates the hydrological processes, hydrological models clearly contribute much more to the total uncertainty.

For the Upper Yellow in Asia, both the hydrological models and climate models contribute to uncertainty in the impacts, though an increase in high flows in future is a robust result ensured by all three hydrological models. In this basin, also having a monsoonal type of climate but lower temperatures than in the Niger basin, the snowmelt processes contribute to runoff, and the highest contribution of the hydrological models to the total uncertainty occurs at the end of the rainy season and in winter.

5.4.3. Uncertainty related to RCPs

The uncertainty related to RCPs (also called scenario uncertainty) arises due to incomplete knowledge about future emissions. For temperature changes, other studies found an increased contribution of scenario uncertainty to the overall uncertainty for the second half of the twenty-first century (Yip et al., 2011). Regarding precipitation projections, Hawkins and Sutton (2011) found that uncertainties are in general outperformed by climate models, also at the end of the century. The large uncertainty contribution of climate models for precipitation projections is probably the reason for the small contribution of RCPs to the overall uncertainty in the present study. Only in the Rhine do RCPs represent an important "driving" factor, where the more certain projected trends in temperature are probably more relevant for projected discharges than the precipitation projections.

5.4.4. Uncertainty related to GCMs

The dominance of GCM-related uncertainty in impact studies is also reported in other studies (e.g., Kay et al., 2009). This is not surprising, as GCMs are not able yet to reproduce some variables (like precipitation) due to their coarse resolution and current model structure describing related processes. Besides, they cannot be calibrated and validated in the same way against observed data, as is usually done for hydrological models (see Blöschl and Montanari, 2010, and the related discussion). In addition, GCMs have more degrees of freedom, as they have to model atmosphere and hydrosphere and all feedbacks within one model system on the global scale with only greenhouse gas emissions as a driver, whereas the hydrological models are specialized to simulate hydrological processes and are usually calibrated and validated for the region of interest. Also, the hydrological models are very sensitive to climate variability and change, making the climate boundary conditions as given by climate scenarios even more important. Summarizing all the results, it can be concluded that providing more robust climate scenarios is a precondition for obtaining more robust hydrological impacts.

5.4.5. Uncertainty related to hydrological models

It is likely that uncertainty in hydrological models increases with the increase in complexity of hydrological processes in the studied basins. As a result, the largest uncertainty related to hydrological models was found for the Upper Yellow River, where both snowmelt and precipitation are important for the runoff generation. Only a minor uncertainty related to hydrological models was found for the Upper Niger, where a simple rainfall–runoff process prevails.

Looking at the projected long-term average seasonal dynamics, we can see that, in certain periods of the year, hydrological models contribute almost as much to the total uncertainty as the driving GCMs. The analysis shows that this is normally the case when certain processes simulated by the hydrological models dominate the generation of river runoff, and these processes are simulated differently by three models. During the summer season in the Rhine basin, for example, the water balance is negative (viz. monthly evapotranspiration is higher than precipitation). The evapotranspiration is a process modeled by the hydrological models, and the different approaches implemented in the three models contribute more to the overall uncertainty whenever evapotranspiration dominates the water balance. The second period when the contribution of the hydrological models to the overall uncertainty is relatively high in the Rhine basin is during the late winter, when snowmelt processes, also simulated by the hydrological models, become relevant.

It is important, when discussing the contribution of hydrological models to the entire scenario uncertainty, to compare the processes considered in the hydrological models, and the complexity of their description. It is often argued that the complex physically based models ought to be the better choice when performing model projections (Bergström, 1991; Abbott and Refsgaard, 1996). However, the more complex models normally need more parameter input, and problems may occur whenever the additional parameters and processes are sensitive to changes in the boundary conditions. For example, vegetation processes are usually considered in the more complex hydrological models (like SWIM), and parameterized in the simpler hydrological models (like HBV). On the one hand, this may be advantageous for a more realistic description of evapotranspiration, but, on the other hand, under climate change and especially under high end scenarios, vegetation cover may change (i.e., summer to winter crops, coniferous to mixed or deciduous forest, etc.), and the corresponding adjustment of the vegetation module would be needed. Another example is water management: it can be implemented during the reference period, but may become obsolete under climate change conditions, so that for hydrological models that are considering water management, relevant management scenarios should also be defined.

In the present study, only three hydrological models have been used. This might underestimate the overall uncertainty related to hydrological models. A larger number of models (11) and more river basins (11) will be considered in the second phase of the ISI-MIP project, allowing for a more detailed intercomparison of climate change impacts.

5.4.6. Uncertainties from different sources: what are the ways to reduce them?

The ideal case would be to improve the description of processes in climate and hydrological models so that the climate models agree better in the climate trends for one specific RCP scenario and region, and the hydrological models agree better in impact

projections. However, climate processes are very complex due to different feedbacks within the climate system (IPCC, 2007), and some uncertainties will always remain. For example, looking at the changes in precipitation as outlined in the latest IPCC report (IPCC, 2013), one can identify regions where most climate models agree in the trend direction (for example, in the tropics with an increase in precipitation and the sub-tropics with mostly a decrease in precipitation), but the transition zones will always be subject to uncertainty, as one cannot expect that all climate models will exactly agree on the borderline between changes in precipitation and other climate variables. Regarding hydrological models, more efforts are needed to improve the simulation of different processes and their performance in complex basins, e.g., those at higher altitudes where snow and glacier processes are important, and those with human water management playing an important role in overall water balance.

When accepting the fact that it is not really possible to decrease substantially the range of uncertainty, one should invest more in analyzing the distribution of uncertainty by gathering more information (e.g., integrating ensembles of climate and hydrological models into the impact study). Doing so, conclusions will get a higher explanatory power, as one will learn more about, e.g., focal points of change and possible outliers, and thus increase the robustness of the overall results.

Besides, some scientists (Greene et al., 2006; Zhu et al., 2013) recommend a model-weighting scheme as a feasible approach to reducing uncertainties in climate impact studies. This method gives large weights to the skillful models and minor weights to the models that do not match the observed dynamics. The Impact model intercomparison is still a relatively new field of research (Schewe et al., 2014), and most studies now are focusing on robust results and the sources of uncertainty in terms of model types and data processing (climate models, impact models, bias correction). Less attention is paid to the specific and fundamental processes implemented, and how to improve their description in the models. Regarding the hydrological part, this concerns mainly the runoff generation and related processes, including evapotranspiration, vegetation dynamics, snowmelt, etc. The differences in the description of these processes contribute to the total impact uncertainty differently over the season and in various regions. In general, our study shows that the intercomparison of impacts is very important for producing more reliable results of climate impact assessment for the regions and for reducing fragmentarity of impacts on the global scale. Besides, the model intercomparison and analysis of results allow finding the ways to improve climate and impact models and reduce uncertainty for more reliable impact studies in future.

Acknowledgements

This work was financed by the project PROGRESS (Potsdam Research Cluster for Georisk Analysis, Environmental Change and Sustainability). For their roles in processing the climate data we like to thank the the ISI-MIP modeling group. Edited by: R. Pavlick

References

Abbott, M. B. and Refsgaard, J. C.: Distributed hydrological modeling, Distributed hydrological modeling. Kluwer Academic Publishers,Dordrecht, Boston, London, 1996.

Ad-hoc AG-Boden: Bodenkundliche Kartieranleitung, 5. Verbesserte und erweiterte Auflage, Bundesanstalt für Geowissenschaften und Rohstoffe, Stuttgart, 2006.

Aich, V., Liersch, S., Vetter, T., Huang, S., Tecklenburg, J., Hoffmann, P., Koch, H., Fournet, S., Krysanova, V., Müller, E. N., and Hattermann, F. F.: Comparing impacts of climate change on streamflow in four large African river basins, Hydrol. Earth Syst. Sci., 18, 1305–1321, doi:10.5194/hess-18-1305-2014, 2014.

Andersson, L., Samuelsson, P., and Kjellström, E.: Assessment of climate change impact on water resources in the Pungwe river basin, Tellus A, 63, 138–157, 2011.

Arnold, J. G., Allen, P. M., and Bernhardt, G.: A comprehensive surface-groundwater flow model, J. Hydrol., 142, 47–69, 1993.

Bartholomé, E. and Belward, A.: GLC2000: a new approach to global land cover mapping from Earth observation data, Int. J. Remote Sens., 26, 1959–1977, 2005.

Bergström, S.: Principles and confidence in hydrological modelling, Nord. Hydrol., 22, 123–136, 1991.

Bergström, S. and Forsman, A.: Development of a conceptual deterministic rainfall-runoff model, Nord. Hydrol., 4, 147–170, 1973.

Bergström, S. and Singh, V. P.: The HBV model, Computer models of watershed hydrology, Water Resources Publications, Highlands Ranch, Colorado, USA, 443–476, 1995.

Blöschl, G. and Montanari, A.: Climate change impacts—throwing the dice?, Hydrol. Process., 24, 374–381, 2010.

Bosshard, T., Carambia, M., Goergen, K., Kotlarski, S., Krahe, P., Zappa, M., and Schaer, C.: Quantifying uncertainty sources in an ensemble of hydrological climate-impact projections, Water Resour. Res., 49, 1523–1536, doi:10.1029/2011WR011533, 2013.

Breuer, L., Huisman, J. A., Willems, P., Bormann, H., Bronstert, A., Croke, B. F. W., Frede, H. G., Graeff, T., Hubrechts, L., Jakeman, A. J., Kite, G., Lanini, J., Leavesley, G., Lettenmaier, D. P., Lindstroem, G., Seibert, J., Sivapalan, M., and Viney, N. R.: Assessing the impact of land use change on hydrology by ensemble modeling (LUCHEM). I: Model intercomparison with current land use, Adv. Water Resour., 32, 129–146, doi:10.1016/j.advwatres.2008.10.003, 2009.

Chen, X., Yang, T., Wang, X., Xu, C.-Y., and Yu, Z.: Uncertainty Intercomparison of Different Hydrological Models in Simulating Extreme Flows, Water Resour. Manage., 27, 1393–1409, 2013.

Christensen, N. S. and Lettenmaier, D. P.: A multimodel ensemble approach to assessment of climate change impacts on the hydrology and water resources of the Colorado River Basin, Hydrol. Earth Syst. Sci., 11, 1417–1434, doi:10.5194/hess-11-1417-2007, 2007.

Deb, K., Pratap, A., Agarwal, S., and Meyarivan, T.: A fast and elitist multiobjective genetic algorithm: NSGA-II, IEEE T. Evolut. Comput., 6, 182–197, doi:10.1109/4235.996017, 2002.

Déqué, M., Rowell, D., Lüthi, D., Giorgi, F., Christensen, J., Rockel, B., Jacob, D., Kjellström, E., De Castro, M., and van den Hurk, B.: An intercomparison of regional climate simulations for Europe: assessing uncertainties in model projections, Climatic Change, 81, 53–70, 2007.

Doherty, J.: PEST: Model Independent Parameter Estimation, 5th Edn. of user manual, Watermark Numerical Computing, Brisbane, Australia, 2005.

FAO, IIASA, ISRIC, and ISSCAS: JRC (2009) Harmonized world soil database (version 1.1), FAO, Rome and IIASA, Laxenburg, 2009.

Finger, D., Heinrich, G., Gobiet, A., and Bauder, A.: Projections of future water resources and their uncertainty in a glacierized catchment in the Swiss Alps and the subsequent effects on hydropower production during the 21st century, Water Resour Res., 48, W02521, doi:10.1029/2011WR010733, 2012.

Graham, P.: Modelling runoff to the Baltic basin, Ambio, 28, 328– 334, 1999.

GRDC: Global Runoff Data, The Global Runoff Data Centre, Koblenz, Germany, 1998.

Greene, A. M., Goddard, L., and Lall, U.: Probabilistic multimodel regional temperature change projections, J. Climate, 19, 4326– 4343, doi:10.1175/JCLI3864.1, 2006.

Haddeland, I., Clark, D. B., Franssen, W., Ludwig, F., Voss, F., Arnell, N. W., Bertrand, N., Best, M., Folwell, S., Gerten, D., Gomes, S., Gosling, S. N., Hagemann, S., Hanasaki, N., Harding, R., Heinke, J., Kabat, P., Koirala, S., Oki, T., Polcher, J., Stacke, T., Viterbo, P., Weedon, G. P., and Yeh, P.: Multimodel Estimate of the Global Terrestrial Water Balance: Setup and First Results, J. Hydrometeorol., 12, 869–884, doi:10.1175/2011JHM1324.1, 2011.

Hagemann, S., Chen, C., Clark, D. B., Folwell, S., Gosling, S. N., Haddeland, I., Hanasaki, N., Heinke, J., Ludwig, F., Voss, F., and Wiltshire, A. J.: Climate change impact on available water resources obtained using multiple global climate and hydrology models, Earth Syst. Dynam., 4, 129–144, doi:10.5194/esd-4-129-2013, 2013.

Hamlet, A. F. and Lettenmaier, D. P.: Effects of Climate Change on Hydrology and Water Resources in the Columbia River Basin, J. Am. Water Resour. Assoc., 35, 1597–1623, 1999.

Hattermann, F. F., Weiland, M., Huang, S., Krysanova, V., and Kundzewicz, Z. W.: Model-supported impact assessment for the water sector in Central Germany under climate change – a case study, Water Resour. Manage., 25, 3113–3134, 2011.

Hawkins, E. and Sutton, R.: The potential to narrow uncertainty in projections of regional precipitation change, Clim. Dynam., 37, 407–418, doi:10.1007/s00382-010-0810-6, 2011.

Hempel, S., Frieler, K., Warszawski, L., Schewe, J., and Piontek, F.: A trend-preserving bias correction – the ISI-MIP approach, Earth Syst. Dynam., 4, 219–236, doi:10.5194/esd-4-219-2013, 2013.

Huang, S., Krysanova, V., Österle, H., and Hattermann, F. F.: Simulation of spatiotemporal dynamics of water fluxes in Germany under climate change, Hydrol. Process., 24, 3289–3306, doi:10.1002/hyp.7753, 2010.

Huang, S., Hattermann, F. F., Krysanova, V., and Bronstert, A.: Projections of climate change impacts on river flood conditions in Germany by combining three different RCMs with a regional eco-hydrological model, Climatic Change, 116, 631–663, 2013.

Huber, P. J.: Robust regression: asymptotics, conjectures and Monte Carlo, Ann. Stat., 1, 799–821, 1973.

IPCC: IPCC Special Report Emission Scenarios – Summary for Policymakers. A Special Report of IPCC Working Group III, Intergovernmental Panel on Climate Change, Cambridge University Press, Cambridge, UK and New York, NY, USA, 2000.

IPCC: Climate Change 2007: Impacts, Adaptation and Vulnerability – Summary for Policymakers, Working Group II Contribution to the Fourth Assessment Report of the Intergovernmental Panel on Climate Change, IPCC Secretariat, Cambridge University Press, Cambridge, UK and New York, NY, USA, 2007.

IPCC: Climate Change 2013: The Physical Science Basis, Cambridge University Press, Cambridge, UK and New York, NY, USA, 2013.

Jacob, D., Petersen, J., Eggert, B., Alias, A., Christensen, O. B., Bouwer, L. M., Braun, A., Colette, A., Déqué, M., Georgievski, G., Georgopoulou, E., Gobiet, A., Menut, L., Nikulin, G., Haensler, A., Hempelmann, N., Jones, C., Keuler, K., Kovats, S., Kröner, N., Kotlarski, S., Kriegsmann, A., Martin, E., van Meijgaard, E., Moseley, C., Pfeifer, S., Preuschmann, S., Radermacher, C., Radtke, K., Rechid, D., Rounsevell, M., Samuelsson, P., Somot, S., Soussana, J.-F., Teichmann, C., Valentini, R., Vautard, R., Weber, B., and

Yiou, P.: EURO-CORDEX: new highresolution climate change projections for European impact research, Reg. Environ. Change, 14, 1–16, 2013.

Jarvis, A., Reuter, H., Nelson, A., and Guevara, E.: Hole-filled SRTM for the globe Version 4, available from the CGIAR-CSI SRTM 90m Database, http://srtm.csi.cgiar.org (last access: 8 January 2015), 2008.

Kay, A., Davies, H., Bell, V., and Jones, R.: Comparison of uncertainty sources for climate change impacts: flood frequency in England, Climatic Change, 92, 41–63, doi:10.1007/s10584-008-9471-4, 2009.

Koller, M. and Stahel, W. A.: Sharpening Wald-type inference in robust regression for small samples, Comput. Stat. Data Anal., 55, 2504–2515, doi:10.1016/j.csda.2011.02.014, 2011.

Krysanova, V., Meiner, A., Roosaare, J., and Vasilyev, A.: Simulation modelling of the coastal waters pollution from agricultural watershed, Ecol. Model., 49, 7–29, 1989.

Krysanova, V., Müller-Wohlfeil, D.-I., and Becker, A.: Development and test of a spatially distributed hydrological/water quality model for mesoscale watersheds, Ecol. Model., 106, 261–289, 1998.

Krysanova, V., Bronstert, A., and Muller-Wohlfeil, D.: Modelling river discharge for large drainage basins: from lumped to distributed approach, Hydrolog. Sci. J. – Journal des Sciences Hydrologiques, 44, 313–331, doi:10.1080/02626669909492224, 1999.

Krysanova, V., Hattermann, F., Huang, S., Hesse, C., Vetter, T., Liersch, S., Koch, H., and Kundzewicz, Z.: Modelling climate and land use change impacts with SWIM: lessons learnt from multiple applications, Hydrolog. Sci. J., accepted, 2015.

Liang, X., Lettenmaier, D. P., Wood, E. F., and Burges, S. J.: A simple hydrologically based model of land surface water and energy fluxes for general circulation models, J. Geophys. Res.-Atmos., 99, 14415–14428, 1994.

Liang, X., Wood, E. F., and Lettenmaier, D. P.: Surface soil moisture parameterization of the VIC-2L model: Evaluation and modification, Global Planet. Change, 13, 195–206, 1996.

Lidén, R., Harlin, J., Karisson, M., and Rahmberg, M.: Hydrological modelling of fine sediments in the Odzi River, Zimbabwe, Water SA, 27, 303–314, 2001.

Liersch, S., Cools, J., Kone, B., Koch, H., Diallo, M., Reinhardt, J., Fournet, S., Aich, V., and Hattermann, F. F.: Vulnerability of rice production in the Inner Niger Delta to water resources management under climate variability and change, Environ. Sci. Policy, 34, 18–33, 2013.

Menzel, L., Thieken, A. H., Schwandt, D., and Bürger, G.: Impact of climate change on the regional hydrology–scenario-based modelling studies in the German Rhine catchment, Nat. Hazards, 38, 45–61, 2006.

Nash, J. and Sutcliffe, J.: River flow forecasting through conceptual models part I – A discussion of principles, J. Hydrol., 10, 282– 290, 1970.

Ott, I., Duethmann, D., Liebert, J., Berg, P., Feldmann, H., Ihringer, J., Kunstmann, H., Merz, B., Schaedler, G., and Wagner, S.: High-Resolution Climate Change Impact Analysis on MediumSized River Catchments in Germany: An Ensemble Assessment, J. Hydrometeorol., 14, 1175–1193, doi:10.1175/JHM-D- 12-091.1, 2013. Reed, S., Koren, V., Smith, M., Zhang, Z., Moreda, F., Seo, D.-J., and Participants, D.: Overall distributed model mintercomparison project results, J. Hydrol., 298, 27–60, doi:10.1016/j.jhydrol.2004.03.031, 2004.

Refsgaard, J. C. and Knudsen, J.: Operational Validation and Intercomparison of Different Types of Hydrological Models, Water Resour. Res., 32, 2189–2202, doi:10.1029/96WR00896, 1996.

Saelthun, N. R.: The Nordic HBV model, Norwegian Water Resources and Energy Administration Publication 7, Norwegian Water Resources and Energy Administration, Oslo, Norway, 1– 26, 1996.

Schewe, J., Heinke, J., Gerten, D., Haddeland, I., Arnell, N. W., Clark, D. B., Dankers, R., Eisner, S., Fekete, B. M., ColonGonzalez, F. J., Gosling, S. N., Kim, H., Liu, X., Masaki, Y., Portmann, F. T., Satoh, Y., Stacke, T., Tang, Q., Wada, Y., Wisser, D., Albrecht, T., Frieler, K., Piontek, F., Warszawski, L., and Kabat, P.: Multimodel assessment of water scarcity under climate change, P. Natl. Acad. Sci. USA, 111, 3245–3250, doi:10.1073/pnas.1222460110, 2014.

Smith, M. B., Seo, D.-J., Koren, V. I., Reed, S. M., Zhang, Z., Duan, Q., Moreda, F., and Cong, S.: The distributed model intercomparison project (DMIP): motivation and experiment design, J. Hydrol., 298, 4–26, doi:10.1016/j.jhydrol.2004.03.040, 2004.

Su, F. and Xie, Z.: A model for assessing effects of climate change on runoff in China, Prog. Nat. Sci., 13, 701–707, 2003.

Velázquez, J. A., Schmid, J., Ricard, S., Muerth, M. J., Gauvin StDenis, B., Minville, M., Chaumont, D., Caya, D., Ludwig, R., and Turcotte, R.: An ensemble approach to assess hydrological models' contribution to uncertainties in the analysis of climate change impact on water resources, Hydrol. Earth Syst. Sci., 17, 565–578, doi:10.5194/hess-17-565-2013, 2013.

Warszawski, L., Frieler, K., Huber, V., Piontek, F., Serdeczny, O., and Schewe, J.: The Inter-Sectoral Impact Model Intercomparison Project (ISI-MIP): Project framework, P. Natl. Acad. Sci., 111, 3228–3232, 2014.

Weedon, G. P., Gomes, S., Viterbo, P., Shuttleworth, W. J., Blyth, E., Österle, H., Adam, J. C., Bellouin, N., Boucher, O., and Best, M.: Creation of the WATCH Forcing Data and Its Use to Assess Global and Regional Reference Crop Evaporation over Land during the Twentieth Century, J. Hydrometeorol., 12, 823–848, 2011.

Wilby, R. L. and Harris, I.: A framework for assessing uncertainties in climate change impacts: Low-flow scenarios for the River Thames, UK, Water Resour. Res., 42, WR004065, doi:10.1029/2005WR004065, 2006.

Yip, S., Ferro, C. A. T., Stephenson, D. B., and Hawkins, E.: A Simple, Coherent Framework for Partitioning Uncertainty in Climate Predictions, J. Climate, 24, 4634–4643, doi:10.1175/2011JCLI4085.1, 2011.

Yohai, V. J.: High Breakdown-point and High-efficiency Robust Estimates For Regression, Ann. Stat., 15, 642–656, doi:10.1214/aos/1176350366, 1987.

Yu, P.-S. and Wang, Y.-C.: Impact of climate change on hydrological processes over a basin scale in northern Taiwan, Hydrol. Process., 23, 3556–3568, 2009.

Zhang, X. and Lindström, G.: A comparative study of a Swedish and a Chinese hydrological modell, J. Am. Water Resour. Assoc., 32, 985–994, doi:10.1111/j.1752-1688.1996.tb04067.x, 1996.

Zhu, J., Forsee, W., Schumer, R., and Gautam, M.: Future projections and uncertainty assessment of extreme rainfall intensity in the United States from an ensemble of climate models, Climatic Change, 118, 469–485, doi:10.1007/s10584-012-0639-6, 2013.

:

Hydrol. Earth Syst. Sci., 18, 1–17, 2014
doi:10.5194/hess-18-1-2014

6. COMPARING IMPACTS OF CLIMATE CHANGE ON STREAMFLOW IN FOUR LARGE AFRICAN RIVER BASINS

Valentin Aich [1,*], Stefan Liersch [1], Tobias Vetter [1], Shaochun Huang [1], Julia Tecklenburg[1], Peter Hoffmann[1], Hagen Koch[1], Samuel Fournet[1], Valentina Krysanova[1], Eva N. Müller [2] and Fred F. Hattermann [1]

[1] Potsdam Institute for Climate Impact Research (PIK), Potsdam, Germany
[2] Institute of Earth and Environmental Science, University of Potsdam, Potsdam, Germany

* Corresponding author: Valentin Aich

Journal: Hydrology and Earth System Sciences (Hydrol. Earth Syst. Sci.)
Status: Published

Abstract: This study aims to compare impacts of climate change on streamflow in four large representative African river basins: the Niger, the Upper Blue Nile, the Oubangui and the Limpopo. We set up the eco-hydrological model SWIM (Soil and Water Integrated Model) for all four basins individually. The validation of the models for four basins shows results from adequate to very good, depending on the quality and availability of input (observed climate, soils, land use, water management) and calibration (discharge) data.
For the climate impact assessment we drive the model with outputs of five bias corrected Earth System Models of Coupled Model Intercomparison Project Phase 5 (CMIP5) for the Representative Concentration Pathways (RCPs) 2.6 and 8.5. This climate input is put into the context of climate trends of the whole African continent and compared to a CMIP5 ensemble of 19 models in order to test their representativeness. Subsequently, we compare the trends in mean discharges, seasonality and hydrological extremes in the 21st century. The uncertainty of results for all basins is high, mainly due to the climate input. Still, climate change impact is clearly visible for mean discharges but also for extremes in high and low flows. The uncertainty of the projections is the lowest in the Upper Blue Nile, where an increase in streamflow is most likely. In the Niger and the Limpopo basins, the magnitude of trends in both directions is high and has a wide range of uncertainty. In the Oubangui, impacts are the least significant. Our results confirm partly the findings of previous continental impact analyses for Africa. However, contradictory to these studies we find a tendency for increased streamflows in three of the four basins (not for the Oubangui). Guided by these results, we argue for attention to the possible risks of increasing high flows in the face of the dominant water scarcity in Africa. In conclusion, the study shows that impact intercomparisons have added value to the adaptation discussion and may be used for setting up adaptation plans in the context of a holistic approach.

6.1. Introduction

Climate change impacts are commonly assessed on two different scales: the global or continental scale allows for a general view of the larger context and patterns, whereas regional studies focus on details, for example flood or drought hazards. By comparing climate change impacts between different regions, advantages of both approaches can be combined. This way of bridging these two scales is likely to give new insights into the characteristics of climate change in the actual regions, but also beyond.

Especially in the African context, this approach could be beneficial where climate change impacts are very likely to be most severe (Boko et al., 2007), and adaptation measures will increasingly stand in competition for finance and precedence (NWP, 2011). Here, regional intercomparison of climate impacts could be beneficial not only scientifically but also for developing regional adaptation strategies.

On the continental level, there have been several climate impact studies focusing on water resources in Africa. In a recent study, Faramarzi et al. (2013) modeled the whole African continent with the SWAT (Soil and Water Assessment Tool) model on a coarse spatial resolution (1496 subbasins), using five CMIP4 (Coupled Model Intercomparison Project Phase 4) Global Circulation Models (GCM: HadCM3, PCM, CGCM2, CSIRO2, ECHAM4). They compared their results to the available literature sources on future projections of streamflow in Africa, namely De Wit and Stankiewicz (2006) and (Strzepek and McCluskey (2007), and several projections for smaller regions. They generally found similar trends in the studies, with decreases in the Sahel region and southern Africa between 10% and 20% and an increase in Central and Eastern Africa between 10% and 20%, but with significant spatial variability. De Wit and Stankiewicz (2006) defined three different regimes according to a precipitation threshold for the African continent and calculated for these three regimes the perennial drainage density as a function of mean annual rainfall. By using six GCMs (not specified) to assess the projected changes in mean annual rainfall across Africa, they found that 25% of the continent will be significantly affected by a decrease in streamflow by the end of this century. Strzepek and McCluskey (2007) simulated changes in streamflow and soil moisture with a conceptual rainfall-runoff model called WatBal. It was applied on grids for five CMIP4 models (CSIRO2, HadCM3, CGCM2, ECHAM, PCM) and the scenarios A2 and B2 across the African continent, and results were provided by country. A study of Mahe et al. (2013) analyzed observed streamflow of the past decades in West and Central Africa and found a modification of seasonal regimes in the Equatorial area and a decrease in the groundwater table in the tropical humid area of West Africa.

However, no impact studies currently exist that investigate projected change in hydrological extremes on a regional resolution consistently across the African continent, that could for the first time enable an intercomparison of the future severity of change and consequently allow an assessment of the urgency of required adaptations. In this modeling

study, we attempt to overcome this apparent lack by quantifying the impact of climate change on the mean river discharge as well as extremes for four major African basins that cover the main Sub-Saharan climate zones: the Niger, the Upper Blue Nile, the Oubangui (Upper Congo basin) and the Limpopo. For these basins, we focus on water as the key resource for development and flood security as well as economic development and livelihood. Moreover, we applied the most up-to-date knowledge (the model outputs from CMIP5 for the Representative Concentration Pathways, RCPs, Van Vuuren et al., 2011) to investigate climate impacts in Africa. Therefore, the objectives of the study are 1. to investigate differences in the sensitivity of modeled annual discharge to climate parameters between the basins, 2. to study climate impacts on river discharge for four basins in terms of quantity and seasonality, 3. to explore changes in hydrological extremes (high flow, low flow) for the four basins, 4. to analyze the uncertainties of the projections, and finally 5. to identify and discuss the implications for adaptation.

To achieve these objectives, we analyze the output of 19 CMIP5 model with regard to temperature and precipitation trends. Then, data for five of these climate models which have been bias corrected by the method of Hempel et al. (2013) are used to drive the eco-hydrological model SWIM (Soil and Water Integrated Model, Krysanova et al. 1998) for each basin. In the main part of this study, we compare projections of future discharge trends for mean discharges as well as for robust indicators of extremes considering 30-year periods in the first and second halves of the 21st century under the RCPs 2.6 and 8.5. These quantitative results are interpreted and compared across the four case studies qualitatively. In a final discussion, we evaluate the potential of such an impact comparison to contribute to developing an agenda for climate change adaptation.

6.2. Study sites

6.2.1. Hydrology of the basins

The selected basins of the Niger, Upper Blue Nile, Oubangui and Limpopo are distributed over all Sub-Saharan Africa, in the West, East Center and South (Figure 46). In addition they cover all climate groups of Sub-Saharan Africa according to the Köppen (1936) classification after Strahler (2013). Besides the tropical humid climates (A), dry climates (B), subtropical climates (C) and highland climates (H) they also cover most of the climatic types and subtypes of the continent. The hydrological regimes of all four rivers are characterized by the alternation of dry and wet seasons. However, the diverse climates, topographical and geological conditions, soils, and vegetation types result in characteristic hydrological conditions in each of the basins. This can exemplarily be seen in the broad spectrum of runoff coefficients in the catchments, ranging from about 2% in the Limpopo catchment to 21% in the Oubangui (Figure 46 and Table 11).

The Niger River is the longest and largest river of West Africa. Its source is located in the Guinean highlands, from which the Niger flows in a northern arc through the dry Sahelian zone until it again enters the wetter tropical region north of the Gulf of Guinea. Topographically the basin also includes Algeria, but from this northernmost part in the Central Sahara, no water contributes to the streamflow. Geographically, the Niger basin spreads over six different large agro-climatic and hydrographic regions. These range from the Central Sahara with less than 100 mm/yr average annual rainfall to tropical rain forests in the Guinean zone with more than 1400 mm/yr. Besides this broad range of climates, the regime of the Niger is substantially influenced by the Inner Niger Delta by delaying the peak runoff and smoothening the hydrograph. The fluvial regime at the analyzed Lokoja gauge is mainly shaped by the wetter climate of upstream parts of the basin and the Niger tributaries, particularly the Benue. However, the influence of the dynamics of the Inner Niger Delta and the Guinean headwaters is still noticeable (Andersen et al., 2005b; Ogilvie et al., 2010).

The Oubangui River is a main tributary of the Congo River in the north-east of the basin. The source of the Oubangui is located in the mountains near Lake Albert. From the Bangui gauging station the Oubangui still flows 600 km further until it reaches the Congo River. Its regime follows the rainy season, with highest discharges from August to December and a total annual rainfall between 1300 mm/yr and 1700 mm/yr. The basin is dominated by a vast peneplain and only 5% of its area is covered with mountains, mainly at the eastern and northeastern edges. The Oubangui basin is the least investigated of all four African basins and data is - even for African conditions – sparse (Shahin, 2006; Tshimanga and Hughes, 2012; Tshimanga, 2012; Wesselink et al., 1996).

The Upper Blue Nile is the Ethiopian segment of the Blue Nile. After the White Nile, the Blue Nile is the second longest tributary to the Nile River. It contributes up to 80% of the mean annual discharge to the Stem Nile. The source of the Blue Nile is Lake Tana and its tributaries. From Lake Tana, the Blue Nile flows across northwestern Ethiopia through numerous incised valleys and canyons and crosses the border to Sudan at El Diem. The major influences on the hydrological regime of the catchment are a distinct topography and a wide range of climatic conditions. The altitude within the basin ranges from 4050 m a.s.l. in the Ethiopian highlands to 500 m a.s.l. at the outlet at El Diem. Besides the influence of this landform, the effects of the summer monsoon determine the climate in the basin. Annual rainfall ranges from 1077 mm/yr to over 2000 mm/yr in the highlands (Conway 2000).

The Limpopo River originates in Witwatersrand, South Africa, from which it flows in a northern arc and then enters the Indian Ocean. The hydrology of the Limpopo is characterized by its location in the transition zone between the intertropical convergence zone and the tropical dry zone, with additional maritime influence in the east. Its topography is dominated by plains of higher altitude in the inland and lower coastal plains, both separated by the Great Escarpment, which runs through the center of the basin from

north to south. This geographical setting results not only in a typical subtropical intra-annual, but also a very distinct inter-annual variability of flow (FAO, 2004; Frenken and Faurès, 1997; Murwira and Yachan, 2007).

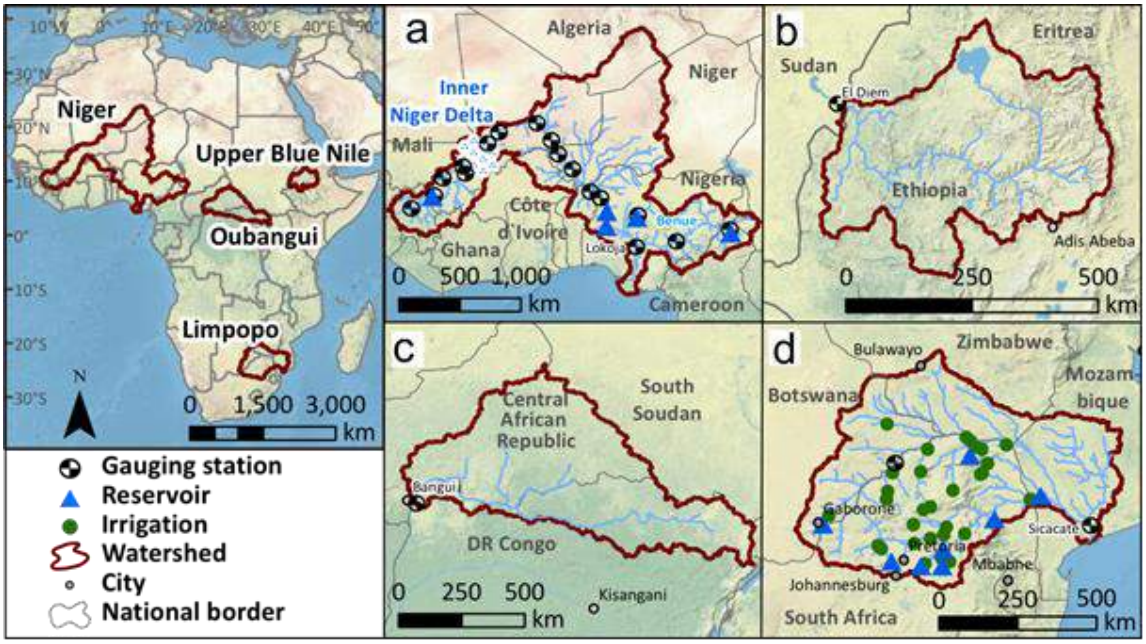

Figure 46 Map of the four modeled basins: Niger (a), Upper Blue Nile (b), Oubangui (c), Limpopo (d).

6.2.2. Human influence on discharge dynamics in the basins

The intensity of human influence on the hydrological processes differs remarkably in the four basins. The Limpopo River basin is located in an arid to semi-arid region where water is the critical limiting factor on all development. Water resources including groundwater are heavily utilized due to the densely populated area and many irrigation schemes (UN-HABITAT 2007). In order to satisfy the intensive use of water resources, the Limpopo River is quite developed in terms of storage reservoirs and dams. In the South African part of the Limpopo basin alone, there are 160 dams classified as large dams in accordance with the criteria of the International Committee on Large Dams. Among these 160 dams, 15 of them have storage capacities above 100 Mm³, and 34 are between 10 Mm³ and 100 Mm³ (LBPTC, 2010). In addition, there are a lot of mining activities in the Limpopo River Basin with about 1900 mines over the years (Ashton et al., 2001), and many of them have extensive impacts on water resources (Ashton et al., 2005).”

However, water management infrastructure does not influence the streamflow fundamentally on the basin scale. Currently there are only five major reservoirs in the catchment with volumes over 1000 Mm³, mainly built for irrigation and hydropower: Selingué (Mali), Kainji, Jebba, Shiroro (all three in Nigeria) and Lagdo (Cameroon). These influence the streamflow locally and are included in the model. According to Frenken and

Fauré (1997), there is a large potential for more irrigated agriculture in the Niger Basin, with an additional 2.8 Mha of natural savannah that could be transformed into cultivated areas. In recent years, plans for new irrigation schemes as well as for additional reservoirs have been developed and some are under construction. The Niger is navigable from Koulikoro in central Mali to Lokoja in Nigeria, mainly in the season of highest discharge from October to January (Andersen 2005).

In the Upper Blue Nile Basin, water management still plays a moderate role. At the end of the 1990s, the irrigation potential was estimated by the FAO to be more than 2.2 Mha (Frenken and Faurès 1997). Since then, efforts to exploit this potential have been moderate. However, over the last decade many efforts have been made for intensification of irrigated agriculture and other management measures, of which the Grand Ethiopian Renaissance Dam is the most prominent. After planned completion in 2017, the dam should store a water volume of 63,000 Mm3 and will serve power generation of 5000 MW (Salman, 2013). The Upper Blue Nile is not navigable for larger boats (Awulachew et al., 2007).

In the Oubangui basin, information and data on water management is very sparse. There are three reservoirs in the headwater part that generate hydropower. The river serves as a major traffic route for the Central African Republic, though there are reports of insufficient streamflow for navigation over an increasing period throughout the year (UN, 2009). Consumption and small-scale irrigation along the river play a minor role and the influence on the discharge and hydrological regime is small (Vanden Bossche and Bernacsek, 1990).

Table 11 Basin and river characteristics

	Niger	Upper Blue Nile	Oubangui	Limpopo
Area in km²	2,156,000	167,000	489,000	413,000
Alt. range in m a.s.l.	0 – 2961	526 - 4187	341 – 2046	0 – 2326
Mean temp. in °C	28	19	25	21
Mean temp. warmest/ coldest month in °C	32 in May / 24 in Jan.	21 in April/ 17 in Dec.	26 in March/ 24 in Dec.	25 in Feb./ 15 in July
Mean prec. in mm/ a	682	1382	1507	530
Dominant land uses in %	cropland: 20 grassland: 18 savannah 14	cropland: 57 savannah: 30	forest: 50 cropland: 32	forest: 34 cropland: 32 savannah: 20
Length of river in km*	~3650	~800	~1670	~1750
Mean annual discharge in mm/a	~170	~370	~224	~13
Runoff coefficient**	~18%	~17%	~21%	~2%

*Until the relevant gauging stations. Niger: Lokoja, Upper Blue Nile: El Diem, Oubangui: Bangui, Limpopo: Sicacate.

**Amount of precipitation that reaches the outlet.

6.3. Methodology

6.3.1. Model

All four African basins were modeled using the eco-hydrological model SWIM (Krysanova et al., 1998). The model was chosen because it is able to reproduce discharge on the mesoscale on a daily basis with high efficiency and has been used extensively in many catchments of various sizes all over the world, including in Africa (Koch et al., 2013a; Liersch et al., 2013). This semi-distributed model is based on the models SWAT (Arnold et al., 1993) and MATSALU (Krysanova et al., 1989). SWIM is a process-based model and simulates the dominant eco-hydrological processes such as evapotranspiration, vegetation growth, runoff generation and river discharge, and also considers feedbacks among these processes (Krysanova et al., 2005) (Figure 47).

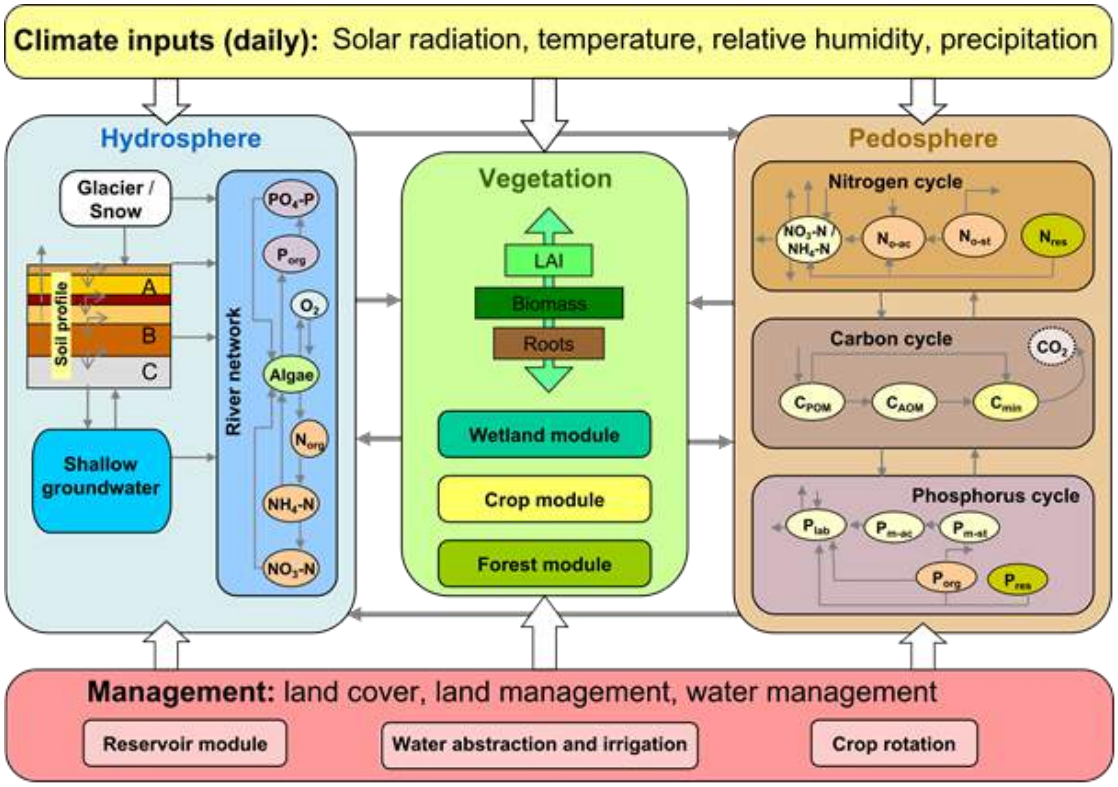

Figure 47 Structure of the eco-hydrological model SWIM.

SWIM disaggregates a river basin to subbasins and hydrotopes. The subbasins were delineated on the basis of flow accumulation in a Digital Elevation Model (DEM). The size of the subbasins usually ranges between 150-1500km², depending on topography and the focused precision. In large basins as modeled in this study, the size of the subbasins derived in the delineation process is a trade between the exactness of the model and its manageability. The resulting subbasins are then subdivided into hydrotopes, each with same type of soils and land use class. The daily weather input is interpolated to subbasin

centroids, and includes mean, minimum and maximum temperature, as well as precipitation, relative humidity and global radiation. On each hydrotope within a subbasin the daily weather is added. Subsequently in each of these hydrotopes, the model is calculating water fluxes and the water balance for the soil column subdivided into several layers. Its hydrological system includes the soil surface, the root zone of the soil and the shallow aquifer. The output of each hydrotope is then aggregated at subbasins level, taking retention into account, and then the routing of lateral fluxes starts. The basin can be subdivided into subcatchments which can be separately parameterized if discharge data is available for the outlet of each subcatchment. The model is described in detail in Krysanova et al. (2000) and (Krysanova et al. (2005). Recent model developments and extensions that are used in the different basin model projects for this study are described in the model set-up.

For each African basin, the model has been individually adapted and calibrated with regard to its geographical and bio-physical settings (see Chapter 6.3.3).

6.3.2. Data

For all four regions, a digital elevation model derived from the Shuttle Radar Topography Missions with 90 m resolution (Jarvis et al., 2008). Soil parameters were derived from the Digital Soil Map of the World (FAO et al., 2012). Relevant soil data for SWIM includes its depth, clay, silt and sand content, bulk density, porosity, available water capacity, field capacity, and saturated conductivity for each of the soil layers. Land use data were reclassified from the Global Land Cover (Bartholomé and Belward, 2005). Land use classes of SWIM include water, settlement, industry, road, cropland, meadow, pasture, mixed forest, evergreen forest, deciduous forest, wetland, savannah (heather) and bare soil.

Climatic observations are generally sparse in Africa and very inhomogeneously distributed over the continent. Therefore, and for better comparability of the results, we calibrated the model for four basins using a reanalysis climate data set produced within the EU FP6 WATCH project (Weedon et al., 2011; WFD, 2011). This data contains all variables required for SWIM on a daily basis on a 0.5°x0.5° grid. Observed river discharge data from the Global Runoff Data Centre was used to calibrate and validate the model (Fekete et al., 1999).

For analyzing climate trends we used the output of an ensemble of 19 CMIP5 ESMs. Of this ensemble, five ESMs (HadGEM2-ES, IPSL-5 CM5A-LR, MIROC-ESM-CHEM, GFDL-ESM2M, NorESM1-M) outputs were used for driving the hydrological model (Table 12). The accurate way of choosing the ESMS for the regions would have been a skill test (see IPCC-TGICA, 2007 and Tshimanga and Hughes, 2012). But as we compare different regions and have to maintain the same ESMs for the intercomparison we used all five models which are available in a bias corrected version (Hempel et al., 2013), taking

into account that the relative performance of the ESMs in reproducing historical patterns will be ignored. Instead we added an analysis where we compare the chosen ESMs with the whole ensemble in order to see their characteristics in terms of precipitation and temperature (Figure 50 and Figure 51).

The five chosen ESMs have been downscaled using a trend-preserving bias correction method with the WFD reanalysis data, and have been resampled on a 0.5 ×0.5 grid for the time period 1950–2099 (Hempel et al., 2013). "Representative Concentration Pathways" (RCP) cover different emission concentrations, and in this study the RCP 2.6 and 8.5 scenarios were used for all 5 ESMs to cover the low and high ends of possible future climatic projections. The RCP 2.6 corresponds likely to a warming of less than 2°C increase of global temperature above the pre-industrial level until the end of the century (Van Vuuren et al., 2011a), and the RCP 8.5 to a likely increase of 3.8–5.7°C (Rogelj et al., 2012). The trend-preservation in the bias correction can lead to extreme precipitation corrections in exceptional cases. An example of this can be seen in the case of the IPSL model in the Upper Blue Nile basin, where the almost rainless October was corrected by a high factor during the base period. In the future scenarios, this factor resulted in a very strong increase in precipitation during October, which exceeds the usual peak of the rainy season in August (see supplementary material, Fig. 2).

Table 12 Earth System Models driving the SWIM model

Model name	Institution
HadGEM2-ES	Met Office Hadley Centre Earth System Modeling group, England
IPSL-5 CM5A-LR	Institut Pierre-Simon Laplace, France
MIROC-ESM-CHEM	Japan Agency for Marine-Earth Science and Technology, Atmosphere and Ocean Research Institute, Japan
GFDL-ESM2M	Geophysical Fluid Dynamics Laboratory of the National Oceanic and Atmospheric Administration, USA
NorESM1-M	Norwegian Climate Centre, Norway

6.3.3. Model set-up and calibration

Table 13 summarizes the basic model set-up and calibration information as well as the results of the validation. The Niger basin is geographically the most heterogeneous of the four basins and covers the largest area (Table 11). Therefore, the availability of a sufficient number of discharge gauging stations to cover the heterogeneity of the basins was crucial for the set-up of the model. The 1,923 subbasins were integrated to form 18 subcatchments, each associated with a gauge at its outlet. These subcatchments were

calibrated individually in order to adapt the model as closely as possible to the regional conditions (Appendix Table S 2).

In addition to this heterogeneity the flood plains of the Inner Niger Delta (IND) in Mali have a significant impact on the flow regime of the Niger River. About 40% percent of the inflowing water evaporates from the huge floodplain and discharge patterns at the outlet differ significantly. It is therefore indispensable to incorporate processes such as flooding and release into the hydrological model in order to account for increased infiltration and evaporation from the additional water surface. Based on the Digital Elevation Modell, inundation zones are delineated for each subbasin in the floodplain. Moreover, ponds were identified where water gets trapped and is not allowed to flow back to the channel system. It is assumed that if discharge exceeds the water holding capacity of the river at a subbasin inlet, the surplus flows into the inundation zone(s). This threshold is computed by multiplying cross-sectional area by flow velocity. At each time step, water is released from the storages into the downstream subbasin according to the routing scheme. The volume of water to be released from storage is a linear function of the current storage volume. Areas (hydrotopes) in the flood plain switch dynamically from water to land phase implementing different functions for land cover, infiltration, percolation and evapotranspiration. The SWIM inundation module which is described in detail in Liersch et al. (2013) significantly improved discharge simulations at the IND outlet. The five largest reservoirs were included in the model set-up (see 2.2). A reservoir module developed by Koch et al. (2013) was used for this purpose.

The calibration of the model for the Upper Blue Nile basin was limited to one gauging station, namely El Diem at the Sudanese-Ethiopian border. For this basin, the quality of radiation data within the WFD dataset was insufficient when compared with the World Radiation Data Center (WRDC, 2000) data. Radiation was underestimated, especially during the rainy season. Therefore, global radiation was estimated for this basin by means of the latitude as well as minimal and maximal daily temperatures, using the method of Hargreaves and Samani (1982). Further, the vegetation module was adapted to spatially varying temperature conditions in the topographically very heterogeneous catchment to provide more realistic regional vegetation growth. Water management was not implemented in the model of this basin because the influence of streamflow management is still negligible.

The Oubangui Basin consists mainly of a peneplain and contains a broad range of different soil and vegetation types. The model for the catchment was calibrated for the gauging station Bangui. Precipitation data for the Oubangui basin in the WFD are based on very sparse climate observation data from the Global Precipitation Climatology Centre's precipitation data (GPCC). The interpolation and correction method for precipitation of WFD thus produced unrealistically high precipitation values for the Oubangui. Therefore, WFD precipitation was replaced by original uncorrected GPCC data for the calibration in this basin while all other parameters are still from the original WFD (Schneider et al.,

2013). Another particularity of the Oubangui basin is the almost complete cover by tropical evergreen forest. As the SWIM vegetation module has not yet been adapted to this type of vegetation, it was not been simulated in the Oubangui catchment. Instead, Leaf Area Index and rooting depth were used as additional calibration parameters. Due to the sparse data, the reservoirs of the Oubangui basin could not be included in the model.

Table 13 Characteristics of basin models and validation results

	Niger	Upper Blue Nile	Oubangui	Limpopo
Number of subbasins	1,923	558	377	2,020
Number of hydrotopes	13,883	1,700	1,734	13,085
Number of included reservoirs	5	0	0	8
Number of included irrigation schemes	0	0	0	31
Number of gauging stations used for calibration	18	1	1	2
Gauging station(s) used for calibration/ validation	Lokoja[a]	El Diem	Bangui	Sicacate, Oxenham Ranch
Calibration period	1972-1982[a]	1961-1970	1981-1990	1971-1978
NSE[b] (daily)	0.92	0.81	0.66	0.72, 0.73
PBIAS[c]	8.6	20.9	19.1	11.5, -6.7
Validation period	1983-1992[a]	1971-1980	1971-1980	1980-1987[d]
NSE[b] (daily)	0.89	0.63	0.6	0.55
NSE[b] (monthly)	0.9	0.73	0.63	0.8
PBIAS[c]	2.1	39	15.7	3.4

a) In the Niger basin 18 gauging stations have been used for the calibration. For the additional 17 calibration periods and results see Appendix Table S 2.

b) Nash-Sutcliffe Efficiency.

c) Percent bias of monthly average.

d) The gauging station Oxenham Ranch was only used for calibration and not validated.

The SWIM model was calibrated for the Limpopo basin using discharge data from the

Sicacate gauging station in South Africa and the Botswanian station Oxenham Ranch. However, the main challenge for the modelling of this basin was a strong effect of human intervention on the river discharge. Therefore, the largest eight reservoirs were included in the model with the input data on reservoir capacity and withdrawal amount from the reservoirs. In addition, 31 intensive irrigation sites with an annual abstraction rate over 6.3 Mm3 were identified and included in the model. Taking into account the annual abstraction rate, the monthly share of irrigation and the estimated return flow after irrigation, the daily irrigation demand was calculated for each irrigation site. The irrigation module of SWIM abstracts the irrigation demand from the specific river reaches as long as the amount of irrigation water is available in the river.

6.4. Results

6.4.1. Validation of the model

The SWIM model was validated for the gauging stations at the outlets of the four basins; the results are presented in Figure 48. To quantify the efficiency of the model we applied the method of Nash and Sutcliffe (1970) (NSE), and percent bias (PBIAS) was used for evaluation of model error. The validation period was chosen independently from the calibration period and lasted at least eight years (Table 13). The focus of the calibration and model set-up for all four basins was to achieve adequate efficiency for streamflow simulations for daily time steps, for mean as well as high and low flows. The high flows refer in this context for discharge peaks during the rainy season and low flows as the minimum discharge during the dry season, and are quantified as Q10 and Q90, correspondingly.

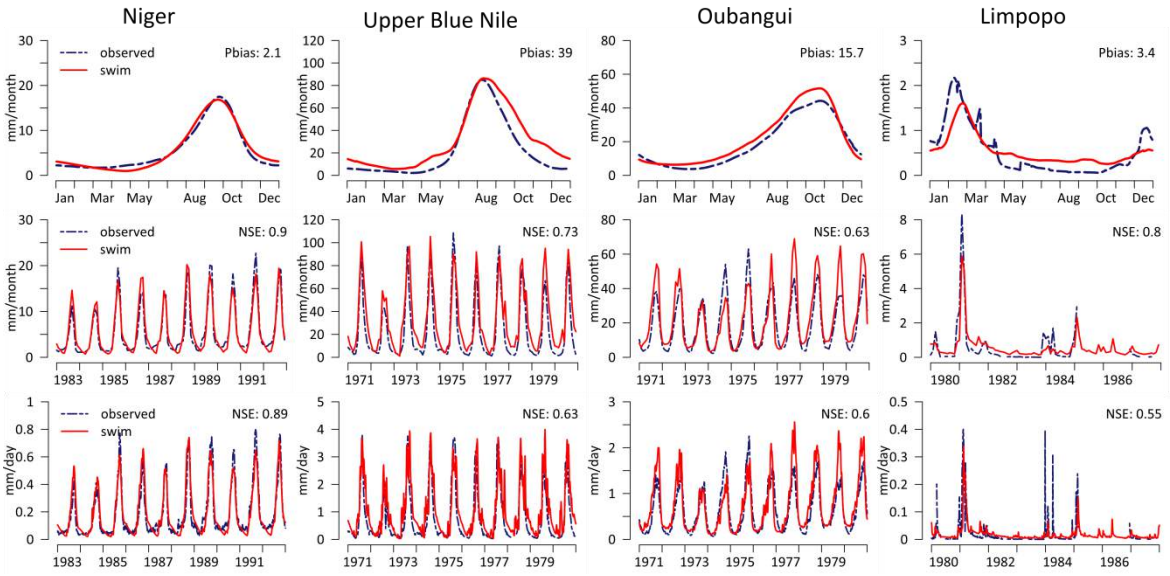

Figure 48 Validation of SWIM at the outlets of the four basins. In the top row the seasonality of monthly runoff rate in validation period and PBIAS, in the middle row the monthly runoff rate and in the bottom row the daily runoff rate in the validation period, both with Nash-Sutcliffe Efficiency.

The SWIM model was basically able to reproduce the hydrological characteristics of each basin reasonably well, with NSE of the monthly runoff rate ranging between 0.63 and 0.9 and the daily runoff rate ranging from 0.55 to 0.89. However, the validation showed heterogeneous results in terms of the NSE, ranging from adequate in the Oubangui basin and Limpopo basin to very good in the Niger basin. The model was able to reproduce high and low flows for the Niger basin well, and in terms of seasonality the results are very good for both daily and aggregated monthly model output. The Upper Blue Nile basin shows good results for the modelling of seasonality for daily and monthly output data with adequate representation of high flows but an overestimation during the low flow. For the Limpopo basin the difference between daily and monthly runoff rate is high. When aggregated to monthly time series, the validation shows a slight underestimation of high flow and overestimation of low flow, but the total efficiency is good. For the daily time series, some peaks were well modeled but others are missing almost completely. The model for the Oubangui basin has distinct deficiencies in reproducing high and low flows, but regarding discharge seasonality the model gives adequate results during the validation period for monthly and daily data.

6.4.2. Climate trends

Precipitation and temperature are the key drivers for the hydrological regime of rivers, and climate change has its main impact through changes in these two variables. In Figure 49, we show the mean trends for these two parameters from 2006 until 2100 projected by

19 CMIP5 models for the whole African continent. Shown are the results for RCP 8.5 in order to illustrate the most pronounced trends under extreme scenario conditions.

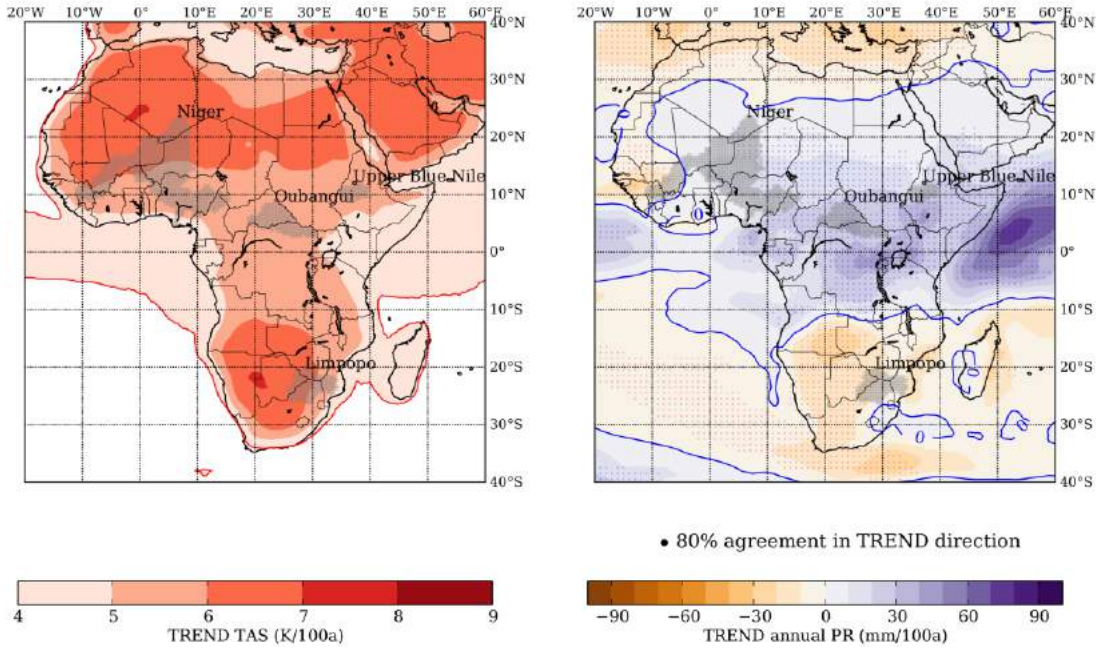

Figure 49 Mean temperature (left) and precipitation (right) trends over the African continent for 19 CMIP5 models from 2006-2100 for RCP 8.5. For precipitation, an agreement in trend direction of 80% or more of the models is marked with a dot.

All models agree on a distinct temperature rise over the whole African continent, while in the tropics much of the additional energy input is converted to latent heat. The highest increase of 6°C to 7°C, in some parts even up to 8°C, is projected over the already driest and hottest areas in the Sahara and southern African savannahs and deserts. The catchments of the Niger and Limpopo are partly located in these zones of the most extreme temperature increases. The Upper Blue Nile and Oubangui basins are located in regions with a lower but still very distinct warming trend. Here, temperatures rise between 4°C and 6°C, whereas the coastal zones generally show a lower rise in temperature.

For precipitation, the model agreement is considerably lower. The Niger basin can be divided into an area with a negative precipitation trend in the headwaters of the river in the west, and a positive trend in the eastern part. The longitudinal trend intensifies eastwards, and in the headwaters of the Benue tributary in Cameroon most models agree on a distinct precipitation increase. The Upper Blue Nile and the Oubangui are located in the inner tropical belt, where at least 80% of the models agree on the positive precipitation trends. The precipitation trend for the Limpopo basin is negative, with a high agreement in the western part of the basin, where most of the rain falls. Here major changes seem most probable.

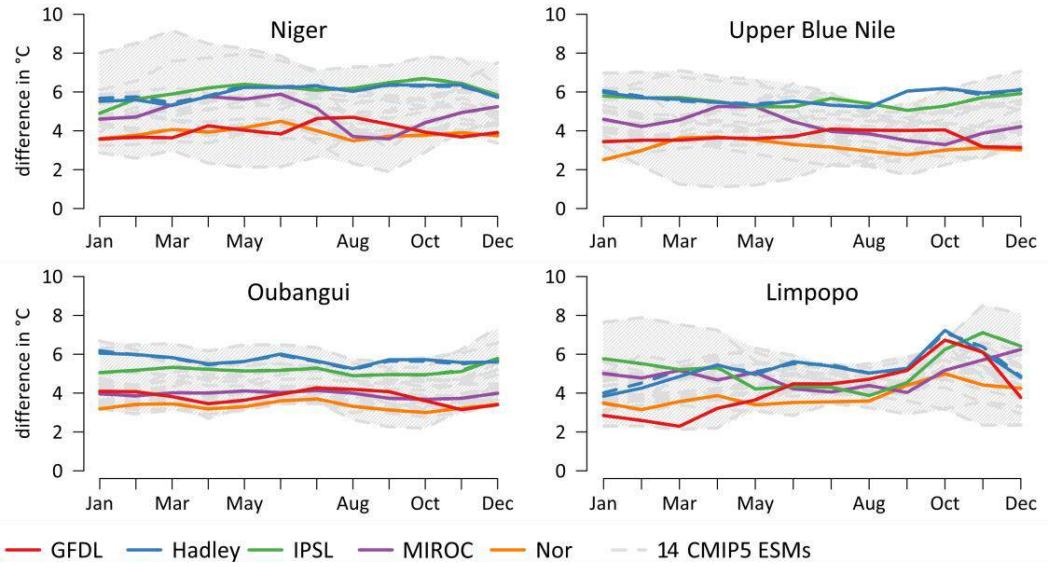

Figure 50 Difference in monthly mean temperature in the far projection period (2070-2099) relative to the base period (1970-1999) for RCP 8.5 for five bias corrected model projections (colored lines), the uncorrected ESMs (colored dashed lines) and 14 ENSEMBLE ESMs (grey dashed lines).

For the projection of streamflow we use the bias corrected model output of 5 ESMs (HadGEM2-ES, IPSL-5 CM5A-LR, MIROC-ESM-CHEM, GFDL-ESM2M, NorESM1-M). In Figure 50 and Figure 51, temperature and precipitation of these climate runs were compared to the uncorrected runs and 14 other CMIP5 models in order to display the influence of the bias correction and where the respective models lie in a larger ensemble, i.e. if the model is especially dry or wet, warm or cold or in the middle of the whole ensemble. In Figure 50, the seasonal changes between mean monthly temperatures show a distinctly homogeneous pattern. In all four basins, the temperature rises between ~3°C and ~6°C. In the basins of the Niger, Oubangui and Upper Blue Nile, all 5 models chosen project a homogeneous increase throughout the year; Hadley and IPSL outputs are the most extreme with increases between 5°C and 6°C, GFDL and Nor project a moderate increase of less than 4°C, and MIROC results are in the middle with the highest variance. In the Limpopo basin, all models agree on the range of warming between 2.5°C and 6.5°C, and on the same pattern of warming, most pronounced from August to December. Hadley and GFDL again show the highest mean annual warming, and GFDL reaches the same level of warming during the first half of the rainy season from August to December. The bias correction hardly influenced the temperature. The five selected model outputs cover the temperature range of the CMIP5 ensemble in all four basins well.

In Figure 51, we compare monthly precipitation in the same periods for the RCP 8.5. For the Niger, the range of uncertainty for the five models chosen is very high. It ranges from ~150 mm/month increase during the rainy season (MIROC model) to 25 mm/month decrease (GFDL model), which means a range between ~120% and minus ~-20 %. Compared with the uncorrected model runs, the MIROC model unexpectedly shows a

distinct increase in trend, caused by the correction (see discussion in 6.5). For the other models, the correction slightly decreases the means of the monthly trend. During the dry season from November to March, there is no visible trend in precipitation. The selection of five models represents the precipitation range of the CMIP5 ensemble well for the Niger basin though there are deficits between March and June.

The five bias corrected models for the Upper Blue Nile basin all agree on an increasing trend in precipitation. The increase in the IPSL model of almost 400 mm/month (~100%) at the end of the rainy season is striking. All other bias corrected models show a slight increase in precipitation of less than 40 mm/month during the rainy season, which corresponds to less than 20%. The difference from the uncorrected model runs is minor in this basin, except for the IPSL run which again unexpectedly shows a distinct increase in trend as a result of the correction (see discussion in Chapter 6.5.2). During the dry season from December to May, there is no trend in precipitation (except IPSL). In this basin, selection of the five corrected climate runs diminishes the range of the whole CMIP5 ensemble particularly from June to September, which should be taken into account when interpreting the results.

In the Oubangui catchment, the trends of the five CMIP5 models chosen are rather minor. All models agree on an increasing precipitation trend from ~20 mm/month to ~50 mm/month, which is less than 20% with no obvious pattern. The effects of the bias corrections are minor for all five models. As the dry season is not significant in this region and lasts not longer than two months, the precipitation trends are distinct throughout the entire year. The selection of the five corrected climate runs results in a substantially reduced range of the whole CMIP5 ensemble, which also reduces the informative value for the discussion.

Precipitation trends for the five models chosen in the Limpopo basin all agree on a decrease at the beginning of the rainy season in October. During the main rainy season from December to March, Hadley and GFDL show an increase of over 50 mm/month, which corresponds to an increase of over 50%. The other three models show minor decreases or no trend at all. The correction of the models with the ISI-MIP method results in less distinct trends for increases as well as for decreases (see discussion in Chapter 6.5.2). In the Limpopo basin, the dry season lasts from May to November and during this period there are no trends in precipitation. The selection of five models of the CMIP5 ensemble covers the whole range of precipitation trends in the Limpopo basin with deficits from August to November.

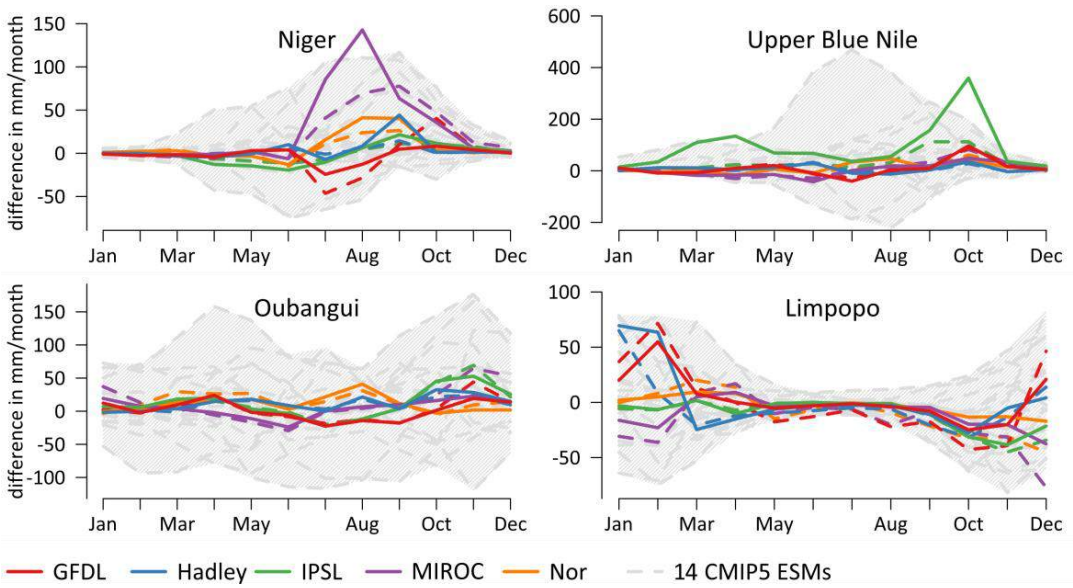

Figure 51 Difference in monthly precipitation in the far projection period (2070-2099) relative to the base period (1970-1999) for RCP 8.5 for five bias corrected model projections (colored lines), the uncorrected ESMs (colored dashed lines) and 14 ENSEMBLE ESMs (grey dashed lines).

6.4.3. Climate sensitivity

Figure 52 illustrates the sensitivity of river discharge to climate variability and change in the four basins. Shown is the change in percentage for the total precipitation over 12 months beginning with the driest month, against the total discharge during the related hydrological year. As base values for all five selected climate models runs of RCP 8.5 serve the means of the base period (1970-1999). The anomalies are then plotted for each year from 2006 until 2099. Additionally, we show the anomalies for the runs with the reanalysis WFD climate input from 1960-2001. Changes in precipitation are shown in the range from -50% to 100%, and for discharge from -100% to 200%. Values outside this range are not shown but are included in the calculation of the fitted local regression, plotted as a black line.

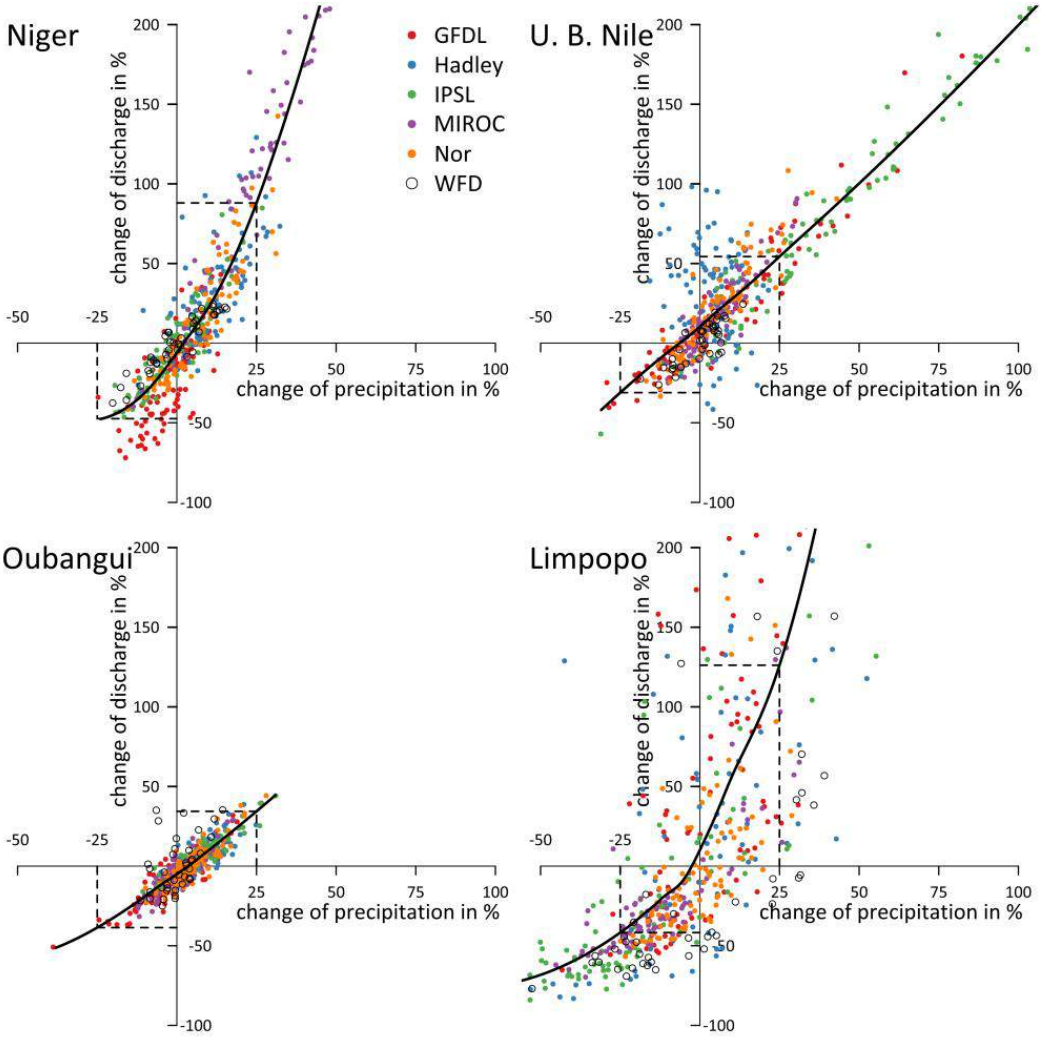

Figure 52 Climate sensitivity in the four basins. Change in modeled annual discharge [percent] per change of precipitation [percent] for 2006-2099 compared to the mean of base period 1970-1999 for five climate models in RCP 8.5 and WFD. Curve shows fitted local regression over all values.

The sensitivity varies distinctly from basin to basin. In the Niger basin, an increase in annual precipitation by 25% results in an increase in modeled discharge by ~90%, and 25% less precipitation causes a decrease in annual discharge of almost 50%. In the Upper Blue Nile, a 25% increase in precipitation leads to ~50% higher modeled discharge, whereas a 25% reduction in annual rainfall leads to ~ 25% reduction in discharge. In the Oubangui, climate sensitivity is least pronounced. Namely, a 25% increase in precipitation results in less than 30% increase in annual discharge, and a 25% decrease reduces discharge by ~40%. In the Limpopo basin sensitivity is highest, and already small changes in the precipitation regime may cause huge effects on the discharge regime. So, a 25% increase in annual precipitation results in ~125% higher discharge, and a 25% reduction in precipitation leads to a decrease in discharge of ~40%. In addition, the spread of impacts in the Limpopo basin is the largest of all four basins.

The response of discharge to rainfall anomalies for the model runs with the observed WFD agrees with the scenario runs in the Niger and the Upper Blue Nile basins. In the Limpopo basin, the form of the curve corresponds to the scenario values, whereas the position shifts. This can be explained by the distribution of rainfall that changes in the scenarios, and rainfall during the dry period becomes more likely (Figure 50). In the Oubangui basin, the runs with WFD data agree with the scenario runs, though there are some years with an outlying relation of annual precipitation to discharge. This can be explained by a temporal concentration of rainfalls and hence an increased runoff coefficient.

6.4.4. Impact of climate change on discharge and seasonality

Figure 53 shows mean monthly discharge values or their changes, derived from the daily model output for all 4 basins and 5 models in the different time periods and for both RCPs. For the base period (1970-1999), the agreement between the simulated discharge driven by WFD and the five chosen climate models is good for the Niger and Oubangui (Fig. 8, topmost row), yet there are some differences for the Oubangui. However, for the Limpopo and Upper Blue Nile basins the results differ more distinctly. Especially in the Limpopo catchment, only the simulation driven by climate input from one model, HadGEM2-ES, gives results comparable to that driven by the WFD input. However, with regard to the small absolute numbers of discharge in the Limpopo basin, these results are still acceptable.

Regarding the changes in river discharge from the base period to the near (2021-2050) and far (2070-2099) scenario periods, we focus mainly on the rainy season of each basin (Figure 53, grey shaded area). The spread between the simulations driven by different climate models is high for all basins, ranging from strong increase to little or moderate decrease, depending on basin and climate model (Figure 52, four lower rows).

For the Niger basin the directions of change differ, which corresponds to the location of the basin in the transition zone of increasing and decreasing precipitation projections of the whole CMIP5 ensemble (Figure 49). The SWIM model projects changes of monthly discharge when driven by the climate simulation results of Hadley, Nor, IPSL and GFDL for both periods and both RCPs, ranging from an increase of up to 50% to a decrease of up to 50%. The change in discharge produced with the MIROC climate projections is remarkably higher than that simulated by other climate models. The discharge for the near and far scenario periods increases by the end of the rainy season by 200% and for the RCP 8.5 in the far period even by 500%.

In the Upper Blue Nile basin, the projections of the SWIM model driven by the five corrected climate models agree almost completely on positive trends which correspond to the precipitation trends shown in Figure 49. In the near scenario period, there is a slight

increase of fluctuations around 0% at the beginning of the rainy season from June to August for both RCPs. Furthermore, the climate scenarios show an increase at the end of the rainy season. This holds also for the far scenario period, with a slightly stronger increase for the RCP 8.5 at the end of the rainy season. The discharge projections driven by IPSL show the most extreme results, with increases between 50% and 100% and even 300% in October of the far period. According to the results obtained, all models including IPSL agree on a shift in peak discharge for both RCPs of around one month.

According to Figure 52, the Oubangui River is least sensitive to climate variability. This is in line with projections, which show the smallest trends out of all four basins, with the highest increase of discharge up to 60% in the second period for the RCP 8.5. The projections of the SWIM model driven by the five corrected climate models for both RCPs range from decreases of 15% to increases up to 20%. However, as the selected climate models in this case do not represent the whole CMIP5 spectrum very well, the validity of this information is limited (Figure 51).

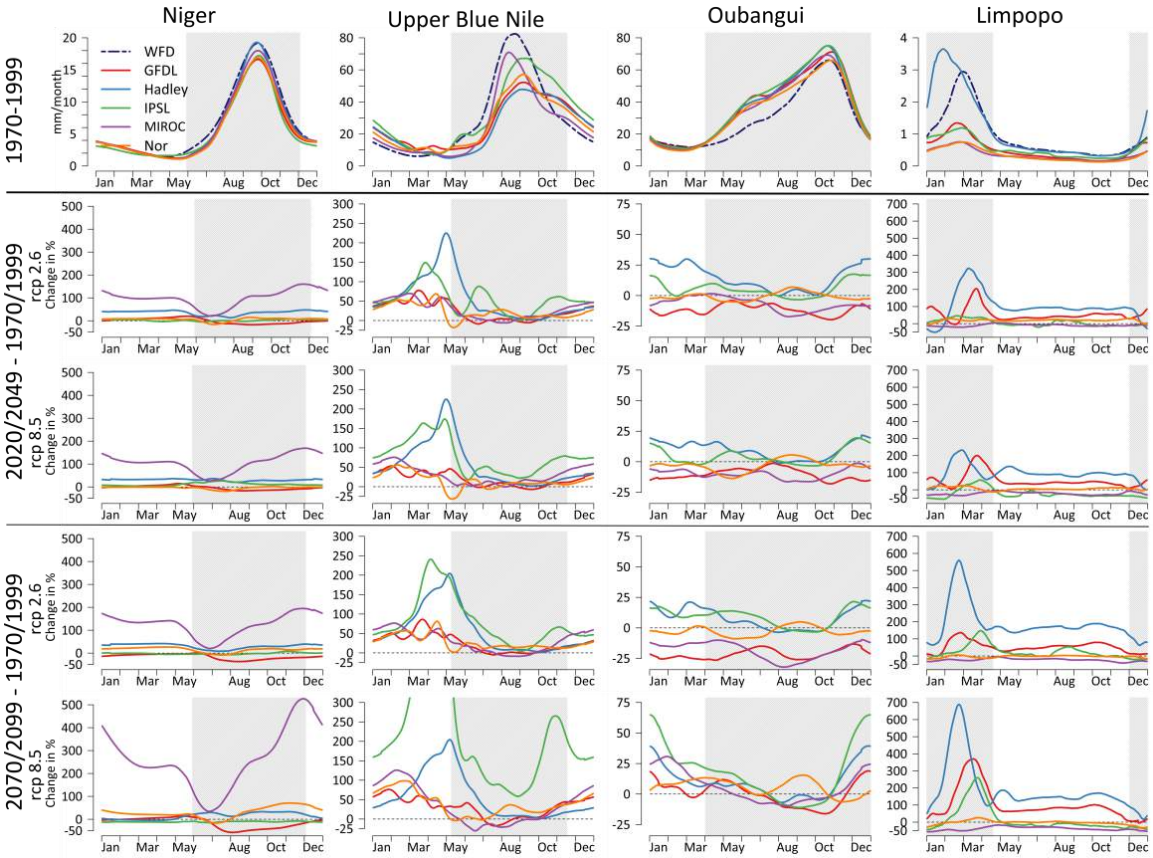

Figure 53 First row: seasonality of monthly discharge for the reference period; second and third rows: changes in % of discharge between a near scenario period and reference periods for RCP2.6 and RCP 8.5; fourth and fifth rows: changes in % of discharge between a far scenario period and reference periods for RCP 2.6 and RCP 8.5. Recent rainy season as grey shaded area

In the Limpopo basin with its extremely low runoff coefficient and very high sensitivity to climate variability (Figure 52), the projected trends are the most extreme of all of the four basins. However, analyzing the results in percentage, the small amount of discharge in absolute numbers has to be taken into account, which implies that the annual runoff is still limited. The GFDL-driven model runs show an increase in discharge during the peak of the rainy season of ~200% in the near period for both RCPs and in the far period for RCP 2.6. The discharge for RCP 8.5 in the far period increases by 350%. The discharge projected with IPSL output also increases by ~50% in the near period and in the far period by 100% for RCP 2.6, and by 200% for RCP 8.5. The model output with Nor climate input produces no visible trends for both periods and RCPs. The MIROC model driven runs result in a slightly reduced discharge by ~25% in the near period and RCP 2.6 in the far period. The projected discharge driven by RCP 8.5 for the far period decreases even up to 50% in the rainy season. The Hadley-driven simulation produces a striking increase in discharge of ~300% during the peak of the rainy season in February in the near period for RCP 2.5, and of ~250% for RCP 8.5. For the far period, the increase is even more extreme in February at ~550% and ~700% for both RCPs.

6.4.5. Changes in extremes

The Q10 value is a robust indicator for high flows and designates a value of river discharge which is only exceeded 10% of the time. A negative trend in Q10 means a reduction in flood risk, and a positive trend represents an increase. The results for changes in Q10 under scenario conditions are presented in Figure 54 for two periods and two RCPs.

In the Niger catchment, Q10 produced with input from all climate models reflects the direction of changes in mean discharge. The MIROC-driven outputs show a rise in Q10 to over 100% in all four cases. The RCP 8.5 scenario for the far period shows the most extreme increase of over 300%. The outputs driven by all other models show rather moderate changes in Q10, which correspond roughly to the percentage of change in the mean discharge during peak flow in the rainy season.

In the Upper Blue Nile basin, the discharge projections for almost all climate models and both RCPs show an increase from ~10% to ~50%. Only for the RCP 8.5 in the far period, IPSL-driven output projects an increase in Q10 of 150%.

The scenarios for the Oubangui produce the lowest Q10 trends out of all four basins. An increase in Q10 is not projected. The GFDL and MIROC-driven results show a decrease in Q10 of ~15%, and the other outputs fluctuate around 0% for both scenario periods and both RCPs.

In the Limpopo basin, the patterns of changes identified for the mean discharge also hold for Q10. The Hadley climate-driven output yields the strongest positive Q10 trend of almost 250% for RCP 2.6 in the far period. For RCP 8.5 the increase is about 200%. In

contrast, the increase in the near scenario period is higher for RCP 8.5 at almost 150% than for RCP 2.6 at ~100%. The projections with GFDL input in the near future are almost the same for both RCPs at ~75%. For the far period, the trend reduces to 50% in the RCP 2.6 case, and for RCP 8.5 it strengthens to 120%. The IPSL-driven projection shows slight increases in both periods for RCP 2.6 and a decrease of almost 50% in the near period for RCP 8.5. This decrease tends to zero in the far period. The MIROC-driven output shows negative Q10 trends for both RCPs in both periods.

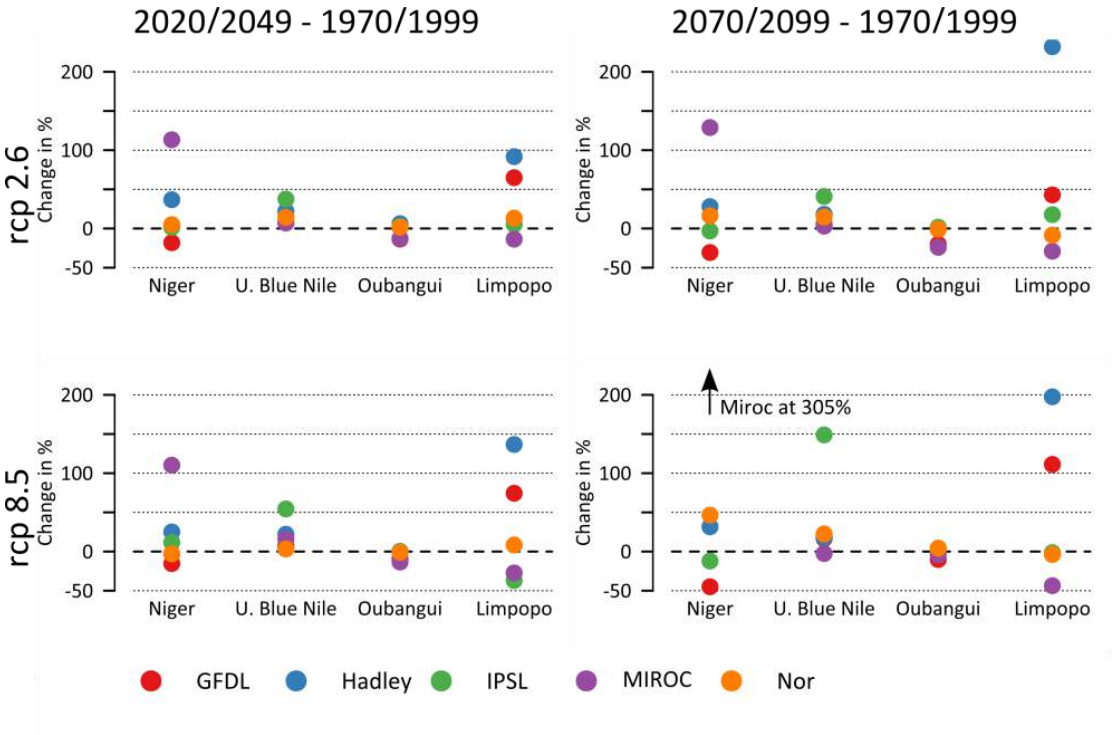

Figure 54 Change in Q10 (high flows) of five bias corrected model projections in near (2020-2049, left column) and far (2070-2099, right column) scenario periods compared to the reference period (1970-1999) for RCP 2.6 (upper row) and RCP 8.5 (lower row) in percent.

A Q90 value is used for identifying low flows, indicating that 90% of the time the value is exceeded (Figure 55). If the value shows a negative trend, it implicates that low flow is further decreasing and river droughts are likely to occur more often.

In the Niger basin, the Q90 trend is mostly positive for both RCPs and both scenario periods. Only GFDL and IPSL-driven outputs show slight negative trends in the far period, between 10% and 20%.

In the Upper Blue Nile basin all trends are positive, showing strong increases. The IPSL-driven simulations again produce extreme results, with increases up to 450% in the far period for RCP 8.5. The Nor-driven scenarios result in a Q90 increase of ~100% in the far period for both RCPs and ~50% in the near period for both RCPs. Simulations driven by all other climate models lead to increased Q90 trends in a range of 40% to 60%.

In the Oubangui basin, only model runs driven by GFDL and MIROC climate inputs produce a decrease in Q90. For GFDL, Q90 is reduced by ~25% for both periods and both RCPs. The MIROC-driven results show a ~20% decrease in Q90 for both RCPs in the near period, a ~25% decrease for RCP 2.6 in the far period, and almost no trend for RCP 8.5 in the far period. All other simulations produce trends that fluctuate around 0%.

For the Limpopo catchment, MIROC and IPSL climate inputs lead to negative Q90 trends. In the near period of RCP 2.6 scenario, only the MIROC climate input leads to a slightly negative trend, whereas for RCP 8.5 the IPSL-driven runs project a decrease of ~15% and MIROC ~30%. In the far future period, the IPSL and MIROC-driven outputs show a decrease of ~40% to ~50%. Simulations driven by the other 3 climate models project a positive Q90 trend.

Summarizing the results for changes in extremes, it can be said that the direction of changes identified for the mean discharge holds mostly also for the high and low flow extremes.

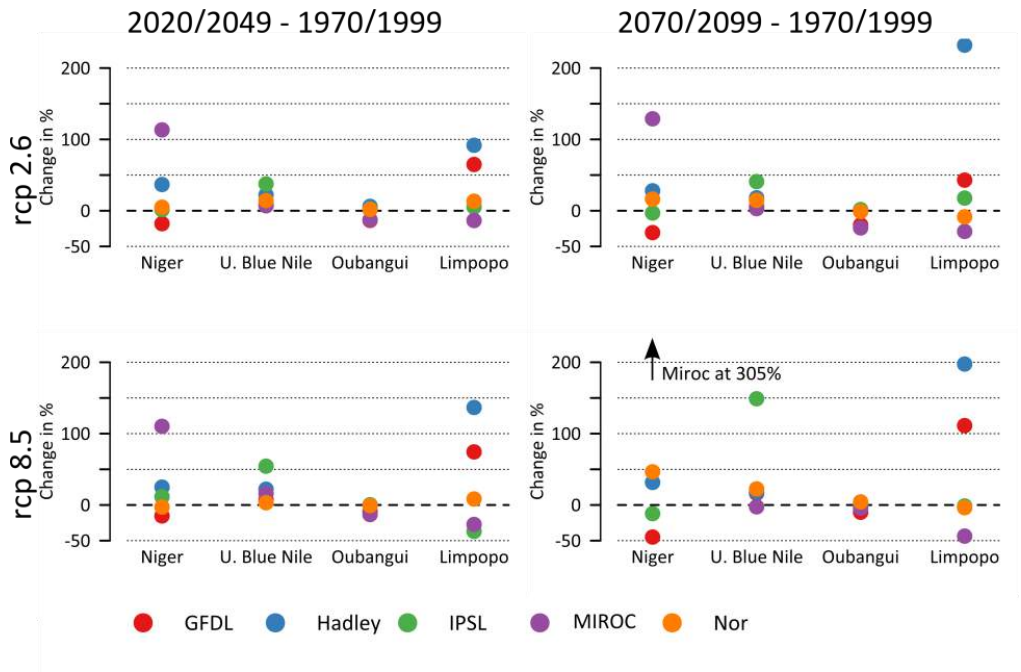

Figure 55 Change in Q90 (low flows) of five bias corrected model projections in near (2020-2049, left column) and far (2070-2099, right column) scenario periods compared to the reference period (1970-1999) for RCP 2.6 (upper row) and RCP 8.5 (lower row) in percent.

6.5. Discussion

The following discussion is structured according to the research objectives presented in the introduction.

6.5.1. Differences in climate change sensitivity among the basins

First aim was to investigate differences in the sensitivity of modeled annual discharge to climate parameters between the basins. The response to changes in precipitation is not a linear process but rather depends on the basin's characteristics. Figure 52 shows that the response to changes in annual precipitation is augmented with regard to percent change in streamflow in all basins.

The relationship between changes in precipitation to changes in discharge is most extreme in the Limpopo basin, where we also found the highest probability of major changes to the precipitation regime. This high sensitivity can be explained by the very low runoff coefficient of the Limpopo basin, which makes the catchment very sensitive to changes in precipitation (Table 11). Also for the Upper Blue Nile and Niger basins, the changes in precipitation are likely to intensify the impacts of climate change on discharge in both directions for both drier and wetter years.

These findings are independent of the projected climate scenarios and their uncertainties. Hence, climate change will most likely have significant impacts on river discharge in the Limpopo, even if climate change is more moderate than in other basins studied.

6.5.2. Changes of streamflow under climate change

Our results related to objective 2. on the seasonality of discharge for the four basins in the future mainly confirm the results of former studies on streamflow projections in Africa. Possible decreases in streamflow for the Limpopo, Niger and Oubangui are in the same range (up to -20% per year, Figure 53) as in the studies discussed in the introduction. For the Niger basin, the results on increasing streamflow at the downstream part of the river where the Lokoja gauge is located (Table 14) agrees with the findings of other studies (Faramarzi et al., 2013; Mahe et al., 2013). The results for the Oubangui basin are also in line with previous studies, which project varying results with a tendency for decreasing flow as a mean over all projections (Strzepek and McCluskey, 2007; De Wit and Stankiewicz, 2006).

However, the increasing discharge produced for the Upper Blue Nile basin by all climate models and for the Limpopo basin by the majority of the climate projections are partly contradictory to previous studies' results (Strzepek and McCluskey, 2007; De Wit and Stankiewicz, 2006) and also to the African chapter of the Fourth Assessment Report of the IPCC (AR4) (Boko et al., 2007). Especially for the Upper Blue Nile basin, simulations driven by all climate input runs chosen resulted in higher annual discharge, on average even up to 40% for the first half of the 21st century. However, also for the Limpopo basin where other studies projected decreases in streamflow (De Wit and Stankiewicz, 2006; Zhu and Ringler, 2012), the multi-model mean of the climate models resulted in an

increase of mean annual streamflow for both scenario periods with a high agreement for the first half of the century at RCP 2.6. As both previous studies focused on the continental scale on a defined grid, it is difficult to compare the outputs directly.

Regarding the differences between RCP 2.6 and 8.5, our findings agree with the observations of the AR4, which states that the differences between the emission scenarios mainly take effect in the second half of the 21st century (Solomon et al., 2007). This holds for all four basins. The projections of increasing streamflow in the basins are especially remarkable as in all catchments a substantial increase of temperature (Figure 50) and hence potential evapotranspiration is projected, which would lead under constant rainfall to a reduction of streamflow. In the Oubangui basin it can be seen exemplarily that the increase of rainfall in the climate models does not automatically lead to an increase of discharge but the increase in evapotranspiration leads to a decrease of streamflow despite increasing rainfall. This is in line with other studies in this basin (Tshimanga and Hughes, 2012).

Table 14 Summary of modeling results.

	Change between 2020-2049 and 1970-1999 (RCP 2.6/ 8.5)[a]					
	Direction of trend in %[b]			**Mean amount of change in %**		
	Mean	Q10	Q90	Mean	Q10	Q90
Niger	60/ 60	80/ 60	<50/ 60	28/ 27	32/ 30	28/ 26
U. Blue Nile	100/ 100	100/ 100	100/ 80	38/ 40	56/ 57	18/ 21
Oubangui	<50/ <50	<50/ <50	<50/ <50	0/ −2	2/ 0	−3/ −5
Limpopo	80/ 60	80/ <50	80/ 60	34/ 23	14/ 10	32/ 31
	Change between 2070-2099 and 1970-1999					
	Direction of trend in %			**Mean change in %**		
	Mean	Q10	Q90	Mean	Q10	Q90
Niger	60/ 60	60/ 60	60/ 60	30/ 56	38/ 44	28/ 65
U. Blue Nile	100/ 100	100/100	80/ 80	44/ 81	68/ 132	16/ 41
Oubangui	<50/ 80	>50/ 60	<50/ <50	−5/ 7	−4/ 12	−9/ −2
Limpopo	60/ 60	60/ 60	60/ 60	48/ 53	16/ −4	51/ 52

a Changes in annual mean discharge above 5% or under -5% have been counted as positive/negative. Less than 5% trend was counted as no trend

b Percent values have been calculated by comparing the five corresponding model runs driven by the chosen climate projections.

6.5.3. Changes in hydrological extremes

Results with regard to research question 3. on changes in hydrological extremes affirm the occurrence of trends found previously. Concerning flood risk in Africa at the continental scale or for large regions in Africa, most previous assessments focused on changing vulnerability (Di Baldassarre et al., 2010; Hastenrath et al., 2010; Mngutyo, 2012; Tschakert et al., 2010) and less on climate change. However, a recent study by Jury, (2013) found a return to wet conditions throughout Africa in the period 1995–2010 by

means of trends in monthly river flow records, meteorological reanalysis data, and satellite observations. This tendency of increasing high flows in the observations matches our findings in all basins studied except the Oubangui basin (Figure 54, Figure 49). However, the Oubangui basin modelling has shown a substandard efficiency in terms of high flows in the PBIAS criteria and the projections of decreasing or stable high flows should be interpreted carefully. Still the performance of the model in the other basins in terms of high flows during the validation, especially in the Niger basin and the Upper Blue Nile basin, was good and the increase of high flows holds especially for the Upper Blue Nile basin, where simulations driven by all climate models resulted in a distinct increase in high flows for both RCPs and both scenario periods.

Our study also shows that climate change might play a major role in the increasing risk of hazardous floods in Africa. For a few model runs, these trends are extreme, especially for the Limpopo and the Niger. For the Oubangui basin, the model results agree on a relatively low change in high floods and show discrepancies in the direction of the trend. As flood risk is caused not only by a higher frequency or amplitude of the hazard itself, but is also linked to a rising vulnerability in Sub-Saharan Africa, flood hazards should be taken into account when assessing climate change impacts and adaptation in Africa.

When it comes to low flows, the existing literature agrees mostly on an increase of frequency and magnitude of river droughts throughout the African continent (e.g. Boko et al. 2007; Faramarzi et al. 2013). These findings are not always connected to climate change, but to the increase in water use. As we focus on climate change and neglect changes in land use, it is difficult to compare the results. However, the mean changes in Q90 are positive for the Niger basin, Upper Blue Nile basin and Limpopo basin (Table 14). In regard of the deficiencies in terms of PBIAS during the low flows in the Upper Blue Nile basin, these results should be interpreted with caution also when looking on relative changes. In the Limpopo basin, where previous studies mainly agreed on an increase of hydrological droughts (Zhu and Ringler 2012), our results driven by three of the five climate model outputs show a positive tendency for the low flow level, which means a reduced likelihood of riverine droughts (Figure 55). In the Niger basin, where droughts are also an issue (Oguntunde and Abiodun, 2013), the Q90 trend is mostly positive, and only results driven by two climate models show slightly negative trends. Only for the Oubangui basin do the results indicate an increased likelihood of low flows, but with a very high degree of uncertainty (based on results driven by only two climate models). Hence, taking climate change into account, our study with the five chosen climate projections does not support the widespread view of a distinctly higher probability of decreasing low flows for these regions in Africa.

6.5.4. Sources of uncertainties

Our research objective 4. focuses on the sources of uncertainty in this climate impact study. As with the first finding, we see a broad range of projected changes in precipitation in the five chosen ESMs in each basin, and the associated uncertainties are striking for the near future but even greater for the far future (Figure 49). In contrast, the analysis shows that the direction of the temperature trend on the African continent is confirmed by all CMIP5 models; the temperature change in the four basins ranges from 3°C to 6°C until the end of the century under RCP 8.5 (Figure 50). Hence, the uncertainty in terms of streamflow, which is largely influenced by both, temperature and precipitation, derives mainly from uncertainties in precipitation. This uncertainty could not be reduced with the bias correction method used.

For the Niger, Oubangui and Limpopo there is one climate model for each that produces outlying results that should be interpreted with particular caution when discussing the impacts. The MIROC model for the Niger and the IPSL model for the Upper Blue Nile show outlying increases in discharge, distinctly different from the other results. These extreme increases can be explained by the extreme increase in precipitation, produced by the bias correction of the climate output using the method of Hempel et al. (2013) (Figure 51). "In the Limpopo basin, the extreme discharge resulting from the simulation driven by the Hadley model can be explained by extremely high rainfall. The high sensitivity to weather extremes in the Limpopo Basin most often results in the very high discharge peaks (Table 11; Figure 54). However, in the Limpopo basin not only the uncertainties originating from the climate models are high but also the performance of the hydrological model for peak discharges is rather weak (Figure 48).

The uncertainties derived from the climate model runs are propagated in the cascade of uncertainty to the hydrological model, resulting in the broad range of changes in discharge for each basin. Here, the intercomparison of model set-ups and validation results among the four basins confirmed the dependency of model performance on availability and quality of the input data. With increasing basin size, the data requirements grow, but even more influential are the basins' characteristics in terms of heterogeneity and complexity, including water management, wetlands, etc. Nevertheless, as the performance of the SWIM model is adequate for all basins, the hydrological model probably plays a minor role in this uncertainty. This assumption is supported by the small differences between river discharge amounts simulated with the WFD climate input and the climate models' input during the reference period. Especially in areas with very low runoff coefficient and high sensitivity as in the Limpopo basin, the model is very sensitive to climate input and the requirements for consistent and reliable climate scenarios are very high.

6.5.5. Implications for adaptation

The final research question takes a broader view and looks at the general suitability of a regional intercomparison in order to assess adaptation. Compared to literature reviews in which the comparison of results is usually hampered by the differences between the applied models, scenario assumptions and periods applied, a regional impact comparison study as shown here gives more coherent and comparable results. This holds for the mean changes as well as for the ranges of uncertainty with which they are affected.

As far as adaptation is concerned, we are able to distinguish two types of uncertainty in our results: in one case, the simulations driven by the climate models agree on the direction of the trend. This is mostly the case for the Upper Blue Nile basin, where the trend agreement for the mean, Q10 and Q90 was far higher than in the other catchments (Table 14). In other cases, they do not even agree on the trend's direction. For the purposes of adaptation, the latter case seems to be the most difficult to react to. Regarding an agenda for adaptation, this might be a factor for decision making where impact comparisons may be involved. In addition, the magnitude of change for high flows is the highest in the Upper Blue Nile basin, and additional studies could focus on this particular issue.

In terms of adaptation planning in Africa, there is additional information that can be derived from the comparison. For all four basins, basin-wide action plans for water management (and in many of the riparian states, the additional national plans as well) exist or are in development (Niger: Niger Basin Authority (2007); Upper Blue Nile: Block et al. (2007); Oubangui: Commission Internationale du Bassin Congo-Oubangui-Sangha, (2007); Limpopo: UN Habitat et al. (2007). These plans all include adaptation to climate change in the water sector. However, due to the overwhelming threat of droughts and water scarcity in many regions of Africa, all of these plans account mainly or solely for decreasing streamflow and river droughts. In our study, we show that in the Niger, Upper Blue Nile and Limpopo the risk of high flows will increase. Of course, these results have to be interpreted carefully, as our projections are driven by five bias corrected climate models that do not cover the entire range of the whole CMIP5 ensemble (Figure 50), and uncertainty in the projections is still unavoidable even if the whole ensemble were to be used. Still, disastrous floods in the past decades in many parts of Africa have shown that these catastrophes represent one of the main challenges and an increasing threat under global change in many regions in Africa (e.g. Di Baldassarre and Uhlenbrook, 2012; Di Baldassarre et al., 2010; Jury, 2013). Our findings support this perception and underpin the need for broad adaptation strategies, taking projections for future flooding into account.

However, in the face of these high uncertainties deriving mainly from the climate projections, adaptation is very challenging. Recent studies argue for a "bottom-up" approach to reduce vulnerability instead of adapting "top-down" on the basis of uncertain projections (Few et al., 2007; Richardson et al., 2011). Also, with state-of-the-art climate projections and modeling approaches, these conclusions cannot be disproved and

uncertainties reduced. Still, a comparison of climate change impacts on river discharge and their uncertainties, even using a very general and basic approach, may support decision makers in answering the challenges of climate change.

6.6. Summary and conclusions

The differences between the sensitivities of streamflow regimes to climate variability among the four basins studied are remarkably large; the Limpopo basin with the lowest runoff coefficient being the most sensitive. With regard to future changes in quantity and seasonality of streamflow, we show that the most extreme changes in discharge are likely to happen in the Upper Blue Nile catchment. Here, all climate model projections result in increased streamflow and an extension of the streamflow peaks at the beginning and end of the rainy season. In the Niger and Limpopo basins, the direction of the trend is unclear, whereas the magnitude of change is large for simulations driven by single climate models. In contrast, impacts on the Oubangui River are not so significant compared to others, but still do not all lead in the same direction. In general, this also holds for the extremes. In the Upper Blue Nile basin, there is a clear picture of increasingly high flows for all model runs and a reduction of risk for low flows. For the Limpopo and Niger the trends are diverse, but the majority of runs project increasingly high flows and higher low flows (reduction of risk for low flows). In the Oubangui, the trend for the extremes is unclear and the magnitude of changes is less significant.

In terms of uncertainty, our results confirm that the most uncertainty in regional impact studies derives from climate models, even if the input is bias corrected. In our case, an improvement in the regional hydrological model's performance seems unlikely to diminish uncertainties in streamflow projections substantially, due to the huge range of uncertainty deriving from the climate models' projections. In order to identify and quantify the whole cascade of uncertainty, communication between regional impact modelers and regional climate modelers should be intensified. Particularly the efforts toward improvement of bias correction methods of the climate model outputs should be strengthened.

These broad uncertainty ranges, in which the probabilities of trend directions are in some cases even equally distributed, are of little use for planning actual adaptation measures. Moreover, it should be noted that only five bias corrected ESMs were applied in our study, and a larger number of climate projections would most likely have resulted in an even broader range of uncertainty (Figure 50). However, some robust trends still can be detected:

•The direction of trends for the Upper Blue Nile basin is almost uniform, and our results clearly suggest an increase in discharge and high flows. This strongly indicates that water management in this region should adapt to a longer and more intense rainy season and more intense and frequent flooding in the future.

•The agreement of the projections on increasingly high flows in three of the four regions (except the Oubangui) is remarkable. It agrees with many studies on increased flood frequency and amplitude in past decades in many rivers (e.g. Di Baldassarre and Uhlenbrook, 2012; Di Baldassarre et al., 2010; Jury, 2013). Adaptation efforts in Africa should consider this threat, even if water scarcity is still the main challenge in most of the African regions.

For the Niger and the Limpopo, the diversity of projected trends in average runoff suggests a need for implementation of a wider range of possible adaptation measures. In both cases, our results imply that the focus of adaptation strategies should be broad and include a general reduction of vulnerability of the riverine population. In the Oubangui basin, the trends are unclear and more moderate, which would imply a lower priority level for climate change adaptation for this catchment.

Still, the results should be interpreted carefully, not only because the uncertainties are remarkably high. For very large basins such as the Niger, future studies should also consider the main sub-regions in order to be able to compare impacts for different climate zones. In addition, detailed future studies for planning adaptation strategies have to consider the need for development of flood protection measures.

Acknowledgments

We thank the IMPACT2c project for financing this study and ISI-MIP for providing us with bias corrected climate scenarios.

References

Aich, V., Liersch, S., Vetter, T., Huang, S., Tecklenburg, J., Hoffmann, P., Koch, H., Fournet, S., Krysanova, V., Müller, E. N. and Hattermann, F. F.: Comparing impacts of climate change on streamflow in four large African river basins, Hydrol. Earth Syst. Sci., 18(4), 1305–1321, doi:10.5194/hess-18-1305-2014, 2014a.

Aich, V., Koné, B., Hattermann, F. F. and Müller, E. N.: Floods in the Niger basin – analysis and attribution, Nat. Hazards Earth Syst. Sci. Discuss., 2(8), 5171–5212, doi:10.5194/nhessd-2-5171-2014, 2014b.

Altman, N. S.: An Introduction to Kernel and Nearest-Neighbor Nonparametric Regression, , 46(3), 175–185 [online] Available from: http://www.tandfonline.com/doi/abs/10.1080/00031305.1992.10475879# (Accessed 23 April 2015), 2012.

Amogu, O., Descroix, L. and Yéro, K.: Increasing river flows in the Sahel?, Water [online] Available from: http://www.mdpi.com/2073-4441/2/2/170 (Accessed 11 November 2013), 2010.

Andersen, I., Dione, O., Jarosewich-Holder, M. and Olivry, J.-C.: The Niger River Baisn: A Vision for Sustainable Management, edited by K. G. Golitzen, Dir. Dev., 144 [online] Available from: http://books.google.com/books?hl=de&lr=&id=DQj7Zpv-IwkC&pgis=1 (Accessed 11 November 2013), 2005.

Andersson, J. C. M., Zehnder, A. J. B., Wehrli, B., Jewitt, G. P. W., Abbaspour, K. C. and Yang, H.: Improving crop yield and water productivity by ecological sanitation and water harvesting in South Africa., Environ. Sci. Technol., 47(9), 4341–8, doi:10.1021/es304585p, 2013.

Andréassian, V., Parent, E. and Michel, C.: A distribution-free test to detect gradual changes in watershed behavior, Water Resour. Res., 39(9), doi:10.1029/2003WR002081, 2003.

Arnold, J., Williams, J., Nicks, A. and Sammons, N.: SWRRB; a basin scale simulation model for soil and water resources management. [online] Available from: http://www.cabdirect.org/abstracts/19911960464.html (Accessed 26 April 2015), 1990.

Arnold, J. G., Allen, P. M. and Bernhardt, G.: A comprehensive surface-groundwater flow model, J. Hydrol., 142(1), 47–69 [online] Available from: http://www.sciencedirect.com/science/article/pii/002216949390004S, 1993.

Arnold, J. G., Moriasi, D. N., Gassman, P. W., Abbaspour, K. C., White, M. J., Srinivasan, R., Santhi, C., Harmel, R. D., Griensven, A. van, Liew, M. W. Van and N. Kannan, M. K. J.: SWAT: Model use, calibration, and validation, Trans. Am. Soc. Agric. Biol. Eng., 55(4), 1491–1508 [online] Available from: http://swat.tamu.edu/media/70993/azdez.asp.pdf (Accessed 26 April 2015), 2012.

Arnold, J. G., Kiniry, J. R., Srinivasan, R., Williams, J. R., Haney, E. B. and Neitsch, S. L.: SWAT 2012 Input/Output Documentation., 2013.

Ashton, P., Love, D., Mahachi, H. and Dirks, P.: An Overview of the Impact of Mining and Mineral Processing Operations on Water Resources and Water Quality in the Zambezi, Limpopo and Olifants Catchments in Southern Africa. Contract Report to the Mining, Minerals and Sustainable Development (SOUTHERN AF., 2001.

Ashton, P., Love, D., Mahachi, H. and Dirks, P.: Impacts of Mining and Mineral Processing on Water Resources in the Zambezi, Limpopo, and Olifants Catchment, World Bank Publications., 2005.

Awotwi, A., Yeboah, F. and Kumi, M.: Assessing the impact of land cover changes on water balance components of White Volta Basin in West Africa, Water Environ. J., n/a–n/a, doi:10.1111/wej.12100, 2014.

Awulachew, S. B., Loulseged, A. D., Loiskandl, M., Ayana, W. and M Alamirew, T.: Water resources and irrigation development in Ethiopia, International Water Management Institute, Colombo, Sri Lanka., 2007.

Baker, T. J. and Miller, S. N.: Using the Soil and Water Assessment Tool (SWAT) to assess land use impact on water resources in an East African watershed, J. Hydrol., 486, 100–111, doi:10.1016/j.jhydrol.2013.01.041, 2013.

Di Baldassarre, G. and Uhlenbrook, S.: Is the current flood of data enough? A treatise on research needs for the improvement of flood modelling, Hydrol. Process., 26(1), 153–158, doi:10.1002/hyp.8226, 2012.

Di Baldassarre, G., Montanari, A., Lins, H., Koutsoyiannis, D., Brandimarte, L. and Blschl, G.: Flood fatalities in Africa: From diagnosis to mitigation, Geophys. Res. Lett., 37(22), L22402, doi:10.1029/2010GL045467, 2010.

Bartholomé, E. and Belward, a. S.: GLC2000: a new approach to global land cover mapping from Earth observation data, Int. J. Remote Sens., 26(9), 1959–1977, doi:10.1080/01431160412331291297, 2005.

Block, P. J., Strzepek, K. and Rajagopalan, B.: Integrated Management of the Blue Nile Basin in Ethiopia, Washington D.C. [online] Available from: http://water.columbia.edu/files/2011/11/Block2007Integrated(1).pdf, 2007.

Boko, M., Niang, I., Nyong, A., Vogel, C., Githeko, A., Medany, M., Osman-Elasha, B., Tabo, R. and Yanda, P.: Africa. Climate Change 2007: Impacts, Adaptation and Vulnerability. Contribution ofWorking Group II to the Fourth Assessment Report of the Intergovernmental Panel on Climate Change, edited by M. L. Parry, O. F. Canziani, J. P. Palutikof, P. J. van der Linden, and C. E. Hanson, pp. 433–467., Cambridge University Press, Cambridge UK. [online] Available from: http://results.waterandfood.org/handle/10568/17019 (Accessed 2 December 2013), 2007.

Vanden Bossche, J.-P. J. P. and Bernacsek, G. M. M.: Source book for the inland fishery resources of Africa Vol. 2, Rome., FAO. [online] Available from: http://www.fao.org/docrep/005/t0360e/T0360E00.htm#TOC, 1990.

Cleveland, W. S. and Devlin, S. J.: Locally Weighted Regression: An Approach to Regression Analysis by Local Fitting, J. Am. Stat. Assoc., 83(403), 596–610, doi:10.1080/01621459.1988.10478639, 1988.

Commission Internationale du Bassin Congo-Oubangui-Sangha: Plan d'Action Stratégique, [online] Available from: http://www.cicos.info/siteweb/uploads/media/1.1._Amelioration_du_Plan_d_Action_Strategique__PAS_.pdf, 2007.

Descroix, L., Genthon, P., Amogu, O., Rajot, J.-L., Sighomnou, D. and Vauclin, M.: Change in Sahelian Rivers hydrograph: The case of recent red floods of the Niger River in the Niamey region, Glob. Planet. Change, 98-99, 18–30, doi:10.1016/j.gloplacha.2012.07.009, 2012.

Descroix, L., Bouzou, I., Genthon, P., Sighomnou, D., Mahe, G., Mamadou, I., Vandervaere, J.-P., Gautier, E., Faran, O., Rajot, J.-L., Malam, M., Dessay, N., Ingatan, A., Noma, I., Souley, K., Karambiri, H., Fensholt, R., Albergel, J. and Olivry, J.-C.:

Impact of Drought and Land – Use Changes on Surface – Water Quality and Quantity: The Sahelian Paradox, in Current Perspectives in Contaminant Hydrology and Water Resources Sustainability, edited by P. Bradley, pp. 243–271, InTech, Rijeka, Croatia., 2013.

Doherty, J.: PEST—Model-independent parameter estimation, User Manual, 5th ed., edited by W. N. Computing, Watermark Numerical Computing. [online] Available from: http://www.pesthomepage.org/files/pestman.pdf, 2005.

Durbin, J. and Watson, G.: Testing for serial correlation in least squares regression. I, Biometrika, 37(3-4), 409–428 [online] Available from: http://www.jstor.org/stable/2332325 (Accessed 10 March 2014), 1950.

Durbin, J. and Watson, G.: Testing for serial correlation in least squares regression. II, Biometrika, 38(1-2), 159–178 [online] Available from: http://www.jstor.org/stable/2332325 (Accessed 10 March 2014), 1951.

FAO: Drought Impact Mitigation and Prevention in the Limpopo River Basin: A Situation Analysis, FAO Sub-Regional Office for Southern and East Africa Harare., 2004.

FAO, IIASA, ISRIC, ISSC and JRC: Harmonized World Soil Database v 1.2, [online] Available from: http://webarchive.iiasa.ac.at/Research/LUC/External-World-soil-database/HTML/, 2012.

Faramarzi, M., Abbaspour, K. C., Ashraf Vaghefi, S., Farzaneh, M. R., Zehnder, A. J. B., Srinivasan, R. and Yang, H.: Modeling impacts of climate change on freshwater availability in Africa, J. Hydrol., 480, 85–101, doi:10.1016/j.jhydrol.2012.12.016, 2013.

Fekete, B. M., Vorosmarty, C. J. and Grabs, W.: Global, composite runoff fields based on observed river discharge and simulated water balances., Water System Analysis Group, University of New Hampshire, and Global Runoff Data Centre. Koblenz, Germany: Federal Institute of Hydrology (BfG), Koblenz, Germany., 1999.

Few, R., Brown, K. and Tompkins, E. L.: Public participation and climate change adaptation: avoiding the illusion of inclusion, Clim. Policy, 7(1), 46–59, doi:10.1080/14693062.2007.9685637, 2007.

Frenken, K. and Faurès, J. M.: Irrigation Potential in Africa: A Basin Approach, FAO, Rome. [online] Available from: https://books.google.de/books?id=VzqBfdeSjgQC&printsec, 1997.

Gebrehiwot, S. G., Seibert, J., Gärdenäs, A. I., Mellander, P.-E. and Bishop, K.: Hydrological change detection using modeling: Half a century of runoff from four rivers in the Blue Nile Basin, Water Resour. Res., 49(6), 3842–3851, doi:10.1002/wrcr.20319, 2013.

Giuntoli, I., Renard, B., Vidal, J.-P. and Bard, A.: Low flows in France and their relationship to large-scale climate indices, J. Hydrol., 482, 105–118, doi:10.1016/j.jhydrol.2012.12.038, 2013.

Hargreaves, G. H. and Samani, Z. A.: Estimating Potential Evapotranspiration, J. Irrig. Drain. Div., 108(3), 225–230 [online] Available from: http://cedb.asce.org/cgi/WWWdisplay.cgi?35047, 1982.

Harrigan, S., Murphy, C., Hall, J., Wilby, R. L. and Sweeney, J.: Attribution of detected changes in streamflow using multiple working hypotheses, Hydrol. Earth Syst. Sci. [online] Available from: http://eprints.maynoothuniversity.ie/4947/1/CM_Attribution.pdf (Accessed 20 January 2015), 2013.

Hastenrath, S., Polzin, D. and Mutai, C.: Diagnosing the Droughts and Floods in Equatorial East Africa during Boreal Autumn 2005–08, J. Clim., 23(3), 813–817, doi:10.1175/2009JCLI3094.1, 2010.

Hattermann, F., Kundzewicz, Z. W., Huang, S., Vetter, T., Kron, W., Burghoff, O., Merz, B., Bronstert, A., Krysanova, V., Gerstengarbe, F.-W., Werner, P. C. and Ylva, H.: Flood risk from a holistic perspective–observed changes in Germany, in Changes of flood risk in Europe, edited by Z. W. Kundzewicz, pp. 212–237, IAHS Press, Wallingford. [online] Available from: https://scholar.google.de/scholar?hl=en&as_sdt=0,5&q=flood+risk+holistic+hattermann#0 (Accessed 7 May 2015), 2012.

Hempel, S., Frieler, K., Warszawski, L., Schewe, J. and Piontek, F.: A trend-preserving bias correction – the ISI-MIP approach, Earth Syst. Dyn. Discuss., 4(1), 49–92, doi:10.5194/esdd-4-49-2013, 2013.

Huang, S., Krysanova, V. and Hattermann, F.: Projection of low flow conditions in Germany under climate change by combining three RCMs and a regional hydrological model, Acta Geophys., 61(1), 151–193 [online] Available from: http://link.springer.com/article/10.2478/s11600-012-0065-1 (Accessed 26 April 2015), 2013.

Hundecha, Y. and Merz, B.: Exploring the relationship between changes in climate and floods using a model-based analysis, Water Resour. Res., 48(4), n/a–n/a, doi:10.1029/2011WR010527, 2012.

Hurtt, G. C., Chini, L. P., Frolking, S., Betts, R. a., Feddema, J., Fischer, G., Fisk, J. P., Hibbard, K., Houghton, R. a., Janetos, a., Jones, C. D., Kindermann, G., Kinoshita, T., Klein Goldewijk, K., Riahi, K., Shevliakova, E., Smith, S., Stehfest, E., Thomson, a., Thornton, P., van Vuuren, D. P. and Wang, Y. P.: Harmonization of land-use scenarios for the period 1500-2100: 600 years of global gridded annual land-use transitions, wood harvest, and resulting secondary lands, Clim. Change, 109(1-2), 117–161, doi:10.1007/s10584-011-0153-2, 2011.

IPCC-TGICA: General Guidelines on the Use of Scenario Data for Climate Impact and Adaptation Assessment. Version 2., 2007.

Jarvis, a, Reuter, H. I., Nelson, a and Guevara, E.: Hole-filled seamless SRTM data V4, Int. Cent. Trop. Agric., available from http://srtm.csi.cgiar.org [online] Available from: http://srtm.csi.cgiar.org/ (Accessed 13 January 2015), 2008.

Jury, M. R.: A return to wet conditions over Africa: 1995–2010, Theor. Appl. Climatol., 111(3-4), 471–481, doi:10.1007/s00704-012-0677-z, 2013.

Kandji, S. T., Verchot, L. and Mackensen, J.: Climate change and variability in the Sahel region: Impacts and adaptation strategies in the agricultural sector, Nairobi, Kenya. [online] Available from: http://www.unep.org/Themes/Freshwater/Documents/pdf/ClimateChangeSahelCombine.pdf (Accessed 23 January 2015), 2006.

Kim, H.: GSWP3, Glob. Soil Wetness Proj. Phase 3, Surf. Meteorol., 1 [online] Available from: http://hydro.iis.u-tokyo.ac.jp/GSWP3/exp1.html (Accessed 24 April 2015), 2014.

Klein Goldewijk, K., Beusen, A. and Janssen, P.: Long-term dynamic modeling of global population and built-up area in a spatially explicit way: HYDE 3.1, The Holocene, 20(4), 565–573, doi:10.1177/0959683609356587, 2010.

Klein Goldewijk, K., Beusen, A., Van Drecht, G. and De Vos, M.: The HYDE 3.1 spatially explicit database of human-induced global land-use change over the past 12,000 years, Glob. Ecol. Biogeogr., 20(1), 73–86, doi:10.1111/j.1466-8238.2010.00587.x, 2011.

Koch, H., Liersch, S. and Hattermann, F. F.: Integrating water resources management in eco-hydrological modelling, Water Sci. Technol., 67(7), 1525, doi:10.2166/wst.2013.022, 2013.

Köppen, W.: Das geographische System der Klimate, in Handbuch der Klimatologie., edited by W. Köppen and R. Geiger, p. 44, Gebrüder Borntraeger, Berlin., 1936.

Krysanova, V., Meiner, A., Roosaare, J. and Vasilyev, A.: Simulation modelling of the coastal waters pollution from agricultural watershed, Ecol. Modell., 49(1), 7–29 [online] Available from: http://www.sciencedirect.com/science/article/pii/0304380089900410, 1989.

Krysanova, V., Müller-Wohlfeil, D.-I. and Becker, A.: Development and test of a spatially distributed hydrological/water quality model for mesoscale watersheds, Ecol. Modell., 106(2–3), 261–289, doi:10.1016/S0304-3800(97)00204-4, 1998.

Krysanova, V., Arnold, J. G., Wechsung, F., Srinivasan, R. and Williams, J.: SWIM (Soil and Water Integrated Model) Users Manual, Potsdam Institute for Climate Impact Research, Potsdam, Germany., 2000.

Krysanova, V., Hattermann, F. and Wechsung, F.: Development of the ecohydrological model SWIM for regional impact studies and vulnerability assessment, Hydrol. Process., 19(3), 763–783 [online] Available from: http://onlinelibrary.wiley.com/doi/10.1002/hyp.5619/abstract, 2005.

LBPTC, L. B. P. T. C.: Joint Limpopo River Basin Study Scoping Phase. Final Report, 2010.

Liersch, S., Cools, J., Kone, B., Koch, H., Diallo, M., Reinhardt, J., Fournet, S., Aich, V. and Hattermann, F. F.: Vulnerability of rice production in the Inner Niger Delta to water resources management under climate variability and change, Environ. Sci. Policy, 34, 8–33, doi:10.1016/j.envsci.2012.10.014, 2013.

Mahe, G., Lienou, G., Descroix, L., Bamba, F., Paturel, J. E., Laraque, A., Meddi, M., Habaieb, H., Adeaga, O., Dieulin, C., Chahnez Kotti, F. and Khomsi, K.: The rivers of Africa: witness of climate change and human impact on the environment, Hydrol. Process., 27(15), 2105–2114, doi:10.1002/hyp.9813, 2013.

Mahé, G.: Surface/groundwater interactions in the Bani and Nakambe rivers, tributaries of the Niger and Volta basins, West Africa, Hydrol. Sci. J., 54(4), 704–712, doi:10.1623/hysj.54.4.704, 2009.

Mediero, L., Santillán, D., Garrote, L. and Granados, A.: Detection and attribution of trends in magnitude, frequency and timing of floods in Spain, J. Hydrol., 517, 1072–1088, doi:10.1016/j.jhydrol.2014.06.040, 2014.

Merz, B., Vorogushyn, S., Uhlemann, S., Delgado, J. and Hundecha, Y.: HESS Opinions "More efforts and scientific rigour are needed to attribute trends in flood time series," Hydrol. Earth Syst. Sci. Discuss., 16, 1379–1387, doi:10.5194/hessd-16-1379-2012, 2012.

Mngutyo, A.: An Investigation of the Influence of the Flooded Household Environments on Maternal Health of Flood Plain Dwellers in Makurdi, OIDA Int. J. Sustain. Dev., 4(8), 29–38 [online] Available from: http://papers.ssrn.com/sol3/papers.cfm?abstract_id=2131849, 2012.

Moriasi, D. and Arnold, J.: Model evaluation guidelines for systematic quantification of accuracy in watershed simulations, Trans. …, 50(3), 885–900, doi:10.13031/2013.23153, 2007.

Murphy, C., Harrigan, S., Hall, J. and Wilby, R. L.: Climate-driven trends in mean and high flows from a network of reference stations in Ireland, Hydrol. Sci. J., 58(4), 755–772, doi:10.1080/02626667.2013.782407, 2013.

Murwira, A. and Yachan, A.: Limpopo Basin Strategic Plan for Reducing Vulnerability to Floods and Droughts. Draft for Discussion with Riparian Governments. UN-HABITAT/UNEP, Manager, (July), 25 [online] Available from: http://scholar.google.de/, 2007.

Nash, J. E. and Sutcliffe, J. V.: River flow forecasting through conceptual models part I — A discussion of principles, J. Hydrol., 10(3), 282–290, doi:10.1016/0022-1694(70)90255-6, 1970.

Niger Basin Authority: NIGER-HYCOS, [online] Available from: http://nigerhycos.abn.ne/ (Accessed 1 March 2012), 2008.

Niger Basin Authority, (NBA): Elaboration of an Action Plan for the Sustainalble Development of the Niger Basin. Phase 2: Master Plan for the Development and Managment, Niamey, Niger., 2007.

Nobert, J. and Jeremiah, J.: Hydrological Response of Watershed Systems to Land Use/Cover Change. A Case of Wami River Basin, Open Hydrol. J., 6(1) [online] Available from: http://benthamopen.com/ABSTRACT/TOHYDJ-6-78 (Accessed 24 April 2015), 2012.

NWP: Summary note of the Nairobi work programme on impacts, vulnerability and adaptation to climate change, UNFCC, Durban, South Africa. [online] Available from: http://unfccc.int/adaptation/workstreams/nairobi_work_programme/items/3633.php, 2011.

Nyeko, M., D'Urso, G. and Immerzeel, W. W.: Adaptive simulation of the impact of changes in land use on water resources in the lower Aswa basin, J. Agric. Eng., 43(4), 24, doi:10.4081/jae.2012.e24, 2013.

Ogilvie, A., Mahé, G., Ward, J., Serpantié, G., Lemoalle, J., Morand, P., Barbier, B., Diop, A. T., Caron, A., Namarra, R., Kaczan, D., Lukasiewicz, A., Paturel, J.-E., Liénou, G. and Clanet, J. C.: Water, agriculture and poverty in the Niger River basin, Water Int., 35(5), 594–622 [online] Available from: http://www.tandfonline.com/doi/abs/10.1080/02508060.2010.515545 (Accessed 11 November 2013), 2010.

Oguntunde, P. G. and Abiodun, B. J.: The impact of climate change on the Niger River Basin hydroclimatology, West Africa, Clim. Dyn., 40(1-2), 81–94, doi:10.1007/s00382-012-1498-6, 2013.

Panthou, G., Vischel, T., Lebel, T., Blanchet, J., Quantin, G. and Ali, A.: Extreme rainfall in West Africa: A regional modeling, Water Resour. Res., 48(8), doi:10.1029/2012WR012052, 2012.

Panthou, G., Vischel, T. and Lebel, T.: Recent trends in the regime of extreme rainfall in the Central Sahel, Int. J. Climatol., doi:10.1002/joc.3984, 2014.

Prosdocimi, I., Kjeldsen, T. R. and Svensson, C.: Non-stationarity in annual and seasonal series of peak flow and precipitation in the UK, Nat. Hazards Earth Syst. Sci., 14(5), 1125–1144, doi:10.5194/nhess-14-1125-2014, 2014.

Ramankutty, N.: Croplands in West Africa: A Geographically Explicit Dataset for Use in Models, Earth Interact., 8(23), 1–22, doi:10.1175/1087-3562(2004)8<1:CIWAAG>2.0.CO;2, 2004.

Richardson, K., Steffen, W. and Liverman, D.: Climate change: Global risks, challenges and decisions, Cambridge University Press. [online] Available from: Richardson, K., Steffen, W. and Liverman, D.: Climate change: Global risks, challenges and decisions, Cambridge University Pres, 2011.

Ritchie, J.: Model for predicting evaporation from a row crop with incomplete cover, Water Resour. Res., 8(5), 1204–1213 [online] Available from: http://onlinelibrary.wiley.com/doi/10.1029/WR008i005p01204/full (Accessed 26 April 2015), 1972.

Rogelj, J., Meinshausen, M. and Knutti, R.: Global warming under old and new scenarios using IPCC climate sensitivity range estimates, Nat. Clim. Chang., 2(4), 248–253, doi:10.1038/nclimate1385, 2012.

Salman, S. M. A.: The Nile Basin Cooperative Framework Agreement: a peacefully unfolding African spring?, Water Int., 38(1), 17–29, doi:10.1080/02508060.2013.744273, 2013.

Schreider, S. Y., Jakeman, A. J., Letcher, R. A., Nathan, R. J., Neal, B. P. and Beavis, S. G.: Detecting changes in streamflow response to changes in non-climatic catchment conditions: farm dam development in the Murray–Darling basin, Australia, J. Hydrol., 262(1-4), 84–98, doi:10.1016/S0022-1694(02)00023-9, 2002.

Seibert, J. and McDonnell, J. J.: Land-cover impacts on streamflow: a change-detection modelling approach that incorporates parameter uncertainty, Hydrol. Sci. J., 55(3), 316–332, doi:10.1080/02626661003683264, 2010.

Sen, P.: Estimates of the regression coefficient based on Kendall's tau, J. Am. Stat. Assoc., 63(324), 1379–1389 [online] Available from: http://amstat.tandfonline.com/doi/abs/10.1080/01621459.1968.10480934 (Accessed 10 March 2014), 1968.

Shahin, M.: Hydrology and Water Resources of Africa, Springer Science & Business Media. [online] Available from: https://books.google.com/books?id=MmjjBwAAQBAJ&pgis=1 (Accessed 26 August 2015), 2006.

Sheffield, J., Goteti, G. and Wood, E. F.: Development of a 50-year high-resolution global dataset of meteorological forcings for land surface modeling, J. Clim., 19(13), 3088–3111, doi:10.1175/JCLI3790.1, 2006.

Solomon, S., Qin, D., Manning, M., Alley, R. B., Berntsen, T., Bindoff, N. L., Chen, Z., Chidthaisong, A., Gregory, J. M. and Hegerl, G. C.: Climate change 2007: The physical science basis, contribution of working group 1 to the fourth assessment report of the Intergovernmental Panel on Climate Change, [online] Available from: http://www.esrl.noaa.gov/search/publications/3792/, 2007.

Strahler, A. H.: Introducing Physical Geography, Wiley. [online] Available from: https://books.google.de/books?vid=ISBN9781118396209&redir_esc=y (Accessed 26 August 2015), 2013.

Strömqvist, J., Arheimer, B., Dahné, J., Donnelly, C. and Lindström, G.: Water and nutrient predictions in ungauged basins: set-up and evaluation of a model at the national scale, Hydrol. Sci. J., 57, 229–247, doi:10.1080/02626667.2011.637497, 2012.

Strzepek, K. and McCluskey, A.: The impacts of climate change on regional water resources and agriculture in Africa, World Bank Policy Res. Work. Pap., (4290) [online] Available from: http://papers.ssrn.com/sol3/papers.cfm?abstract_id=1004404, 2007.

Tarhule, A.: Damaging Rainfall and Flooding: The Other Sahel Hazards, Clim. Change, 72, 355–377, doi:10.1007/s10584-005-6792-4, 2005.

Theil, H.: A rank-invariant method of linear and polynomial regression analysis, Ned. Acad. Wetensch. Proc, 53, 386–392 [online] Available from: http://link.springer.com/chapter/10.1007/978-94-011-2546-8_20 (Accessed 10 March 2014), 1950.

Tschakert, P., Sagoe, R., Ofori-Darko, G. and Codjoe, S. N.: Floods in the Sahel: an analysis of anomalies, memory, and anticipatory learning, Clim. Change, 103(3-4), 471–502, doi:10.1007/s10584-009-9776-y, 2010.

Tshimanga, R. M.: Hydrological uncertainty analysis and scenario-based streamflow modelling for the Congo River Basin, Rhodes University, South Africa. [online] Available from: http://agris.fao.org/agris-search/search.do?recordID=AV2012089066 (Accessed 26 August 2015), 2012.

Tshimanga, R. M. and Hughes, D. A.: Climate change and impacts on the hydrology of the Congo Basin: The case of the northern sub-basins of the Oubangui and Sangha Rivers, Phys. Chem. Earth, Parts A/B/C, 50–52, 72–83, doi:10.1016/j.pce.2012.08.002, 2012.

UN: Water in a changing world, The United Nations World Water Development Report 3, World Water Assess. Program. [online] Available from: http://webworld.unesco.org/water/wwap/wwdr/wwdr3/tableofcontents.shtml, 2009.

Vetter, T., Huang, S., Aich, V., Yang, T., Wang, X., Krysanova, V. and Hattermann, F.: Multi-model climate impact assessment and intercomparison for three large-scale river basins on three continents, Earth Syst. Dyn., 6(1), 17–43, doi:10.5194/esd-6-17-2015, 2015.

Villarini, G. and Strong, A.: Roles of climate and agricultural practices in discharge changes in an agricultural watershed in Iowa, Agric. Ecosyst. Environ., 188, 204–211, doi:10.1016/j.agee.2014.02.036, 2014.

Vorogushyn, S. and Merz, B.: What drives flood trends along the Rhine River: climate or river training?, Hydrol. Earth Syst. Sci. Discuss., 9(12), 13537–13567, doi:10.5194/hessd-9-13537-2012, 2012.

Van Vuuren, D. P., Stehfest, E., Elzen, M. G. J., Kram, T., Vliet, J., Deetman, S., Isaac, M., Klein Goldewijk, K., Hof, A., Mendoza Beltran, A., Oostenrijk, R. and Ruijven, B.: RCP2.6: exploring the possibility to keep global mean temperature increase below 2°C, Clim. Change, 109(1-2), 95–116, doi:10.1007/s10584-011-0152-3, 2011a.

Van Vuuren, D. P., Edmonds, J., Kainuma, M., Riahi, K., Thomson, A., Hibbard, K., Hurtt, G. C., Kram, T., Krey, V. and Lamarque, J.-F.: The representative concentration

pathways: an overview, Clim. Change, 109(1-2), 5–31 [online] Available from: http://link.springer.com/article/10.1007/s10584-011-0148-z, 2011b.

weADAPT: weADAPT 4.0, Climate adaptation planning, research and practice, [online] Available from: https://weadapt.org/ (Accessed 21 January 2015), 2015.

Weedon, G. P., Gomes, S., Viterbo, P., Shuttleworth, W. J., Blyth, E., Österle, H., Adam, J. C., Bellouin, N., Boucher, O. and Best, M.: Creation of the WATCH Forcing Data and Its Use to Assess Global and Regional Reference Crop Evaporation over Land during the Twentieth Century, J. Hydrometeorol., 12(5), 823–848, doi:10.1175/2011JHM1369.1, 2011.

Wendling, U. and Schellin, H.: Neue Ergebnisse zur Berechnung der potentiellen Evapotranspiration, Zeitschrift für Meteorol., 36(3), 214–217 [online] Available from: http://cat.inist.fr/?aModele=afficheN&cpsidt=8792552 (Accessed 26 April 2015), 1986.

Wesselink, A. J., Orange, D. and Feizouré, C. T.: Les régimes hydroclimatiques et hydrologiques d'un bassin versant de type tropical humide: l'Oubangui (République Centrafricaine), vol. 238, edited by P. Chevallier and B. Pouyaud, pp. 179–194, IAHS Publication, Wallingford, UK. [online] Available from: http://books.google.de/books?hl=de&lr=&id=azUCAebIN-YC&oi=fnd&pg=PA179&dq=, 1996.

WFD: EU WATCH - Home, [online] Available from: http://eu-watch.org/templates/dispatcher.asp?page_id=25222705, 2011.

Williams, J. R., Renard, K. G. and Dyke, P. T.: EPIC: A new method for assessing erosion's effect on soil productivity, J. Soil Water Conserv., 38(5), 381–383 [online] Available from: http://www.jswconline.org/content/38/5/381.short (Accessed 26 April 2015), 1983.

De Wit, M. and Stankiewicz, J.: Changes in surface water supply across Africa with predicted climate change, Science (80-.)., 311(5769), 1917–1921 [online] Available from: http://www.sciencemag.org/content/311/5769/1917.short, 2006.

WOCAT: World Overview of Conservation Approaches and Technologies, [online] Available from: https://www.wocat.net/ (Accessed 21 January 2015), 2015.

WRDC: World Radiation Data Centre, [online] Available from: http://wrdc-mgo.nrel.gov/, 2000.

Yue, S., Pilon, P., Phinney, B. and Cavadias, G.: The influence of autocorrelation on the ability to detect trend in hydrological series, Hydrol. Process., 16(9), 1807–1829, doi:10.1002/hyp.1095, 2002.

Zhu, T. and Ringler, C.: Climate Change Impacts on Water Availability and Use in the Limpopo River Basin, Water, 4(4), 63–84, doi:10.3390/w4010063, 2012.

7. FLOOD PROJECTIONS FOR THE NIGER RIVER BASIN CONSIDERING FUTURE LAND USE AND CLIMATE CHANGE

Valentin Aich [1,*], Stefan Liersch [1], Tobias Vetter [1], Samuel Fournet [1], Jafet C.M. Andersson [2], Sandro Calmanti [3], Frank H.A. van Weert [4], Fred F. Hattermann [1], Eva N. Müller [5]

[1] Potsdam Institute for Climate Impact Research (PIK), Potsdam, Germany

[2] Swedish Meteorological and Hydrological Institute (SMHI), Norrköping, Sweden

[3] Italian National Agency for New Technologies, Energy and Sustainable Economic Development (ENEA), Roma , Italy

[4] Wetlands International (WI), Wageningen, The Netherlands

[5] Institute of Earth and Environmental Science, University of Potsdam, Potsdam, Germany

* Corresponding author: Valentin Aich

Journal: Science of the Total Environment (Sc. Total Environ.)
Status: Submitted

Abstract: This study assesses future flood risk in the Niger River basin considering for the first time simultaneously the effects of projected climate change and land use changes. For this purpose, an eco-hydrological process-based model (SWIM) was set-up and validated for past climate and land-use dynamics for the entire Niger basin. Model runs for future flood risks were driven with an ensemble of 18 climate models, 13 of them dynamically downscaled from the CORDEX Africa project and 5 of them statistically downscaled Earth System Models. Two climate (Representative Concentration Pathways 4.5 and 8.5) and two land use change scenarios (Harmonized Global Land Use scenarios 4.5 and 8.5 (Hurtt et al., 2011)) were used to cover a broad range of potential developments in the region. Two flood indicators (annual 90th percentile and the 20-year return flood) were used to assess the future flood risk for four sub-catchments of the Niger basin, representing the Upper, the Middle and the Lower Niger as well as the Benue region. The modelling results show generally increases of flood magnitudes when comparing a scenario period in the near future (2021-2050) with a base period of 1976-2005. Land use effects are more uncertain but trends and relative changes for the different catchments of the Niger basin seem robust. The dry areas of the Sahelian and Sudanian region of the basin show a particularly high sensitivity against climatic and land use changes, with a partly alarming increase of flood magnitudes. A scenario with continuing transformation of natural vegetation into agricultural land and urbanization intensifies the flood risk in all parts of the Niger basin while a "regreening" scenario can reduce flood magnitudes to some extent. Yet, land use change effects were smaller when compared relatively to the effects of climate change. In the face of the already existing adaptation deficit to catastrophic flooding in the region, the authors argue for a mix of adaptation but also mitigation efforts in order to reduce the flood risk in the Niger River basin.

Graphical abstract:

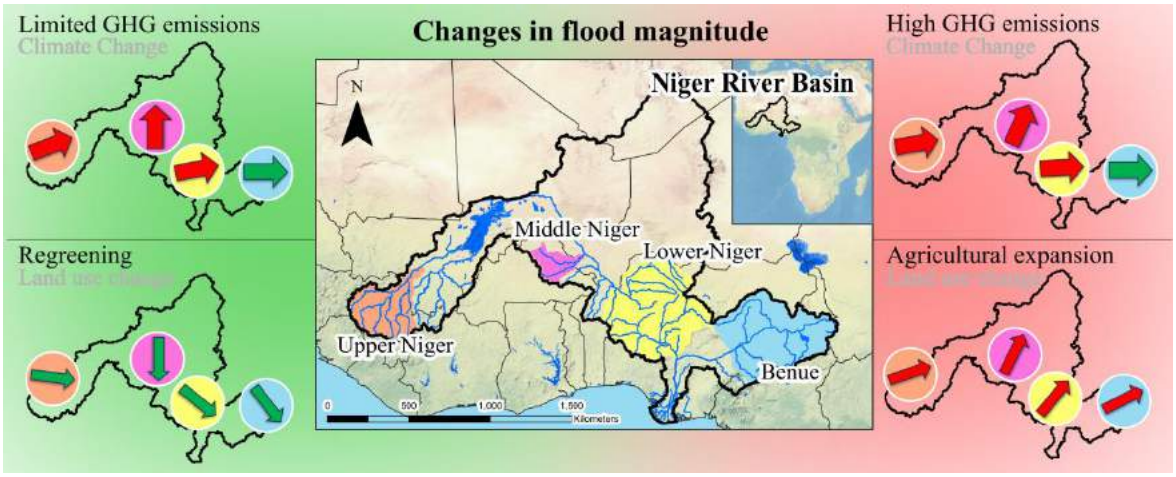

Projected changes in flood magnitudes in the Niger River Basin between a near future period (2021-2050) and the base period (1976-2005), modelled with an eco-hydrological model (SWIM) and driven with 18 Regional Climate projections. The results of a limited emission (RCP 4.5) (top left) and a high emission (RCP 8.5) (top right) scenario are depicted as medians of 18 runs for each sub-region as arrow, with red for increasing and green for decreasing trends. The angles of the arrows are relative to the highest increase (Middle Niger limited emission: +30.4% ≙ 90°). For land use and land cover changes a regreening scenario (bottom left) and a businesses as usual scenario (bottom right) with strong agricultural expansion are depicted as changes from the mean of both climate scenarios. The angles of the arrows are relative to the highest decrease (Middle Niger regreening: -21.2% ≙ -90°). This means, that in the Middle Niger, the increase of the climate scenarios is reduced by 21.2% under a regreening scenario and raised by 14.9% (14.9% ≙63.3°) in a business as usual scenario with agricultural intensification.

Highlights:

- Modelling suggests increased floods of the Niger for future climate and land-use
- Dry areas of the Sahelian and Sudanian region show a particularly high sensitivity
- Projections for climate and land-use change result in diametrical impacts
- Modelled land-use change effects were smaller than climatic effects
- Ecohydrological modelling is a valuable tool to disentangle the impacts and drivers

Keywords: Niger, Floods, Land use change, Climate Change, eco-hydrological modelling, Cordex

7.1. Introduction

Catastrophic flooding in the Niger River Basin (NRB) is increasingly perceived as a major threat, affecting people in the order of magnitudes of millions (Aich et al., 2014b; Tarhule, 2005; Tschakert et al., 2010). Simultaneous increasing vulnerability, population growth and discharges in absolute terms were identified as reasons for this enlarged flood risk (e.g. Aich et al., 2014a; Descroix et al., 2012; Di Baldassarre et al., 2010). A study of Jury (2013) for the entire Sub-Saharan African region found a general return to wetter conditions, when looking on streamflows during the last decades, including the Niger River. More specifically for the Niger River, Tarhule et al., (2015) found increasing flows in all parts since the extremely dry period of the 1970s and 1980s. However, for most regions of the NRB, the water levels do not reach the levels that have been observed before this dry period (e.g. Paturel et al., 2003). Hydrological projections for the West African region have recently been reviewed by Roudier et al. (2014). For the NRB, they found a tendency for increasing river flows with a mean increase among all studies above 5 %, however, with a strong variability and a strong spatial heterogeneity. Roudier et al. (2014) concluded that there is a general agreement on the high vulnerability to climate change for this region. However this vulnerability analysis lacks of projections of future floods. In addition, they state that there is an urgent need to take into account the other factors influencing runoff, especially water and land use changes, in order to acquire a more comprehensive flood risk assessment. Especially for the drier parts of the basin, in the Sahelian Zone, Amogu et al. (2010) and Descroix et al. (2013) and Séguis et al. (2004) identified Land Use Land Cover (LULC) change as the main driver of the increasing flood magnitudes. To assess these past changes, Aich et al. (2015) used a modelling attribution approach to quantify the share of LULC change and climatic variability on the recent flood increases and concluded that LULC and climatic changes have approximately equal shares on the flood increase. Future flood projections for the NRB should therefore include both drivers, climate and LULC, in order to support the elaboration of sound flood mitigation and adaptation strategies.

The study intends to assess this research gap by addressing the research question on how will flood magnitudes in the Niger basin evolve under the influence of expected climatic changes and LULC changes? In order to answer this question, projected changes in LULC and climate dynamics are analyzed first, and based on these scenarios, a process-based, ecohydrological model is employed to assess future high flows. For the climate and LULC projections, respectively, two specific scenarios were selected: one ‘optimistic’ scenario, which is based on a globally limited Green House Gas (GHG) emissions (Representative Concentration Pathways (RCP) 4.5) and conservational land management; and the ‘pessimistic’ scenario (RCP 8.5), which assumes business as usual, with increasing emissions, economically focused land management and further expansion of agricultural land. Due to the huge extent and the diversity of the study area, four different example

regions of the Niger basin are analyzed (Figure 56). The projections concentrate on the near-future period of 2021-2050, because of its specific relevance for adaption measures. In particular, the near future period considered for the analysis corresponds approximately to the occurrence of +2 °C global warming with respect to the pre-industrial period. The +2 °C global warming is still considered a critical guidance for mitigation strategies, in order to avoid the most severe socio-economic impacts of climate change. The results are being discussed and interpreted, taking into account the uncertainties. Finally, implications for the management of future flood risks in the NRB are discussed.

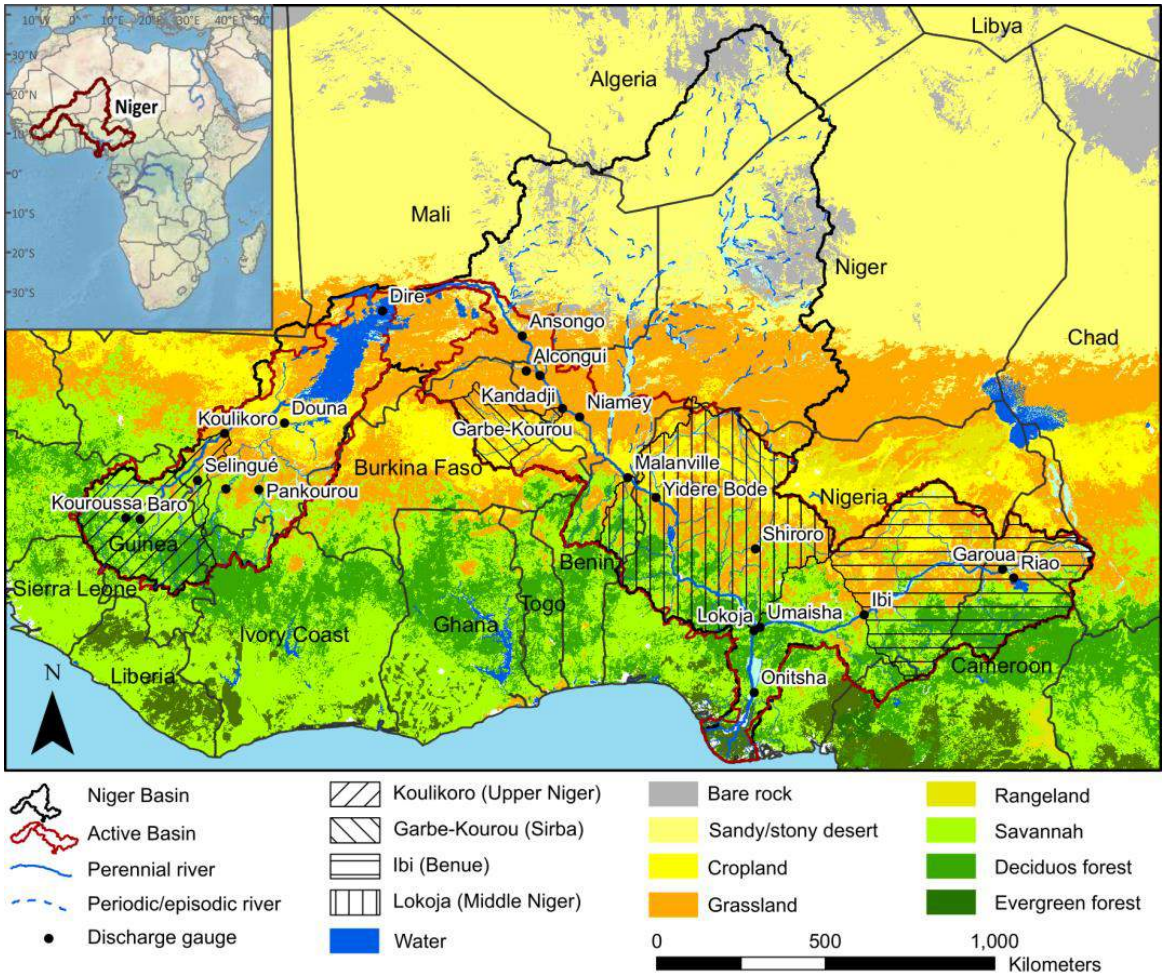

Figure 56: Overview map with four focus sub-regions and land use and land cover of 2005.

7.2. Materials and Methods

7.2.1. Study area

The NRB in West Africa covers an area of approximately 2,156,000 km², of which only approximately 1,270,000 km² contribute to the river discharge (Figure 56). Guinea, Ivory Coast, Mali, Burkina Faso, Benin, Niger, Chad, Cameroon and Nigeria fall within this

active basin. These countries are members of the Niger Basin Authority (NBA), an intergovernmental body which coordinates the management and development of the Niger Basin water resources, including the development and implementation of a joint flood policy.

The basin comprises sub-regions with very different hydrographic and/or climatic conditions: The Upper, the Middle and the Lower Niger Basins (UNB, MNB, LNB), the Benue and the Niger Delta all have individual topographic and drainage characteristics. This study focuses on exemplary catchments in all sub-regions but the Delta (Table 15). Discharge data of individual catchments in the LNB was not available for the study. The drainage area of the analyzed gauge Lokoja in the LNB comprises the other sub-regions. In the UNB, headwaters of the Niger arise on low-altitude plateaus with annual precipitation of up to over 1,500 mm (all precipitation magnitudes derived from Hijmans et al. 2005). These headwaters flow into the Inner Niger Delta (IND), a vast wetland. The catchment until the gauging station Koulikoro (approximately 120,800 km²) has been selected to represent the discharge in the UNB.

The MNB is the driest sub-region of the NRB and ranges from the IND to the border of Nigeria, including the Sahel and the northern part of the Sudan zone of the basin. The climate is arid to semiarid with strongly annually varying precipitation, ranging from average 300 mm in the North to 1,000 mm in the South. Most of the inflow in this area comes from the plateaus of the Right-Bank sub-basins. The basin of the Sirba River until the gauging station Garbe-Kourou (approximately 39,000 km²) was selected as a sample catchment for this sub-region.

The LNB ranges from the Nigerian border to the confluence of the Niger and the Benue at Lokoja. The climate in this region is wetter than in the MNB with average precipitation between 1,000 mm and 1,500 mm. Although the Benue River also influences it, the station of Lokoja has been selected to represent this sub-basin, because there was no other gauging station available for this section of the Niger basin. This region has an extent of approximately 289,900 km² without the Benue basin.

The basin of the Benue in the East of the Niger basin is the largest tributary in terms of discharge. Its headwaters are on the north slope of the Adamawa Plateau in Cameroon and the annual precipitation ranges from 750 mm in the North to over 1,500 mm in the South. For this basin, the station Ibi was selected with an approximate drainage area of 264,000 km².

Finally the Niger discharges into the Gulf of Guinea forming the Niger Delta, which is not part of this study. The Niger basin is described in more detail in Andersen et al. 2005.

Table 15: Hydrological parameters for catchments. Values for precipitation are derived from the PGFv2 dataset and discharges are modelled outputs using the same climate input, bot during the base period (1976-2005).

	Koulikoro catchment (UNB)	Garbe-Kourou catchment (MNB)	Lower Niger Basin	Ibi catchment (Benue)
Average annual discharge in m³/s	1,177	46	5,577 (with Inflow from other areas)	2,039
Average annual rainfall in mm	1,439	556	975	1,177
Area in km²	120,821	39,038	289,941	263,962
Runoff coefficient	21 %	6 %	NA: Inflow from other areas	20 %

7.2.2. Data

7.2.2.1. Climate Data

In West-Africa, meteo-station data is rare and the spatial coverage coarse. Hence, reanalyzed climate data from the second version of the Global Meteorological Forcing Dataset for land surface modeling of Princeton University (PGFv2) (Sheffield et al., 2006) has been used for the calibration and validation of the eco-hydrological model. It contains all relevant climatic forcing parameters of the model on a 0.5°x0.5° grid and on a daily basis (mean, maximum and minimum temperature, humidity, precipitation, short wave downwelling radiation (rsds, after the standard naming adopted in climate model output)). The performance of this data set has been tested by interpolating and comparing it to observed station data by Aich et al. (2015) for the MNB and showed in general satisfying results. In order to check the suitability of PGFv2 for all four sub-regions and to estimate the uncertainty, it was compared to other reanalysis datasets (Figure 57). Annual precipitation, mean temperature and rsds have therefore been analyzed from the WATCH Forcing Data 20th Century (WATCH): 1950–2001 (Weedon et al., 2011), from the WATCH-Forcing-Data-ERA-Interim (WFDEI): 1979-2012 (Weedon et al., 2014) and from the reanalysis data set of from the Global Soil Wetness Project Phase 3 (GSWP3): 1950-2010 (Kim, 2014). The comparison showed generally a strong agreement of all datasets for all regions beside exceptions for the heavy precipitation (Figure 57, Supplementary material). Heavy precipitation is higher for PGFv2 and WATCH compared to GSWP3 and WFDEI. Another exception is rsds of the WATCH data-set, which is between 300 W/m² and 500 W/m² lower than for the other three data-sets in three of the four regions. Only in the MNB, WATCH is on the same level as PGFv2.

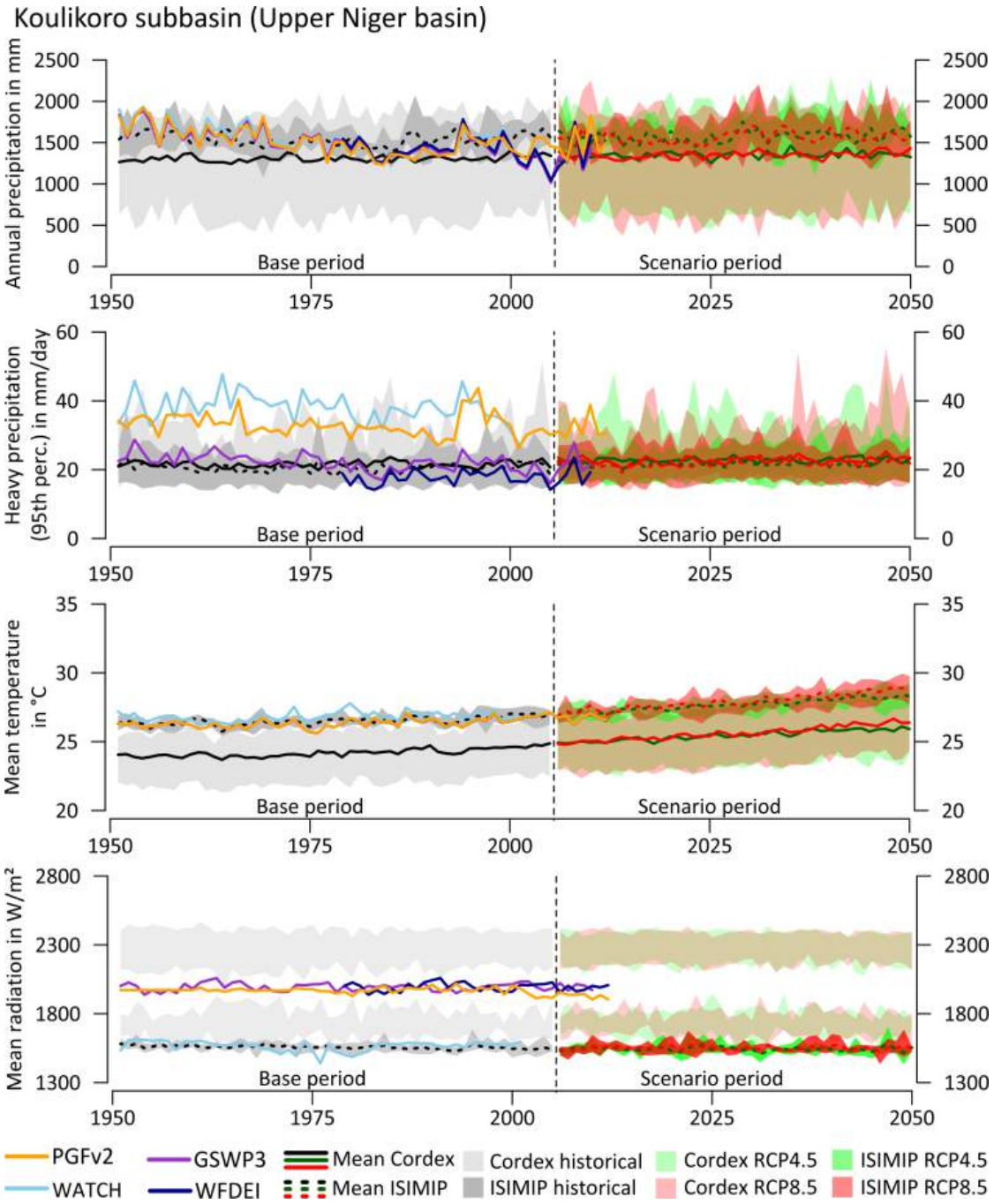

Figure 57: Annual precipitation, mean temperature and mean short wave downwelling radiation for the Koulikoro catchment in the Upper Niger Basin with four reanalysis datasets (PGFv2: 1950-2012, GSWP3: 1950-2010, WATCH: 1950-2001, WFDEI: 1979-2012), and climate scenarios for the base and the future period of five ISIMIP models and 13 CORDEX Africa GCM-RCM combinations for RCP 4.5 and RCP 8.5.

In order to have a broad spectrum of climate scenarios, dynamically and statistically downscaled climate models have been applied in the study (Table 16). Five Earth System Models (ESM) from the Coupled Model Intercomparison Project Phase 5 (CMIP-5), available in a bias corrected version, have been selected as statistically downscaled

models. Since they have been provided in the context of the Inter-Sectoral Impact Model Intercomparison Project, this ensemble is further on referred to as ISIMIP. The five chosen ESMs have been resampled on a 0.5°×0.5° grid and have been downscaled using a trend-preserving bias correction method to the WATCH reanalysis data (Hempel et al., 2013). Since the WATCH data set has been used for the bias-correction and showed significantly lower rsds values than the PGFv2 data-set for most of the region, also the bias-corrected ESMs show this deviation (Figure 57). Therefore rsds of the statistically downscaled climate scenarios have been neglected and instead, rsds was calculated applying the method of Hargreaves and Samani (1982). This led to similar radiation values compared to the other data-sets. These statistically ISIMIP models have been used for several impact studies in Africa and also the NRB (e.g. Aich et al., 2014; Vetter et al., 2015)

As dynamically downscaled climate scenarios, 13 ESM-Regional Climate Model (RCM) combinations from the Coordinated Regional Downscaling Experiment for Africa (CORDEX Africa) have been applied (Hewitson et al., 2012; Jones et al., 2011). This data is available on a 0.5°×0.5° grid with all necessary parameters. This data is regularly used for regional impact studies in Africa. Validations for their performance in West Africa, show a general capability of all models to simulate the basic regional climate system (Andersson et al., 2014; Kim et al., 2013; Nikulin et al., 2012). Nevertheless, rsds data for these climate model simulations are problematic. The values for rsds of the CORDEX runs show a strong bias compared to the reanalysis data. Some models are higher and some are lower and none is in the same magnitude then the reanalysis. Bias-correction of the parameters is an option, but it produces significant and strongly dis-homogeneous distortion of the climate signal produced by each model simulation. Therefore, we choose the raw climate model data as an input to the hydrological model. As a consequence we will need to explicitly discuss the range of uncertainties related to this modeling strategy (Chapter 7.4.1).

For the statistically as well as for the dynamically downscaled climate simulations, two different

RCPs have been applied: RCP 4.5 and RCP 8.5. Differently from the projections described in the previous Special Report on Emission Scenarios (SRES) (Nakicenovic and Swart, 2000), RCPs do not imply a unique framework for evaluating the impact of socio-economic assumptions such as population growth, economic development and technology. Instead, each RCP is the result of a different set of modelling assumption such that the scenarios are not directly comparable. However, they have been defined in order to span a significant range of radiative forcing scenarios. Each RCP is named after the level of additional radiative forcing achieved by 2100, with respect to the pre-industrial value. For example, the RCP 4.5 adopted in this study corresponds to a low stabilization scenario, whereby in 2100 the radiative forcing is 4.5 W above the pre-industrial level. On the other

hand, the RCP 8.5 corresponds to a high end stabilization scenario, mainly driven by a sustained population growth, whereby in 2100 the radiative forcing is 8.5 W above the pre-industrial level. The RCP 4.5 corresponds likely to a warming between 1.1 °C to 2.6 °C increase of global temperature above the pre-industrial level until the end of this century and the RCP 8.5 to a likely increase of 2.6 °C to 4.8 °C (IPCC, 2013).

In order to check the ability of the climate models to reproduce the climate, that leads to the typical discharge regime for each catchment, the modelled annual regime driven with the historical simulations of the CORDEX Africa and the ISIMIP models have been compared with a run driven be the reanalysis PGVf2 (see supplementary). Some of the climate models did not result in satisfactory discharges or even show completely wrong patterns. However, since the estimation of uncertainties is clearer if the same amount of model runs are used for all regions and relative changes are analyzed in the study, all runs were taken into account.

Table 16: Overview on the climate models used in the study.

	ESMs	RCMs
CORDEX	CNRM-CERFACS-CNRM-CM5	CLMcom-CCLM4-8-17
	CNRM-CERFACS-CNRM-CM5	SMHI-RCA4
	ICHEC-EC-EARTH	CLMcom-CCLM4-8-17
	ICHEC-EC-EARTH	DMI-HIRHAM5
	ICHEC-EC-EARTH	KNMI-RACMO22T
	ICHEC-EC-EARTH	SMHI-RCA4
	MPI-M-MPI-ESM-LR	CLMcom-CCLM4-8-17
	MPI-M-MPI-ESM-LR	SMHI-RCA4
	CCCma-CanESM2	SMHI-RCA4
	NOAA-GFDL-GFDL-ESM2M	SMHI-RCA4
	IPSL-IPSL-CM5A-MR	SMHI-RCA4
	MIROC-MIROC5	SMHI-RCA4
	NCC-NorESM1-M	SMHI-RCA4
ISIMIP	GFDL-ESM2M	-
	HadGEM2-ES	-
	IPSL-CM5ALR	-
	MIROCESM-CHEM	-
	NorESM1-M	-

7.2.2.2. Discharge Data

The observed daily discharges from 22 monitoring stations (Figure 56) were used to calibrate and validate the model. The observations are part of the Niger-HYCOS monitoring network, managed by the NBA, which consists of daily water-level readings as well as accompanying rating curves to compute discharge at these locations (Niger Basin Authority, 2008). The time periods of available data differs from gauge to gauge and used periods read from Table 17.

Table 17: Calibration and validation results for daily values.

Gauging Stations	Subregion	Calibration			Validation		
		Period	NSE	PBIAS	Period	NSE	PBIAS
Onitsha (Niger)	Niger Delta	1970-1980	0.93	11	1959-1966	0.92	12.5
Lokoja (Niger)	Lower Niger	1965-1975	0.93	3.6	1957-1964	0.87	15.1
Umaisha (Benue)	Benue	1981-1991	0.89	13.7	-	-	-
Ibi (Benue)	Benue	1981-1991	0.7	28.8	1992-2008	0.75	-3.1
Garoua (Benue)	Benue	1953-1963	0.68	12.7	1964-1970	0.76	-1.8
Ria (Benue)	Benue	1958-1968	0.64	-3.5	1951-1957	0.59	-5.8
Yidére Bodé (Niger)	Middle Niger	1993-2003	0.59	24	1984-1992	0.74	10.2
Malanville (Niger)	Middle Niger	1974-1984	0.66	16.9	1966-1973	0.74	4.3
Niamey (Niger)	Middle Niger	1974-1984	0.82	-9.3	1966-1973	0.65	-9.1
Garbe-Kourou (Sirba)	Middle Niger	1981-1991	0.73	14.5	1973-1980	0.18	52.2
Alcongui (Goroul)	Middle Niger	1976-1986	0.25	-50.7	1968-1975	0.39	-20.1
Ansongo (Niger)	Middle Niger	1974-1984	0.84	-7.4	1966-1973	0.58	-14.1
Diré (Niger)	Middle Niger	1974-1984	0.87	-10	1966-1973	0.72	-14.1
Douna (Bani)	Upper Niger	1965-1975	0.92		1957-1964	0.96	0.5
Pankourou (Bagoé)	Upper Niger	1964-1974	0.91	-4.3	1956-1963	0.92	-1
Bougouni (Baoulé)	Upper Niger	1969-1979	0.88	14.7	1961-1968	0.84	-12.7
Koulikoro (Niger)	Upper Niger	1964-1974	0.94	4	1956-1963	0.93	9.2
Selingué (Sankarani)	Upper Niger	1972-1982	0.9	-2.1	1964-1971	0.85	3.9
Baro (Milo)	Upper Niger	1962-1972	0.82	-6.5	1954-1961	0.83	4.9
Kouroussa (Niger)	Upper Niger	1965-1975	0.87	-3.5	1957-1964	0.76	19.5

7.2.2.3. Land Use and Land Cover Change Data

The only available LULC change dataset for the study region, which provides information on past LULC changes and consistent scenarios on future LULC changes is currently provided by the Land Use Harmonization project (Hurtt et al., 2011). For this dataset, historical LULC change reconstructions have been harmonized with different future scenarios on a global basis and served as basis for the ESMs of the fifth Assessment Report of the Intergovernmental Panel on Climate Change (IPCC). Historical LULC information for the period 1500–2005 is reconstructed using the model HYDE (Klein Goldewijk et al., 2010, 2011). It contains information on areal changes of cropland, pasture and urban land at a 0.5° × 0.5° resolution on an annual basis. The reconstruction is based on satellite maps when available and for the more distant past by combining information on population density, soil suitability, distance to rivers or lakes, slopes, and specific biomes. For each of the grid points information for the respective percentage of crop, pasture and urban land is provided.

The future scenarios are based on different storylines which are related to the RCP emission scenarios. For this study we used, accordingly to the climate scenarios, the LULC scenarios of the RCPs 4.5 and 8.5, from now on called LULC 4.5 and LULC 8.5. LULC 4.5 was modelled with the Global Change Assessment Model (GCAM) (Kim et al., 2006). It is a stabilization scenario, assuming the preservation of large stocks of terrestrial carbon in forests and an overall expansion of non-cultivated area throughout the 21st century. LULC 8.5 was modelled using the MESSAGE model (Riahi et al., 2007). This scenario assumes a strong increase in cultivated land while other natural vegetation decreases.

This data on past and future LULC changes, is however not detailed enough for the meso-scale eco-hydrological model and it does not include further information on non-agricultural LULC. Therefore, the LULC information has been generated via combining the above-mentioned LULC data with a detailed Global Land Cover database for the year 2000 (GLC2000) (Bartholomé and Belward, 2005). The process is described in detail in Aich et al. (2015) and is therefore just explained in summary here. GLC2000 has 27 land classes and a spatial resolution of 1/112°, which corresponds to 1 km at the equator. It is based on remote sensing data and includes a detailed legend. The GLC2000 classes occurring in the research area have been transformed to the classes of the ecohydrological model (Figure 56). The LULC change information was added to the base map on the sub-basin level of the model, and existing land classes changed accordingly. The land classes of water, wetlands, sandy/stony desert and bare rock have been kept constant as in the year 2000. When pasture, crop and/or urban land increase in a sub-basin, other natural vegetation land classes like savannah or forest are proportionally reduced in the respective subbasin. If crop, pasture and/or urban land decrease, the land classes of the natural vegetation increase proportionally. By that means LULC maps have been generated for the base-period from 1950 until 2005 and two scenarios from 2005 until 2050 in 5-year time steps.

Crop types were derived from a data set for West African crops (Ramankutty, 2004). The four main types in the region are millet, sorghum, cowpea and rice. For every sub-basin, the same crop type has been used for the whole period, according to the dominant crop in the sub-basin.

7.2.2.4. Soil and Topographic Data

Information on the soils used by the model was derived from the Digital Soil Map of the World (FAO et al., 2012). Relevant parameters for the model include depth, clay, silt and sand content, bulk density, porosity, available water capacity, field capacity, and saturated conductivity for each of the soil layers. The sub-basins were delineated using the topographic information of the Digital Elevation Model derived from the Shuttle Radar Topography Missions at a 90 m resolution (Jarvis et al., 2008).

7.2.3. Ecohydrological Model and Model Set-Up

The ecohydrological Soil and Water Integrated Model (SWIM) is a process-based and spatially semi-distributed model of intermediate complexity for river basins. It integrates hydrological processes and vegetation growth at the basin scale on a daily time step. SWIM was developed based on the Soil and Water Assessment Tool (SWAT) (Arnold et al., 1993) and MATSALU (Krysanova et al., 1989) as a tool for climate and land use change impact assessment from intermediate to large river basins. The SWIM model disaggregates a river basin in sub-basins which then again are subdivided into hydrotopes. The sub-basins are delineated on the basis of flow accumulation in a Digital Elevation Model. The hydrotopes are created by overlaying the sub-basin with land use and soil maps. They represent the spatial units used to simulate all water flows in the soil as well as vegetation growth, based on the principle of similarity (i.e. assuming that units that have the same land use and soil types behave hydrologically similarly). Potential evapotranspiration is calculated using the method of Turc-Ivanov (Wendling and Schellin, 1986). If rsds is not available or has a strong bias, the estimation method of Hargreaves and Samani (1982) is used, which is based on the latitude and daily minimum and maximum temperatures. The simulation of the vegetation (Figure 56), including arable land, is based on the Environmental Policy Integrated Climate (EPIC) approach (Williams et al., 1983) and similar to SWAT. In the SWIM model, vegetation effects on hydrological processes include the cover-specific retention coefficient, impacting surface runoff and influencing the amount of transpiration. Transpiration is simulated as a function of potential evapotranspiration and leaf area index. A more detailed description of SWIM's representation of hydrological processes is given in Huang et al. (2013).

To account for specific characteristics of tropical land, land use types parametrization is derived from SWAT's newest parameter setting (ArcSWAT, 2012). This includes LULC types like savannah and rangeland, specifically parametrized for the African context with an uncertainty framework of which the optimum parameters have been used in this study (Schuol et al., 2008b). These parameter settings have been widely used for LULC change studies in Africa (e.g. Andersson et al., 2013; Awotwi et al., 2014; Baker and Miller, 2013; Bossa et al., 2012a, 2012b). Cornelissen et al., (2013) tested different hydrological models for LULC change studies in West Africa and stated that SWAT is suitable for assessing LULC change. Due to the similarity of the modelling approaches, this statement is assumed to hold also for the SWIM model.

The model has recently been used in several studies for the Niger basin or parts of the basin to assess climate impacts (Aich et al., 2014a; Liersch et al., 2013; Vetter et al., 2014) but also the effects of land use and LULC changes on hydrology (Aich et al., 2015).

For this study, the model has been set up for the entire NRB. The Niger model is based on 1,152 sub-basins with areas ranging from approximately 50 to 28,500km² with smaller sub-basins in areas with higher altitudinal differences and large sub-basins in flat areas, for

example in the inactive desert zones of the basin. Since the flooding process in the IND is not part of the study, the routing of water between the major inflows at Bani and Koulikoro to the outlet at Diré is represented by the inflow-outflow relation, including storage and evapotranspiration on the flooded area as power law modified from Zwarts (2010).

$$A^{flood} = a * (Q^{ind^b}) \quad (20)$$

A^{flood} is the inundated area, Q^{ind} the combined inflow from Douna and Koulikoro and a and b are dimensionless factors. The evapotranspiration Et^{ind} over the flooded area is calculated using the potential evapotranspiration Et^{pot}:

$$Et^{ind} = A^{flood} * Et^{pot} \quad (21)$$

The daily change in the water storage of the flood plain dS^{ind} is:

$$dS^{ind} = -(k * S_{t-1}^{ind}) + Q^{inflow} - Et^{ind} \quad (22)$$

k is a factor that controls the daily outflow of the water storage S_{t-1}^{ind} of the day before, Q^{inflow} as added daily inflow from Douna and Koulikoro the actual evapotranspiration is subtracted. The daily outflow of the IND at Diré $Q^{Diré}$ is finally calculated with the new value of the storage S_t^{ind}

$$S_t^{ind} = S_{t-1}^{ind} + dS^{ind} \quad (23)$$

$$Q^{Diré} = k * S_t^{ind} \quad (24)$$

The factors $a = 35.0$, $b = 0.874$ and $k = 0.0072$ have been set using the the Model independent Parameter Estimation software package (PEST) (Doherty, 2005), which uses the mean square error between the observed and the simulated discharge as objective function.

In regard of infrastructure, six reservoirs are represented in the model via the reservoir module developed by Koch et al. 2013 (Table 18).

Table 18 Reservoirs of the Niger River Basin included in the model.

Reservoir	Country	Year	Max. capacity in mio m³
Selingué	Mali	1982	2,135
Kainji	Nigeria	1968	15,000
Jeeba	Nigeria	1984	3,880
Shiroro	Nigeria	1990	7,000
Lagdo	Cameroon	1982	7,800

LULC changes for the past and the future are represented in the model with changes each five years, using the dynamic land use change module as described in detail by Aich et al. 2015. It changes the land classes at any frequency or given point in time, while keeping the instantaneous balance of water and other modelled fluxes constant during the change, for example soil water content. This means that the number and the areas of

hydrotopes within a sub-basin can change and new hydrotopes can appear or existing ones disappear.

7.2.4. Indicators and statistics

In order to assess catastrophic flooding, besides the hazard, also the vulnerability of people and their goods should be considered. However, thresholds for catastrophic flooding or damage functions are not available for the NRB and the relation between high flows and catastrophic flooding has not been clarified yet. In this study, we used two different indicators to assess flooding: the 90th percentile of annual discharges, which is a robust indicator for high flows and additional the 20-year return period floods, which indicate more extreme floods with a higher likelihood of causing catastrophic flooding. Still, these measures are no direct pointer for catastrophic flooding, but indicators. The terms “flood”, “high flow” and “peak flow” are consequently related to the annual flood, not to catastrophic flooding.

As indicator for an increase in flood magnitude, the 20-year return period flood (RP20) and the 90th percentile of the daily discharge (Q10) are used. The RP20 was calculated on the basis of General Extreme Value (GEV) distributions (Coles et al., 2001) of the annual maximum discharges. The GEV method has been widely used for assessing flood risks (e.g. Huang et al., 2012) The distribution has been fitted to the annual maximum discharges using the “fevd” function of the “extRemes” package (Gilleland, 2012) and the 20-year return period has been identified using the “return-level” function of the same package for the R statistical software (R Core Team, 2013). A 20-year flood is a rarer event for which the uncertainty is higher than for example for annual return intervals. The Q10 value is a more robust indicator for high flows and used commonly for assessing changes in high flows and flood risk (e.g. Aich et al., 2014b; Vetter et al., 2014). It designates a value of river discharge which is only exceeded 10 % of the time. A negative trend in Q10 implies a reduction in flood magnitude, and a positive trend an increase. When interpreted together, these indicators can also add additional information about the characteristics of the flood behavior, in order to get an indication whether the distribution or frequency of flood events change. For example would a decrease in Q10 accompanied by an increase in RP20 indicate a general decrease of common annual high flows but accompanied by an increase of more rare extreme floods. This would imply a change of the flood distribution to a distribution curve with a longer tail.

Heavy precipitation is analyzed as 95th percentile of days above 1 mm precipitation. This is a standard indicator for precipitation extremes and for example used by the European Union (EEA, 2014).

In order to quantify the model efficiency, the Nash Sutcliff Efficiency (NSE) (Nash and Sutcliffe, 1970), and the percent bias (PBIAS) have been used. The NSE is calculated using simulated (Q_{sim}) and observed (Q_{obs})discharge.

$$NSE = 1 \frac{\sum_{i=1}^{n}(Q_{obs} - Q_{sim})^2}{\sum_{i=1}^{n}(Q_{obs} - \overline{Q_{obs}})^2} \quad (25)$$

The NSE is a value in the range from $-\infty$ to 1, with $NSE = 1$ implying perfect model performance, $NSE = 0$ implying that the model is performing as good as the observed average as a predictor and $NSE < 0$ implying that the choice of the model is increasingly questionable since the residual variance is larger than the observed variance. The PBIAS indicates the over- or underestimation of discharge during the calibration or validation period as a percentage. For the evaluation of the NSE and PBIAS the terminology of Moriasi and Arnold (2007) is used. The terminology is commonly applied to monthly values, however, in this study to daily values (for NSE: very good: $0.75-1.0$, good: $0.65-0.75$, satisfactory: $0.5-0.65$, unsatisfactory: < 0.5; for PBIAS: very good: $< |10|$, good: $|10|-|15|$, satisfactory: $|15|-|25|$, unsatisfactory: $\geq |25|$).

7.2.5. Calibration and Validation of the Model

Dynamic implementation of LULC scenarios are a challenge for eco-hydrological modeling in regard of process representation and hence also their calibration – a problem which is being built up by to the data scarcity in West Africa. The calibration procedure, including a sensitivity analysis, is explained in more detail in Aich et al. (2015). The focus of the calibration was the accurate representation of daily streamflow regimes with a focus on high flows, in order to achieve a good representation of floods. The main parameters for the calibration were related to groundwater, river routing, saturated conductivity and potential evapotranspiration. Since the study area are is very large for a mesoscale modeling framework and the climatic and geographic conditions are very heterogenic, the model was calibrated independently for 22 different catchments, where discharge data were available (see chapter 7.2.2.2). The catchments in the model have been calibrated using PEST (Doherty, 2005). After the automatic calibration, the result for the respective subcatchment were checked visually with focus on the performance during high flows and, if necessary, recalibrated with narrower value band for the parameters. During the calibration, the LULC dynamics and the effect of the reservoirs was taken into account in order to calibrate the model as closely as possible to the real conditions. The calibrated parameters are static and do not change within a catchment and over time in order to avoid overfitting.

The calibration period of the model was chosen according to data availability of at least 11 consecutive years, if available (ranges of calibration and validation periods as given in Table 17). If more than 11 years were available, a period was selected, which included years with distinctly high and low flows, in order to account for different climatic conditions. The validation period was selected as 8-year period before the calibration, if available. For stations with limited and/or erratic data availability, other periods with more

data have been used for the validation, which can be exemplarily seen for the station Ibi (Figure 58). The results of the calibration and validation are shown in Table 17.

To quantify the efficiency of the model, the commonly used measures NSE and PBIAS were applied (see Chapter 7.2.4). The results for the calibration and validation differ for the sub-regions of the catchment. In the Upper and Lower Niger Basin (LNB, UNB) as well as for the Benue and the Niger Delta, calibration results were mostly very good or at least good with NSE values between 0.64 and 0.94 and PBIAS with the poorest value 28.8 and best -2.1. The validation in these regions showed generally comparable efficiency with NSE ranging from 0.59 to 0.96 and PBIAS 19.5 and 0.5. For the Middle Niger Basin (MNB) the model showed distinctly lower efficiency with NSE for the calibration of 0.25 and 0.87 and PBIAS between -50.7 and -7.4. The validation values were slightly lower with NSE ranging from 0.18 to 0.74 and PBIAS 52.2 to 4.3. This regional differences for the calibration efficiency was already observed in Aich et al. (2015) and other modelling studies like Schuol et al. (2008a, 2008b), showing monthly NSE for the UNB, the LNB, and the Benue mainly between 0.0 and 0.7 and between -1.0 to 0 in the MNB.

The mean efficiency for the whole basin for the calibration is a NSE of 0.78 and PBIAS of 2.4 and for the validation a NSE of 0.74 and PBIAS of 2.7. Besides the gauging stations of Alcongui and Garbe-Kourou in the MNB, the calibration and validation results were at least satisfactory.

The results for the stations which are analyzed in this study are depicted in Figure 58. Since absolute numbers of discharge are not analyzed in this study but only relative changes, NSE is more meaningful than PBIAS. The NSE was at least good for all stations during calibration and validation with the exception of the validation of the station Garbe-Kourou. The poor model performance for this station is similar in the study of Aich et al. (2015) and discussed in detail there. Possible reasons might be deficient discharge observations, deficient climatic forcing, incorrect or inexact land-use, the higher sensitivity to wrong data due to the high runoff-coefficient in dry areas and/or other deficits in the model structure, e.g., for the representation of the groundwater or other runoff flowpaths. This source of uncertainty for the analysis of the Garbe-Kourou catchment, but also for the other catchments, is taken into account in the discussion (see Chapter 7.4).

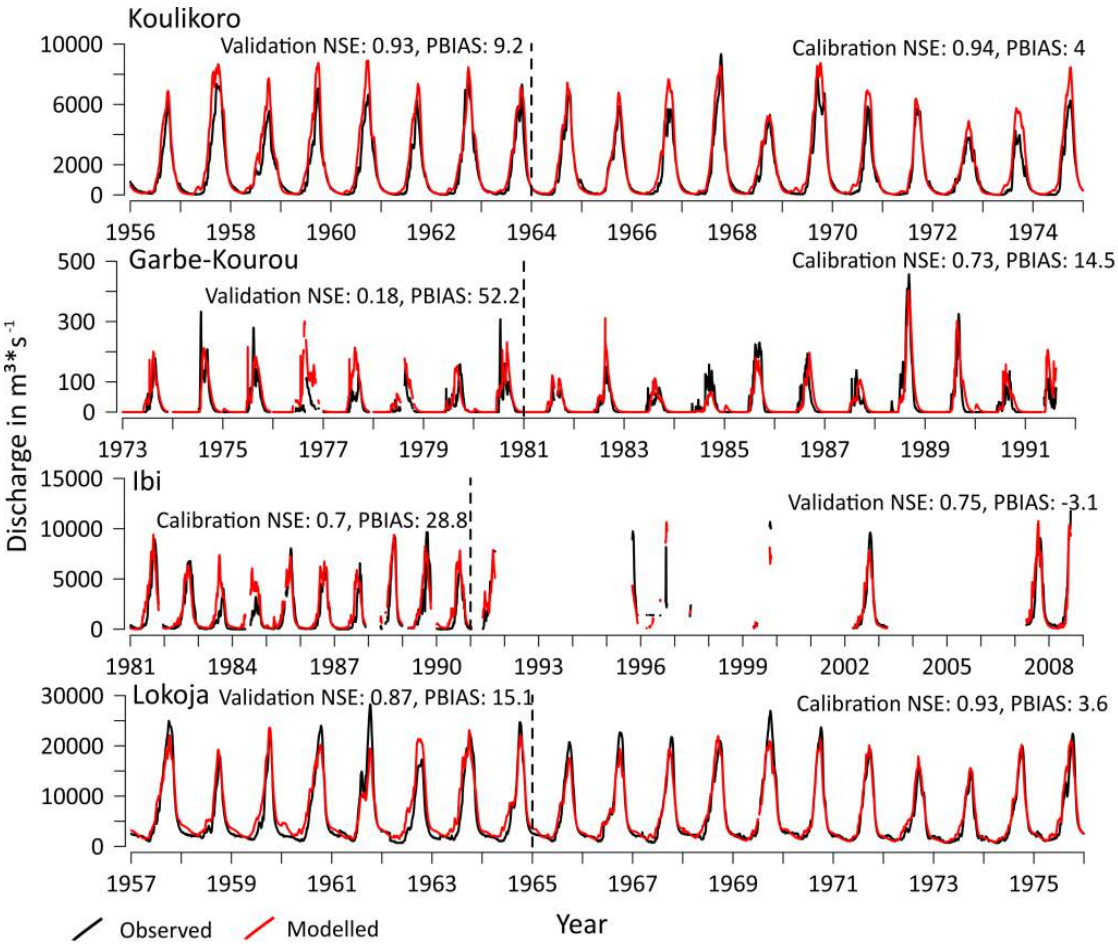

Figure 58: Calibration and validation results (daily values) for the stations analyzed in the study.

7.3. Results

7.3.1. Assessment of future climate projections in the Niger Basin

The historical simulations of the CORDEX Africa models have been evaluated against station data by Kim et al. (2013) and Nikulin et al. (2012). They stated that in general all RCMs provide a reasonable description of the observed climatology and, that the multimodal ensemble outperformed the individual models. They recommended especially for impact studies, to evaluate the performance of the models individually for each region and all relevant parameters in order to assess the uncertainty. This exercise has been conducted for all climate models and the case of the Koulikoro catchment (UNB) is reported as an example, (Figure 57, other regions in the Supplementary material: Figs S1-S3). The four regions in the Niger show generally the same patterns when compared to reanalysis data. The mean for all CORDEX models for annual precipitation is similar to the reanalysis data in all four regions. The strong variability of annual precipitation seems to be reflected by most of the models. The mean for heavy precipitation is in the same range as the GSWP3 and WFDEI reanalysis products, however the values of PGFv2 and

WATCH are higher and for the LNB and the Ibi catchment (Benue) the range of the CORDEX model does not cover the values of these two data sets. For temperature, the mean of the 13 RCMs is lower than the reanalysis data. The range for rsds is interestingly divided in two groups, of which one (RCMs: RCA4, HIRHAM5, RCA4) is above the reanalysis products and the other (RCM: CCLM4-8-17) is below or on the same level as the WATCH data set. In all four regions, the temperature increase between 2006 and 2050 is around 2 °C, with RCP 8.5 scenarios slightly warmer than RCP 4.5. The projections for RCP 4.5 are slightly below RCP 8.5. For rsds, there is no trend.

The results for the ISMIP models, also shown in Figure 57, are closer to the reanalysis during the base period. For annual precipitation, temperature and rsds the tested parameters the band of the five models is narrowly around the WATCH data set, which has been used for the bias correction (see chapter 7.2.2.1). Heavy precipitation is, however, below the values of WATCH and rather on the level of the CORDEX simulations. For the scenario period, the climate change signal is similar to the CORDEX simulations. Temperature increase is approximately 2 °C until 2050, while rsds remains constant.

The changes in precipitation and heavy precipitation are shown separately in Figure 59 for the CORDEX runs and for the ISIMIP models in more detail. For all regions the medians for annual mean precipitation are between 2 % and 6 % higher during the scenario period (2021-2050) compared to the base period (1976-2005). The model medians for heavy precipitation are distinctly higher with values in the UNB, LNB and Benue between approximately 5 % and 10 % and in the MNB even 10 % and above. The values for RCP 8.5 are in all cases at least slightly higher than for RCP 4.5, in the MNB even distinct higher.

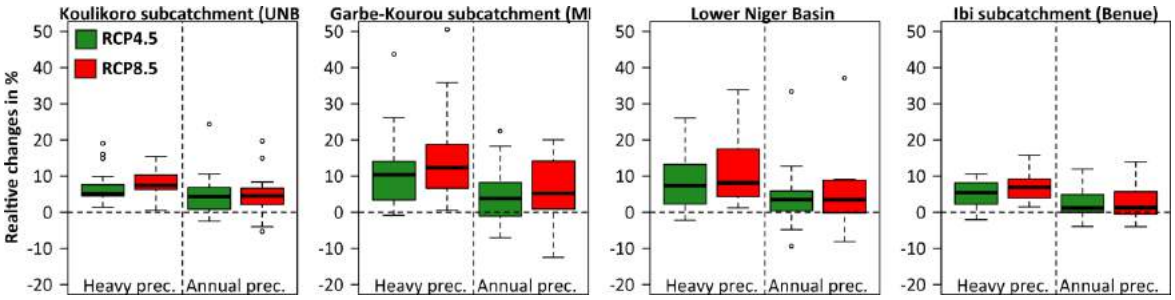

Figure 59: Relative changes of heavy (95th percentile of days >1 mm) and annual mean precipitation for all 18 climate models and scenarios RCP 4.5 (green) and RCP 8.5 (red) between a base period (1976-2005) and the scenario period (2022-2050).

7.3.2. Assessment of future land use and land cover changes in the Niger Basin

According to the reconstruction of Hurtt et al. (2011), the main LULC in the NRB for the period from 1950 until 2005 were a strong increase in cropland and pasture (Figure 60 and Figure 61). Pasture increased mainly in the Sahel zone and cropland further South, in the Sudanian zone and the Benue. Urban areas did not significantly increase. The main

increase in pasture happened from 1950 to 1960 with increases in the UNB from approximately 37 % to 42 %, in the Garbe-Kourou catchment (MNB) from approximately 20 % to 23 %, in the LNB from approximately 40 % to 45 % and in the Ibi catchment (Benue) from 30 % to 35 %. The changes after 1960 until 2005 were rather small or the area of pasture stayed constant. For cropland, the changes differ more distinctly within the basin with the strongest changes in the MNB and LNB from approximately 20 % to 35 % respectively 18 % to 30 %. In the UNB there is almost no cropland during the whole period and in the Benue, it increases from approximately 17 % to 20 %. Urbanization stays low, under 1 % during the whole historical period for all sub-regions.

The 'optimistic' LULC 4.5 regreening scenario predicts a stabilization of LULC in the Niger basin from 2005 onwards with decreases of croplands and pastures in the Guinean Highlands, the Niger Delta and of cropland in the Sahelian/Sudanian zone. In the UNB, this scenario is thought to result in a reduction of pasture from approximately 42 % to 20 %. In the other sub-regions, the areal coverage of pasture is assumed to remain approximately constant from 2005 onwards. Cropland would decrease in all sub-regions between approximately 2 % and 5 %. The urban areas are assumed to stay almost constant as in 2005 or decrease even.

The business as usual scenario LULC 8.5 would lead to an increase of crop and pasture almost in the entire basin south of the Sahara desert and is assumed to result in a strong urbanization in the now already densely populated areas of the basin, mainly in the Delta (starting in the north around the area of Lokoja) and the right-bank tributaries in the MNB. The historic trend of cropland would continue until 2050 with an increase of approximately 10 percentage points in the MNB and LNB and 5 percentage points in the UNB and Benue. Urbanization is thought to increase distinctly in the MNB by approximately 5 %. In the other catchments, the urbanized areas would grow slower to approximately 1.5 % in the LNB and 0.5 % in the UNB and Benue.

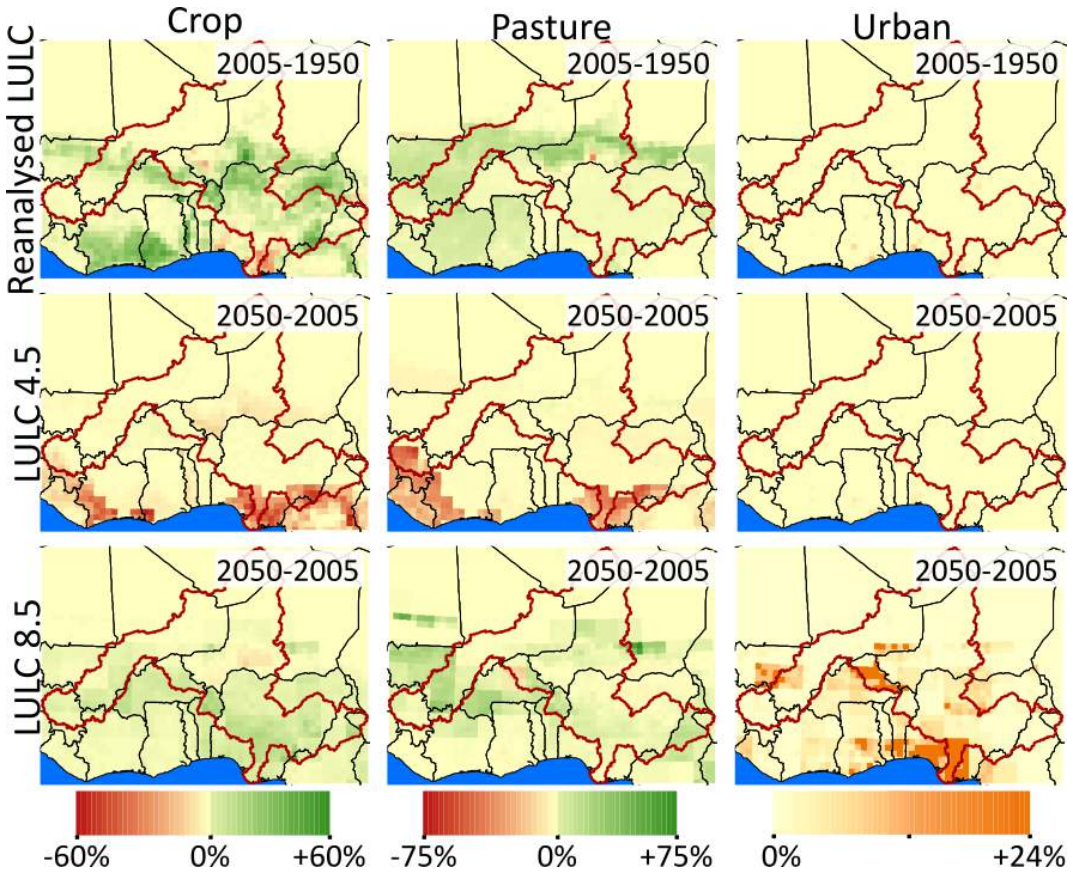

Figure 60: Land use and land use and land cover changes for cropland, pasture and urban land. Top row: differences between 2005 and 1950 of reanalyzed data. Middle row: differences between 2050 and 2005 for the scenario 4.5. Bottom row: differences between 2050 and 2005 for the scenario 8.5.

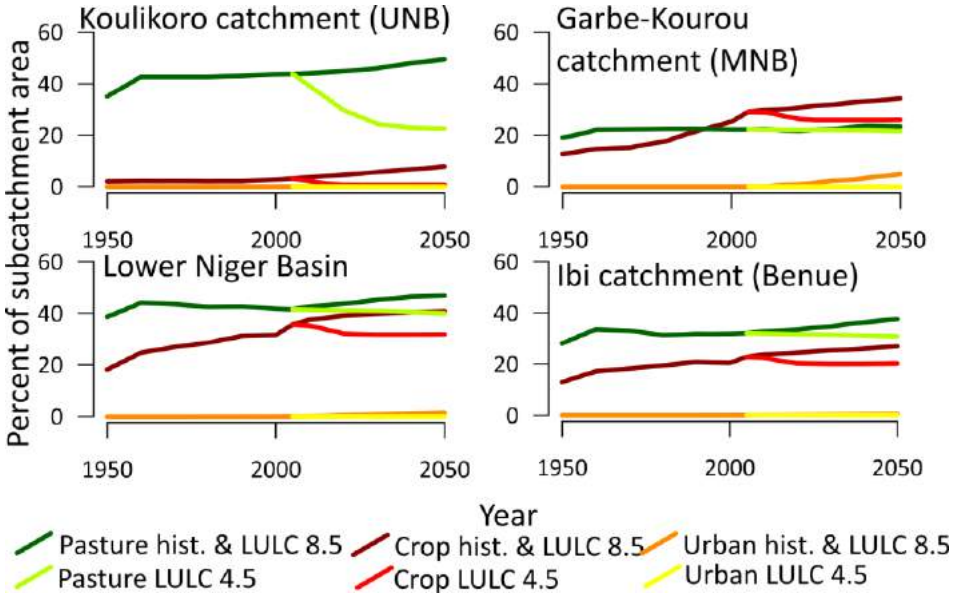

Figure 61: Quantification of changes of % crop and pasture areas of the catchments for the land use and land cover change scenarios 4.5 and 8.5.

7.3.3. Assessment of future flood projections in the Niger Basin

In general, most modeling scenarios show a consistent increase of high flows (Q10) for the scenario period of 2021-2050 in comparison to the base period of 1976-2005 (Figure 7) for any climate or LULC scenarios (with the only exceptions of the "regreening" scenario LULC 4.5 at Ibi and Lokoja). The model results give a slightly smaller increase of high flows for the RCP 8.5 scenarios in comparison to the optimistic RCP 4.5 climate scenarios.

At the same time, the modelling results show an opposed trend for the LULC scenarios: a larger increase of high flows for the "business as usual" LULC 8.5 scenarios in comparison to the "regreening" scenarios: the "regreening" LULC 4.5 scenarios show only a slight increase of high flows for Koulikoro and Garbe-Kourou and a decrease of high flows for Ibi and Lokoja (in comparison to the base period).

The mean annual flow for the period of 2021-2050 increases under the scenario with constant LULC as of 2005 and for the "business as usual" scenario and decreases for the "regreening scenario" in comparison to the base period of 1976-2005 for all four regions. Similar to the high flows, the mean discharges are slightly reduced under climate scenario RCP 8.5 compared to 4.5, but to a smaller degree than at the high flows.

Koulikoro is the only station, where the LULC 4.5 scenario leads to almost similar results compared to the constant LULC scenario as of 2005. The relative changes between the scenario and the base period of the medians for the flood indicators for all LULC scenarios are between +1 % and 12 %. For the Garbe-Kourou catchment shows two main deviations from the results of the other catchments. It shows the most extreme increases and the differences between the LULC as well as the RCP scenarios are very distinct. The medians of the flood indicators Q10 change for all LULC scenarios between +15 % and +44 % for RCP 4.5 and between -5 % and +37 % for RCP 8.5. At Ibi and at Lokoja, the regreening scenario leads to a slight decrease of high flows; for the constant LULC scenario, the medians stay almost stable and for the LULC 8.5 scenario there is an increase up to 15 %.

In regard of the spread of the different driving climate models, the interquartile ranges of the boxplots of Koulikoro, Ibi and Lokoja are similar, between approximately 15 and 50 percentage points. For Garbe-Kourou, the range is slightly larger, particularly for the Q10 indicator with over 50 percentage points. There is no visible systematic difference between the constant and the two LULC scenarios. This holds also for the two climate scenarios.

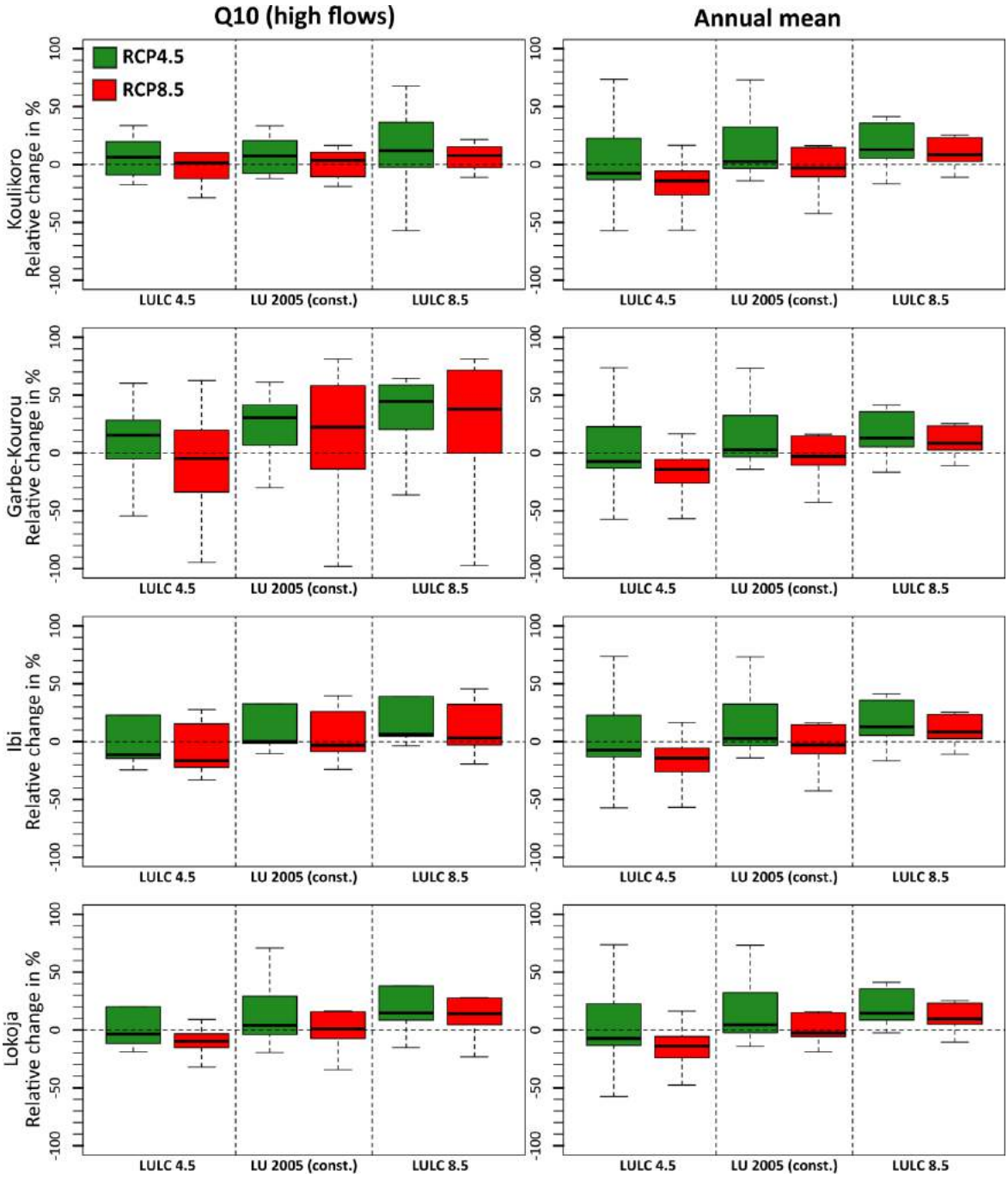

Figure 62 Boxplots for relative change (in %) for the 90th percentile of annual discharges (Q10) and the mean annual discharge in the four study catchments, for the different land management scenarios (LULC 4.5, constant LULC of 2005, and LULC 8.5) and different climate scenarios (RCP 4.5 and RCP 8.5). Differences are given between the scenario period (2021-2050) and the base period (1976-2005). Note that outliers are not depicted. A figure with outliers is in the supplementary material (Fig S 3).

The relative changes of the 20-year return period floods (RP20) are given in Figure 63 to assess the potential impacts on more extreme floods. In general, their relative changes show the same pattern as the ones for the Q10 indicators above. Only for the Koulikoro

and the Garbe-Kourou catchment, there was a distinct systematic difference between the Q10 indicator and RP20 indicator visible for RCP 4.5. In these catchments, the RP20 increases significantly stronger than the Q10 indicator for constant LULC and scenario 8.5 in Koulikoro and 4.5 for Garbe-Kourou. Interestingly, there are even reductions for the medians of RCP 8.5 at Garbe-Kourou. In general there is no overall pattern visible. The lack of significant differences between Q10 and RP20 shows a rather stable statistical distribution of discharges, which seems to change mainly linear, thus confirms the findings of a non-stationary General Extreme Value distribution analysis on annual maximum discharges presented by Aich et al. (2014a).

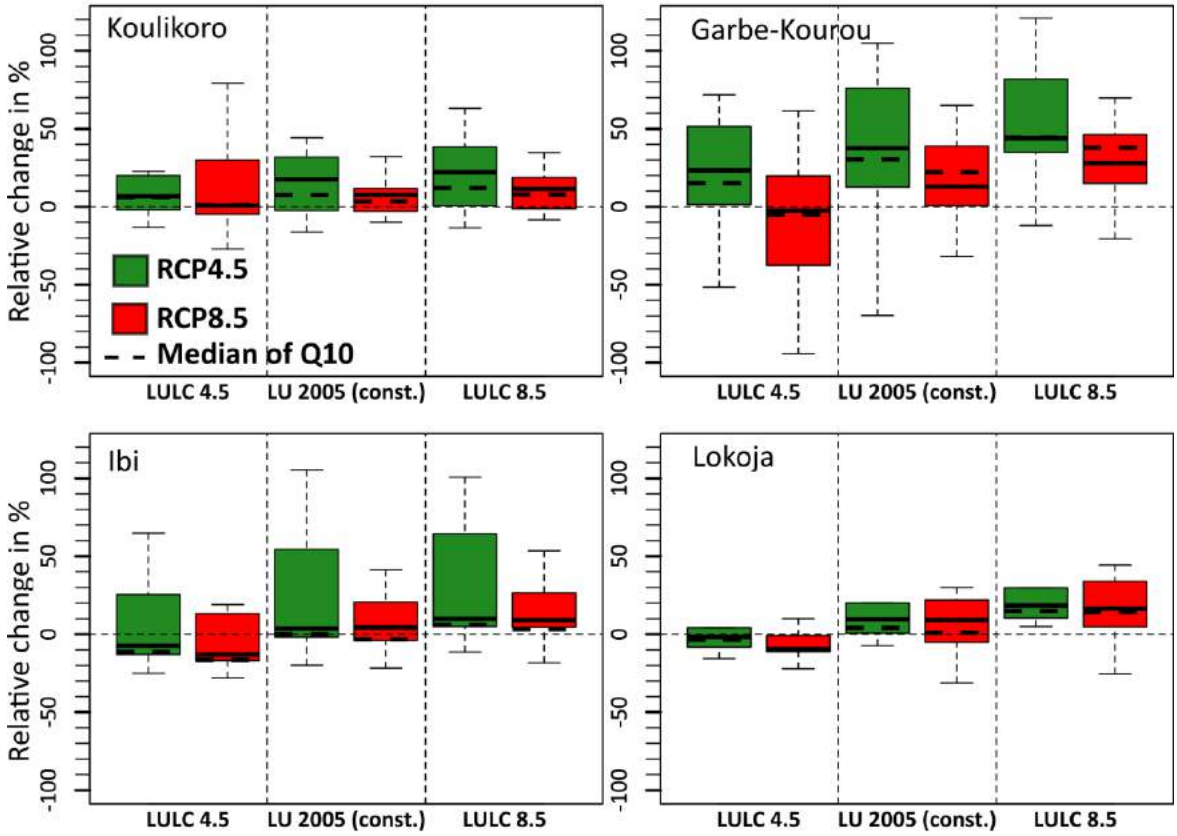

Figure 63 Boxplots for relative change (in %) for the 20th-year flood in the four study catchments, for the different land management scenarios (LULC 4.5, constant LULC of 2005, and LULC 8.5) and different climate scenarios (RCP 4.5 and RCP 8.5). The medians of the90th percentile of annual discharges (Q10) are depicted as dotted line. Differences are given between the scenario period (2021-2050) and the base period (1976-2005). Note that outliers are not depicted. A figure with outliers is in the supplementary material.

7.4. Discussion

7.4.1. Uncertainty

The cascade of uncertainty in this study is characteristic for impact studies and arises from different assumptions and limitations in the modelling chain (Beven and

Romanowicz, 2005; Jones, n.d.; Rodríguez-Rincón et al., 2015; Willgoose et al., 1991). The uncertainty of the projections starts with the assumption of the RCPs for GHG emissions and respective LULC. For each, climate and LULC, two rather opposed but plausible scenarios have been selected in order to cover a broad range of societal pathways. Regarding climate, the differences between both RCPS are not distinct during the study period until 2050, which confirms other climate studies in the region (e.g. Aich et al., 2014b). In regard of LULC changes, the scenarios differ substantially in the assumptions and also in the impacts. In addition, only scenario information on changes in cropland, pasture and urban land are available. Other potential relevant changes like population increase in rural areas, degeneration of natural vegetation, the effects of sealing, changes of flow paths etc. are not taken into account in this study. Therefore already at this stage of the uncertainty cascade it is obvious, that the study can only provide limited absolute quantitative information on future flood trends.

The uncertainty coming from the different climate models is the next level of the cascade. One can differentiate between the general performance of the models to represent the climate system and the regional trends they project when simulating climate change scenarios. The general performance of the models in the regions seems low, when comparing the river regimes driven with the historical simulations of the climate models (Supplementary material Figure S 24). In particular the climate models' performance on temperature and rsds is rather weak and a specific test on the influence of the parameters in regard of river flow is still missing. Concerning climatic trends, the model agreement on temperature increase is very robust. For precipitation, most models agree in an increase of annual precipitation and heavy precipitation. The increase in precipitation can be explained physically with higher temperatures carrying more water and more convection and confirms former studies in the region, summarized by Roudier et al. (2014). Therefore an increase in precipitation seems plausible. Still, the observed natural decadal variability in the region is enormous as seen for example during the Sahel drought during the 1970s and 1980s (e.g. Paturel et al., 2003). The effects and characteristics of the natural variability are still not sufficiently understood. On the short and intermediate term until the end of the study period 2050, natural variability might therefore counter the projected increase in precipitation. The sensitivity is probably highest in the drier areas of the NRB due to the low runoff-coefficient as shown in Aich et al. (2014b). This is confirmed in the analysis with the highest model spread for the Garbe-Kourou catchment. Here, the impacts deriving from the climate models are not only strongest in this regions but also most uncertain.

The next step on the cascade of uncertainty derives from the hydrological model itself. The validation showed good results and Vetter et al., (2014) showed that in this region the share of the hydrological models on the overall uncertainty is rather low, when compared to climate model uncertainty. However large uncertainties stem from the lack of observations that would be required to calibrate key model parameters like overland or groundwater flows. For different smaller regions, other studies confirm our modelling

results of the catchment. Ramier et al. (2009) measured the water balances of millet croplands and savannah in the Sahelian part of the NRB. They found increased groundwater and reduced evapotranspiration for the millet compared to the savannah. This confirms the modelling results of increasing discharges when LULC is changing from savannah to cropland. The same trend was also found by Favreau et al. (2009). Aich et al. (2015) compared trends of annual maximum discharges in the Sahel region using modelling with and without LULC changes. For cropland, results showed similar flood trend directions and approximately similar trend magnitudes as observed, when taking into account LULC changes. In case of turning savannah into pasture, the trend direction was still correct but the magnitude much smaller than observed. In regard of changes in forest cover as for example in the Upper Niger Basin, there is no literature available to the authors. Other studies like Awotwi et al. (2014) and Cornelissen et al. (2013) found a more generally suitability of the model parameterization for the area (see Chapter 7.2.3). Therefore we generally assume that the model is capable of reproducing the correct effects of the LULC change processes (that are reflected in the model code). However, the absolute magnitude is uncertain and other relevant processes might be missing. Feedbacks of ecohydrological LULC processes, for example soil property changes like infiltration rates and friction factor are yet missing in the model. This implies a careful interpretation of the results in regard of LULC change effects and the magnitudes should only be interpreted relatively among the different parts of the catchment and not as absolute projections for the changes.

Finally, the certainty of different results of this study has to be estimated individually. The projections without LULC changes seem robust in the face of solid results during the validation and at least for all catchments beside Garbe-Kourou, also rather small IQR, showing the same direction (increase). The tendencies for the LULC processes seem robust as well, however, the magnitudes are uncertain and many effects that might be connected with LULC processes are not represented in the modelling chain.

7.4.2. Flood trends

The results imply mostly an increase in flood magnitudes in the different regions of the Niger basin. These findings complete and confirm the overall picture of a return to wet conditions in West Africa, as found by Tarhule et al. (2015), Aich et al. (2014b), Jury (2013) and Roudier et al. (2014). Divergent to our approach, in a modelling study by Hirabayashi et al. (2013), global climate models of RCP 8.5 were used to drive a global river routing model without considering land-use change. They found a decrease of the return-period for a projected 100-year flood for most of the model runs for the Niger basin. Their findings do not contradict our findings, since the climate scenario RCP 8.5 and constant LULC as of 2005 in our simulations also led to a decrease of flood magnitude near the outlet of the Niger basin at Lokoja for most of models. However, this does not

hold for other climate and LULC scenarios and especially not for other subregions within the basin, which underlines the need and importance for detailed regional studies.

When looking more detailed into the results, interestingly the LULC and the climate scenarios which actually are related (LULC 4.5 with RCP 4.5 and LULC 8.5 with RCP 8.5) point in opposite directions. Whereas the "regreening" scenario LULC 4.5 generally reduces flood magnitudes, the related climate scenario RCP 4.5 leads to an increase in heavy precipitation and flood risk (Figure 62). The opposite is true for the "pessimistic" scenarios, with a substantial flood increase under the LULC scenario 8.5 and general reductions of flood magnitudes under the related climate scenario RCP 8.5. Still, the results imply that the climatic influence will be stronger than the effect of LULC changes. Even with a constant LULC as of 2005, for all regions an increase of the flood magnitude is projected under RCP 4.5 and most runs of RCP 8.5 in accordance to the precipitation and particularly heavy precipitation projections (Figure 59). These increases are likely related to the rise of temperature under climate change and the associated increase in humidity due to the higher water holding capacity of air and increased convection in the atmosphere (Müller and Pfister, 2011; O'Gorman and Schneider, 2009; Trenberth, 2011). The generally lower values for mean precipitation and mean annual flow also support this hypothesis. The increase in evapotranspiration due to the high temperatures counter this effect, especially under the warmer climate scenario RCP 8.5, where high flows are projected to be more stable under climate change. The study showed, that the combined effects of LULC and climatic changes will have a very significant influence on the flood risk particularly in the drier subregions, due to the high hydrological sensitivity which comes with low runoff-coefficients. The Sahelian and Sudanian areas of the MNB, are therefore especially vulnerable to increasing flood risk, which has already be observed during the last decade (Aich et al., 2014b).

Another interesting subregional finding is related to the "regreening" scenario LULC 4.5. The mean discharge decreases even stronger by approximately 20 % than high flows in the Koulikoro catchment. This might be an effect of the afforestation measures of former cropland and pasture areas in this catchment (Figure 56). This effect is also reported by Wahren et al. (2012), who found that peak flows are less reduced by afforestation when soils are already wet, which applies regularly for the rainy season in the Guinean Highlands. In contrast, high flows increase less than mean flows in the Ibi catchment, which might be explained similarly to the afforestation effect in the Koulikoro catchment. The forest cover in the Ibi catchment (Figure 56) led to high mean annual evapotranspiration (low discharge) with still rather high levels of high flows. In the LULC 8.5 scenario, the forest cover is replaced by cropland and pasture. This leads to a stronger increase in mean flows than high flows. This means, that afforestation in forests can lead to a decrease in mean annual discharge via increased evapotranspiration, whilst high flows are reduced distinctly less.

7.4.3. Managment implications

Already the increasing flood risk due to climate change, without considering LULC, implies a strong need to react. The recent hydro-climatic conditions in the NRB and the relative magnitudes of floods are already leading regularly to catastrophic floods (Aich et al., 2014b; Tarhule, 2005; Tschakert et al., 2010). This means, that the societies of the riverine nations along the Niger are not adapted to the situation. In addition the results seem robust and the uncertainty deriving from the climate models in regard of an increasing trend of flood magnitudes in the near future is low. In the face of an existing adaptation deficit on the current situation, this increase in flood magnitude will likely aggravate the current situation in regard of flood risk.

Most of the different scenarios led to an increase of flood magnitude, also the optimistic climate and LULC scenario. This means that an increase of flood risk is likely, under the given uncertainty, even if globally strong efforts are undertaken to reduce GHG emissions. Therefore, quick action is necessary in the NRB in order to prevent further loss of lives and damage to goods and the developing economies. Flood adaptation has to be an integral component of infrastructure planning, settlement policy, public awareness and development plans. Furthermore, effective early warning systems should be implemented in the basin. Infrastructural measures like reservoirs, dams etc. should be considered in the most flood prone areas and before implemented, subject of detailed regional studies.

Results of the LULC analysis open another perspective, though they come with higher uncertainty. The differences for the LULC scenarios show that adaptation is not the only option and regional flood mitigation is, to a certain extent, possible. In this context, mitigation means the mitigation of flood intensities and frequencies whereas adaptation means to be prepared for the expected flood intensities and frequencies. Mitigation efforts could be the transformation of agricultural land (crop and pasture) into grasslands, savannah or forest, which can reduce flood increases or, as in the case of Ibi and Lokoja, even reverse them. Especially, reduction of croplands like in Garbe-Kourou and Lokoja as well as an increase of grasslands and savannah seem to have positive effects, whilst afforestation, as mainly simulated in the Koulikoro catchment, reduces the peak flows less than the mean flows. Especially in water scarce areas and in countries with an increasing food demand due to extreme population growth, this trade off might be problematic and should be object to further analysis. Another interesting finding is that dry areas, which have the highest sensitivity to also profit the most from mitigation efforts. Particularly urbanization and increase of cropland, as in the MNB and LNB, have a strong effect. In these highly vulnerable areas, flood mitigation should be a guiding idea of land management in order to not aggravate the already tenuous situation.

In summary, efforts at catchment scales are possible and smart land use plans can help to reduce flood risk locally. Especially for the developing countries in the NRB, a flexible strategy of mitigation and adaptation measures seems a necessary but also realistic way to

increase resilience against catastrophic flooding. This holds even more, as many measures in regard to land management, come with further positive, mainly economic and agricultural effects and are therefore “no regrets options”. An example might be new plowing techniques that increase the productivity and reduce surface flow. By this means, the uncertainty, which is still large in regard of the absolute numbers of flood magnitude increase, is also taken into account and trade-offs between flood adaptation and development can be avoided. In addition, regional measures and no regrets options might help to reduce the need for large and expensive infrastructural measures like reservoirs, which come often with harmful effects on the environment.

7.5. Conclusions

The simulation study projects that risk of catastrophic floods in the modelled sub-catchments of the Niger Basin is likely to increase under most climate and land-use scenarios. It also stresses the needs and importance for detailed regional studies to understand and quantify the at times opposing or counterbalancing impacts of climate and LULC changes in different vegetational and climatic settings of the Niger Basin.

The modeling results suggest that there is an urgent need for the implementation of adaption measures to lessen the effects of future large floods, especially for the drier parts of the Niger Basin, where flood risk is likely to increase at an alarming rate. The results of the LULC scenarios show that mitigation of catastrophic floods is at least partly possible with reasonable land management on the catchment scale. At the same time, the effects of LULC are subject to large uncertainty, mainly due a lack of potentially relevant processes in the model as well as data quality, data availability, and LULC parameterization constraints; more research effort is required to minimize these uncertainties.

Besides, the effects of climate change are not independent from LULC changes. The relation is complex since the global development in regard of GHG emissions, trade, economy, etc. will influence both the regional climate and LULC in West Africa. Sequently, the regional climate will have an influence on the regional LULC, e.g. in regard of expansion or intensification of agriculture; and the regional LULC, vice versa on the regional climate, e.g. via higher evapotranspiration in afforested areas. The study shows, that this complexity can be approached with state-of-the-art eco-hydrological models and scenario-driven approaches, in order to disentangle the impacts of changes and also to quantify the influence of the different drivers.

Acknowledgments

We thank the IMPACT2C project for financing this study and the Niger Basin Authority (NBA) for providing data.

References

Aich, V., Liersch, S., Vetter, T., Huang, S., Tecklenburg, J., Hoffmann, P., Koch, H., Fournet, S., Krysanova, V., Müller, E. N. and Hattermann, F. F.: Comparing impacts of climate change on streamflow in four large African river basins, Hydrol. Earth Syst. Sci., 18(4), 1305–1321, doi:10.5194/hess-18-1305-2014, 2014a.

Aich, V., Koné, B., Hattermann, F. F. and Müller, E. N.: Floods in the Niger basin – analysis and attribution, Nat. Hazards Earth Syst. Sci. Discuss., 2(8), 5171–5212, doi:10.5194/nhessd-2-5171-2014, 2014b.

Aich, V., Liersch, S., Vetter, T., Andersson, J., Müller, E. and Hattermann, F.: Climate or Land Use?—Attribution of Changes in River Flooding in the Sahel Zone, Water, 7(6), 2796–2820, doi:10.3390/w7062796, 2015.

Amogu, O., Descroix, L., Yéro, K. S., Le Breton, E., Mamadou, I., Ali, A., Vischel, T., Bader, J.-C., Moussa, I. B., Gautier, E., Boubkraoui, S. and Belleudy, P.: Increasing River Flows in the Sahel?, Water, 2(2), 170–199, doi:10.3390/w2020170, 2010.

Andersen, I., Dione, O., Jarosewich-Holder, M. and Olivry, J. C.: Niger River Basin: A Vision for Sustainable Management (Directions in Development), edited by K. G. Golitzen, World Bank Publications, Washington DC. [online] Available from: http://www.amazon.com/Niger-River-Basin-Sustainable-Development/dp/0821362038 (Accessed 11 November 2013), 2005.

Andersson, J. C. M., Zehnder, A. J. B., Wehrli, B., Jewitt, G. P. W., Abbaspour, K. C. and Yang, H.: Improving crop yield and water productivity by ecological sanitation and water harvesting in South Africa., Environ. Sci. Technol., 47(9), 4341–8, doi:10.1021/es304585p, 2013.

Andersson, J. C. M., Andersson, L., Arheimer, B., Bosshard, T., Graham, L. P., Nikulin, G. and E, K.: Experience from Assessments of Climate Change Effects on the Water Cycle in Africa, in Proceedings of the 15th WaterNet/WARFSA/GWP-SA Symposium "IWRM for harnessing socio-economic development in Eastern and Southern Africa," Lilongwe, Malawi., 2014.

ArcSWAT: ArcSWAT |ArcGIS-ArcView extension and graphical user input interface for SWAT, [online] Available from: http://swat.tamu.edu/software/arcswat/ (Accessed 9 July 2015), 2012.

Arnold, J. G., Allen, P. M. and Bernhardt, G.: A comprehensive surface-groundwater flow model, J. Hydrol., 142(1), 47–69 [online] Available from: http://www.sciencedirect.com/science/article/pii/002216949390004S, 1993.

Awotwi, A., Yeboah, F. and Kumi, M.: Assessing the impact of land cover changes on water balance components of White Volta Basin in West Africa, Water Environ. J., n/a–n/a, doi:10.1111/wej.12100, 2014.

Baker, T. J. and Miller, S. N.: Using the Soil and Water Assessment Tool (SWAT) to assess land use impact on water resources in an East African watershed, J. Hydrol., 486, 100–111, doi:10.1016/j.jhydrol.2013.01.041, 2013.

Di Baldassarre, G., Montanari, A., Lins, H., Koutsoyiannis, D., Brandimarte, L. and Blschl, G.: Flood fatalities in Africa: From diagnosis to mitigation, Geophys. Res. Lett., 37(22), L22402, doi:10.1029/2010GL045467, 2010.

Bartholomé, E. and Belward, a. S.: GLC2000: a new approach to global land cover mapping from Earth observation data, Int. J. Remote Sens., 26(9), 1959–1977, doi:10.1080/01431160412331291297, 2005.

Beven, K. and Romanowicz, R.: The uncertainty cascade in flood forecasting, in International conference on innovation advances and implementation of flood forecasting technology, 17 to 19 October 2005, Tromsø, Norway ., p. 9. [online] Available from: http://www.actif-ec.net/conference2005/proceedings/pdf docs/session_04_uncertainty/beven_keith.pdf (Accessed 8 July 2015), 2005.

Bossa, A. Y., Diekkrüger, B., Igué, A. M. and Gaiser, T.: Analyzing the effects of different soil databases on modeling of hydrological processes and sediment yield in Benin (West Africa), Geoderma, 173-174, 61–74, doi:10.1016/j.geoderma.2012.01.012, 2012a.

Bossa, A. Y., Diekkrüger, B., Giertz, S., Steup, G., Sintondji, L. O., Agbossou, E. K. and Hiepe, C.: Modeling the effects of crop patterns and management scenarios on N and P loads to surface water and groundwater in a semi-humid catchment (West Africa), Agric. Water Manag., 115, 20–37, doi:10.1016/j.agwat.2012.08.011, 2012b.

Coles, S., Bawa, J., Trenner, L. and Dorazio, P.: An introduction to statistical modeling of extreme values, Springer London, London, UK., 2001.

Cornelissen, T., Diekkrüger, B. and Giertz, S.: A comparison of hydrological models for assessing the impact of land use and climate change on discharge in a tropical catchment, J. Hydrol., 498, 221–236, doi:10.1016/j.jhydrol.2013.06.016, 2013.

Descroix, L., Genthon, P., Amogu, O., Rajot, J.-L., Sighomnou, D. and Vauclin, M.: Change in Sahelian Rivers hydrograph: The case of recent red floods of the Niger River in the Niamey region, Glob. Planet. Change, 98-99, 18–30, doi:10.1016/j.gloplacha.2012.07.009, 2012.

Descroix, L., Bouzou, I., Genthon, P., Sighomnou, D., Mahe, G., Mamadou, I., Vandervaere, J.-P., Gautier, E., Faran, O., Rajot, J.-L., Malam, M., Dessay, N., Ingatan, A., Noma, I., Souley, K., Karambiri, H., Fensholt, R., Albergel, J. and Olivry, J.-C.: Impact of Drought and Land – Use Changes on Surface – Water Quality and Quantity: The Sahelian Paradox, in Current Perspectives in Contaminant Hydrology and Water Resources Sustainability, edited by P. Bradley, pp. 243–271, InTech, Rijeka, Croatia., 2013.

Doherty, J.: PEST—Model-independent parameter estimation, User Manual, 5th ed., edited by W. N. Computing, Watermark Numerical Computing. [online] Available from: http://www.pesthomepage.org/files/pestman.pdf, 2005.

EEA, (European Environment Agency): Precipitation extremes (CLIM 004), (CLIM 004) [online] Available from: http://www.eea.europa.eu/data-and-maps/indicators/precipitation-extremes-in-europe-2/assessment (Accessed 27 June 2015), 2014.

FAO, IIASA, ISRIC, ISSC and JRC: Harmonized World Soil Database v 1.2, [online] Available from: http://webarchive.iiasa.ac.at/Research/LUC/External-World-soil-database/HTML/, 2012.

Favreau, G., Cappelaere, B., Massuel, S., Leblanc, M., Boucher, M., Boulain, N. and Leduc, C.: Land clearing, climate variability, and water resources increase in semiarid southwest Niger: A review, Water Resour. Res., 45, W00A16, doi:10.1029/2007WR006785, 2009.

Gilleland, E.: extRemes: Extreme Value Analysis, [online] Available from: http://www.assessment.ucar.edu/toolkit/, 2012.

Hargreaves, G. H. and Samani, Z. A.: Estimating Potential Evapotranspiration, J. Irrig. Drain. Div., 108(3), 225–230 [online] Available from: http://cedb.asce.org/cgi/WWWdisplay.cgi?35047, 1982.

Hewitson, B., Lennard, C., Nikulin, G. and Jones, C.: CORDEX-Africa: a unique opportunity for science and capacity building, , 60, 6–7 [online] Available from: http://www.researchgate.net/publication/259813034_CORDEX-Africa_a_unique_opportunity_for_science_and_capacity_building (Accessed 24 June 2015), 2012.

Hijmans, R. J., Cameron, S. E., Parra, J. L., Jones, P. G. and Jarvis, A.: Very high resolution interpolated climate surfaces for global land areas, Int. J. Climatol., 25(15), 1965–1978, doi:10.1002/joc.1276, 2005.

Hirabayashi, Y., Mahendran, R., Koirala, S., Konoshima, L., Yamazaki, D., Watanabe, S., Kim, H. and Kanae, S.: Global flood risk under climate change, Nat. Clim. Chang., 3(9), 816–821, doi:10.1038/nclimate1911, 2013.

Huang, S., Hattermann, F. F., Krysanova, V. and Bronstert, A.: Projections of climate change impacts on river flood conditions in Germany by combining three different RCMs with a regional eco-hydrological model, Clim. Change, 116(3-4), 631–663, doi:10.1007/s10584-012-0586-2, 2012.

Huang, S., Krysanova, V. and Hattermann, F.: Projection of low flow conditions in Germany under climate change by combining three RCMs and a regional hydrological model, Acta Geophys., 61(1), 151–193 [online] Available from: http://link.springer.com/article/10.2478/s11600-012-0065-1 (Accessed 26 April 2015), 2013.

Hurtt, G. C., Chini, L. P., Frolking, S., Betts, R. a., Feddema, J., Fischer, G., Fisk, J. P., Hibbard, K., Houghton, R. a., Janetos, a., Jones, C. D., Kindermann, G., Kinoshita, T., Klein Goldewijk, K., Riahi, K., Shevliakova, E., Smith, S., Stehfest, E., Thomson, a., Thornton, P., van Vuuren, D. P. and Wang, Y. P.: Harmonization of land-use scenarios for the period 1500-2100: 600 years of global gridded annual land-use transitions, wood harvest, and resulting secondary lands, Clim. Change, 109(1-2), 117–161, doi:10.1007/s10584-011-0153-2, 2011.

IPCC: Summary for Policymakers, in The Physical Science Basis. Contribution of Working Group I to the Fifth Assessment Report of the Intergovernmental Panel on Climate Change, edited by StockerT.F., D. Qin, G.-K. Plattner, S. K. A. M. Tignor, A. N. J. Boschung, Y. Xia, V. Bex, and P. M. Midgley, p. 29, Cambridge University Press Cambridge, Cambridge UK. [online] Available from: http://www.climatechange2013.org/images/report/WG1AR5_SPM_FINAL.pdf, 2013.

Jarvis, a, Reuter, H. I., Nelson, a and Guevara, E.: Hole-filled seamless SRTM data V4, Int. Cent. Trop. Agric., available from http://srtm.csi.cgiar.org [online] Available from: http://srtm.csi.cgiar.org/ (Accessed 13 January 2015), 2008.

Jones, C., Giorgi, F. and Asrar, G.: The Coordinated Regional Downscaling Experiment: CORDEX–an international downscaling link to CMIP5, Clivar Exch. [online] Available from: https://scholar.google.de/scholar?hl=en&q=The+Coordinated+Regional+Downscaling+Experiment%3A+CORDEX%2C+An+international+downscaling+link+to+CMIP5%3A+CLIVAR+Exchanges&btnG=&as_sdt=1%2C5&as_sdtp=#0 (Accessed 24 June 2015), 2011.

Jones, R. N.: Managing Uncertainty in Climate Change Projections – Issues for Impact Assessment, Clim. Change, 45(3-4), 403–419, doi:10.1023/A:1005551626280, n.d.

Jury, M. R.: A return to wet conditions over Africa: 1995–2010, Theor. Appl. Climatol., 111(3-4), 471–481, doi:10.1007/s00704-012-0677-z, 2013.

Kim, H.: GSWP3, Glob. Soil Wetness Proj. Phase 3, Surf. Meteorol., 1 [online] Available from: http://hydro.iis.u-tokyo.ac.jp/GSWP3/exp1.html (Accessed 24 April 2015), 2014.

Kim, J., Waliser, D. E., Mattmann, C. A., Goodale, C. E., Hart, A. F., Zimdars, P. A., Crichton, D. J., Jones, C., Nikulin, G., Hewitson, B., Jack, C., Lennard, C. and Favre, A.: Evaluation of the CORDEX-Africa multi-RCM hindcast: systematic model errors, Clim. Dyn., 42(5-6), 1189–1202, doi:10.1007/s00382-013-1751-7, 2013.

Kim, S. H., Edmonds, J., Lurz, J., Smith, S. J. and Wise, M.: The (OECTS)-E-bj framework for integrated assessment: Hybrid modeling of transportation, Energy J., Hybrid Mod(2), 63–91, doi:10.2307/23297046, 2006.

Klein Goldewijk, K., Beusen, A. and Janssen, P.: Long-term dynamic modeling of global population and built-up area in a spatially explicit way: HYDE 3.1, The Holocene, 20(4), 565–573, doi:10.1177/0959683609356587, 2010.

Klein Goldewijk, K., Beusen, A., Van Drecht, G. and De Vos, M.: The HYDE 3.1 spatially explicit database of human-induced global land-use change over the past 12,000 years, Glob. Ecol. Biogeogr., 20(1), 73–86, doi:10.1111/j.1466-8238.2010.00587.x, 2011.

Koch, H., Liersch, S. and Hattermann, F. F.: Integrating water resources management in eco-hydrological modelling, Water Sci. Technol., 67(7), 1525, doi:10.2166/wst.2013.022, 2013.

Krysanova, V., Meiner, A., Roosaare, J. and Vasilyev, A.: Simulation modelling of the coastal waters pollution from agricultural watershed, Ecol. Modell., 49(1), 7–29 [online] Available from: http://www.sciencedirect.com/science/article/pii/0304380089900410, 1989.

Liersch, S., Cools, J., Kone, B., Koch, H., Diallo, M., Reinhardt, J., Fournet, S., Aich, V. and Hattermann, F. F.: Vulnerability of rice production in the Inner Niger Delta to water resources management under climate variability and change, Environ. Sci. Policy, 34, 8–33, doi:10.1016/j.envsci.2012.10.014, 2013.

Moriasi, D. and Arnold, J.: Model evaluation guidelines for systematic quantification of accuracy in watershed simulations, Trans. …, 50(3), 885–900, doi:10.13031/2013.23153, 2007.

Müller, E. N. and Pfister, A.: Increasing occurrence of high-intensity rainstorm events relevant for the generation of soil erosion in a temperate lowland region in Central Europe, J. Hydrol., 411(3-4), 266–278, doi:10.1016/j.jhydrol.2011.10.005, 2011.

Nakicenovic, N. and Swart, R.: Special Report on Emissions Scenarios. [online] Available from: http://adsabs.harvard.edu/abs/2000sres.book.....N%EF%BF%BD%C3%9C (Accessed 14 August 2015), 2000.

Nash, J. E. and Sutcliffe, J. V.: River flow forecasting through conceptual models part I — A discussion of principles, J. Hydrol., 10(3), 282–290, doi:10.1016/0022-1694(70)90255-6, 1970.

Niger Basin Authority: NIGER-HYCOS, [online] Available from: http://nigerhycos.abn.ne/ (Accessed 1 March 2012), 2008.

Nikulin, G., Jones, C., Giorgi, F., Asrar, G., Büchner, M., Cerezo-Mota, R., Christensen, O. B., Déqué, M., Fernandez, J., Hänsler, A., van Meijgaard, E., Samuelsson, P., Sylla, M. B. and Sushama, L.: Precipitation Climatology in an Ensemble of CORDEX-Africa Regional Climate Simulations, J. Clim., 25(18), 6057–6078, doi:10.1175/JCLI-D-11-00375.1, 2012.

O'Gorman, P. A. and Schneider, T.: The physical basis for increases in precipitation extremes in simulations of 21st-century climate change., Proc. Natl. Acad. Sci. U. S. A., 106(35), 14773–7, doi:10.1073/pnas.0907610106, 2009.

Paturel, J.-E., Ouedraogo, M., SERVAT, E., MAHE, G., DEZETTER, A. and BOYER, J.-F.: The concept of rainfall and streamflow normals in West and Central Africa in a context

of climatic variability, Hydrol. Sci. J., 48(1), 125–137, doi:10.1623/hysj.48.1.125.43479, 2003.

R Core Team: R: A language and environment for statistical computing, [online] Available from: http://www.r-project.org/, 2013.

Ramankutty, N.: Croplands in West Africa: A Geographically Explicit Dataset for Use in Models, Earth Interact., 8(23), 1–22, doi:10.1175/1087-3562(2004)8<1:CIWAAG>2.0.CO;2, 2004.

Ramier, D., Boulain, N., Cappelaere, B., Timouk, F., Rabanit, M., Lloyd, C. R., Boubkraoui, S., Métayer, F., Descroix, L. and Wawrzyniak, V.: Towards an understanding of coupled physical and biological processes in the cultivated Sahel – 1. Energy and water, J. Hydrol., 375(1-2), 204–216, doi:10.1016/j.jhydrol.2008.12.002, 2009.

Riahi, K., Grübler, A. and Nakicenovic, N.: Scenarios of long-term socio-economic and environmental development under climate stabilization, Technol. Forecast. Soc. Change, 74(7), 887–935, doi:10.1016/j.techfore.2006.05.026, 2007.

Rodríguez-Rincón, J. P., Pedrozo-Acuña, A. and Breña-Naranjo, J. A.: Propagation of hydro-meteorological uncertainty in a model cascade framework to inundation prediction, Hydrol. Earth Syst. Sci., 19(7), 2981–2998, doi:10.5194/hess-19-2981-2015, 2015.

Roudier, P., Ducharne, A. and Feyen, L.: Climate change impacts on runoff in West Africa: a review, Hydrol. Earth Syst. Sci., 18(7), 2789–2801, doi:10.5194/hess-18-2789-2014, 2014.

Schuol, J., Abbaspour, K. C., Srinivasan, R., Yang, H., Jurgen, S., Karim, C. A., Raghavan, S. and others: Estimation of freshwater availability in the West African sub-continent using the SWAT hydrologic model, J. Hydrol., 352(1-2), 30–49, doi:10.1016/j.jhydrol.2007.12.025, 2008a.

Schuol, J., Abbaspour, K. C., Yang, H., Srinivasan, R. and Zehnder, A. J. B.: Modeling blue and green water availability in Africa, Water Resour. Res., 44(7), n/a–n/a, doi:10.1029/2007WR006609, 2008b.

Séguis, L., Cappelaere, B., Milési, G., Peugeot, C., Massuel, S. and Favreau, G.: Simulated impacts of climate change and land-clearing on runoff from a small Sahelian catchment, Hydrol. Process., 18(17), 3401–3413, doi:10.1002/hyp.1503, 2004.

Sheffield, J., Goteti, G. and Wood, E. F.: Development of a 50-year high-resolution global dataset of meteorological forcings for land surface modeling, J. Clim., 19(13), 3088–3111, doi:10.1175/JCLI3790.1, 2006.

Tarhule, A.: Damaging Rainfall and Flooding: The Other Sahel Hazards, Clim. Change, 72, 355–377, doi:10.1007/s10584-005-6792-4, 2005.

Tarhule, A., Zume, J. T., Grijsen, J., Talbi-Jordan, A., Guero, A., Dessouassi, R. Y., Doffou, H., Kone, S., Coulibaly, B. and Harshadeep, N. R.: Exploring temporal

hydroclimatic variability in the Niger Basin (1901-2006) using observed and gridded data, Int. J. Climatol., 35(4), 520–539, doi:10.1002/joc.3999, 2015.

Trenberth, K.: Changes in precipitation with climate change, Clim. Res., 47, 123–138, doi:10.3354/cr00953, 2011.

Tschakert, P., Sagoe, R., Ofori-Darko, G. and Codjoe, S. N.: Floods in the Sahel: an analysis of anomalies, memory, and anticipatory learning, Clim. Change, 103(3-4), 471–502, doi:10.1007/s10584-009-9776-y, 2010.

Vetter, T., Huang, S., Aich, V., Yang, T., Wang, X., Krysanova, V. and Hattermann, F.: Multi-model climate impact assessment and intercomparison for three large-scale river basins on three continents, Earth Syst. Dyn., 5(1), 17–43, doi:10.5194/esd-6-17-2015, 2014.

Vetter, T., Huang, S., Aich, V., Yang, T., Wang, X., Krysanova, V. and Hattermann, F.: Multi-model climate impact assessment and intercomparison for three large-scale river basins on three continents, Earth Syst. Dyn., 6(1), 17–43, doi:10.5194/esd-6-17-2015, 2015.

Weedon, G. P., Gomes, S., Viterbo, P., Shuttleworth, W. J., Blyth, E., Österle, H., Adam, J. C., Bellouin, N., Boucher, O. and Best, M.: Creation of the WATCH Forcing Data and Its Use to Assess Global and Regional Reference Crop Evaporation over Land during the Twentieth Century, J. Hydrometeorol., 12(5), 823–848, doi:10.1175/2011JHM1369.1, 2011.

Weedon, G. P., Balsamo, G., Bellouin, N., Gomes, S., Best, M. J. and Viterbo, P.: The WFDEI meteorological forcing data set: WATCH Forcing Data methodology applied to ERA-Interim reanalysis data, Water Resour. Res., n/a–n/a, doi:10.1002/2014WR015638, 2014.

Wendling, U. and Schellin, H.: Neue Ergebnisse zur Berechnung der potentiellen Evapotranspiration, Zeitschrift für Meteorol., 36(3), 214–217 [online] Available from: http://cat.inist.fr/?aModele=afficheN&cpsidt=8792552 (Accessed 26 April 2015), 1986.

Willgoose, G. R., Bras, R. L. and Rodriguez-Iturbe, I.: A physical explanation of an observed link area-slope relationship, Water Resour. Res., 27(7), 1697–1702, 1991.

Williams, J. R., Renard, K. G. and Dyke, P. T.: EPIC: A new method for assessing erosion's effect on soil productivity, J. Soil Water Conserv., 38(5), 381–383 [online] Available from: http://www.jswconline.org/content/38/5/381.short (Accessed 26 April 2015), 1983.

Zwarts, L.: Will the inner Niger delta shrivel up due to climate change and water use upstream. A & W report 1537, Feanwâlden. [online] Available from: http://www.wetlands.org/Portals/0/publications/Report/Will the Inner Niger Delta shrivel up due to climate change and water use upstream.pdf (Accessed 11 November 2013), 2010.

8. DISCUSSION AND CONCLUSIONS

The discussion and conclusions integrate the findings of the individual analysis from the antecedent Chapters 2 to 7 and relate them to the research questions. The results are put into the general context of the increasing flood risk and the current state of the research in the respective fields. The chapter is structured following the four main points of the research strategy introduced in Chapter 1.3.: analysis, attribution, projections and recommendations. Finally, the overall conclusions summarize this thesis´ findings and a short outlook presents potential future assessments of flooding in the NRB.

8.1. Analysis: Features of the changes in flood risk

Catastrophic flooding in the NRB is not a new phenomenon and has always been known. Still, the frequency and the impact of the catastrophic events have increased drastically over the past two decades.

Flood risk is commonly defined as a product of hazard, exposure, and vulnerability (1 and Figure 64). Research has shown that exposure and vulnerability have increased in the NRB. Particularly the extreme population growth has led to increased exposure. The work of Di Baldassarre et al. (2010) has shown that a kind of "levee-effect" increased vulnerability in the NRB, even absent the construction of levees. The "levee-effect" describes the fact that dams, levees, and other flood protections may actually increase flood losses because they encourage new development and settlement in the floodplain. When man-made flood protections fail in an extremely high flood, damages are higher than they would have been, had the protective measures not been installed (Baldassarre and Viglione, 2015). In the context of the Niger, research has shown that the extreme natural variability with its fluctuation of wet and dry periods has caused this effect. During the dry 1970s and 1980s, people settled in flood plains and other places that have traditionally been avoided for settlement due to flood risk.

With regard to the hazard, the annual peak discharge time series were analyzed in order to detect trends or changes in variance. Since the 1990s, peak discharges of floods recovered throughout the basin compared to the previous dry period. Particularly in the dry Sahelian part of the basin, the trends were extreme at the Niger itself and also at its tributaries (see Chapters 2 and 3). An additional statistical analysis of changes in the distribution of flood peaks revealed that, for the Guinean and also the main stem of the Niger in the Sahelian and Sudanian parts, the above-mentioned increase was linear and did not change the form of the distribution but only the magnitudes. The analysis showed that only at the tributaries in the Sahelian part, the distribution did change to a longer tail, indicating that especially the extreme flood peaks have increased over the past two decades (see Chapters 2 and 3).

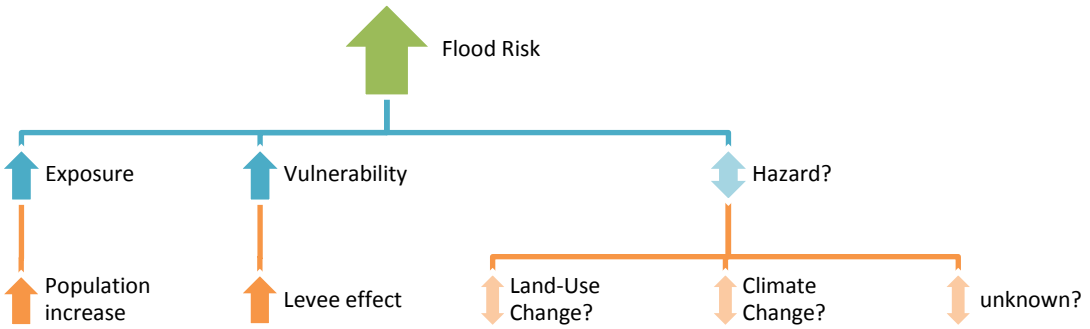

Figure 64 Schematic representation of the causal chain leading to the increase in flood risk in the Niger River Basin, including the unknown consequences of hazard and it´s influencing factors.

The results contained in the present thesis consequently demonstrated and proved that also the hazard itself, i.e. flood magnitudes and frequencies, has changed and contributed to the observed increase in flood risk. The threefold effect of increasing exposure, vulnerability and hazard can explain the extreme increase in catastrophic flooding in the NRB (Figure 64). This holds particularly for the extreme increase in the dry Sahelian and Sudano-Sahelian parts, where the flood magnitudes and the population density increased the most. The reasons for this increase in flood magnitude and the change in variance for some gauges are discussed in the following chapter.

8.2. Attribution: Drivers of the changes in the flood regime

The studies from Chapters 3, 4 and 7 provide answers to the question investigating why peak discharges have increased since the 1990s, as found during the analysis (Chapter 2, Figure 64).

Several studies argue that LULC effects are the main or single cause of the increase in flood magnitudes and frequency in the Sahelian part of the Niger (e.g. Amogu et al., 2010; Descroix et al., 2012, 2013). They describe a chain of LULC processes, such as deforestation, savannah degradation, or increased agricultural production, that are usually related to land degradation and result in sealed soils and crusting and, hence, a reduction in infiltrability. This again leads to increased surface run-off and then to increasing peak flows in the area. Since the analyses in this thesis show mainly increasing precipitation trends until recently (e.g. Figure 59), an attribution study was undertaken in order to determine to what extent LULC and/or climatic changes influenced the peak flows in the NRB.

The attribution followed the approach of Merz et al. (2012), who proposed a framework to attribute trends based on the evidence of consistency, the evidence of inconsistency and the provision of a confidence level. In a data-based approach, presented in the appendix to Chapter 3, a strong consistency between the long term precipitation trends and peak flows could be detected. After the wet 1960s with high peak flows, both precipitation and peak

flows decreased until the end of the 1980s, only to increase again from the beginning of the 1990s (Figures Figure 10 and Figure 18). This parallel is also supported by a significant correlation analysis (Table S 1). This proof of consistency indicates that precipitation variation is a driver of the peak flows´ long-term dynamics.

In order to check the consistency or inconsistency, respectively, of LULC, flashiness of discharge was used as a proxy for the influence of LULC on the hydrology. The test is based on the hypothesis that the impacts of the LULC processes that lead to increased surface-runoff subsequently result in increased heightened flashiness. This increase can indeed be detected for the Upper and Middle Niger, with statistically significant trends beginning in the 1960s (Figure S 8). For other parts of the Niger, appropriate data was not available. These trends show, however, a continuous increase until the recent past without following the decrease in peak flows during the 1970s and 1980s. These partly opposite trends can be interpreted as indicating an inconsistency in LULC changes and flood trends. This implies eventually that the climatic driver seems at least to have more influence on the trend than LULC. Still, the uncertainty of data-based attribution is high and a definite attribution is not possible.

The substantial degree of uncertainty resulting from the use of the data-based approach is particularly evident in a data-scarce region like the NRB. In addition, a quantification of the drivers´ influence is not possible under a data-based method. In order to get more robust results, the simulation-based attribution approach is also applied to the Sahelian part of the Niger and its tributaries (Chapter 4). The eco-hydrological model SWIM was driven by reanalysis climate data. For LULC changes, one run was performed using stable LULC as of 1950 as well as a control run with dynamic LULC changes according to observed changes between 1950 and 2010. Under ideal modelling conditions, this experimental set-up allows the identification of the role of climatic changes and LULC, and even a quantification of the share of the LULC changes´ influence on the peak flows against the influence of the climatic trend. For one subcatchment of the region, the results of the experiment indicate that LULC and climatic changes contribute in roughly equal shares to the observed increase in flooding. For the other parts of the region, the results are less clear but show that climatic changes and LULC are drivers for the flood increase, although their shares cannot be quantified.

The simulation-based approach is also connected with considerable uncertainty, as discussed comprehensively in Chapter 4.3.3. The results strongly depend on the model efficiency, and on the quality of the data for the past LULC changes. Still, this approach has proven to be a more robust and efficient way to attribute changes in AMAX than the data-based approach. In this study, both approaches yielded to similar results regarding the general influence of both, climate and LULC changes, while the data-based approach underestimated the influence of LULC.

By combining these findings with the results given Chapter 7.3, where the effects of the projected LULC and climatic changes have been tested for the whole NRB, an additional conclusion can be drawn. The study showed that the effects of LULC are particularly high in the dry regions of the NRB, i.e. in the Sahelian and Sudano-Sahelian zones. It can be assumed that this finding also holds for the past. It also confirms the finding of the data-based attribution approach, namely the conclusion that in the wetter regions like the Upper NRB, climatic trends and natural variability have more influence on the peak flows than LULC changes.

8.3. Projections: Expected changes in the flood regime

The analyses and attribution studies help to understand the characteristics and causes of the observed flood hazard increase in the NRB in the recent past. However, the knowledge gathered by these analyses is, in and by itself, insufficient for the purposes of reducing flood risk in the future. It is also necessary to anticipate future changes in flood hazard increase, in order to determine how to prepare for and ultimately react to it. A widespread method for anticipating future changes, in order to determine the appropriate measures thereto, is hydrological modelling. Model results, however, are meaningless if they do not include a confidence level, i.e. an estimation of uncertainty, allowing to judge the reliability of their results.

In Chapter 5, the uncertainty levels of climate impact studies was analyzed for the Upper Niger Basin, quantifying the share of different factors (such as emission scenarios and hydrological and climate models – both global and regional) in the existing uncertainty. For the high flows (Q_{10}), the complete known uncertainty results almost exclusively of the climate models, whereas the global models are distinctly more relevant than the regionalization (Figures Figure 44 and Figure 45). The dominance of climate can be explained by the monsoonal type of climate in the NRB. During the rainy season, with high and intense precipitation, the Earth System Models (ESM) dominate river runoff and thus also the total uncertainty. Differences between the hydrological models have little influence, probably due to the relatively simple rainfall-runoff processes in the catchment during the rainy season.

In Chapter 6, the uncertainty derived from the climate models is the subject of further analysis. Nineteen different ESMs were evaluated for the NRB of five were finally used for driving simulations with the eco-hydrological model SWIM. For precipitation, even the future direction of the trend is highly uncertain. During the rainy season when flood peaks occur, most of the models project an increase in precipitation, but some of them also a decrease therein. Only in terms of temperature do all models agree, projecting an increase of, approximately, between 3 °C and 6 °C at the end of the 21st century (depending on the emission scenario and model) compared to a base period at the end of the 20th century. A special feature of the NRB with regard to climatological uncertainty is the high natural

variability, as explained in Chapter 2. According to Janicot et al. (2011), nowhere in the world has a natural variability of similar dimensions been observed during the 20th century. The droughts in the 1970s and 1980s demonstrated that these decadal and sub-decadal climatic variations are probably more important than long-term trends. During the dry period in the 1970s and 1980s no major flooding was reported, a fact confirmed by the AMAX time series. This implies that even if models project a tendency towards a reduction or increase in precipitation, internal variability will probably be the dominant feature, also with regard to flood regime.

The attribution studies showed clear evidence that both LULC and climatic changes have contributed to the increasing flood peaks in the NRB in the recent past. Therefore, LULC processes have also been included in the projections where they add additional uncertainty to the already-known uncertainties resulting from emission scenarios, global and regional climate models, and hydrological models. The uncertainty brought about by LULC stems from the scenario considered, but also, to a large extent, from the way in which LULC processes are represented in the model. In addition to this already large and significant known uncertainty, the unknown uncertainty should also be kept in mind. The lesson extracted from this consideration of uncertainty is modelling results should be interpreted very carefully; over-interpretation, for example, of the exact quantification of changes must be avoided. Still, most results clearly stand out from the white noise; moreover, knowledge of uncertainty levels and causes can also help to design strategies for how to cope with the increasing flood hazards. The results of the projections of future flood hazard in the NRB contained in Chapters 5 to 7 can be summarized in four key findings:

(1) Most of the climate projections for the NRB display a general tendency towards wetter conditions, whilst the high decadal variability is projected to continue in the 21st century. The increase in precipitation appears stronger in the emission scenarios featuring business-as-usual emission trends (RCP 8.5) than in low-emission /stabilization scenarios (RCP 2.6 and 4.5). Heavy precipitation events are projected to increase more sharply than the mean annual precipitation.
(2) These general climatic trends are echoed by the discharge trends for high and annual peak flows. However, the effect of the emission scenarios is inverted. The higher temperature increases of the high-end emission scenarios are projected to enhance evapotranspiration, which again reduces peak flows. Therefore, despite lower precipitation, the limited emission scenarios lead to higher discharges than the business-as-usual scenarios, despite the fact that they feature higher precipitation levels.
(3) Hydrological sensitivity to climatic and LULC changes is distinctly higher in the dry Sahelian and Sudano-Sahelian zones than in the wetter subregions of the NRB.

(4) The effects of LULC on flood magnitudes are generally weaker than those of the projected trends of climate change, but they are still substantial. Extension of agricultural areas leads to higher peak flows whilst regreening reduces the flood magnitudes.

8.4. Recommendations for reducing the flood risk

The conclusions of the individual studies presented here provide a broad basis for recommendations regarding the flood hazard in the NRB. The assessment of vulnerability and exposure are at least as important for adaptation and mitigation of flood risk as of the hazard. This work, however, focuses mainly on the flood hazard in the NRB, a focus these recommendations share as well. The recommendations mainly address research (Recommendations 1 - 5) and policy (Recommendations 6 - 9). Based on the presented assessment of the flood risk in the NRB the following recommendations have been derived:

(1) Modelling

Faced with growing numbers of people affected, research on flood risk in the NRB is deficient. Whilst time series analysis and research on the characteristics of changes in the discharge regime gained some attention in recent years, comprehensive attribution has not. Therefore, this work could only provide an initial assessment of the influence of LULC and climate in the NRB. A robust attribution analysis is a basis for solid adaptation and mitigation efforts, since only with this knowledge can the causes and characteristics of the increasing flood hazard be approached appropriately. Modelling proved to be a promising approach for understanding the drivers of the changing flood hazard. With regard to the individual processes affecting the hydrological system, modelling might be very effective when coupled with field experiments. Especially, awareness of temporal and spatial patterns of flood hazard changes and research on specific transformations and degradations of landscapes are crucial for improving landscape planning and flood mitigation policies.

(2) Prioritizing research on land use impacts

As for of prioritizing research in different fields, LULC seems most promising, compared to common climate impacts. Whilst state-of-the-art climate models and hydrological models are currently at a stage where even small improvements and reductions of uncertainty are connected to extreme efforts in model development, the amount of required work and/or measures to improve a LULC model or the LULC component of an existing model are distinctly fewer.

Due to the large uncertainty in climatic trends under climate change, projections on the impact of LULC changes are still affected by the uncertainty of the climate

models. Therefore, climate data of the 20th century might be an alternative. The large natural variability of the climate with its distinct decadal and sub-decadal variability already includes a wide range of climatic conditions and could be used for adaptation-testing studies. By these means, adaptation measures could be tested for their suitability for flooding (e.g. with climate forcing of the 1960s) as well as droughts (e.g. with climate forcing input of the 1970/1980s) using modelling approaches.

(3) Considering natural variability

The uncertainty analysis has shown that beside the LULC component, climate models entail the highest uncertainty. It is unlikely that climate models will substantially improve during the next few years. In order to bypass this bottleneck, the focus of hydro-climatologic research and adaptation in the NRB should consider the region´s large natural variability. Great steps have been made in the recent past in the understanding of the phenomenon (Dieppois et al., 2013; Nicholson, 2013) and climate models are able to reproduce the patterns (Gbobaniyi et al., 2014). Still these decadal patterns are not included in projections. Paeth and Hense (2002) explained how different starting conditions of a climatological model can lead to diverging results, reflecting in part the natural variability of the climatic system. This effect should also be taken into account when analyzing the West African climate in contrast to the current approach, which relies on ensembles of individual model runs. Experiments with several runs of each model would allow quantification of the natural variability, which would contribute to the understanding of this factor's role – particularly in the case of the NRB, where currently the effects of natural variability seem to be more significant than the repercussions of climate change.

(4) Climate forecasting

Another approach might result from the growing understanding of the processes and underlying mechanism of the West African Monsoon system as illustrated by the African Monsoon Multidisciplinary Analysis (AMMA) project (Hourdin et al., 2010; Ruti et al., 2011). This knowledge might allow for a long-term forecasting of the decadal but also sub-decadal patterns, and would be a milestone towards not only the improvement of the regional flood policy, but also the region´s ability to prepare for droughts and famines.

(5) Integrative and transdisciplinary understanding of flooding

As stated in the beginning, vulnerability and exposure have not been examined in the present thesis. Future studies should, if possible, include these dimensions, since particularly the expected population growth will most likely be the most prominent "game-changer" for livelihoods in West Africa in almost all aspects. The effects of climate and LULC changes on flooding, however, will most likely aggravate the already existing deficit in adaptation to flooding.

Flood policy is commonly part of a broader disaster risk reduction (DRR) policy encompassing all relevant threats. This implies that policy makers require information on all the relevant risks of a region in order to objectively judge the trade-offs in DRR, to prioritize DRR and to create synergies for DRR. An exclusive focus on flood risk would neglect the fact that droughts might affect the life and livelihoods of the population more than floods; all things considered, the construction of a reservoir might help to avoid a future famine as well as reduce future flood risk downstream. This work´s recommendations must therefore not be considered as guidelines or even instructions on how to reduce flood risk, but rather as proposals that should be included in the broader overview of risks in the region.

(6) Public awareness

The recent, general trend of a return to wet conditions in West Africa and a related increase in catastrophic flooding is widely known amongst the local population and also to the respective experts of the global research community. As described in chapter 1.5.7, there exist certain initiatives as to reduce flood risk in the NRB. However, in terms of global awareness and willingness to donate, flooding in the NRB is widely neglected in the face of the dominant drought and famine hazards, which are part of the still widespread “desertification narrative”. Considering the high number of victims during the last decade, and taking into account the fact that floods may also damage food production systems, resulting in food shortages and famines, public awareness of floods as the “other hazard” in West Africa should be systematically raised. Particularly in the face of the current debate on migration from the developing world into the developed world, flood risk in the NRB should receive more attention since it contributes to the deterioration of livelihoods and hinders development.

(7) Technical and institutional adaptation

Conventional technical measures against catastrophic flooding are still rare in the NRB. Five larger reservoirs exist (see Chapter 7) which have proved to be useful against catastrophic flooding. They mostly serve also other functions like for irrigation or generating power and can therefore be categorized as “win-win” adaptation actions that come with other social, economic and/or environmental benefits. However, the impacts of hydrological infrastructures are debated since their side effects often include negative repercussions on the local ecology and livelihoods (e.g. Zwarts et al., 2005). For instance, the inadequate regulation of the Lagdo reservoir in Cameroon has been responsible for repeated flooding in the downstream area of the Benue River, especially in Nigeria around Lokoja (Odunuga et al., 2015). In sum, although these engineering solutions are useful, they should be planned and implemented with caution. Another main technical adaptation measure

is a functional Flood Early Warnings System, which is currently under development but should be extended (Chapter 1.5.7).

Other measures such as, awareness-raising campaigns and a "flood-smart" settlement policy come with generally lower cost. These kinds of measures usually belong to the so-called "no-regret" adaptation actions. They are especially valuably under high uncertainty as in regard of flooding in the NRB. They include actions that do not involve trade-offs with other policy objectives. A precondition for this kind of measures is mainstreaming and integration of flood policy in the broader perspective of infrastructure investments, economic development and other institutional aspects.

(8) Flood-smart land use policy

Despite flood magnitudes' general tendency to further increase with a substantial probability in the NRB, there are also positive implications amongst the results. The fact that regreening and/or smart land-use policy can reduce flood magnitudes constitutes an opportunity for regional policy. Interesting in this regard is the finding that the "optimistic" emission scenarios are projected to lead to a more moderate climatic change, but still come with higher flood magnitudes than the "pessimistic" scenarios. For the high-emission scenarios, the higher temperatures reduce the peak flows via enhanced evapotranspiration. This trade-off is even more pronounced when taking into account that the LULC scenarios related to the "optimistic" emission scenarios project a regreening in the NRB. This regreening, however, cannot reduce the flood magnitudes to the same extent as the climatic changes will increase them. Following the modelling results, an ideal flood policy for the NRB would combine a local regreening with stronger emissions. This is misleading, however, since other effects of increasing temperatures are completely neglected in the projections. Besides other negative effects of increasing temperatures, the likelihood of fundamental and irreversible changes to the ecosystems implies that sustainable regreening might become impossible.

(9) Regional differentiation and prioritization of adaptation

Another main recommendation derived from the results of all individual analyses is a strong regional differentiation in flood policy in the NRB. Particularly the highly vulnerable and flood-prone dry areas of the Sahel and Sudano-Sahelian zones will very likely experience future changes. Particularly, in the context of a trade-off between flood mitigation (regreening) and expansion of agricultural areas, necessary to nourish the increasing population, this spatial heterogeneity should be taken into account. It is in the dry areas where the increase in flood magnitudes due to climate change is projected to be the most severe. At the same time, these are also other areas, where flood mitigation via sustainable land use policy would be the most effective. Since agricultural production in these areas is limited to the semi-arid conditions anyway, a regreening might be reasonable here, despite the need for

an intensification of agriculture. In other areas like the Upper Niger Basin, a regreening would have less effect; sustainable and smart agriculture might provide more advantages than reducing flood magnitudes through reforestation.

8.5. Overall Conclusions

Catastrophic flooding has become a regular and virtually ubiquitous threat in the NRB during the past decade. The annual flooding from tropical rivers in the region is increasing; not only the mean discharge, but also the extremes have rised. This "return to wet conditions" in West Africa after the dry periods in the 1970s and 1980s comes with several positive effects, but also leads to a rise in flood risk.

This process is driven not only by climatic changes, but also by human impact on the hydrology via LULC. For example, the degradation of the savannah and the increase in agriculturally exploited areas have led to more direct run-off and an increase of discharge. Simulation experiments for the Sahelian part of the NRB have shown that the effect of the LULC can contribute up to over 50% of the increase in flood trends, particularly in very dry regions. In these areas of the basin, the combined effects of climatic and LULC drivers have led to a very distinct increase in flood magnitudes, which is also noticeable in the above-average increase in the number of people affected by catastrophic floods in these subregions.

Simulations of future flood regimes project a continuity of these trends. The regional natural variability with its highly variable multi-annual frequency of dry and wet periods is projected to continue during the next century, although without a coherent pattern across the models. Most of the dynamically and statistically downscaled climate simulations reflect continuing variability but also show a further long-term wetting trend. This means that especially during wet periods, like the current one, the likelihood of extreme flood magnitudes in the NRB will rise.

LULC influences these trends and such measures as smart landscape planning can mitigate flood peaks while bad agricultural practices and further land degradation will likely lead to a further increases in flood peaks. Still, even very effective and major mitigation measures and initiatives will only be able to reduce extreme flood magnitudes in the future, not being capable of preventing them completely. Therefore, further research on the risks and adaptation measures at all levels of disaster risk reduction is needed, especially in the highly vulnerable and most greatly affected dry regions of the NRB.

8.6. Outlook

During the 21st United Nations Climate Change Conference of Parties (the COP 21 in Paris), the member nations of the NBA (Niger, Ivory Coast, Cameroon, Nigeria, Togo, Chad, Benin, Burkina Faso, and Guinea) held a press conference on "Niger River Basin Climate Resilience" (COP21, 2015). They announced several large-scale future

investments in the basin, including measures against catastrophic flooding. This positive message, however, was apparently of interest to very few journalists. Still, even if the public awareness and media coverage of floodings in the NRB is still very low compared to the desertification narrative, for example, the investments in flood adaptation in the NRB supported by several international stakeholders such as Kreditanstalt für Wiederaufbau (KfW) constitute steps in the right direction. Ideally, these regional political initiatives should be accompanied by and based on scientific research allowing for a determination of the types of adaptation/flood mitigation measures that are needed/reasonable for each section of the river, taking into account natural climatic variability, climate change, LULC changes and all other relevant factors like demographic growth and vulnerability.

This large variety of variables results in a very high degree of complexity, which necessitates transdisciplinary approaches to research. The present thesis has revealed many gaps in existing knowledge, which could be filled by standard research employed in many nations, e.g. in Europe, even though data deficits and difficult infrastructure complicate and hinder research in the NRB. Due to the considerable geographic heterogeneity in the basin, detailed studies for different regions are needed; especially, human influence and LULC changes should be the focus of future research. In addition, natural variability is a significant factor in the climate of the NRB, and its interaction with the influence of climate change should be considered by climate impact scientists.

As for adaptation, initiatives such as the installation of a functioning Early Warning System (as planned) and a "flood-smart" settlement policy taking into account the changing risk situation would help to reduce the loss of lives and damages in exchange for relatively minor investments. Regarding the extreme demographic growth and the very likely deterioration of the region´s environment and climatic conditions, a comprehensive strategy on flood risk reduction in the NRB would also contribute to reducing the expected environmentally-induced migration. Therefore, not only scientists and regional policy makers, but also the relevant international stakeholders, particularly in the EU, should be involved in the development of a comprehensive flood DRR strategy for the NRB.

9. References

Albergel, J.: Sécheresse, désertification et ressources en eau de surface. Application aux petits bassins du Burkina Faso, in The Influence of Climate Change and Climatic Variability on the Hydrologie Regime and Water Resources (Proceedings of the Vancouver Symposium, August 1987)., vol. 168, pp. 355–445, IAHS Publication. [online] Available from: http://itia.ntua.gr/hsj/redbooks/168/hysj_168_01_0355.pdf (Accessed 6 February 2014), 1987.

Aletan, A., Martins, O. and Idowu, O.: Mitigating the effects of floods and erosion in the Niger south catchment area through integrated flood management (IFM), Coler. Proc. [online] Available from: http://journal.unaab.edu.ng/index.php/COLERM/article/view/258 (Accessed 27 October 2015), 2012.

Amogu, O., Descroix, L., Yéro, K. S., Le Breton, E., Mamadou, I., Ali, A., Vischel, T., Bader, J.-C., Moussa, I. B., Gautier, E., Boubkraoui, S. and Belleudy, P.: Increasing River Flows in the Sahel?, Water, 2(2), 170–199, doi:10.3390/w2020170, 2010.

Andersen, I., Dione, O., Jarosewich-Holder, M. and Olivry, J.-C.: The Niger Basin: a vision for sustainable management, edited by K. G. Golitzen, World Bank Publications, Washington DC. [online] Available from: http://siteresources.worldbank.org/INTWAT/Resources/4602114-1206643460526/Niger_River_Basin_Vision_Sustainable_Management.pdf (Accessed 11 November 2013), 2005.

Baldassarre, G. Di and Viglione, A.: Debates—Perspectives on sociohydrology: Capturing feedbacks between physical and social processes, Water Resour. … [online] Available from: http://onlinelibrary.wiley.com/doi/10.1002/2014WR016416/full (Accessed 27 October 2015), 2015.

Di Baldassarre, G., Montanari, A., Lins, H., Koutsoyiannis, D., Brandimarte, L. and Blschl, G.: Flood fatalities in Africa: From diagnosis to mitigation, Geophys. Res. Lett., 37(22), L22402, doi:10.1029/2010GL045467, 2010.

Black, R., Adger, W. N., Arnell, N. W., Dercon, S., Geddes, A. and Thomas, D.: The effect of environmental change on human migration, Glob. Environ. Chang., 21, Supple(0), S3–S11, doi:10.1016/j.gloenvcha.2011.10.001, 2011.

Breunig, P.: Nok: African sculpture in archaeological context, Africa Magna, 2014.

Collins, R. O. and Burns, J. M.: A History of Sub-Saharan Africa, Cambridge University Press., 2013.

COP21: UNFCCC Webcast - Paris COP 21: Niger River Basin Climate Resilience Investment Plan, UNFCCC Webcast [online] Available from: https://unfccc6.meta-fusion.com/cop21/events/2015-12-01-14-00-niger-ivory-coast-cameroon-nigeria-togo-chad-benin-burkina-faso-guinea-niger-river-basin-climate-resilience-investment-plan (Accessed 4 December 2015), 2015.

Descroix, L., Genthon, P., Amogu, O., Rajot, J.-L., Sighomnou, D. and Vauclin, M.: Change in Sahelian Rivers hydrograph: The case of recent red floods of the Niger River in the Niamey region, Glob. Planet. Change, 98-99, 18–30, doi:10.1016/j.gloplacha.2012.07.009, 2012.

Descroix, L., Bouzou, I., Genthon, P., Sighomnou, D., Mahe, G., Mamadou, I., Vandervaere, J.-P., Gautier, E., Faran, O., Rajot, J.-L., Malam, M., Dessay, N., Ingatan, A., Noma, I., Souley, K., Karambiri, H., Fensholt, R., Albergel, J. and Olivry, J.-C.: Impact of Drought and Land – Use Changes on Surface – Water Quality and Quantity: The Sahelian Paradox, in Current Perspectives in Contaminant Hydrology and Water Resources Sustainability, edited by P. Bradley, pp. 243–271, InTech, Rijeka, Croatia., 2013.

Diallo, I. and Sylla, M.: Multimodel GCM-RCM ensemble-based projections of temperature and precipitation over West Africa for the early 21st century, Int. J. Climatol., 2012.

Diallo, I., Sylla, M., Camara, M. and Gaye, A.: Interannual variability of rainfall over the Sahel based on multiple regional climate models simulations, Theor. Appl., 2013.

Dieppois, B., Diedhiou, A., Durand, A., Fournier, M., Massei, N., Sebag, D., Xue, Y. and Fontaine, B.: Quasi-decadal signals of Sahel rainfall and West African monsoon since the mid-twentieth century, J. Geophys. Res. Atmos., 118(22), 12,587–12,599, doi:10.1002/2013JD019681, 2013.

Druyan, L. M.: Studies of 21st-century precipitation trends over West Africa, Int. J. Climatol., 31(10), 1415–1424, doi:10.1002/joc.2180, 2011.

Falloon, P. D. and Betts, R. A.: The impact of climate change on global river flow in HadGEM1 simulations, Atmos. Sci. Lett., 7(3), 62–68, doi:10.1002/asl.133, 2006.

FAO: Sahel Weather and crop situation report, Report No. 2, 16 July 2004. [online] Available from: ftp://ftp.fao.org/docrep/fao/007/J2780e/J2780e00.pdf, 2004.

Ferguson, W.: Integrating crops and livestock in West Africa, FAO Anim. Prod. Heal. Pap., 41, 112 [online] Available from: http://www.fao.org/docrep/004/x6543e/x6543e00.htm, 1983.

Fontes, J.-C., Andrews, J. N., Edmunds, W. M., Guerre, A. and Travi, Y.: Paleorecharge by the Niger River (Mali) Deduced from groundwater geochemistry, Water Resour. Res., 27(2), 199–214, doi:10.1029/90WR01703, 1991.

Gbobaniyi, E., Sarr, A., Sylla, M. B., Diallo, I., Lennard, C., Dosio, A., Dhiédiou, A., Kamga, A., Klutse, N. A. B., Hewitson, B., Nikulin, G. and Lamptey, B.: Climatology, annual cycle and interannual variability of precipitation and temperature in CORDEX simulations over West Africa, Int. J. Climatol., doi:10.1002/joc.3834, 2013.

Gbobaniyi, E., Sarr, A. and Sylla, M.: Climatology, annual cycle and interannual variability of precipitation and temperature in CORDEX simulations over West Africa, Int. Jour. Clim., 2014.

GIZ, G. für I. Z.: Transboundary disaster risk management along the Niger River in Niger and Mali, [online] Available from: http://www.giz.de/en/worldwide/23292.html (Accessed 27 October 2015), 2013.

Gramont, S. De: Strong Brown God: The Story of the Niger River., 1991.

GRDC: BfG The GRDC - Global Runoff Database, [online] Available from: http://www.bafg.de/nn_266934/GRDC/EN/01__GRDC/03__Database/database__node.html?__nnn=true, 2013.

Hargreaves, G. H. and Samani, Z. A.: Estimating Potential Evapotranspiration, J. Irrig. Drain. Div., 108(3), 225–230, 1982.

Hashizume, M., Wagatsuma, Y. and Faruque, A.: Factors determining vulnerability to diarrhoea during and after severe floods in Bangladesh, J. Water Health, 2008.

Herodotus: Book IV, Melpomene, edited by G. Rawlinson. [online] Available from: http://classics.mit.edu/Herodotus/history.4.iv.html, n.d.

Hogan, C. M.: Ecoregions of the Niger River Basin, [online] Available from: http://www.eoearth.org/view/article/51cbfad67896bb431f6be272, 2013.

Hourdin, F., Musat, I., Grandpeix, J.-Y., Polcher, J., Guichard, F., Favot, F., Marquet, P., Boone, A., Lafore, J.-P., Redelsperger, J.-L., Ruti, P. M., Dell'aquila, A., Filiberti*, M.-A., Pham, M., Doval, T. L., Traore, A. K. and Gallée, H.: AMMA-Model Intercomparison Project, 2010.

IPCC: Managing the Risks of Extreme Events and Disasters to Advance Climate Change Adaptation. A Special Report of Working Groups I and II of the Intergovernmental Panel on Climate Change, edited by C. B. Field, V. Barros, T. F. Stocker, D. J. D. Qin, Dokken, K. L. Ebi, M. D. Mastrandrea, K. J. Mach, G.-K. Plattner, S. K. Allen, M. Tignor, and P. M. Midgley, Cambridge University Press, Cambridge, UK, and New York, NY, USA., 2012.

Jäger, M. and Menge, S.: The Niger River. [online] Available from: http://splash-era.net/downloads/groundwater/7_NBA_final_report.pdf, 2012.

Janicot, S., Lafore, J.-P. and Thorncroft, C.: The West African Monsoon, in The Global Monsoon System: Research and Forecast, edited by C.-P. Chang, Y. Ding, G. N.-C. Lau, R. H. Johnson, B. Wang, and T. Yasunari, pp. 111–135, World Scientific. [online] Available from: https://books.google.com/books?id=DR-7CgAAQBAJ&pgis=1 (Accessed 23 October 2015), 2011.

Jury, M. R.: A return to wet conditions over Africa: 1995–2010, Theor. Appl. Climatol., 111(3-4), 471–481, doi:10.1007/s00704-012-0677-z, 2013.

Kamga, F.: Impact of greenhouse gas induced climate change on the runoff of the Upper Benue River (Cameroon), J. Hydrol. [online] Available from: http://www.sciencedirect.com/science/article/pii/S0022169401004450 (Accessed 14 December 2015), 2001.

Kaptué, A. T., Prihodko, L. and Hanan, N. P.: On regreening and degradation in Sahelian watersheds., Proc. Natl. Acad. Sci. U. S. A., 112(39), 12133–8, doi:10.1073/pnas.1509645112, 2015.

Klutse, N., Sylla, M., Diallo, I. and Sarr, A.: Daily characteristics of West African summer monsoon precipitation in CORDEX simulations, Theor. Appl. … [online] Available from: http://link.springer.com/article/10.1007/s00704-014-1352-3 (Accessed 2 December 2015), 2015.

Kron, W.: Flood Risk = Hazard • Values • Vulnerability, Water Int., 30(1), 58–68, doi:10.1080/02508060508691837, 2005.

Krysanova, V., Hattermann, F., Huang, S., Hesse, C., Vetter, T., Liersch, S., Koch, H. and Kundzewicz, Z. W.: Modelling climate and land use change impacts with SWIM:

lessons learnt from multiple applications, Hydrol. Sci. J., 141217125340005, doi:10.1080/02626667.2014.925560, 2014.

Kundzewicz, Z. W., Kanae, S., Seneviratne, S. I., Handmer, J., Nicholls, N., Peduzzi, P., Mechler, R., Bouwer, L. M., Arnell, N., Mach, K., Muir-Wood, R., Brakenridge, G. R., Kron, W., Benito, G., Honda, Y., Takahashi, K. and Sherstyukov, B.: Flood risk and climate change: global and regional perspectives, Hydrol. Sci. J., 59(1), 1–28, doi:10.1080/02626667.2013.857411, 2013.

L. Perch-Nielsen, S., B. Bättig, M. and Imboden, D.: Exploring the link between climate change and migration, Clim. Change, 91(3), 375–393, doi:10.1007/s10584-008-9416-y, 2008.

Lebel, T. and Ali, A.: Recent trends in the Central and Western Sahel rainfall regime (1990–2007), J. Hydrol., 375(1-2), 52–64, doi:10.1016/j.jhydrol.2008.11.030, 2009.

Liersch, S., Cools, J., Kone, B., Koch, H., Diallo, M., Reinhardt, J., Fournet, S., Aich, V. and Hattermann, F. F.: Vulnerability of rice production in the Inner Niger Delta to water resources management under climate variability and change, Environ. Sci. Policy, 34, 8–33, doi:10.1016/j.envsci.2012.10.014, 2013.

Lupton, K.: Mungo Park the African Traveler, Oxford University Press, Oxford, UK., 1979.

Mahe, G., Lienou, G., Descroix, L., Bamba, F., Paturel, J. E., Laraque, A., Meddi, M., Habaieb, H., Adeaga, O., Dieulin, C., Chahnez Kotti, F. and Khomsi, K.: The rivers of Africa: witness of climate change and human impact on the environment, Hydrol. Process., 27(15), 2105–2114, doi:10.1002/hyp.9813, 2013.

Manabe, S., Milly, P. C. D. and Wetherald, R.: Simulated long-term changes in river discharge and soil moisture due to global warming / Simulations à long terme de changements d'écoulement fluvial et d'humidité du sol causés par le réchauffement global, Hydrol. Sci. J., 2009.

McCarthy, G. T.: The Unit Hydrograph and Flood Routing, Conf. North Atl. Div. US Corps Eng., 1938.

Meek, C. K.: The Niger and the Classics: The History of a Name, J. Afr. Hist., 1(1), 1–17 [online] Available from: http://www.jstor.org/stable/179702, 1960.

Mertz, O. and Mbow, C.: Adaptation strategies and climate vulnerability in the Sudano-Sahelian region of West Africa, Atmos. Sci. Jour., 2011.

Merz, B.: Hochwasserrisiken-Möglichkeiten und Grenzen der Risikoabschätzung, , 2006.

Merz, B., Vorogushyn, S., Uhlemann, S., Delgado, J. and Hundecha, Y.: HESS Opinions "More efforts and scientific rigour are needed to attribute trends in flood time series," Hydrol. Earth Syst. Sci. Discuss., 16, 1379–1387, doi:10.5194/hessd-16-1379-2012, 2012.

Murray, S., Foster, P. and Prentice, I.: Future global water resources with respect to climate change and water withdrawals as estimated by a dynamic global vegetation model, J. Hydrol., 2012.

Nicholson, S.: The West African Sahel: A review of recent studies on the rainfall

regime and its interannual variability, ISRN Meteorol., 2013.

Niger Basin Authority, (NBA): Convention creating the Niger Basin Authority. [online] Available from: http://gis.nacse.org/tfdd/tfdddocs/418ENG.pdf, 1980.

Niger Basin Authority, (NBA) and BRL: Elaboration du modèle de gestion du bassin du Niger. Rapport final., 2007.

Niger Basin Authority, (NBA) and GIZ, G. für I. Z.: Appui à l´ABN - Crue Info., 2015.

Nikulin, G., Jones, C., Giorgi, F., Asrar, G., Büchner, M., Cerezo-Mota, R., Christensen, O. B., Déqué, M., Fernandez, J., Hänsler, A., van Meijgaard, E., Samuelsson, P., Sylla, M. B. and Sushama, L.: Precipitation Climatology in an Ensemble of CORDEX-Africa Regional Climate Simulations, J. Clim., 25(18), 6057–6078, doi:10.1175/JCLI-D-11-00375.1, 2012.

Odunuga, S., Adegun, O., Raji, S. and Udofia, S.: Changes in flood risk in Lower Niger–Benue catchments, Proc. IAHS [online] Available from: http://www.proc-iahs.net/370/97/2015/piahs-370-97-2015.pdf (Accessed 13 November 2015), 2015.

Ogilvie, A., Mahé, G., Ward, J., Serpantié, G., Lemoalle, J., Morand, P., Barbier, B., Diop, A. T., Caron, A., Namarra, R., Kaczan, D., Lukasiewicz, A., Paturel, J.-E., Liénou, G. and Clanet, J. C.: Water, agriculture and poverty in the Niger River basin, Water Int., 35(5), 594–622, 2010.

Oguntunde, P. G. and Abiodun, B. J.: The impact of climate change on the Niger River Basin hydroclimatology, West Africa, Clim. Dyn., 40(1-2), 81–94, doi:10.1007/s00382-012-1498-6, 2013.

Okpara, J. N., Perumal, M., Cluckie, I. D., Chen, Y., Babovic, V., Konikow, L., Mynett, A., Demuth, S. and Savic, D. A.: Hydrological impact assessment of climate change on water resources of the Niger River basin using a water balance model and ANNs., in Hydroinformatics in hydrology, hydrogeology and water resources. Proceedings of Symposium JS.4 at the Joint Convention of the International Association of Hydrological Sciences (IAHS) and the International Association of Hydrogeologists (IAH) held in Hyde, pp. 58–71, IAHS Press., 2009.

Oyerinde, G. T., Hountondji, F. C. C., Wisser, D., Diekkrüger, B., Lawin, A. E., Odofin, A. J. and Afouda, A.: Hydro-climatic changes in the Niger basin and consistency of local perceptions, Reg. Environ. Chang., 1–11, doi:10.1007/s10113-014-0716-7, 2014.

Paeth, H.: The Climate of Tropical and Northern Africa – a Statistical-Dynamical Analysis of the Key Factors in Climate Variability and the Role of Human Activity in Future Climate Change, Bonner Meteorol. Abhandlungen, 61, 316 p., 2005.

Paeth, H. and Hense, A.: Sensitivity of climate change signals deduced from multi-model Monte Carlo experiments, Clim. Res., 2002.

Paeth, H., Fink, A. H., Pohle, S., Keis, F., Mächel, H. and Samimi, C.: Meteorological characteristics and potential causes of the 2007 flood in sub-Saharan Africa, Int. J. Climatol., 31(13), 1908–1926, doi:10.1002/joc.2199, 2011a.

Paeth, H., Hall, N. M. J., Gaertner, M. A., Alonso, M. D., Moumouni, S., Polcher, J., Ruti, P. M., Fink, A. H., Gosset, M., Lebel, T., Gaye, A. T., Rowell, D. P., Moufouma-Okia, W., Jacob, D., Rockel, B., Giorgi, F. and Rummukainen, M.: Progress in regional

downscaling of west African precipitation, Atmos. Sci. Lett., 12(1), 75–82, doi:10.1002/asl.306, 2011b.

Panthou, G., Vischel, T., Lebel, T., Blanchet, J., Quantin, G. and Ali, A.: Extreme rainfall in West Africa: A regional modeling, Water Resour. Res., 48(8), doi:10.1029/2012WR012052, 2012.

Panthou, G., Vischel, T. and Lebel, T.: Recent trends in the regime of extreme rainfall in the Central Sahel, Int. J. Climatol., doi:10.1002/joc.3984, 2014.

Pardé, M.: Fleuves et Rivieres, Collection Armand Colin, Presses Universitaires de France, Paris., 1963.

Park, M.: Travels in the Interior of Africa, Adam and Charles Black, North Bridge, Edinburgh., 1858.

Renaud, F. G., Dun, O., Warner, K. and Bogardi, J.: A Decision Framework for Environmentally Induced Migration, Int. Migr., 49, e5–e29, doi:10.1111/j.1468-2435.2010.00678.x, 2011.

Ritchie, J.: Model for predicting evaporation from a row crop with incomplete cover, Water Resour. Res., 8(5), 1204–1213, 1972.

Rouch, J.: Le Niger en pirogue, Nathan, Paris., 1954.

Roudier, P., Ducharne, A. and Feyen, L.: Climate change impacts on runoff in West Africa: a review, Hydrol. Earth Syst. Sci., 18(7), 2789–2801, doi:10.5194/hess-18-2789-2014, 2014.

Ruelland, D., Ardoin-Bardin, S., Collet, L. and Roucou, P.: Simulating future trends in hydrological regime of a large Sudano-Sahelian catchment under climate change, J. Hydrol., 424-425, 207–216, doi:10.1016/j.jhydrol.2012.01.002, 2012.

Ruti, P. M., Williams, J. E., Hourdin, F., Guichard, F., Boone, a., Van Velthoven, P., Favot, F., Musat, I., Rummukainen, M., Domínguez, M., Gaertner, M. Á., Lafore, J. P., Losada, T., Rodriguez de Fonseca, M. B., Polcher, J., Giorgi, F., Xue, Y., Bouarar, I., Law, K., Josse, B., Barret, B., Yang, X., Mari, C. and Traore, a. K.: The West African climate system: a review of the AMMA model inter-comparison initiatives, Atmos. Sci. Lett., 12(1), 116–122, doi:10.1002/asl.305, 2011.

Shimi, A. C., Parvin, G. A., Biswas, C. and Shaw, R.: Impact and adaptation to flood, Disaster Prev. Manag. An Int. J., 2013.

Sighomnou, D., Descroix, L., Genthon, P., Mahé, G., Moussa, I. B., Gautier, E., Mamadou, I., Vandervaere, J.-P., Bachir, T., Coulibaly, B., Rajot, J.-L., Issa, O. M., Abdou, M. M., Dessay, N., Delaitre, E., Maiga, O. F., Diedhiou, A., Panthou, G., Vischel, T., Yacouba, H., Karambiri, H., Paturel, J.-E., Diello, P., Mougin, E., Kergoat, L. and Hiernaux, P.: La crue de 2012 à Niamey: un paroxysme du paradoxe du Sahel?, Sci. Chang. planétaires / Sécheresse, 24(1), 3–13, doi:10.1684/sec.2013.0370, 2013.

Sun, J., Wang, H. and Yuan, W.: Linkage of the boreal spring Antarctic Oscillation to the West African summer monsoon, J Meteorol Soc Jpn, 2010.

Sylla, M., Diallo, I. and Pal, J.: West African monsoon in state-of-the-science regional climate models, Clim. Var., 2013.

Sylla, M., Elguindi, N., Giorgi, F. and Wisser, D.: Projected robust shift of climate zones over West Africa in response to anthropogenic climate change for the late 21st century, Clim. Change, 2015.

Tarhule, A.: Damaging Rainfall and Flooding: The Other Sahel Hazards, Clim. Change, 72, 355–377, doi:10.1007/s10584-005-6792-4, 2005.

Tarhule, A. A.: Water Resources Scarcity in West Africa: The Imperatives of Regional Cooperation, in Water in the Middle East: Cooperation and Technological Solutions in the Jordan Valley, edited by K. D. Hambright, F. J. Ragep, and J. Ginat, pp. 55–70, University of Oklahoma Press, Brighton., 2006.

Tschakert, P., Sagoe, R., Ofori-Darko, G. and Codjoe, S. N.: Floods in the Sahel: an analysis of anomalies, memory, and anticipatory learning, Clim. Change, 103(3-4), 471–502, doi:10.1007/s10584-009-9776-y, 2010.

UNESCO: State of Conservation: Timbuktu, Mali, State Conserv. 261 [online] Available from: http://whc.unesco.org/en/soc/261, 2012.

Viessman, W., Lewis, G. L. and Knapp, J. W.: Introduction to hydrology., 1989.

Vizy, E., Cook, K., Crétat, J. and Neupane, N.: Projections of a wetter Sahel in the twenty-first century from global and regional models, J. Clim., 2013.

van Vliet, M. T. H., Franssen, W. H. P., Yearsley, J. R., Ludwig, F., Haddeland, I., Lettenmaier, D. P. and Kabat, P.: Global river discharge and water temperature under climate change, Glob. Environ. Chang., 23(2), 450–464, doi:10.1016/j.gloenvcha.2012.11.002, 2013.

Wendling, U. and Schellin, H.: Neue Ergebnisse zur Berechnung der potentiellen Evapotranspiration, Zeitschrift für Meteorol., 36(3), 214–217, 1986.

Wiese, B.: Afrika. Ressourcen, Wirtschaft, Entwicklung, Teubner, Stuttgart., 1997.

World Water Assessment Programme (WWAP): Water Development Report 3: Water in a changing world., Paris. [online] Available from: http://webworld.unesco.org/water/wwap/wwdr/wwdr3/pdf/WWDR3_Water_in_a_Changing_World.pdf, 2009.

Worldbank: CIWA in the Niger Basin, Brief [online] Available from: http://www.worldbank.org/en/region/afr/brief/ciwa-in-the-niger-basin (Accessed 7 December 2015), 2014.

Wright, J. B., Hastings, D. A., Jones, W. B. and Williams, H. R.: Geology and Mineral Resources of West Africa, Springer Science & Business Media., 1985.

Yu, M., Wang, G. and Pal, J. S.: Effects of vegetation feedback on future climate change over West Africa, Clim. Dyn., doi:10.1007/s00382-015-2795-7, 2015.

Zwarts, L., Beukering, P. Van, Kone, B. and Wymenga, E.: The Niger, a Lifeline: Effective Water Management in the Upper Niger Basin, Altenburg & Wymenga Ecologisch Onderzoek BV, Leylstad, Netherlands., 2005.

10. Appendix

10.1. Appendix of Chapter 2

10.1.1. The Sahelian Paradox

The evolution of AMAX for both flood peaks at Niamey is plotted in relation to the annual precipitation in the corresponding source area in Figure S 21. For the Sahelian flow peak, heavy precipitation is plotted as well. For the Guinean peak, heavy precipitation is not shown since the source area in the Guinean highlands is located approximately 1500 km away from the gauge in Niamey, and these events do not have a noticeable effect here.

The systematic detection of the Sahelian peak supports the finding of Descroix et al. (2012) that the AMAX regime in the middle section of the Niger has changed distinctively over the past 30 years. Between 1930 and 1980, years exhibiting a separate peak for the Sahelian flood was rather an exception in Niamey. Since 1983, there was only one year that showed no separate Sahelian peak and, since then, the peak was even higher for nine subsequent years compared to the Guinean flood (Figure S 21, top). This effect is connected to the "Sahelian Paradox", which becomes visible for the Sahelian peak. The positive trend in the AMAX of the Sahelian peak started already in the 1970s. In contrast, the related rainfall data shows a further decrease and then stabilization in annual precipitation until the middle of the 1980s. The data for heavy precipitation in the region shows similar trends and turning points to that for annual precipitation. Therefore, heavy precipitation cannot explain the paradox of increasing discharge despite decreasing or stable rainfall. From the end of the 1980s, all three trends show the same direction and, hence, there is no more paradox, even if the underlying process might still be continuing. For the Guinean peak, this effect is completely absent and the evolution of the AMAX series corresponds to the annual precipitation. For the time series of the Guinean flood peak, the minima for AMAX and precipitation are located in the middle of the 1980s, i.e. analogues to the precipitation in the Sahelian region. Hence, the Sahelian and Guinean flood peaks are decoupled even when observed from the same gauging station.

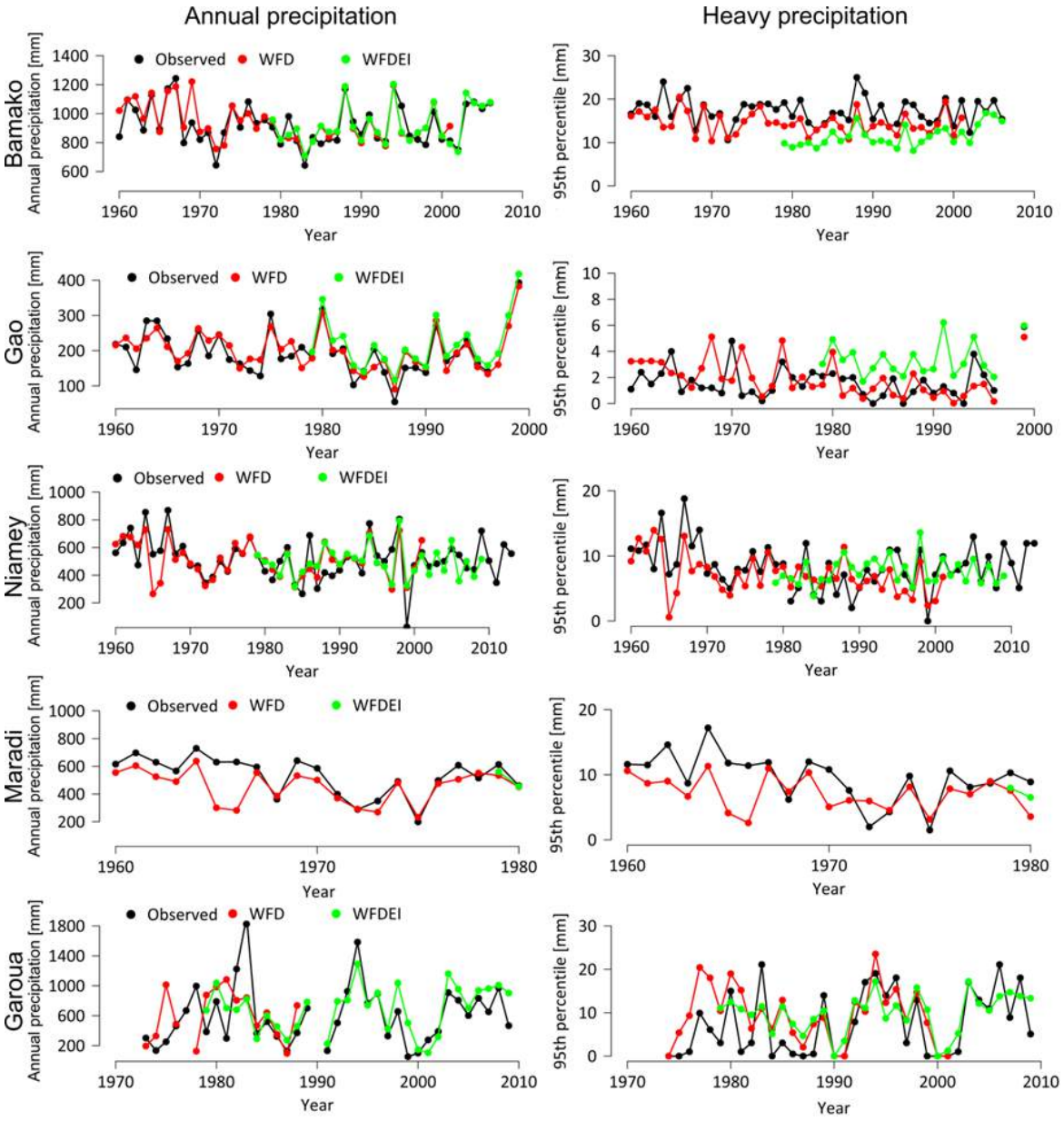

Figure S 1 Validation of precipitation reanalysis data. Left: Annual sum of observed, WFD and WFDEI precipitation in Bamako and Gao (Mali). Right: 95th percentile of daily precipitation for the year for observed, WFD and WFDEI precipitation in Bamako and Gao (Mali).

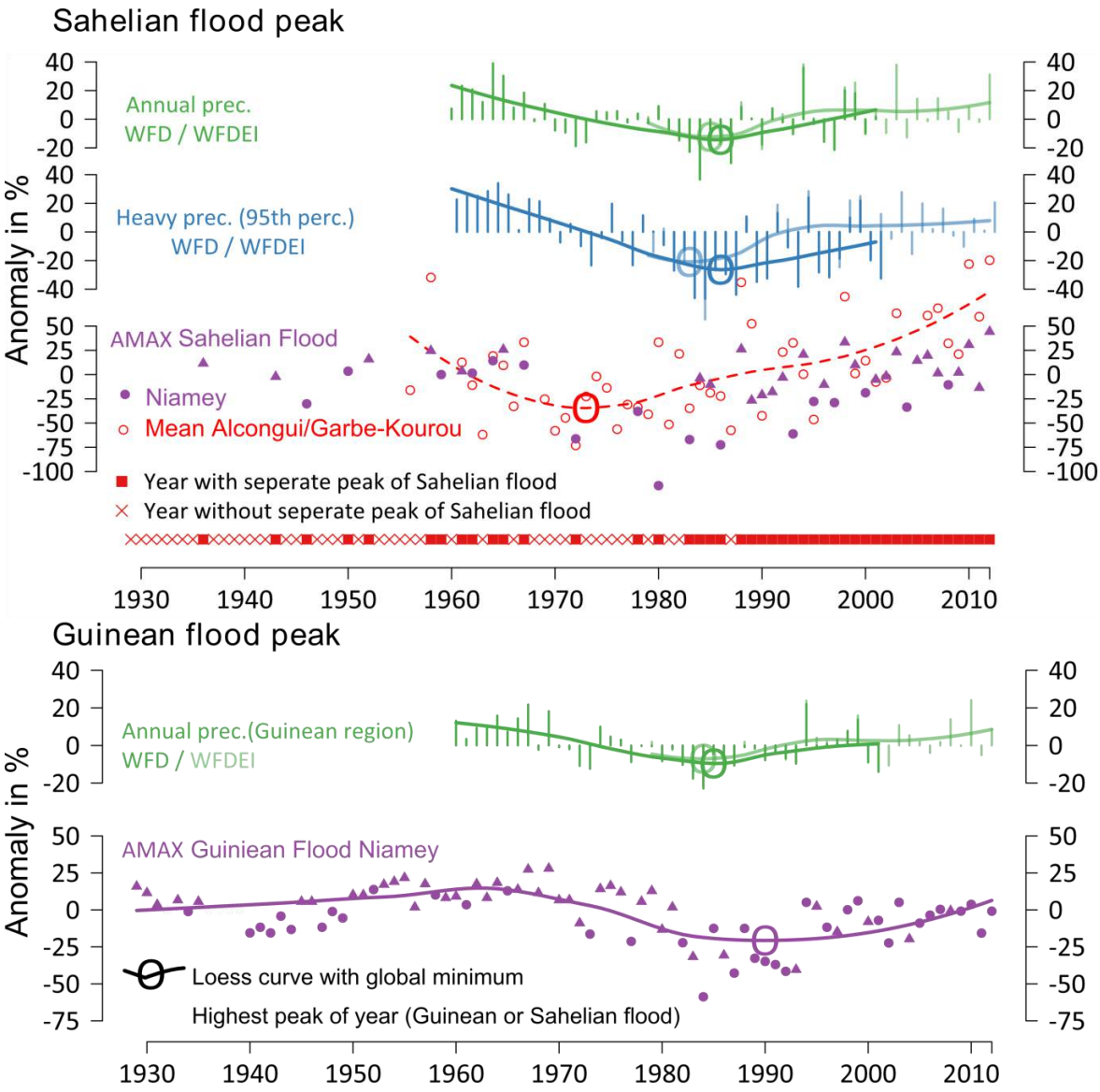

Figure S 2 Top: Annual/ heavy precipitation from WFD and WFDEI and AMAX for Niamey, and the mean of Alcongui and Garbe-Kourou for the Sahelian region. For the generation of the Loess curve only Alcongui and Garbe-Kourou are used. The red squares and crosses at the bottom of the upper figure mark years with and without separate peaks of Sahelian flooding. Bottom: Guinean AMAX for the Niamey station and annual precipitation from WFD and WFDEI for the Guinean region, all with Loess curves and global minima as anomalies in %.

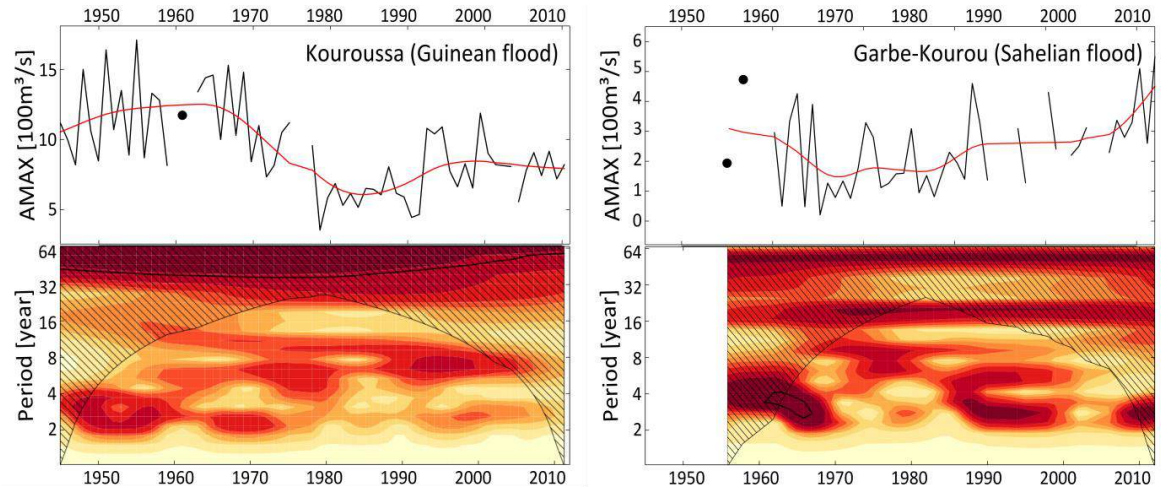

Figure S 3 Top: AMAX time series with local regression curve in red. Bottom: wavelet power spectrum for Guinean, Sahelian, and Sudanian flooding. Brighter colors correspond to smaller wavelet coefficients and darker colors to higher coefficients with the Morlet wavelet. The shaded area is outside the cone of influence and should not be included in the interpretation.

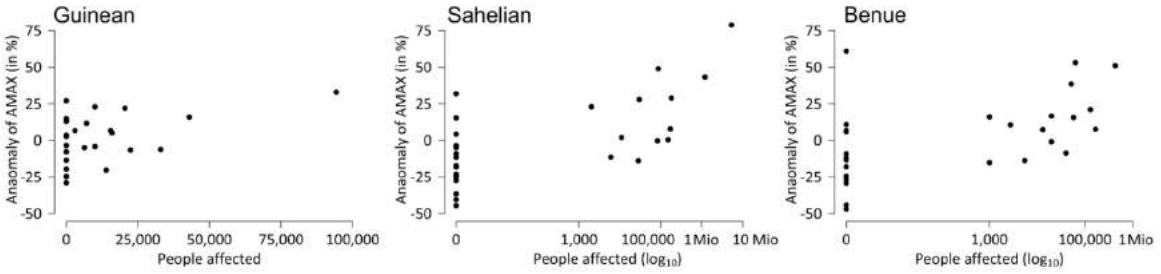

Figure S 4 Correlation between AMAX and people affected by floods for the subregions of the Niger basin. The scales for people affected by floods for the Sahelian region and the Benue are logarithmic. Please note that the number of people affected for the Sahelian basin comprises the whole Middle Niger (Compare 2.3.1.2).

10.2. Appendix of Chapter 3

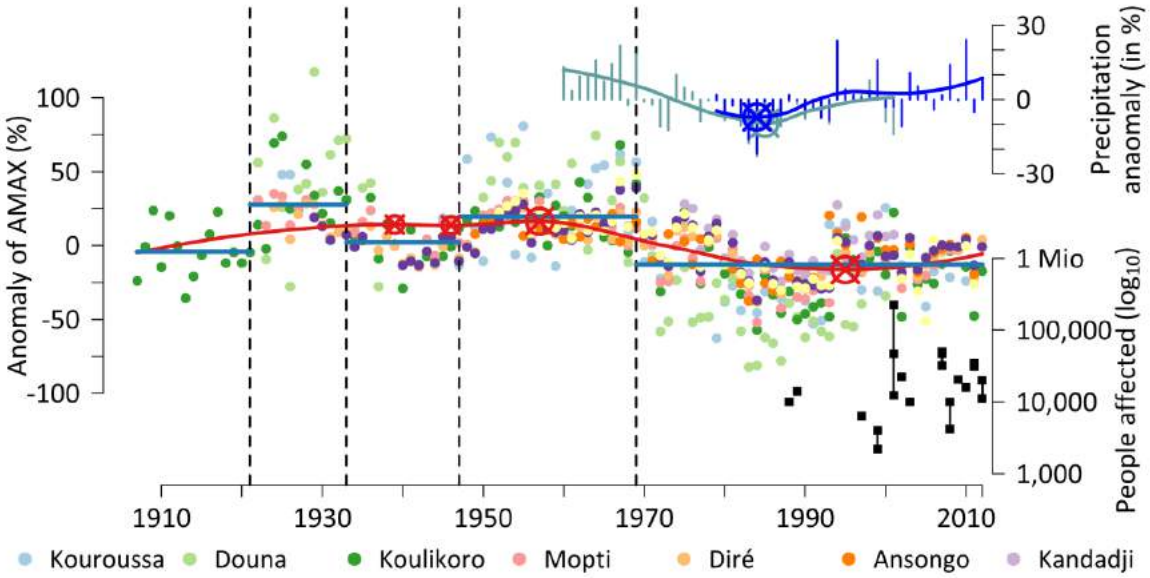

Figure S 5 Decadal changes, trends and people affected by floods for all gauging stations affected primarily by the Guinean flood.

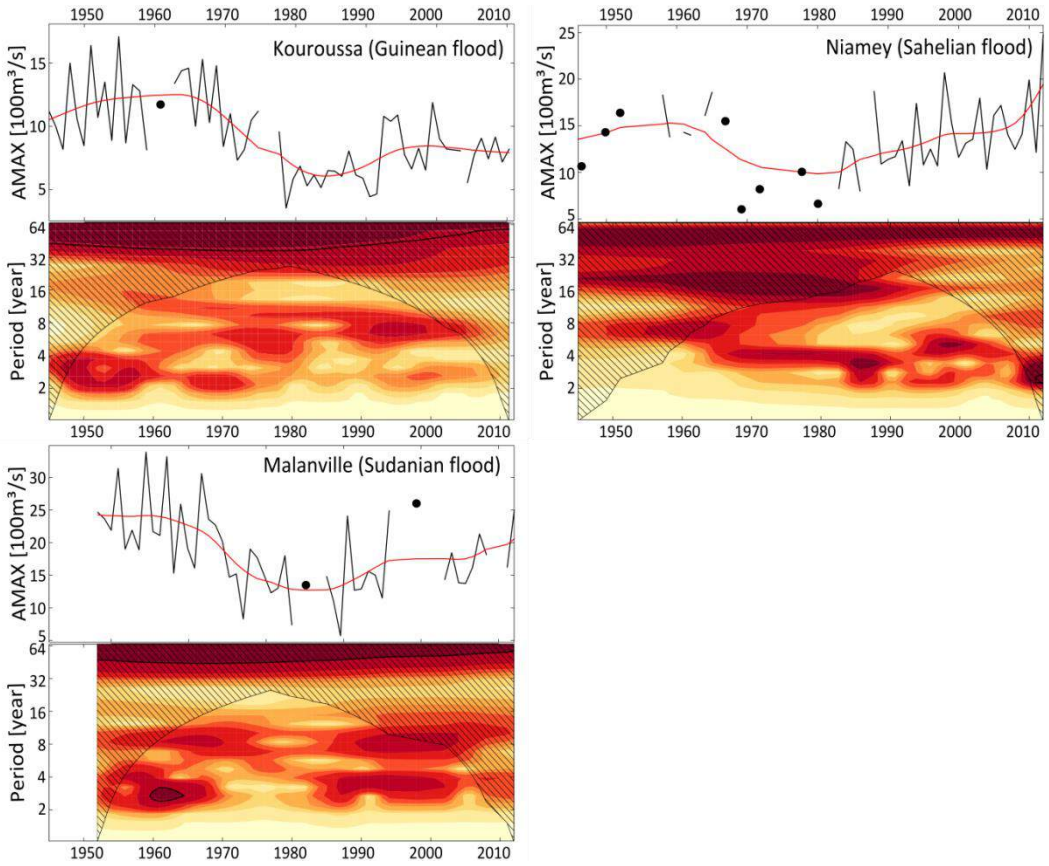

Figure S 6 Top: AMAX time series with local regression curve in red. Bottom: wavelet power spectrum for Guinean, Sahelian, and Sudanian flooding. Brighter colors correspond to smaller wavelet coefficients and darker colors to higher coefficients with the Morlet wavelet. The shaded area is outside the cone of influence and should not be included in the interpretation.

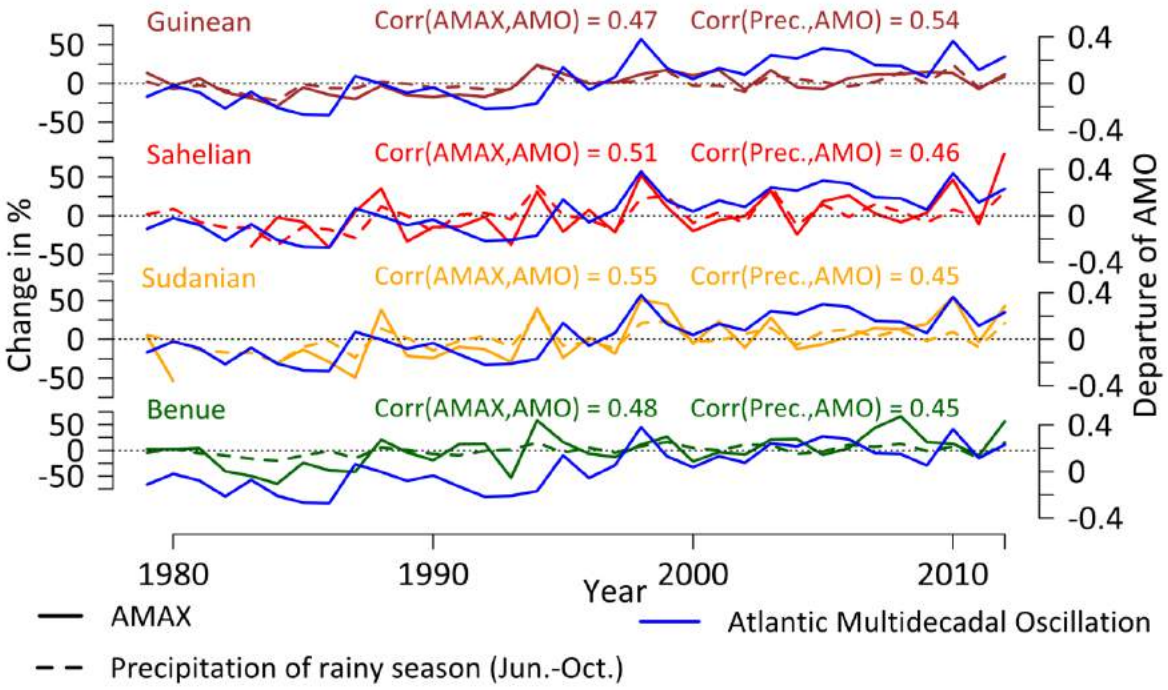

Figure S 7 Correlation between Atlantic Multidecadal Oscillation and AMAX and annual precipitation for the four subregions of the Niger basin.

10.2.1. Revised version of the data based attribution approach

10.2.1.1. The hypothesis-testing framework for flood attribution

Based on the systematic trend analysis, a data-based approach within a hypothesis-testing framework is applied in order to attribute the detected trends (Merz et al., 2012). The framework is based on the evidence of consistency, the evidence of inconsistency, and the provision of confidence level. In this study, the consistency between the climatic variability and the AMAX is shown in order to attribute the flood increase to increasing precipitation. Secondly, the consistency is tested for the influence of land-use change on the discharge. Since there is no direct quantitative land-use change measurement which can be used for a consistency test analogous to the precipitation time series, flashiness is used as a proxy for the influence of land-use change on the runoff regime of the regions. Flashiness is directly linked to land-use changes such as deforestation and increased agricultural production, which results in sealed soils, crusting, smaller infiltration rates and subsequently more direct runoff, as described by Descroix et al. (2012), and thus an increase of flashiness of a river. Although this approach is limited as it only uses a proxy for the influence of land-use change, the combined results allow a qualitative estimation of the magnitude of influence of land-use change compared to climate change signals. The final discussion of these results includes an estimation of the level of confidence of the attribution.

10.2.1.2. Evidence of consistency between precipitation and annual flood peaks

The consistency between AMAX and precipitation is analyzed according to the attribution framework of Merz et al. (2012) (see chapter 10.2.1.1). In chapter 3.4, the analysis showed the general consistency between the AMAX periods (separated by changepoints) and the decadal climatic pattern. In addition, the trend directions between precipitation and AMAX are consistent during the whole time span of available data and for all regions, with the exception of the Sahel Paradox in the Sahelian region and a discrepancy at the end of the Benue precipitation time series (Figure 9). A hypothesis on the Sahel Paradox is explained in chapter 10.1.1, and in the Benue an edge effect of the Loess method can be an explanation for the differences in trends, since in the detailed analysis of this region the trends are consistent (Figure 9).A detailed correlation analysis is only possible for the timespan from 1979 to2012 for which WFDEI rainfall data is available. As precipitation measurements, annual precipitation in the corresponding hydrological year and heavy precipitation as the 95^{th} percentile of the daily precipitation are used and compared to the AMAX (Figure 9). Significant positive trends for the AMAX, annual precipitation and heavy precipitation can be found in all three regions since 1979. The test for autocorrelation was only positive for the AMAX time series of the Guinean region. Here, the autocorrelation was removed as described in chapter 3.2.1. The

strongest trend for AMAX with an increase between 30% and 40% can be found in the Sahelian and Benue regions. In the Guinean region, the trend for AMAX is approximately 20% until 2012. The annual precipitation during the same period increased approximately 15% in the Guinean and Sahelian regions, and only approximately 10% in the Benue region. The heavy precipitation expressed by the 95th percentile increased proportionally in all regions between 20% and 30%. Hence, the trend of AMAX and both precipitation measurements are consistent in all three regions. This consistency is also supported by a correlation analysis. The annual and the heavy precipitation are strongly correlated with the AMAX for all regions (Spearman's ρ: 06-0.72) (Table S 1).

Table S 1 Correlation of AMAX with heavy precipitation (95th percentile) and annual precipitation. All correlations are significant (α = 0.05).

	Guinean	Sahelian	Benue
Heavy precipitation	0.72	0.64	0.71
Annual precipitation	0.72	0.6	0.65

10.2.1.3. Evidence of consistency between land-use change and annual flood peaks

The changes in flashiness have been analyzed using the yearly Richards-Baker index for daily discharge data (Figure S 8). For Koulikoro and Niamey, there are significant positive trends in flashiness since at least 1960. Especially for the Sahelian gauge Niamey, this increase is extreme, ranging from approximately -50% to +40%. In contrast, the gauge at Lokoja indicates a minor decrease in flashiness after the millennium, though due to missing data it was not possible to estimate the trend here. The trends for the Sahelian and Guinean regions are constant and do not show a change in direction. These findings are inconsistent with the time series of the AMAX, which decrease in the case of Koulikoro until the end of the 1980s, and for Niamey until the beginning of the 1970s (Figure 9). This implies that land-use change is not the major driver of AMAX, since their dynamics diverge and another signal influences AMAX more strongly. During the "Sahel Paradox" in the 1970s and 1980s, however, the signal from the rainfall regime is weak because there is little variability and the magnitude is low or decreasing slightly. Over this period, a signal from a driver other than precipitation, which might be otherwise covered or outweighed, can be more easily identified. This is likely to be connected to land-use change, since during this period the land-use change signal and the AMAX are consistent. In the middle of 1980s, the trend of precipitation changes and gets stronger, covering again a potential signal from land-use change.

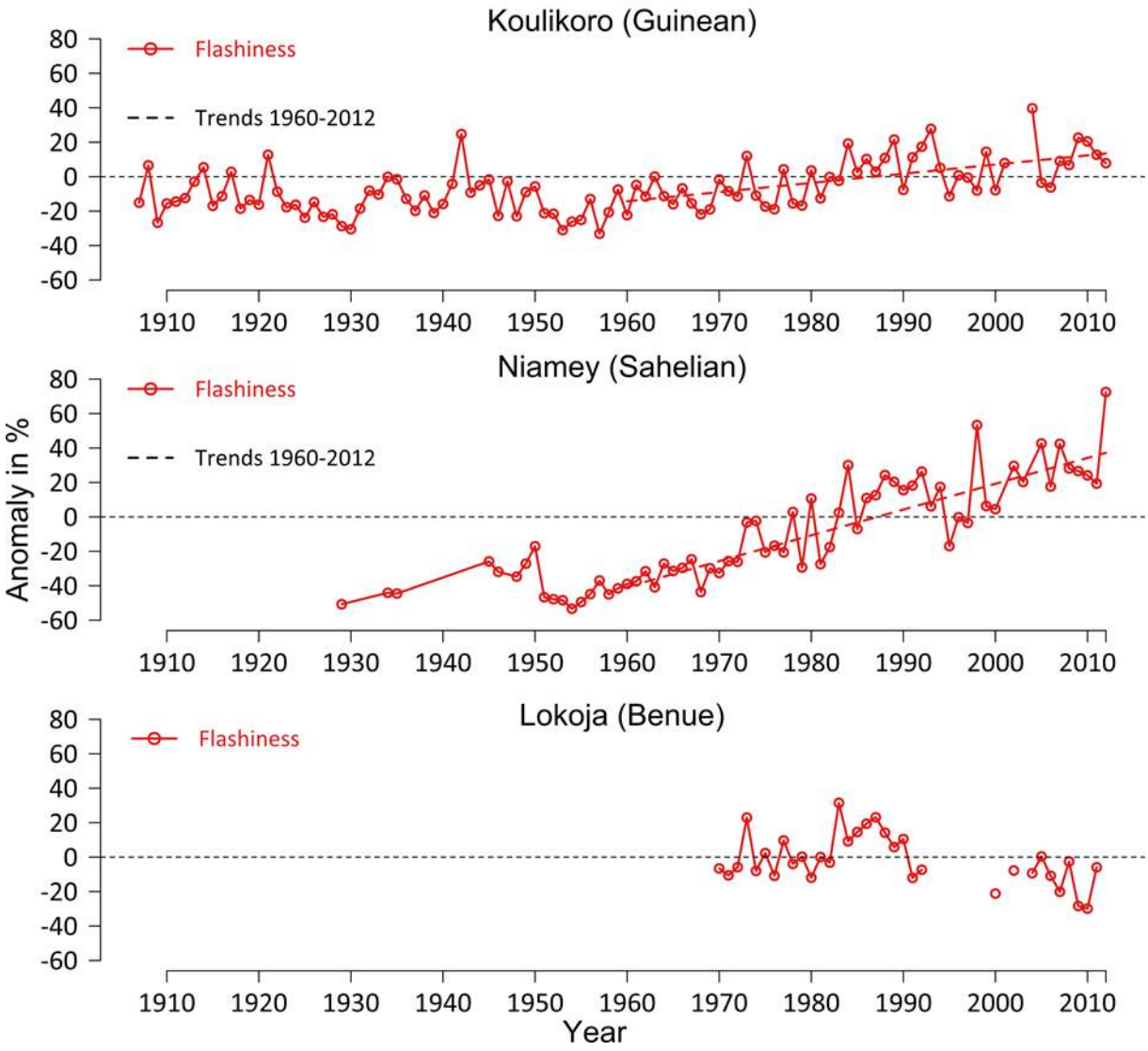

Figure S 8 Anomaly of Richards-Baker flashiness index for representative gauges in the Guinean (Koulikoro), Sahelian (Niamey) and Benue (Lokoja) subregions. The Theil-Sen estimator trend is added as a dashed line for Koulikoro and Niamey from 1960, where the trend is significant (α=0.05). For Lokoja, measurements are not sufficient to estimate the trend.

10.2.1.4. Attribution of the changes in the flood regime and provision of confidence level

The question of whether climatic variabilities or land-use changes are the dominant drivers of the increasing AMAX is complex. Descroix et al. (2012) concluded that, based on their findings of decreasing rainfall, the increase in flooding in the Sahelian region since the 1980s and especially in the region around Niamey are not related to climatic variations but only to land cover changes due to more intensive agricultural use. However, our findings contradict this conclusion for the Sahelian part of the Niger and the other subregions. There is a strong consistency between precipitation and AMAX for the three regions in the Niger basin. The positive trend prevailing since the 1990s in annual rainfall as well as in extreme events is significant and can largely explain the increase in AMAX.

The study by Panthou et al. (2014) supports the results of increasing rainfall occurrence and intensity. The analysis of a multitude of rainfall stations in the Sahel region with up-to-date statistical methods showed a significant trend of increasingly frequent extreme events. These results are in contrast to the findings of Descroix et al. (2012) for the Sahelian region, who detected trends neither for total precipitation nor for heavy precipitation. The increase in precipitation as a driver for the increased flooding in the Sahelian is a finding also supported by Aich et al. (2014). The study shows that for four basins in Africa, an increase in precipitation in drier regions with a rather low runoff coefficient leads to proportionally higher increases in discharge compared to regions with a wetter climate, where an increase in precipitation has less influence. Hence, wet years in the dry Sahelian region lead to proportionally higher discharges than in the Guinean or Benue regions of the Niger basin. The results of the precipitation attribution and the agreement with the existing literature lead to a high confidence level, implying that variability of rainfall is the dominant driver of AMAX in the region. Since changes in annual and heavy precipitation are consistent and the timing is similar, it is not possible to adequately quantify and discuss the influence of heavy precipitation on AMAX with the data-based attribution method.

With regard to land-use change, the trends in flashiness for the Guinean and Sahelian regions indicate an influence of land-use change on the hydrology, beginning at the latest in the 1960s. Both trends are constant without changes in the direction. These findings are not consistent with the AMAX as shown in chapter 10.2.1.3, and this implies that land-use change effects have at least a minor influence on the AMAX (when compared to precipitation). Only during the Sahel Paradox in the 1970s can this other influence on the AMAX be detected, since the signal of the precipitation is weak here (compare chapter 10.2.1.2). The land-use change effect, as described by Descroix et al., (2012), is the most plausible explanation for this “Sahelian Paradox”. However, the level of confidence for the effect of land-use change on the AMAX is rather low, since flashiness can only be a proxy for the influence of land-use change. The combined interpretation of the general consistency between AMAX and precipitation, along with the partial inconsistency with the land-use change signal, implies a major influence of the climate and climate variability on AMAX in the Niger.

Merz et al. (2012) distinguish between hard attribution, in which the consistency of one driver and the inconsistency of another driver can be proven, and soft attribution, in which only the consistency can be shown without ruling out the influence of another driver. In the case of the Niger basin, the conditions for a hard attribution are not completely fulfilled, though there are strong indications for a major influence of climate variability on trends in AMAX and thus flood hazard.

The constraints of the data-based attribution in this study are likely to occur in other data-sparse regions in a similar manner. Even with sufficient data, a final hard attribution of drivers would be difficult. This study shows that the signals of different drivers might

overlap, making it impossible to distinguish their influence on the flooding process. Therefore, it is not possible to exclude the influence of another driver, which might only be hidden under a stronger signal. In the case of the Niger basin, the influence of the land-use change would have remained hidden behind the increasing precipitation if the special context of the "Sahel Paradox" had not revealed it.

10.2.1.5. Conclusions

[…]

Answering our first research question as to the attribution of the increasing hazard is not straightforward: we found some indications that the variability and trends in precipitation in the Niger basin play the dominant role in the increasing AMAX. The changes in flashiness signify an influence of land-use change on the hydrograph for the Guinean and Sahelian regions. However, the analysis of consistency reveals that this effect does not control the AMAX trend, since the trends are partly in the opposite direction. In the special case of the "Sahel Paradox", however, the effect of land-use change on the magnitude of AMAX becomes more apparent. The latter implies that land-use changes in the Guinean and Benue catchments seem not to have a major influence on the generation of catastrophic flooding on the regional scale. The Sahelian catchment is more sensitive to changes, and there are indications that land-use changes in combination with changes in extreme precipitation cause peak flows which have not been observed before. This aspect should be kept in mind for the elaboration of adaptation and development plans, since measures controlling the land-use change effect can mitigate the probability of flooding. However, particularly the results on the influence of land-use change are uncertain and a definite attribution is not possible. A simulation-based attribution approach as suggested by Merz et al. (2012) might give a clearer picture and might even allow the share of each driver to be quantified. This requires, however, a very well-established and calibrated model set up in order to simulate the different influences and provide trustworthy results for hard attribution. In addition, the role of groundwater contributions to flooding in the region is not well understood (Leduc et al., 2001; Mahé, 2009) and should be addressed systematically and included in the discussion.

[…]

10.3. Appendix of Chapter 4

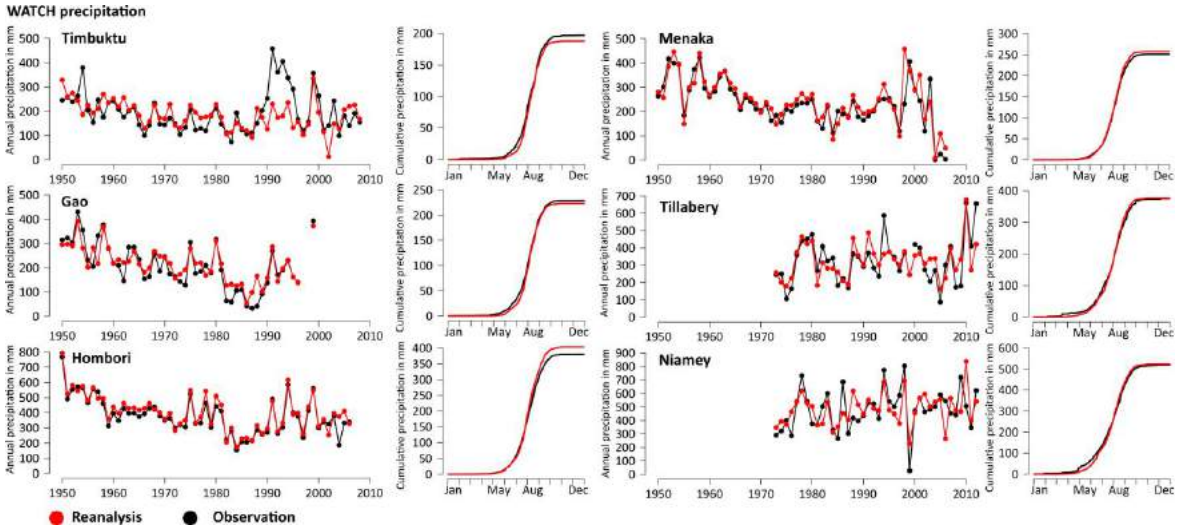

Figure S 9 Comparison of precipitation of interpolated PGFv2 reanalysis data (red) with observations of six weather stations (black) in the research area. For each station the annual precipitation (left) and the cumulative sum of the precipitation of the whole period (right) is depicted.

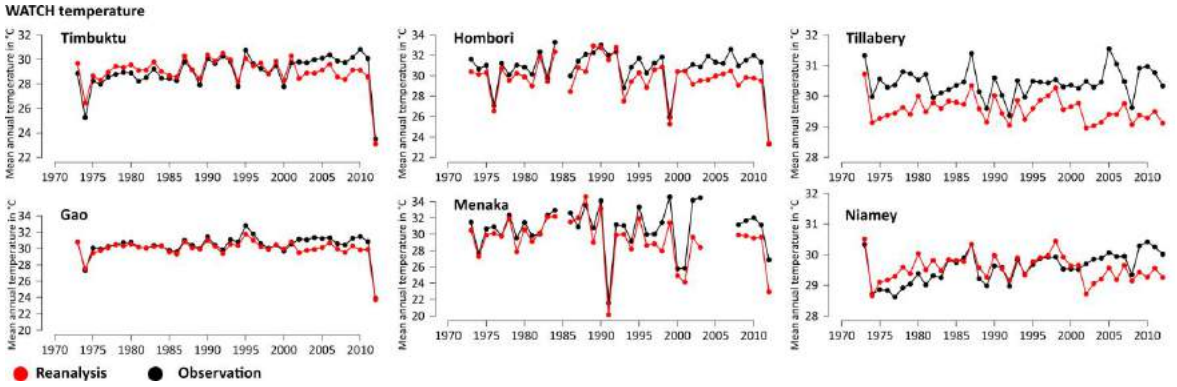

Figure S 10 Comparison of mean annual temperature of interpolated WATCH reanalysis data (red) with observations of six weather stations (black) in the research area.

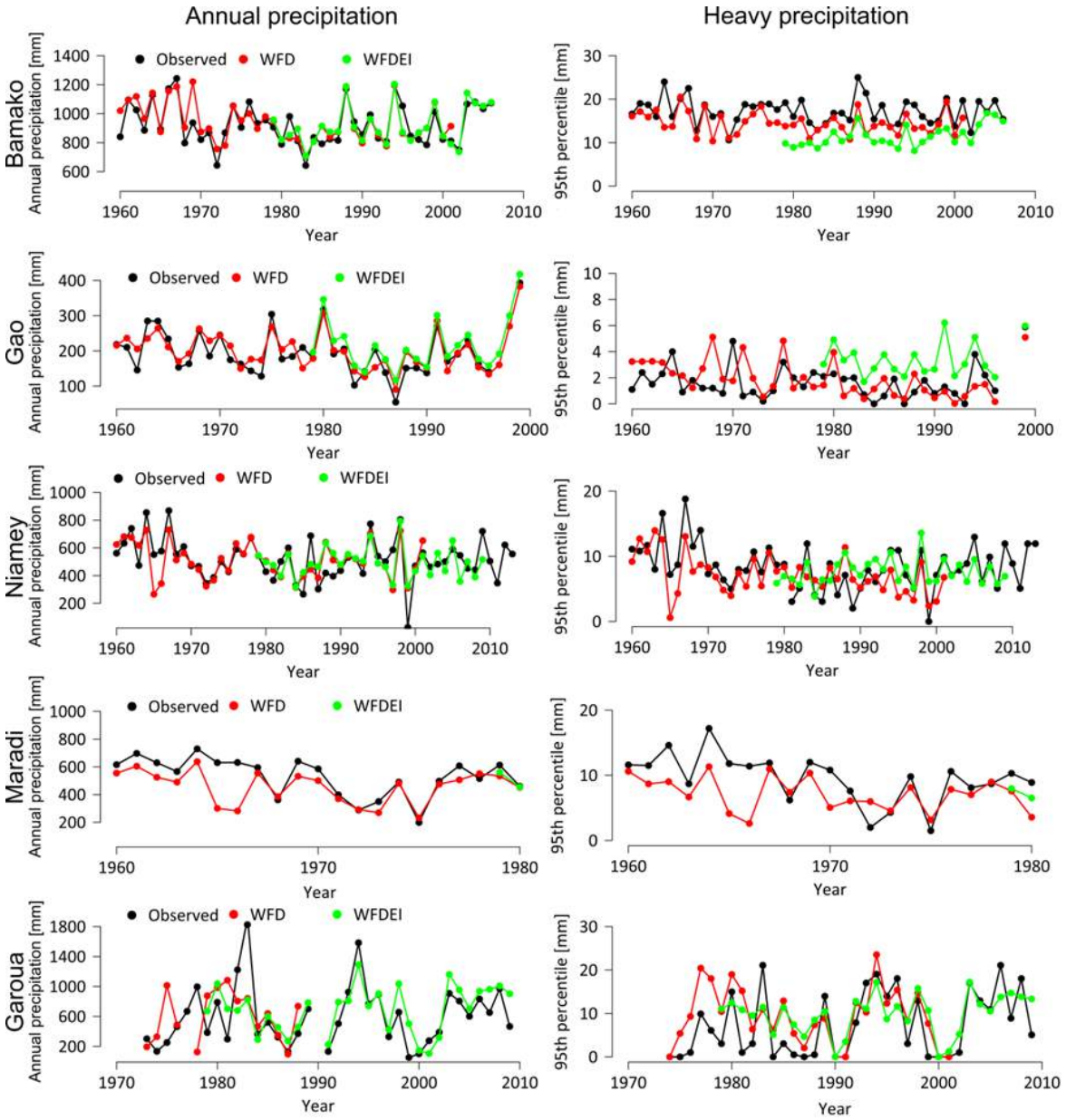

Figure S 11 Validation of precipitation reanalysis data. Left: Annual sum of observed, WFD and WFDEI precipitation in Bamako and Gao (Mali). Right: 95th percentile of daily precipitation for the year for observed, WFD and WFDEI precipitation in Bamako and Gao (Mali).

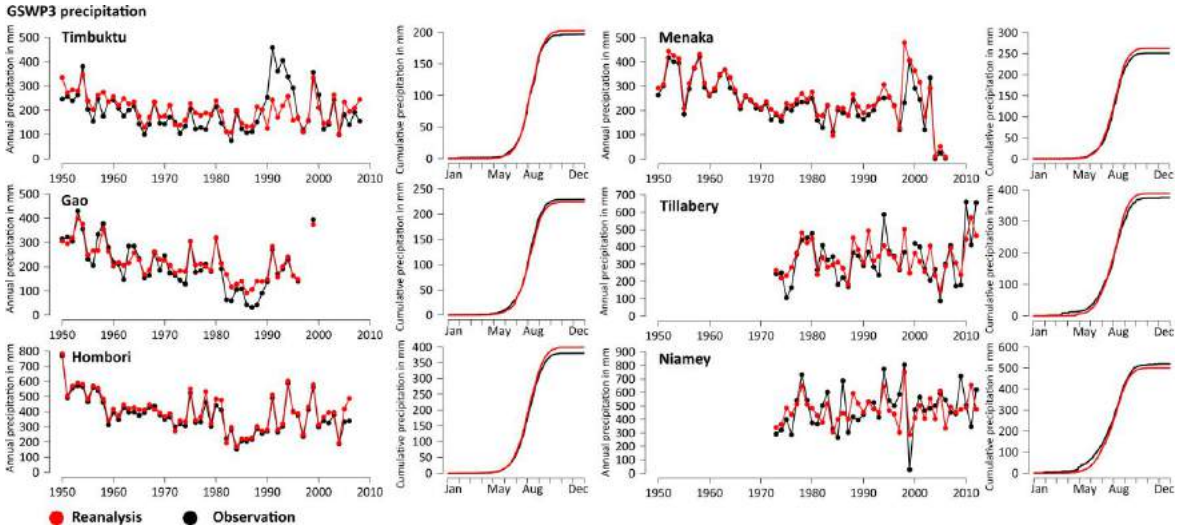

Figure S 12 Comparison of precipitation of interpolated GSWP3 reanalysis data (red) with observations of six weather stations (black) in the research area. For each station the annual precipitation (left) and the cumulative sum of the precipitation of the whole period (right) is depicted.

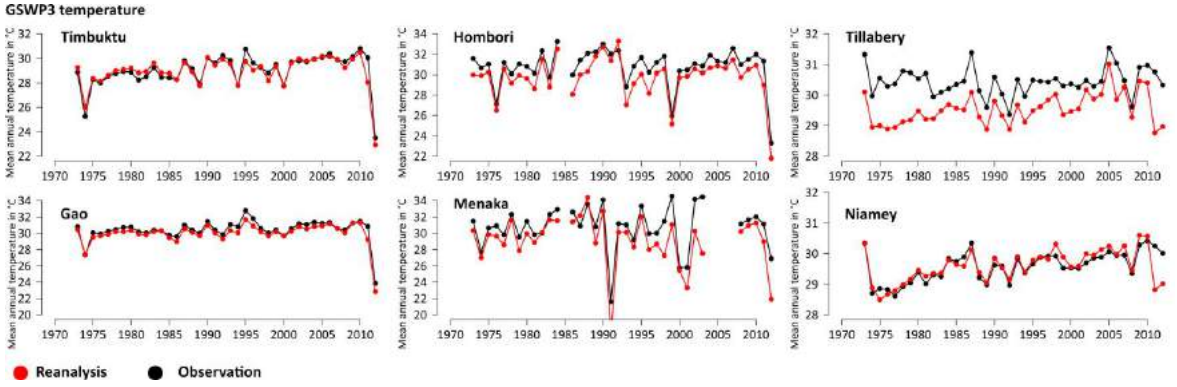

Figure S 13 Comparison of mean annual temperature of interpolated GSWP3 reanalysis data (red) with observations of six weather stations (black) in the research area.

10.4. Appendix of Chapter 5

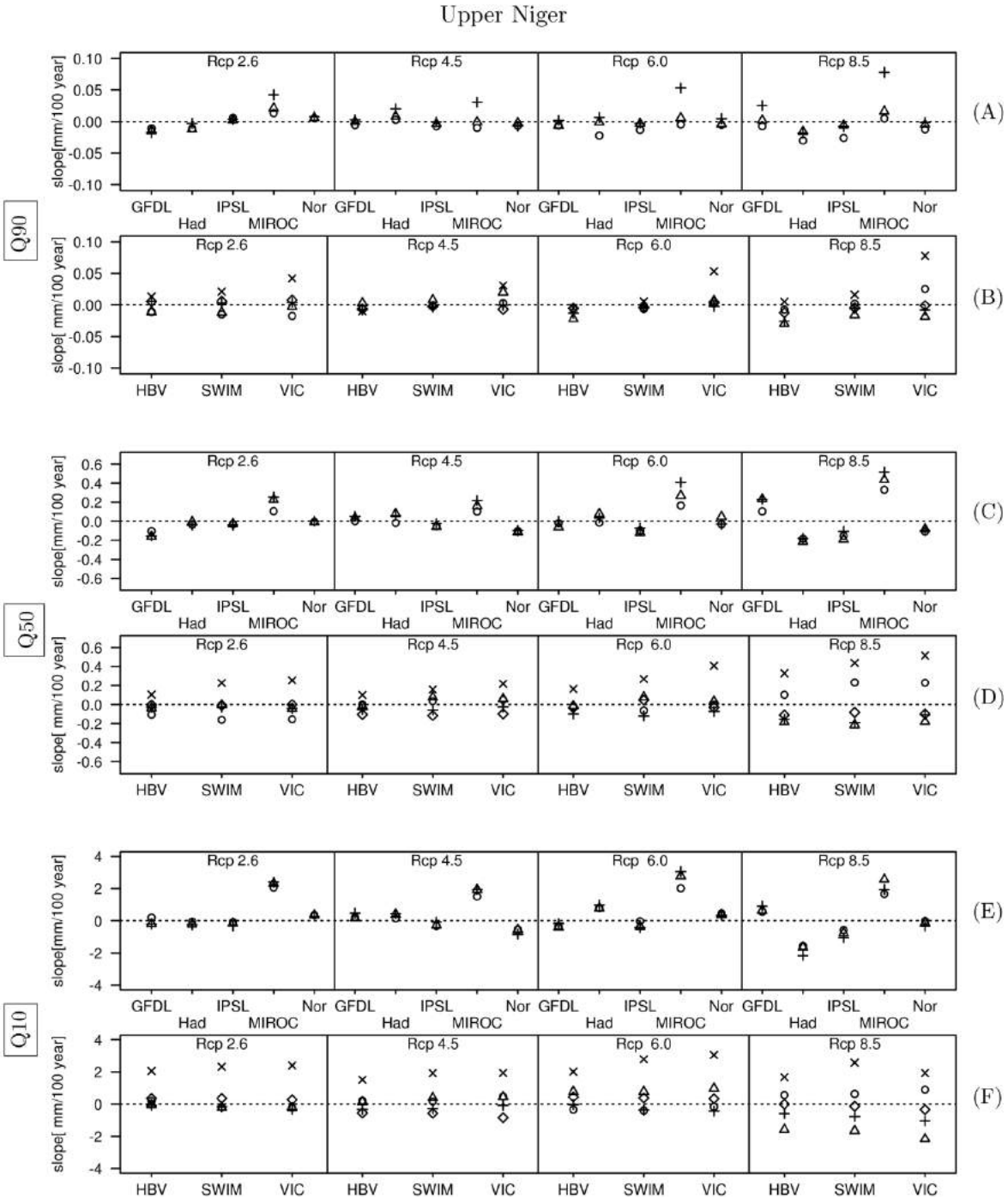

Figure S 14 Slopes of trends in (a, b) low-flow percentile Q_{90}, (c, d) medium discharge Q_{50} and (e, f) high-flow percentile Q_{10} grouped by climate models (a, c, e) and by hydrological models (b, d, f) for the Upper Niger.

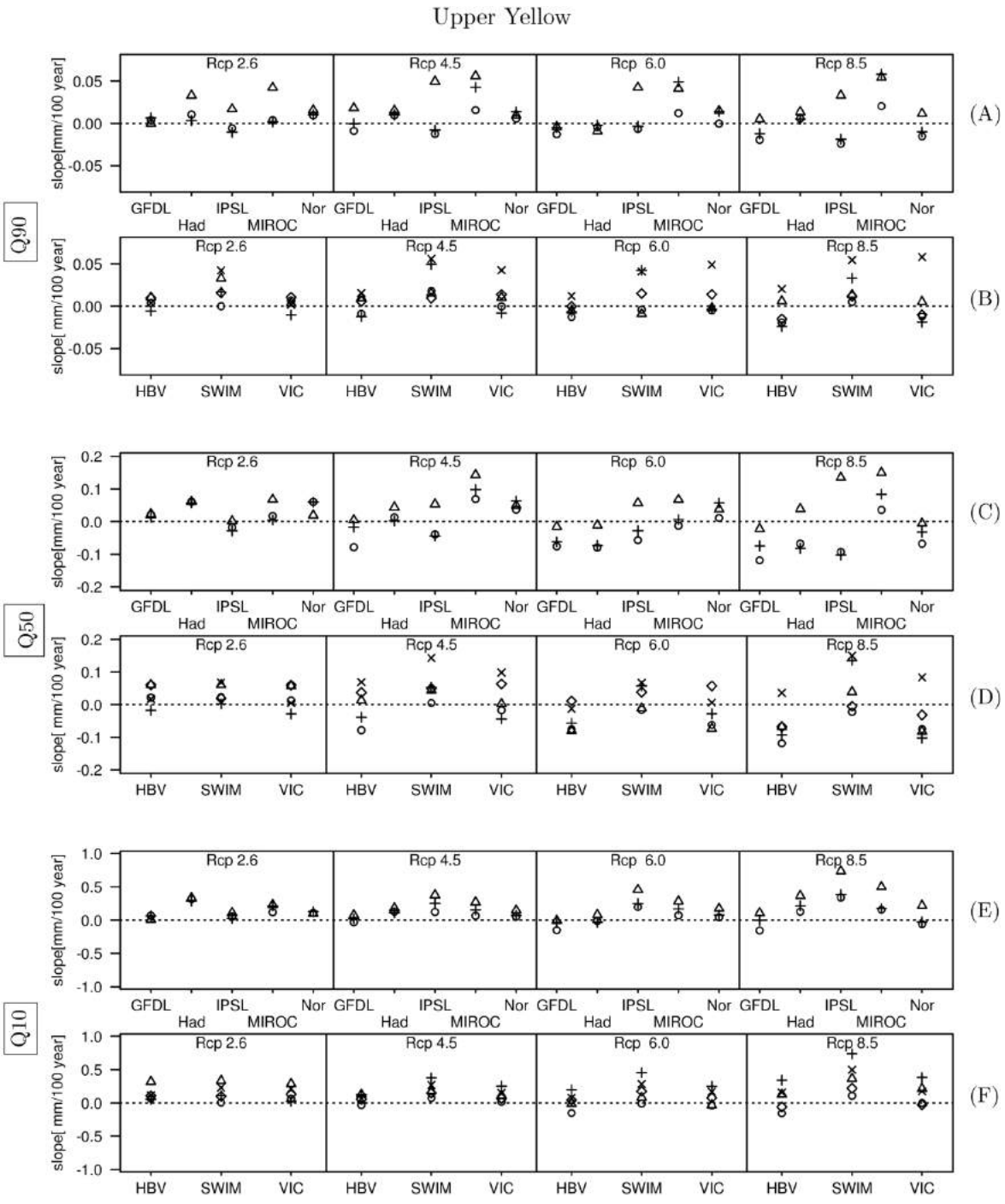

Figure S 15 Slopes of trends in (a, b) low-flow percentile Q_{90}, (c, d) medium discharge Q_{50} and (e, f) high-flow percentile Q_{10} grouped by climate models (a, c, e) and by hydrological models (b, d, f) for the Upper Yellow.

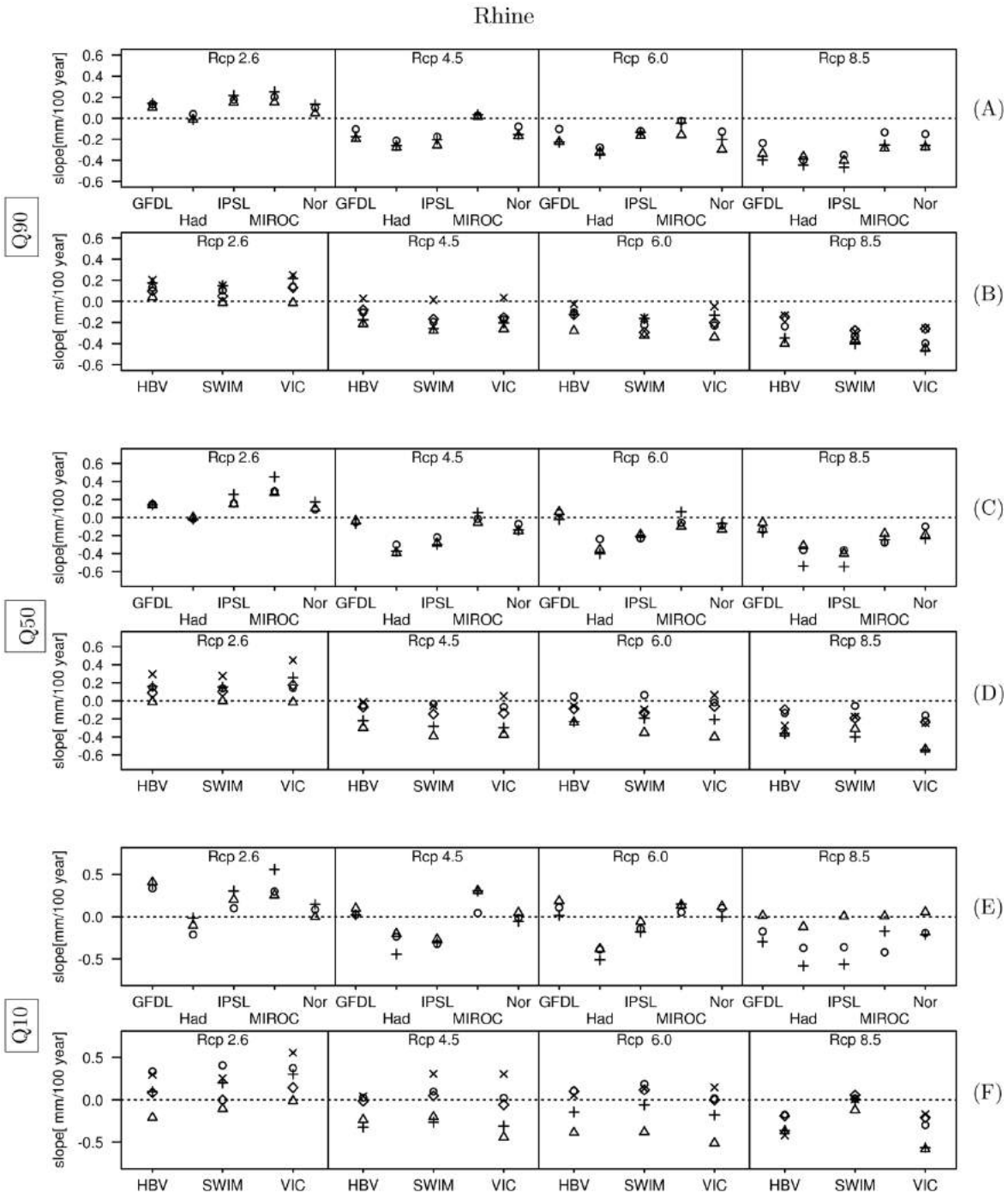

Figure S 16 Slopes of trends in (a, b) low-flow percentile Q_{90}, (c, d) medium discharge Q_{50} and (e, f) high-flow percentile Q_{10} grouped by climate models (a, c, e) and by hydrological models (b, d, f) for the Rhine.

10.5. Appendix of Chapter 6

Table S 2 Calibration results for additional stations in the Niger basin model.

Gauging station	Kouroussa	Selingué	Koulikoro	Douna (Bani River)	Kirango Aval	Akka	Diré	Koryoume	Tossaye
Calibration period	1965-1974	1965-1974	1964-1974	1964-1974	1975-1981	1987-1990	1964-1974	1979-1986	1968-1979
NSE/ PBIAS[a,b]	0.85/ 3.3	0.78/ 6.1	0.92/ 5.8	0.87/ 9.9	0.79/ 29.3	0.48/ -42.6	0.81/ -2.2	0.75/ -4.8	0.82/ 0.2

Gauging station	Ansongo	Kandadji	Niamey	Malanville	Yidere Bode	Shiroro (Kaduna River)[c]	Riao (Benue River)[c]	Ibi (Benue River)
Calibration period	1968-1979	1976-1986	1976-1986	1976-1986	1985-1995	1982-1990	1971-1980	1970-1981
NSE/ PBIAS[a,b]	0.81/ 7.5	0.84/ 9.6	0.76/ 16.2	0.4/ 32.3	0.61/ 27.3	0.52/ 35.4	0.7/ 59.4	0.9/ 14.8

[a] Nash-Sutcliffe Efficiency of daily model output.

[b] Percent bias of monthly average.

[c] At the stations Riao and Shiroro only monthly data has been available and used for calibration and calculation of NSE and PBIAS

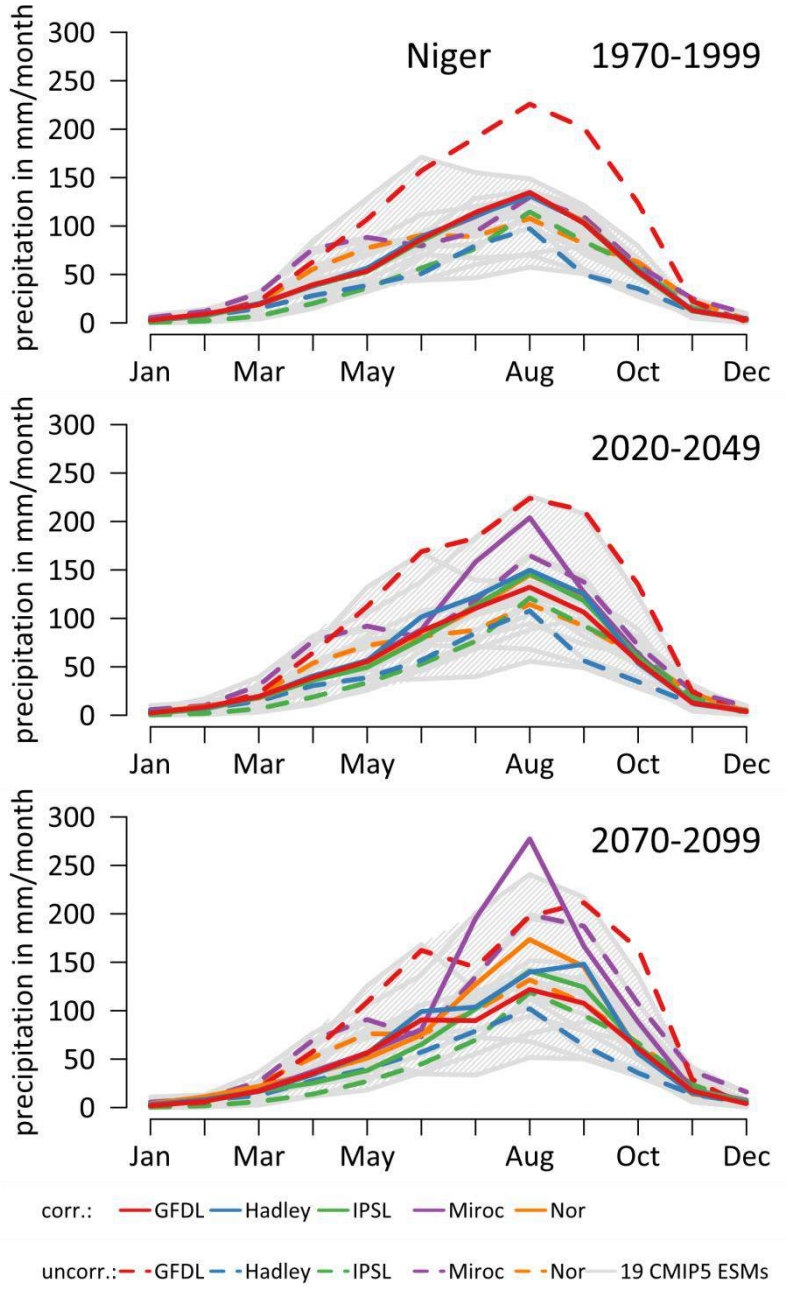

Figure S 17 Mean monthly precipitation of corrected and uncorrected ISI-MIP climate models and 19 other CMIP-5 ESMs for the Niger basin during the periods 1970-1999, 2020-2049 and 2070-2099.

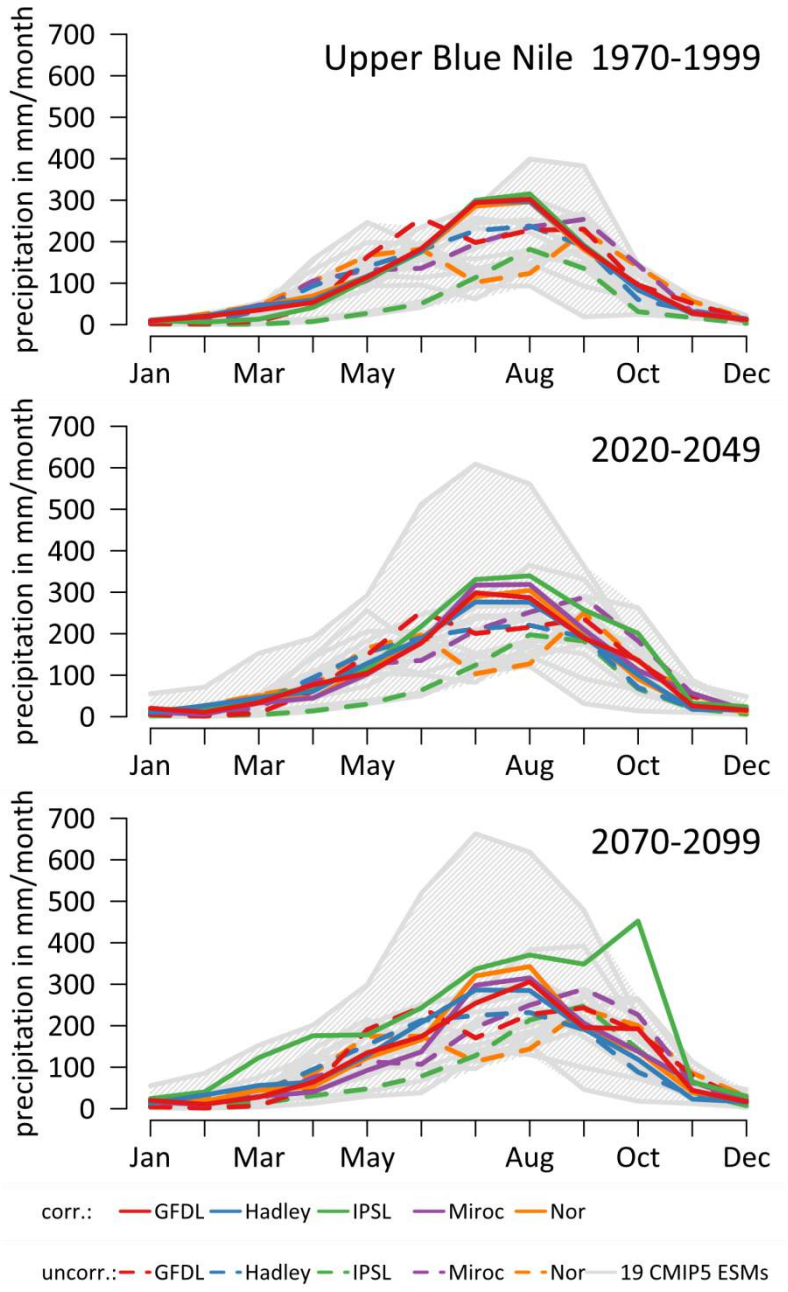

Figure S 18 Mean monthly precipitation of corrected and uncorrected ISI-MIP climate models and 19 other CMIP-5 ESMs for the Upper Blue Nile basin during the periods 1970-1999, 2020-2049 and 2070-2099.

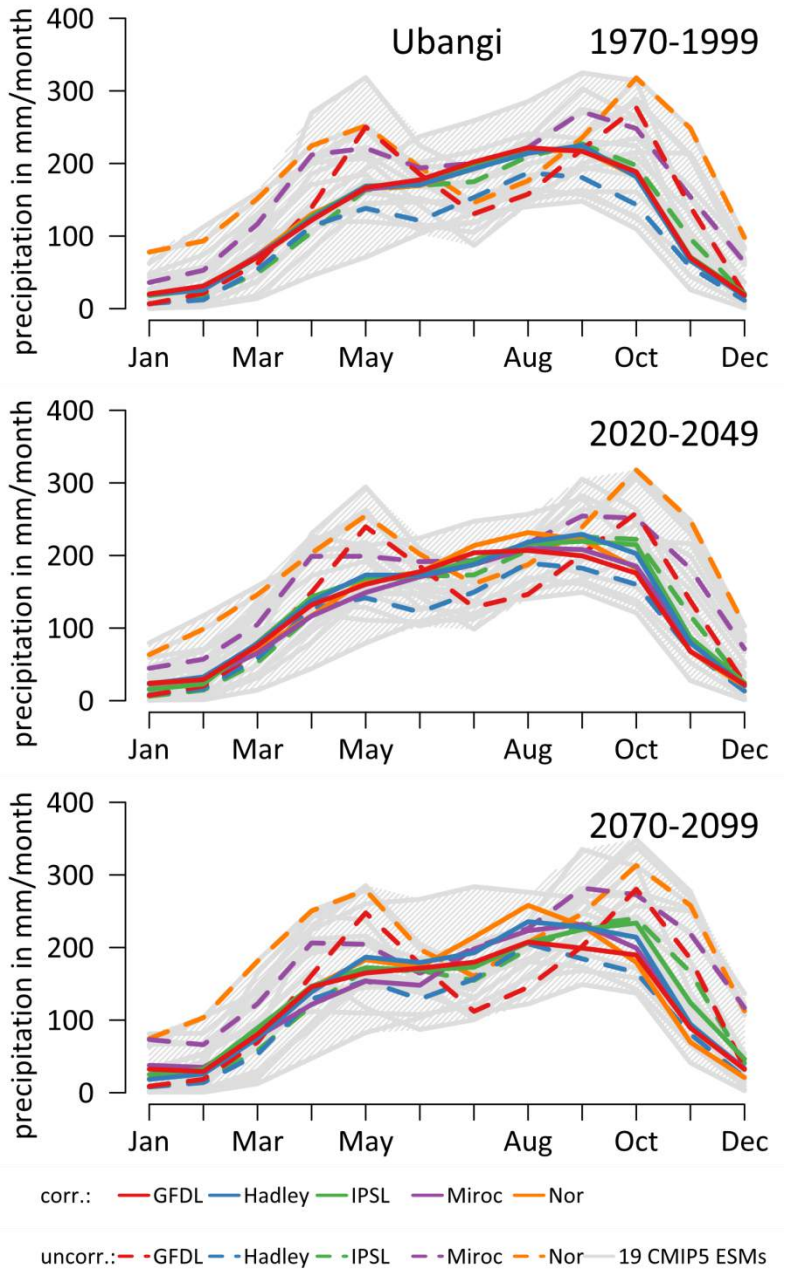

Figure S 19 Mean monthly precipitation of corrected and uncorrected ISI-MIP climate models and 19 other CMIP-5 ESMs for the Ubangi basin during the periods 1970-1999, 2020-2049 and 2070-2099.

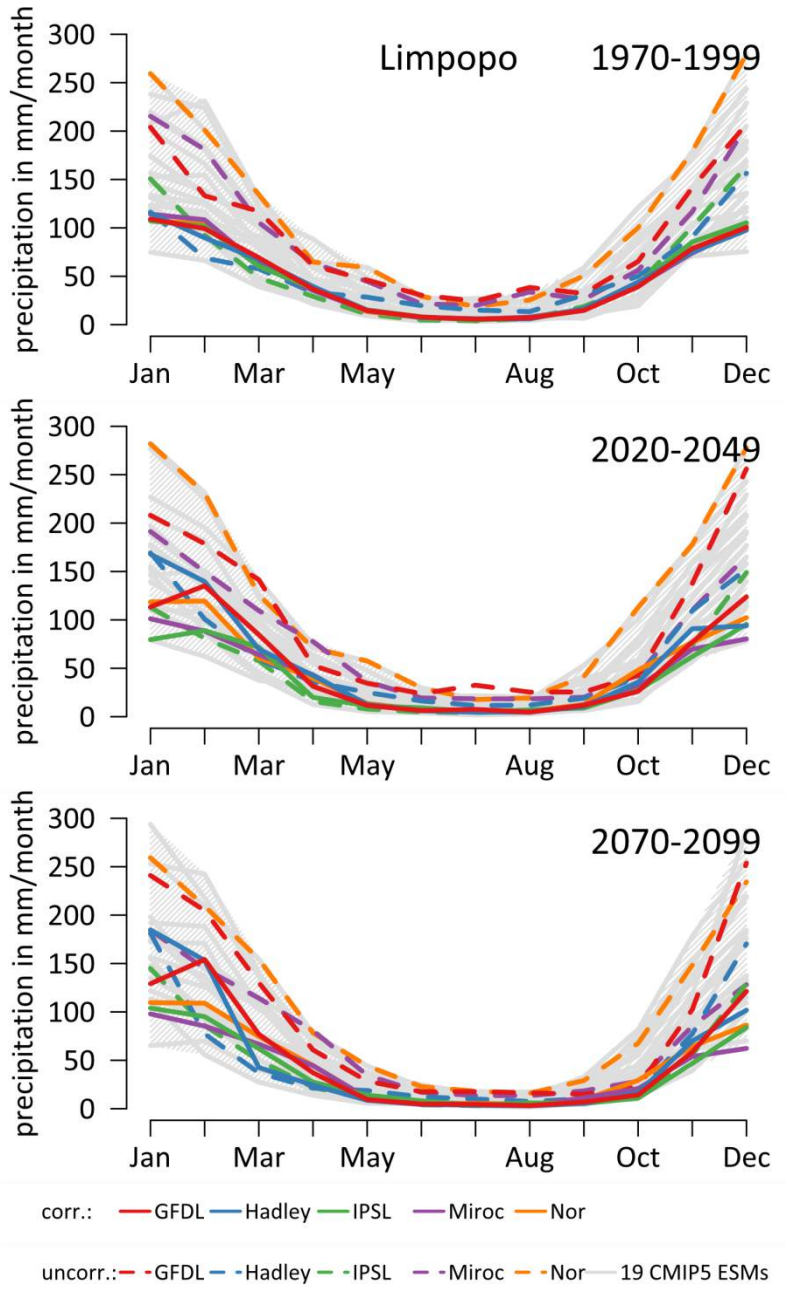

Figure S 20 Mean monthly precipitation of corrected and uncorrected ISI-MIP climate models and 19 other CMIP-5 ESMs for the Limpopo basin during the periods 1970-1999, 2020-2049 and 2070-2099.

10.6. Appendix of Chapter 7

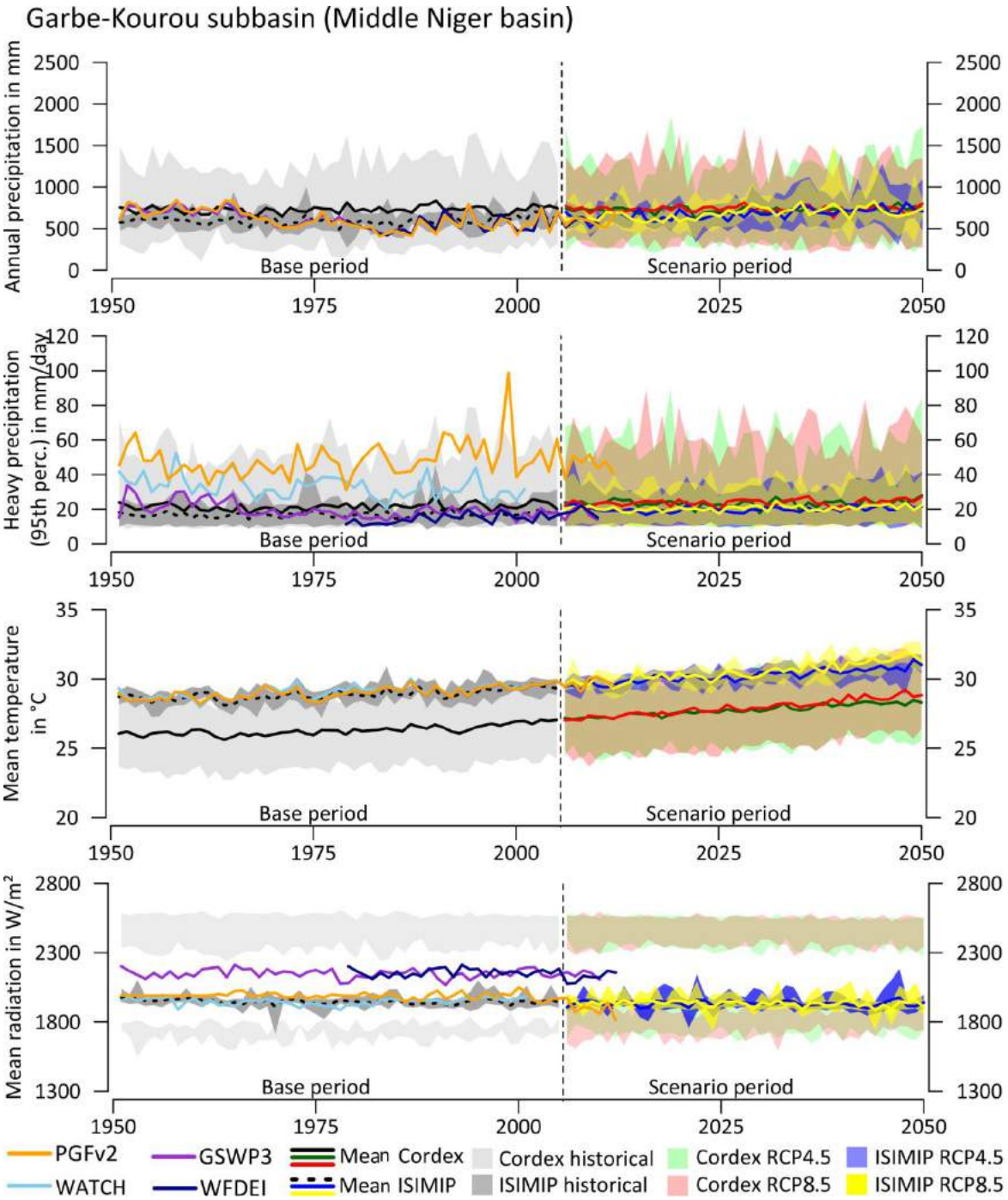

Figure S 21 Annual precipitation, mean temperature and mean short wave downwelling radiation for the Garbe-Kourou subcatchment in the Middle Niger Basin with four reanalysis datasets (PGFv2: 1950-2012, GSWP3: 1950-2010, WATCH: 1950-2001, WFDEI: 1979-2012), and climate scenarios for the base and the future period of five ISIMIP models and 13 CORDEX Africa GCM-RCM combinations for RCP 4.5 and RCP 8.5.

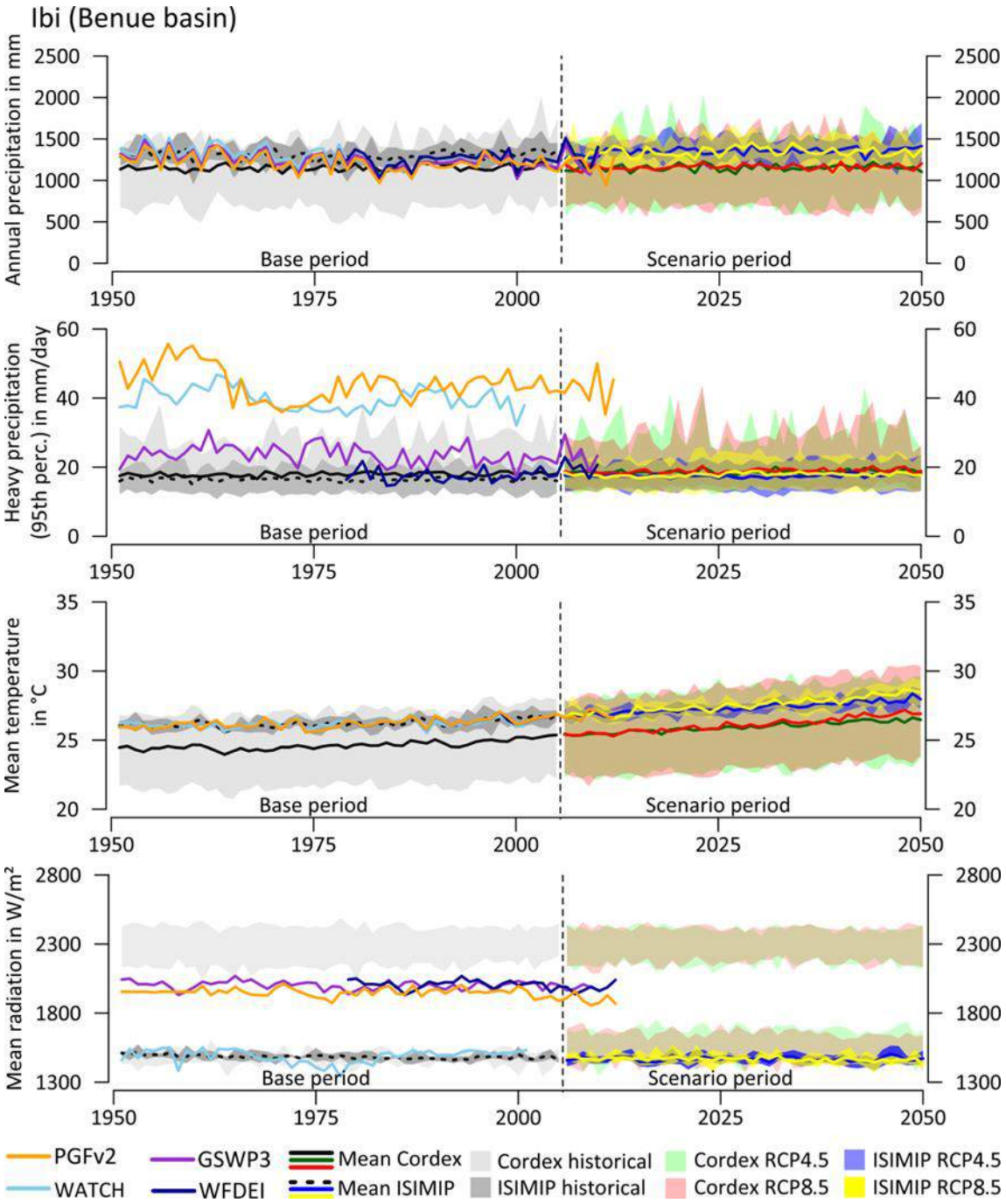

Figure S 22 Similar to Figure S 21 but for the Ibi subcatchment in the Benue Basin.

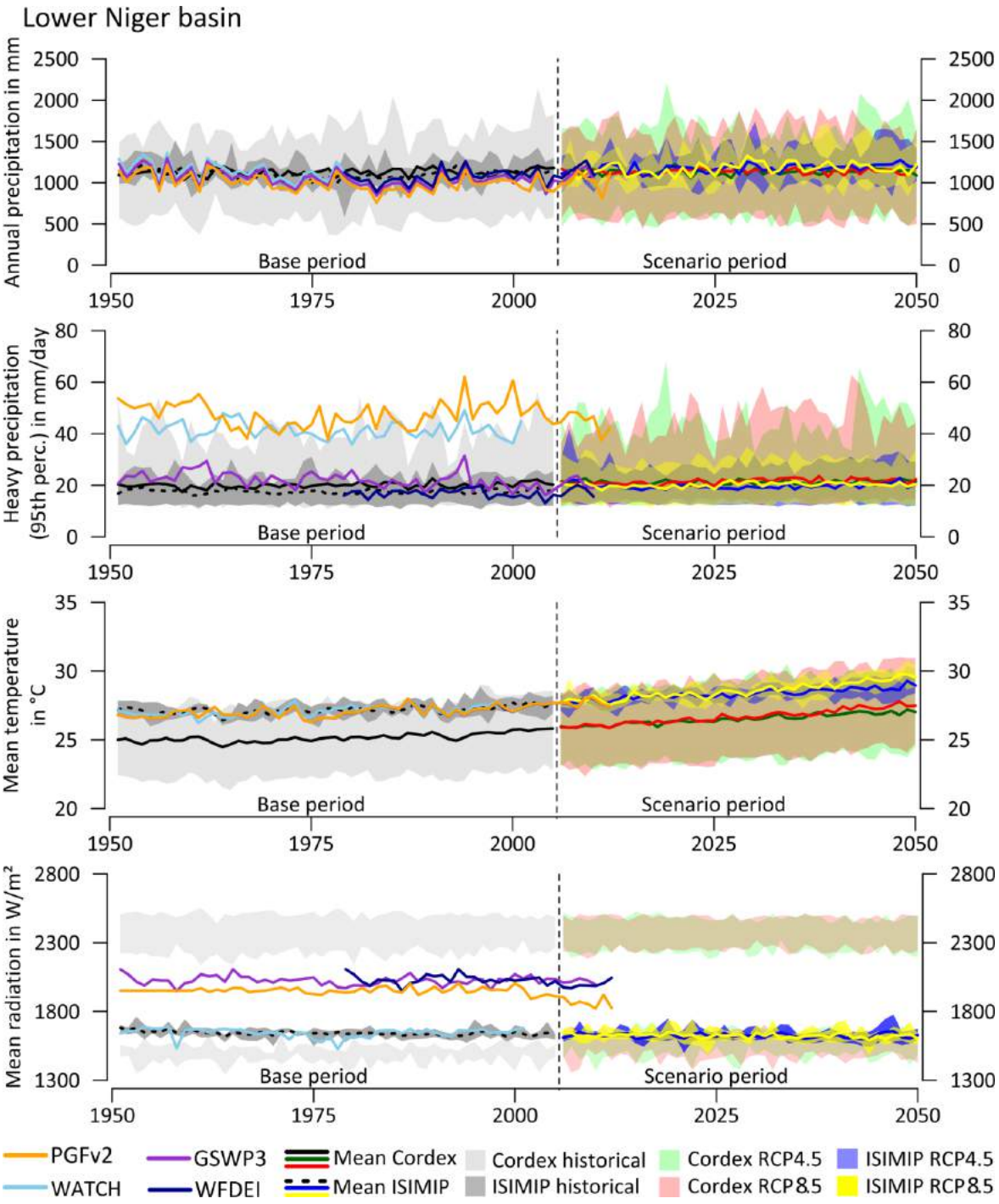

Figure S 23 Similar to Figure S 21 but for the Lower Niger Basin.

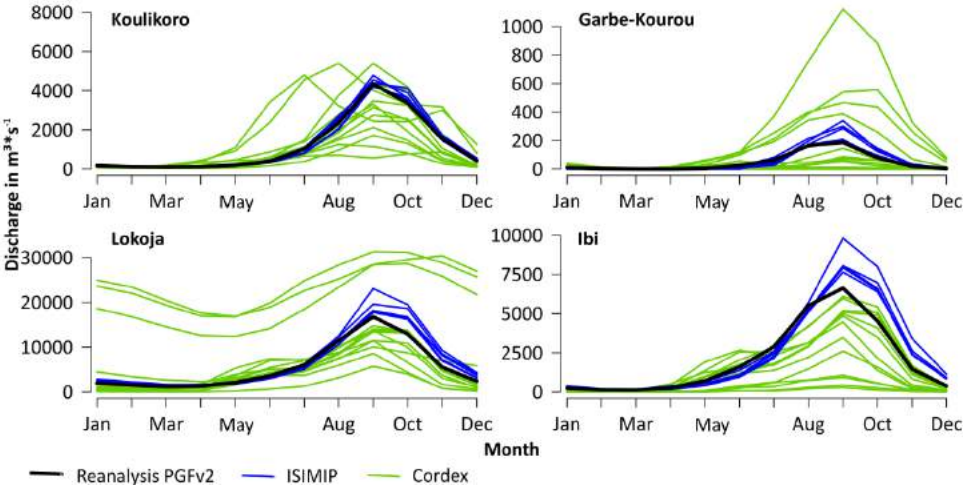

Figure S 24 Annual flow regimes on monthly basis for different parts using climate models input of the base period (1976-2005) compared to reanalysis data which was used for calibration. Green are CORDEX driven simulations, blue are ISMIP driven simulations and the thick black line is the simulation with reanalysis data.

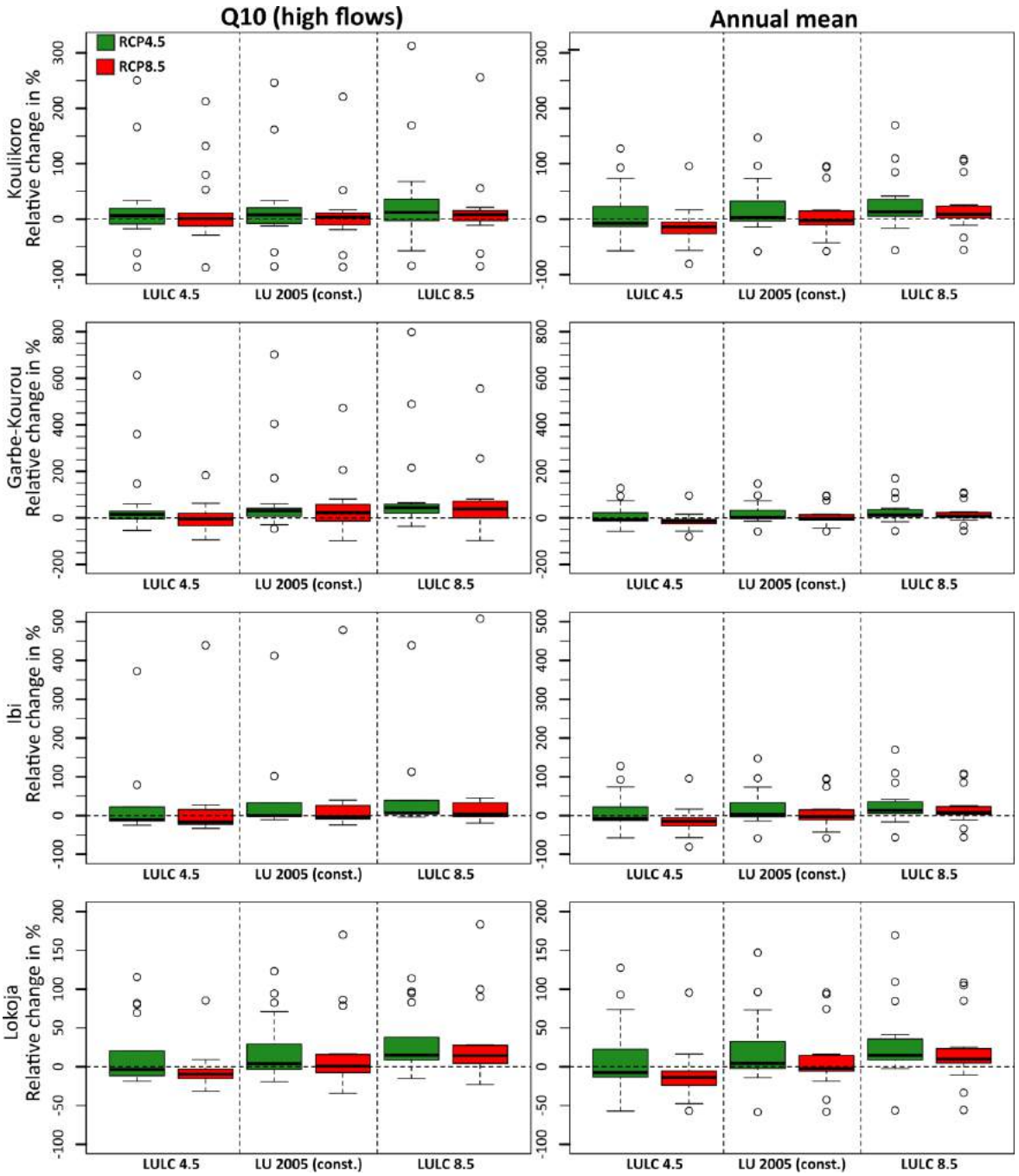

Figure S 25 Similar to Figure 7, but with outliers: Boxplots for relative change (in %) for the 90th percentile of annual discharges (Q10) and the mean annual discharge in the four study catchments, for the different land management scenarios (LULC 4.5, constant LULC of 2005, and LULC 8.5) and different climate scenarios (RCP 4.5 and RCP 8.5). Differences are given between the scenario period (2021-2050) and the base period (1976-2005).

Declaration of authorship

Hereby I declare that this work has not been submitted to any other University or higher education institute, that it is solely my own work – except for the shares of the coauthors in the journal articles as clarified in detail in the overview of articles (chapter 1.6) –, and that all sources used have been listed.

Potsdam, 17th December 2015

Valentin Aich